Author:
Ward, Amy

Title:
Initiation and regulation of experimental autoimmune uveoretinitis

Initiation and Regulation of Experimental Autoimmune Uveoretinitis

Amy Ward

A dissertation submitted to the University of Bristol in accordance with requirements for award of the degree of Doctor of Philosophy in the Faculty of Health Sciences

School of Translational Health Sciences

January 2021

Word Count-61356

Abstract

Non-infectious uveitis is an autoimmune disease characterised by infiltrating leukocytes such as T cells due to loss of immune tolerance to retinal proteins. Experimental autoimmune uveitis (EAU) is an animal model of non-infectious uveitis that shares many features with human disease and can be induced in mice by the transfer of autoantigen specific lymphocytes. The purpose of this thesis was to look at leukocyte trafficking specifically CD4+ T cells during initiation of clinical disease and throughout active clinical disease.

The data presented uses an adoptive transfer to induce clinical disease. This was developed to study antigen specific and non-antigen specific recruitment during EAU. This robust technique also allows investigation into the role of specific chemokine and cytokine receptors during EAU by using knockout mice.

The results demonstrate that antigen specific CD4+ T cells that initiate disease or their progeny persist within the tissue during active clinical disease and after active clinical disease has subsided. At day 2 after transfer, increased recruitment of endogenous CD4+ T cells and retention of transferred CD4+ T cells was observed, this was further investigated using non antigen specific cell transfers using ovalbumin specific CD4+ T cells which showed that the pathogenic stimulus needed to be present locally to initiate clinical disease in recipients. Further to this ovalbumin specific cells are recruited to the eye if the antigen is introduced to the ocular tissue or if a pathogenic stimulus is present. Using the adoptive transfer technique further analysis using chemokine knockout mice showed that during active clinical disease CX3CR1 is expressed on CD4+ T cells which are selectively retained within the eye. Using cytokine receptor knockout mice IL-27R$\alpha^{-/-}$ cells were found to be more potent in nature to drive a more persistent and severe disease phenotype.

Acknowledgements

This thesis and the work behind it would not have been possible without the support and friendship of the great group of people that I have had the chance to work with. It is difficult to put into some short paragraphs how grateful I am towards all those that have supported me throughout my studies.

First and foremost, I would like to thank Lindsay Nicholson for being everything I could have possibly asked for in a supervisor. Thank you for the invaluable advice, continuous support and patience. You have inspired me to become a more rounded scientist and further developed my passion for immunology. I am also very thankful that you encouraged me to continue my work in the lab (even when I should perhaps have been at my desk writing!) and gave me the freedom to explore any experimental ideas that interested me.

I would also like to thank Andrew Dick for all the scientific advice and encouraging words you have given. I have particularly enjoyed your occasionally surprised reactions to new data or experimental ideas that you may not have expected.

My gratitude also goes to National Eye Research Centre and The James Tudor Foundation for funding this project.

I would have made little progress in the lab without the training and guidance from Dave Copland. Thank you so much for your help and patience, as well as everything else you do to support the group. I really enjoyed your company throughout all the experiments we ran together.

I would like to express my gratitude to Gareth Jones for providing me with the IL-27R$\alpha^{-/-}$ mice and all the support and assistance that was given both in terms of experiments and feedback. My thanks also go to David Hill for helping me to run the experiments even while in the midst of writing up his own PhD.

Many thanks to Katy Jepson for the help in acquiring the lightsheet and confocal imaging presented in chapter 7, and also to Andrew Herman and Lorena Sueiro Ballesteros in the flow cytometry facility who helped design panels, trained me to use the cytometers and assisted me with the acquiring and analysis of samples.

Thank you to everyone in the Ophthalmology group both past and present for all their help with experiments and the catch ups over a cup of tea when I needed a break. In particular, Alison Young, Alison Clare, Lydia Bradley, John Pooley, Jian Lui, Colin Chu, Lauren Schewitz-Bowers, Emily Williams and Maddy Stimpson. Also, a massive thank you to my dream team from PhD day 1, Louis Scott and Oli Bell, for celebrating with me when experiments worked, or listening sympathetically when they did not.

I would also like to thank my family and friends, especially my Mum and Pippa for having confidence in me through all my years of studying and in every choice I have made. To Fran and Colin for always being there for me with a drink and a hug if needed. To Jade, Kyle, and Joe for being the best distraction and making me laugh after a stressful week.

To Leighton, thank you for always believing in me, I could not have achieved all I have without your support (even if most of the time you didn't fully understand what I was talking about!).

Lastly, my dad Ian and Grandma Lysaght who I miss dearly. I know both would be proudly supporting me now.

Author's Declaration

I declare that the work in this dissertation was carried out in accordance with the requirements of the University's *Regulations and Code of Practice for Research Degree Programmes* and it has not been submitted for any other academic award. Except where indicated by specific reference in the text, the work is the candidate's own work. Work done in collaboration with, or with assistance of others, is indicated as such. Any views expressed in the dissertation are those of the author.

SIGNED……AMY WARD…… DATE……19/01/2020…….

Publications and Presentations

Publications

Bell OH, Copland DA, **Ward A,** Nicholson LB, Lange CAK, Chu CJ and Dick AD- Single Eye mRNA-Seq reveals normalisation of the retinal microglia transcriptome following acute inflammation Frontiers in Immunology

Presentations

Oral- Enrichment of pioneer CD4+ T cells and upregulation of CX3CR1in Experimental Autoimmune Uveoretinitis **May 2018** School of Cellular and Molecular Medicine Speak Easy, Bristol

Oral- Enrichment of pioneer CD4+ T cells and upregulation of CX3CR1in Experimental Autoimmune Uveoretinitis **September 2018** Infection and Immunity Early Careers Research Day, Bristol

Poster- Upregulation of CX3CR1 on $CD4^+$ T cells in Experimental Autoimmune Uveoretinitis **December 2017** BSI Congress, Brighton

Poster- Enrichment of pioneer $CD4^+$ T cells and upregulation of CX3CR1 in Experimental Autoimmune Uveoretinitis **September 2018** ECI Congress, Amsterdam

Poster- Upregulation of CX3CR1 on CD4+ T cells during Experimental Autoimmune Uveoretinitis **May 2019** ARVO Meeting, Vancouver

Poster- Persistence of transferred pathogenic CD4+ T cells in Experimental Autoimmune Uveoretinitis (EAU) **December 2019** BSI Congress, Liverpool

Poster- $IL27R\alpha^{-/-}$ causes a more severe and persistent Experimental Autoimmune Uveoretinitis disease phenotype **December 2019** BSI Congress, Liverpool

Abbreviations

ACAID	Anterior chamber-associated immune deviation
ACK	Ammonium-chloride-potassium buffer
AIA	Adjuvant Induced Arthritis
AIRE	Autoimmune regulator
Anti-TNF	Anti-tumour necrosis factor
APC	Antigen Presenting Cell
BCR	B cell receptor
CFA	Complete Freund's Adjuvant
CSF	Cerebrospinal fluid
CTLA4	Cytotoxic T lymphocyte antigen 4
DAMP	Danger-associated molecular patterns
DC	Dendritic cell
DNA	Deoxyribonucleic acid
EAAU	Experimental autoimmune anterior uveitis
EAE	Experimental Autoimmune Encephalomyelitis
EAU	Experimental Autoimmune Uveoretinitis
EBI3	Epstein-Barr virus-induced gene 3
EIU	Endotoxin induced uveitis
ELS	Ectopic lymphoid structure
FACS	Fluorescence associated cell sorting
FCS	Fetal Calf Serum
FDC	Follicular dendritic cell
FoxP3	Forkhead box P3
GFP	Green fluorescent protein
GM-CSF	Granulocyte-macrophage colony-stimulating factor
GWAS	Genome wide association studies
HLA	Human leukocyte antigen
ICAM	Intracellular adhesion molecule
IFN	Interferon
Ig	Immunoglobulin

IL	Interleukin
IL27Rα	Interleukin 27 Receptor alpha
ILC	Innate lymphoid cell
IPM	Inter-photoreceptor matrix
IRBP	Interphotoreceptor retinoid-binding protein
iTreg	Induced Tregs
I.P	Intraperitoneal injection
LPS	Lipopolysaccharide
MCP-1	Monocyte chemotactic protein-1
MHC	Major histocompatibility complex
NETS	Neutrophil extracellular traps
NK	Natural killer
OCT	Optical coherence tomography
PAMP	Pathogen associated molecular patterns
PRR	Pattern recognition receptors
pTreg	Peripheral Tregs
RAU	Recurrent anterior uveitis
RBP3	Retinal binding protein-3
RPE	Retinal pigment epithelium
S-Ag	S-antigen
S.C	Subcutaneous injection
STAT	Signal transducer and activator of transcription 4
TCR	T cell receptor
TEFI	Topical endoscopic fundal imaging
Tfh	T follicular helper
Tg	Transgenic
TGFβ	Transforming growth factor beta
Th	T helper
TLR	Toll like receptor
TNF	Tumour necrosis factor
Ttreg	Thymic selected Treg
Treg	Regulatory T

VCAM	Vascular adhesion molecule
WT	Wildtype

Table of Contents

Chapter 1

Chapter 2

Chapter 3

Optimisation of adoptive transfer technique……64

Chapter 4

Recruitment of transferred and endogenous cell populations during EAU…110

Chapter 6

List of Figures

List of Tables

Chapter 1. General Introduction

1. Introduction

Humans are constantly exposed to pathogenic and non-pathogenic microbes. Whilst the immune system is eliminating pathogens and toxic or allergenic proteins it must avoid responding in a way that produces excessive damage to tissues or which eliminate beneficial microbes (2). The three essential properties of the immune system are determined by function: recognition of self and non-self and the ability to discriminate between the two; activation of pathways that eliminate pathogens and the development of long lasting memory (3). The immune system can be divided into the non-specific innate immune response and the highly specific adaptive immune response (3).

The innate immune system can be defined as hard-wired responses that are encoded by genes in the host's germ line, thus allowing recognition of molecular patterns shared by many microbes and toxins that are not found within the mammalian host (2). Although the main role of the innate immune system is defence against infection, the effects of the response allow for surveillance of host tissue damage and protection against progression of malignancy due to mutation (3).

The adaptive immune system uses antigen-specific lymphocyte responses to give successful immune protection (4). The adaptive immune response is composed of cells with specificity (through receptors) for an individual pathogen, allergen or toxin, the responding cells after antigen encounter will then proliferate in order to attain sufficient cell numbers for an effective immune response. An important feature of the adaptive immune response is the production of long-lived cells that are capable of persisting in a dormant state but possess the ability to re-express effector functions quickly after further encounters with the same antigen ensuring the adaptive immune system to manifest immune memory (2).

1.1 Innate immune response

The innate immune system is the first defence mechanism against pathogens and is comprised of cellular components and physiological and chemical barriers to protect against pathogen entry, replication and survival (3). This is achieved by establishing a protective response that has the ability to develop at a rapid pace from initiation to a full inflammatory response, followed by resolution to restore tissue integrity (5). The initial phase of the inflammatory response is focused on the destruction of pathogens that is followed by a phase

of dead and dying cells and cellular debris being eliminated from the site of inflammation. The final phase is a restoration phase in which tissue appears to be repaired and in a healthy condition (5).

1.1.1 Physiological, physical, and chemical barriers of the innate immune system

Anatomical barriers of the innate immune system are comprised of epithelial layers including mucous membranes and the skin which prevent the entry of pathogens into the host (3). Pattern recognition receptors (PPRs) allow recognition of invading organisms and are expressed on various immune cells, they are responsible for the recognition of non-mammalian molecular patterns known as pathogen associated molecular patterns (PAMPs) (6). Activation of protective inflammatory cellular responses can be achieved by binding of PAMPs such as bacterial and fungal cell-wall components and viral nucleic acid (6) to PRRs on the surface and within the cytoplasm of the host cells (3, 7). The recognition of pathogens by PRRs plays a vital role in the generation of an effective innate immune response (7). The sensing of microbes by PRRs expressed on antigen-presenting cells, in particular dendritic cells leads to the activation of adaptive immune responses (6).

1.1.2 Inflammatory mediators and cellular components of innate immunity

Cellular components of the innate immune system include several polymorphonuclear cells such as; neutrophils, eosinophils, basophils, mast cells, phagocytic cells (such as: monocytes, macrophages), dendritic cells and natural killer (NK) cells (3).

Neutrophils are major players during acute inflammation, they are typically the first leukocytes to be recruited to the site of inflammation and are capable of eliminating pathogens by several mechanisms (8). They are continuously generated in the bone marrow from myeloid precursors and during inflammation the neutrophil number within tissues increases. Over time these cells die and are removed by macrophages and dendritic cells. Neutrophils can eliminate pathogens by multiple mechanisms both intracellularly and extracellularly, when microorganisms are encountered phagocytosis occurs, or highly activated neutrophils are capable of eliminating microorganisms by releasing neutrophil extracellular traps (NETs) (8).

Monocytes can be found circulating in the blood, bone marrow and spleen making up roughly 10% of total leukocytes within humans and 2-4% in mice. They can remain in the circulation for up to 1-2 days. If an inflammatory response has not initiated recruitment to the tissue in this time the cells will die and be removed (5). The physiological role of monocyte subsets in

vivo are yet to be fully defined but they are suggested to play roles in inflammation and tissue repair due to their capacity to be activated and secrete inflammatory cytokines, immune defence mechanisms, antigen processing and presentation, pro-angiogenic and patrolling behaviour and also in maintaining homeostasis (5).

Macrophages are professional phagocytes defined as mobile cells with the ability to engulf and digest pathogens, particles and dead cells (9). Resident macrophages are heterogeneous and versatile cells found in tissue in adult mammals, they represent up to 10-15% of total cell number when the tissue is non-inflamed (5). The long-term persistence of adult tissue macrophages relies on replenishment by bone-marrow derived monocytes (10) especially during inflammation (11).

Dendritic cells are a distinctive group of specialised antigen-presenting cells that have the ability to influence both the innate and adaptive immune response (12, 13). Although dendritic cells are only present in a small population within lymphoid tissues, they are also considered important in terms of the initiation of antigen-specific immunity and the T cell mediated response, as well as the induction of immunological tolerance (13). DCs support immunity or tolerance by antigen-presentation to T cells and delivering immunomodulatory signals through cell to cell contact and cytokines (12).

Eosinophils are a minor component of circulating leukocytes that develop and differentiate in the bone marrow; they can be long-lived granulocytes involved in a variety of regulatory functions (14). In normal conditions, eosinophils can be found within the thymus, spleen, blood, lung, uterus, adipose tissue, mammary gland, and lamina propria of the gastrointestinal tract, suggesting a physiological function in each organ. Eosinophils have the ability to regulate lymphocyte recruitment and function but are not known to have the capacity to function as an antigen-presenting cell to T cells. Immunologic regulation of eosinophils has been suggested to extend from innate immunity to adaptive immunity and can involve non-immune cells (14).

Basophils are the least frequent granulocyte population within the mammalian body. The accumulation of basophils has been observed in allergic disease, organ rejection, autoimmunity, and cancer (15). Unlike other granulocyte populations the lifespan of mature basophils is quite short and estimated to be between 1-2 days, therefore the constant presence of basophils in periphery is thought to be down to continuing development and replenishment of the population (15).

Natural Killer (NK) cells are important immune cells with an essential role in tumour immunity, antibacterial immune response, anti-viral immune response and human pregnancy (6). NK cells are now included as a group 1 innate lymphoid cell (ILC) along with ILC1 cells (16). NK cells are recognised as a separate lineage of lymphocytes with effector functions that are considered both cytotoxic and cytokine producing. Accordant with their main function as innate sentinels, NK cells can be found within both lymphoid and nonlymphoid tissues. However, NK cells represent a small fraction of total lymphocytes in most tissues (~2% of murine splenocytes and between 2-18% of lymphocytes detected within human blood). Subsets of NK cells can be distinguished in mice and humans based on their phenotype and anatomical and functional features (17).

1.2 Innate control of adaptive immunity

The innate and adaptive immune systems have been described as two separate contrasting arms of the immune response; however, they are usually found to act together. The host's initial defence being the innate immune response, and the adaptive response becoming the more prominent through clonal expansion of antigen-specific T and B cells after several days (2). Control of adaptive immunity by the innate immune system is considered to be a firmly established paradigm. Microbial pathogens are recognised by the innate immune system using pattern recognition receptors (PRRs) that have the ability to detect conserved pathogen-associated molecular patterns (PAMPs) which are present in bacterial and fungal cell-wall components and viral nucleic acids (6). PAMPs detected by PRRs induces an inflammatory response of innate host defences, the recognition of microbes by PRRs expressed on antigen-presenting cells initiates adaptive immune responses (6).

1.3 Adaptive immune Response

The innate immune system has evolved to sense and eliminate a wide range of pathogens, but the variety of common pathogenic molecular patterns it has the ability to recognise is limited. The variation present in antigenic structures combined with pathogens mutating to avoid host detection can be paralleled with the evolution of the adaptive immune response (18). Unlike the recognition receptors of the innate immune response that are all encoded in the germline genome in their fully functional form, the adaptive immune response depends

on receptors that are specific and selected by somatic recombination of a large array of gene segments (18). After initial pathogen encounter, cells with expression of specific immune receptors can persist in the host for life, thus providing immunological memory and giving the capacity for a highly targeted, rapid response in the event of re-exposure to the same pathogen (3, 18). In response to the inflammatory environment created by the innate immune response, cells of the adaptive immune system (including B and T cells) are stimulated to proliferate and differentiate into cells with various functions that are useful for immunological challenge (19). After the invading pathogen is removed, most of the cells recruited from the adaptive immune response die but leave behind an array of memory subsets against the pathogen within the host (19).

Following host pathogen exposure, cells, and inflammatory mediators from the site of infection travel to local lymph nodes. Non-host antigens presented using MHC molecules on antigen-presenting cells (APCs) are recognised by B and T lymphocyte receptors present in the host (3). Clonal selection involves the processes of clonal deletion and the expansion of lymphocytes to create a population of specific cells capable of targeting the original pathogen (3). Although the adaptive immune response is more specific than the innate response to the pathogen (18).

The principle cells of the adaptive immune response include two major lineages of lymphocytes that have the ability to specifically recognise and respond to antigenic determinants of pathogens and toxins (20). These cells develop in the primary lymphoid organs such as the bone marrow and thymus, then traffic to secondary lymphoid organs which include the lymph nodes and spleen. These organs serve to capture circulating antigens from lymph and blood respectively (18). The cells are named T (thymus-derived) and B (bone-marrow derived) lymphocytes, similar to other blood cells early T and B cells are derived from hematopoietic stem cells (20).

In early stages of development T and B lymphocyte progenitors reorganise various sets of prototypic immunoglobulins (Ig) diversity (d), joining (j) and variable (v) gene segments to produce antigen binding regions of their T cell receptors (TCRs) and B cell receptors (BCRs) (20). The antigen binding regions of the various V(D)J combinations are further diversified through enzymatic addition of nonencoded nucleotides in the joints made during V(D)J assembly. The random nature of this diversification process generates receptors that are capable of recognising self-antigens (20).

Non-host antigens found on antigen-presenting cells can be identified by B and T cell receptors. Clonal selection of lymphocytes gives a population of specific cells that are capable of targeting the original pathogen presented (3).

1.4 Cells of the adaptive immune response

1.4.1 B cell response

The humoral response is mediated by B lymphocytes that are produced in the bone marrow. On activation by T cells they differentiate into plasma cells, memory cells or antigen-presenting cells (21). Memory B cells represent the outcome of the humoral response, these cells express high affinity antigen-specific B cell receptors for specific antigens so that the second response on re-exposure is much quicker and heightened (21, 22).

1.4.2 B cells

B cells are classified by their anatomic localisation and ontogeny. Three main classes exist B1a, B1b and B2 B lymphocytes in both mice and humans, including marginal zone and follicular B cells (23). B1 progenitors develop into B1 lymphocytes present from the foetal liver and survive beyond the neonatal period as a self-renewing population. Whereas B2 lymphocytes are produced from BM precursors that develop from transitional 2 (T2) B cells and continue output throughout life (23). A crucial function of B lymphocytes is antibody production (23).

BCR antigen receptors are present on mature B cells. They are comprised of glycosylated proteins known as membrane-bound or surface immunoglobulins, specifically IgM and IgD classes of antibody (24). Alternatively, antibodies are released from the B cell to target antigens within the extracellular space to bind and neutralise them efficiently (23). Plasma cells secrete antibodies which consist of two similar heavy chains distinguished by the C-terminus regions, which are sustained and do not partake in antigen binding. These chains determine the type of antibody e.g. IgA, IgD and IgE, IgG and Ig(M) with two similar light chains (21, 23). There are four subclasses of IgG antibodies in humans IgG1, IgG2, IgG3 and IgG4 (23), and is the principle mediator of opsonisation, IgA is involved in mucosal immunity, IgD is cell bound and IgE is involved in mast cell degranulation (21). Antibodies apply effector functions in three ways: they activate immune cells including macrophages by binding to the Fc receptor to allow recognition of the constant regions of specific antibody classes, binding

to a specific target to neutralise it and therefore preventing it from entering a cell, or binding to C1q to activate the complement immune response, specifically the classic pathway (23). The chosen effector mechanism of the cell is determined by both the cells affinity to bind and activate the Fc receptor present on immune cells and the isotype of the heavy chain (23).

Follicular B cells are activated after antigen recognition by the BCR and critical helper signals derived from antigen specific CD4 T cells (23). When bound to antigen, the BCR initiates two processes, firstly necessary gene expression programmes are triggered by signals sent from the BCR to the cell, and secondly, the antigen is internalised and brought into the endosomal compartments to be broken down in order to be presented by MHC class II complexes in peptide form to the B cell (23). Recognition of peptide MHC class II complexes by antigen specific CD4+ T cells is achieved through intimate contacts with B cells to form an interaction known as 'cognate' or 'linked' T-B interactions (23).

1.4.3 T cell response

In order to become a mature thymocyte, bone marrow derived precursor cells must go through a highly regulated program of intrathymic development to then leave the thymus and form the peripheral T cell pool (25). The early stages of thymocyte development are defined by a number of molecular events; expression of RAG1 and RAG2 gene products, expression of CD4 and CD8 coreceptor molecules, somatic rearrangement of the T cell receptor β locus and recombination of TCR α locus (25). For a T cell to develop from a haemopoietic progenitor to a mature TCRα/β+ T cell a series of commitment events take place including TCR V(D)J gene rearrangement, TCR β selection and positive/negative selection of thymocytes (26).

T lymphocytes produced in the bone marrow migrate to the thymus and undergo selection (21). During development, the DNA undergoes rearrangement and the T cell receptors (TCRs) become specific for foreign antigens. This is by a process of education that allows the cell to distinguish between self and non-self (21). The ability to recognise self from foreign or non-self is achieved through selection by cell surface molecules known as major histocompatibility complex (MHC) (21). T cells are able to recognise antigen that has been processed and presented to them by MHC molecules on APCs. There are two types of MHC molecules: MHC class I and MHC class II (21). All parenchymal cells express MHC class I molecules and therefore have the capabilities to present internal peptide molecules. Monocytes, macrophage, B cells,

dendritic cells, and endothelial cells express MHC class II and can present external peptides that are processed by APCs (21).

During embryonic development immature T cells interact with epithelial cell surface molecules such as MHC class I and II molecules when passing through the thymus. This is to ensure the T cells are both reactive and specific. From this, immature T cells are processed by functional or positive selection in the thymic cortex, then in the medulla the cells undergo negative selection to ensure elimination of autoreactive T cells (21). In the periphery, regulation of co-stimulation molecules and cytokines control if T cells remain quiescent or become activated; on activation, T cells become either T-helper cells, T-suppressor cells or cytotoxic T cells (21).

1.4.4 T cell activation

Each unique T cell in the periphery carries a TCR that is made up of an α chain and a β chain. The TCR has the potential to recognise a small number of peptide antigens in combination with MHC. These cells are actively surveying but are in a resting state unless they encounter cognate antigen. The generation of the TCR occurs by genomic DNA sequences undergoing recombination during the development of T cells, each TCR is unique and highly specific (19). Recombination to form a functional TCR gives rise to a resting T cell that emerges from the thymus gives. The resting T cell is capable of migrating through secondary lymphoid tissues which include the lymph nodes and spleen or the periphery but cannot yet produce a response that would protect the host from infectious challenge (19).

In order to produce a T cell with the capabilities of mediating immune responses the naïve T cell must be activated, this is achieved through coordinated interactions between the APC and the molecules that are present on the surface of T cells (19). An APC is capable of carrying an antigenic peptide bound to an MHC class molecule non-covalently from an infectious agent. The TCR recognises a peptide antigen when bound to the correct MHC class I or class II molecule (19). In the T cell plasma membrane, the alpha/beta TCR connects with CD3 which is a complex membrane protein comprised of δ-, ε- γ-, and ζ- subunits, an intracellular signal is produced following ligation of the TCR by the cytosolic region of this complex (19). CD4 or CD8 coreceptor together with the TCR bind to class I or class II MHC class molecules; class I for CD8 cells and class II for CD4 cells, this is to stabilise the interaction between the T cell and APC (19). After the recognition of the cognate peptide bound to a MHC molecule by the specific corresponding TCR, the APC and T cell begin forming an immunological synapse by

undergoing actin-mediated membrane reorganisation to facilitate grouping of the TCR on the surface of the cell (19, 27).

However, to induce T cell activation, stimulation with cognate antigen alone is not sufficient and will instead produce a refractory T cell to any further stimulus. The identification of T cell activation needing the primary costimulatory pathway of CD28 confirmed T cell activation requires two signals, firstly association of CD3 with antigenic proteins followed by ligation of CD28 (19).

1.4.5 T cell types

The support that T cells provide to immune responses can be separated in to two categories; generation of T helper cells and generation of cytotoxic T cells, T helper function is associated with CD4 T cells and cytotoxic function is associated with CD8 T cells (19).

Helper CD4+ T cell responses generate cytokines and chemokines to support the immune system. These interact with each other to activate neighbouring T helper cells to perform specific functions including the recruitment of immune cells to encounter pathogen at sites of inflammation (19). The main function of cytotoxic CD8+ T cells is specific elimination of host cells infected by a pathogen by cytotoxic methods, but they are also capable of a producing a diverse array of cytokines. This is done by delivering cytotoxic granules into the cytosol of the infected cell, this process is initiated by TCR binding to specific peptide/MHC molecules on the target cell (19).

Naïve T cells express a specific TCR which allows specificity of the T cell population, however until the TCR is engaged and molecular signals downstream of their cytokine receptor is integrated they remain uncommitted to their T helper fate (19). T cells stimulated with antigen have the potential to differentiate into a variety of effector cell subsets depending on the cytokine milieu present and further modified by the nature of pathogen (19). Helper T cell responses can be classified into T helper subsets such as; Th1, Th2, Th17, Th9, Tfh, Tr1 and Tregs (19).

1.4.6 Th1 Response

Differentiation into Th1 cells is regulated by signal transducer and activator of transcription-4 (STAT-4) and T-bet (28), and cytokines including; interleukin 12 (IL-12), interleukin 18 (IL-18), interferon-γ (IFN-γ) and interferon-α (IFN-α) (Figure 1) these all favour the development of Th1 cells but will inhibit development of Th2 response (28). Th1 cells produce interferon-gamma (IFN-γ), interleukin 2 (IL-2) and tumour necrosis factor (TNF) (Figure 1). The

production of these cytokines initiates macrophage activation that are responsible for phagocyte-dependent protective responses (29).

1.4.7 Th2 Response

In contrast, Th2 development is dependent on STAT-6, GATA-3 and c-maf (30), Th2 cells produce interleukin 4 (IL-4), interleukin 5 (IL-5), interleukin 10 (IL-10) and interleukin 13 (IL-13) (Figure 1) that promote B cells to produce IgE and IgA isoforms of antigen-specific antibody which circulate to mucosal surfaces and neutralise future threats of parasitic encounter (19).

1.4.8 Th17 Response

In response to extracellular bacteria and fungi, innate immune cells produce IL-6 and TGFβ, when naïve T cells receive these signals with additional and constant interleukin 21 (IL-21) and interleukin 23 (IL-23) they differentiate into Th17 helper cells under the control of RORγT (19) (Figure 1), this particular T cell subset is characterised by the expression of the cytokine interleukin 17 (IL-17A and IL-17F), interleukin 22 (IL-22), interleukin 21 (IL-21) and interleukin 10 (IL-10) (Figure 1).

1.4.9 Tregs and Tr1 cells

Unchecked or persistent immune responses lead to immunopathology. To control this, the immune system produces a regulatory subset of T cells (Tregs) that provide negative feedback to terminate the inflammatory process (19). Tregs are produced directly from thymic selection (tTregs), from this $FoxP3^{+}$ CD4+ T cells can be differentiated from naïve $FoxP3^{-}$ CD4+ T cells in the periphery and are known as induced Tregs (iTregs) or peripheral Tregs (pTregs) (19, 31).

Tr1 cells were first described in 1997 by Roncarolo et al (32). It was demonstrated that a specific subset of CD4+ Tregs were of a $FoxP3^{-}$ phenotype that were capable of suppressing antigen-specific responses and preventing the development of colitis (32, 33). This CD4+ FoxP3+ subset appeared to exert their immunosuppressive functions through IL-10 (33). Tr1 cells express CD49b and LAG3 along with normal levels of co-stimulatory molecules including CD40L, CD69,CD28, CTLA4 and HLA-DR and increased levels of glucocorticoid induced transcription factor (GITR), CD134 (OX40), Tumour necrosis factor receptor TNFRSF9, CD18 and inducible costimulator (ICOS) (33).

1.4.10 T Follicular helper cell

Follicular helper T cells (Tfh) are found in lymph nodes, specifically the germinal centres. Cognate interaction between Tfh, B cells and IL-21 induces proliferation of B cells to differentiate into plasma cells and induce the production of antibody (34). Tfh cells and IL-21 are involved in immunodeficiencies, infectious and autoimmune diseases, cancer and vaccination (34).

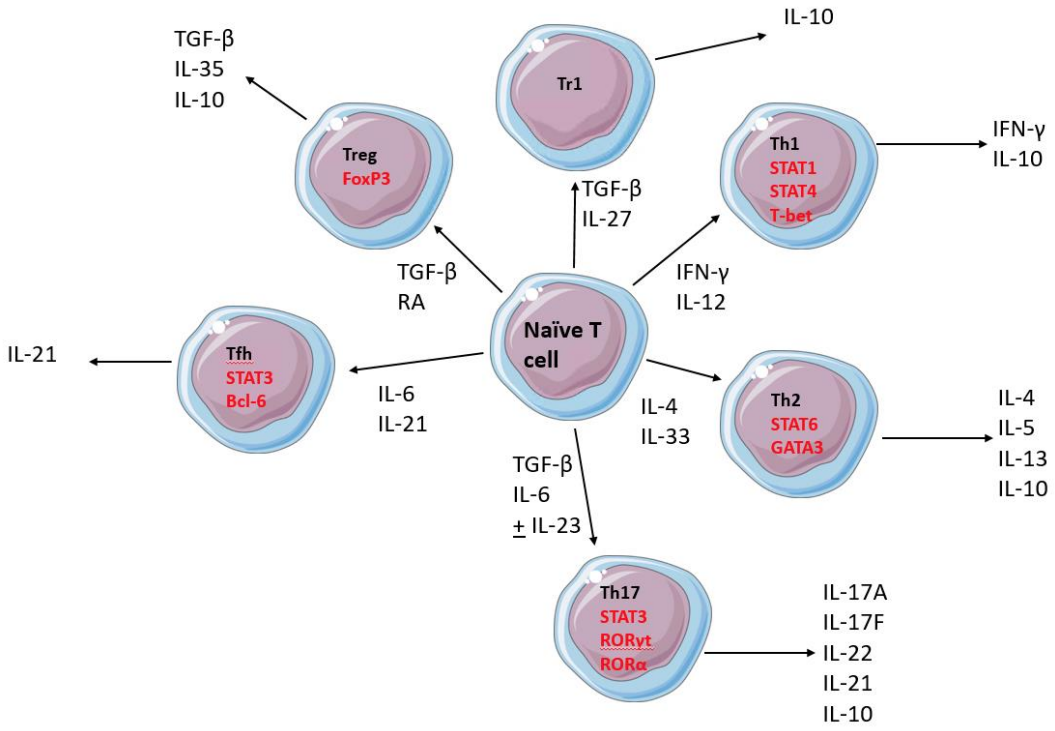

Figure 1.1: T cell subsets in the adaptive immune response. Naïve T cells can differentiate into various CD4+ T cell subsets depending on the cytokine environment and by the signals the cells receive. After differentiation, the cells will produce specific cytokines to mediate the immune response. Figure adapted from Palmer et al. 2010.

1.4.12 T Cell Memory

After the primary response is finished and the infection cleared there is a drastic contraction in the T cell population, leaving a population of T cells known as memory T cells that carry the 'memory' of a specific pathogen that has previously invaded the host and altered functional abilities (19). In comparison to naïve T cells, memory T cells are more easily activated and

have an increased proliferative potential when they come into contact with an antigenic stimulus or costimulatory receptors in order to cause a more rapid response to specific pathogens. They are maintained as a population by a homeostatic proliferation (19). Two main subclasses of memory CD4+ and CD8+ T cells exist: effector-memory (T_{EM}) T cells and central memory (T_{CM}) T cells. T_{CM} cells can be defined by high expression of the adhesion marker CD44 and interleukin 7 (IL-7) receptor (CD127) and high levels of chemokine receptor C-C chemokine receptor type 7 (CCR7), combined with low levels of the adhesion marker CD62L, low levels of the surface marker killer cell lectin-like receptor subfamily G member 1 (KLRG-1) (19).

1.4.12 Antigen-presenting cells

Stimulation of mature T cells requires the presence of a specialised antigen-presenting cell (APC) including macrophages and dendritic cells, however macrophages are unable to initiate a primary immune response which is the principle role of the dendritic cell (35). Dendritic cells express receptors that detect microbial molecules in their environment and then act to promote an adaptive immune response interfacing the innate and adaptive arms of immunity (35). Both macrophages and dendritic cells are strategically placed in T cell dependent areas within lymphoid tissue and express costimulatory molecules at high levels that are required for optimal signalling by T cells (36).

In order to present antigen to T cells, APCs must first degrade native proteins into peptides which are then loaded on to MHC molecules; MHC class I for CD8+ T cells and MHC class II to present to CD4+ T cells (36). Loading of peptide for class I molecules occurs mainly within the endoplasmic reticulum and for class II molecules in the endosomes. When displayed on the cell surface, peptide-bound MHC molecules on APCs are recognised by an antigen-specific αβ T-cell receptor (36). Specialised APCs also express a number of costimulatory molecules including CD28 and CTLA4, high levels of expression of these molecules is mostly restricted to professional APCs such as dendritic cells (36).

1.5 Cytokines and Chemokines

1.5.1 Cytokines

Cytokines are proteins secreted by cells to induce a specific effect on the way cells interact and communicate with each other (37).

The name cytokine can be interchanged with names such as; interleukin (cytokines made by one leukocyte, acting on other leukocytes), lymphokines (cytokines made by lymphocytes), and monokines (cytokines made by monocytes) (37). Cytokines can act in various ways including on cells that produce and secrete them (autocrine action) or neighbouring cell populations (paracrine action) or on faraway cell populations (endocrine action).

It is not unusual for the same cytokine to be secreted by different cell types or several different cell types to be influenced by a single cytokine. They often act in a cascade as one cytokine stimulates its target cell to make additional cytokines that can act synergistically or antagonistically. Cytokines can be produced by many different cell populations, often by helper T cells but also by activated neutrophils, macrophages and non-immune cells such as fibroblasts and endothelial cells during cell injury, infection, invasion and inflammation (37). Major pro-inflammatory cytokines include interleukin 1β (IL-1β), interleukin 6 (IL-6) and tumour necrosis factor-α (TNF-α) and are often associated with inflammasome activation. The pro-inflammatory cytokine response is controlled by a series of immunoregulatory molecules known as anti-inflammatory cytokines.

Specific cytokine inhibitors and soluble cytokine receptors act in harmony with cytokines in order to regulate the immune response. Major anti-inflammatory cytokines include interleukin 1 receptor antagonist, interleukin 4 (IL-4), interleukin 10 (IL-10), interleukin 11 (IL-11) and interleukin 13 (IL-13) (37).

In this thesis the role of IL-27 is interrogated in the mouse model of uveitis. Interleukin 27 (IL-27) is a newly discovered cytokine that belongs to the IL-6/IL-12 cytokine family (38, 39). Similarly, to members of the IL-12 and IL-6 family, IL-27 is a heterodimeric cytokine. It consists of two subunits known as p28 and Epstein-Barr virus-induced gene 3 (EBI3) (39). EBI3 can exist in three forms a homodimer, p35 heterodimer and a p28 heterodimer (39). Secretion of EBI3 is not necessary for the secretion of IL-27p28 and therefore promotion of T cell and NK cell activation can be achieved by the heterodimerisation of IL-27p28 to cytokine-like factor (CLF)

(40). However, there is little evidence of heterodimers being formed between IL-27p28 and IL-12p40 naturally (40).

IL-27 plays a role in the innate and adaptive immune response. In innate immunity, IL-27 has been demonstrated to induce production of IL-1, TNF-α, IL-18 and IL-12 in monocytes and IL-1 and TNF-α in mast cells (39). IL-27 was first described as a proinflammatory cytokine due to its ability to promote IFN-γ production by CD4, CD8 T cells and NKT cells and has been identified as an early initiator of Th1 differentiation but inhibits Th17 responses (39, 41, 42). However, further studies have highlighted the role of IL-27 as a negative regulator of IL-2 and can therefore restrict the development of immune responses (42). Further immunoregulatory functions of IL-27 include the generation of IL-10 producing Tr1 cells and the suppression of the pathogenic Th17 response (43).

1.5.2 Chemokines

A variety of cytokines are known to play a role in chemotaxis (37). Chemokines are small molecules that are related structurally and are capable of regulating cell trafficking of various cell types by interacting with a subset of seven-transmembrane, G protein coupled receptors. In humans roughly 40 chemokines have been identified that mainly act on eosinophils, lymphocytes, monocytes and neutrophils (44). Studies have shown that chemokines play fundamental roles in homeostasis, development, and function of the immune system. They have a wide range of effects on many different cell types beyond the immune system including endothelial cells and various cells of the central nervous system where the effects are angiogenic or angiostatic (44).

Chemokines can be divided into two major subfamilies based on arrangement of the two N-terminal cytosine residues, that is whether the first two cysteine residues have an amino acid between them (CXC) or are adjacent (CC). Further to this two more classes of chemokines have been described; lymphotactin which unlike the typical chemokine structure lacks cysteines one and three so can be described as C or SCYc and fractalkine which is the only chemokine to act through a mucin like stalk to bind to membranes, the structure of fractalkine differs from stereotypical chemokines by the presence of three amino acids between the first two cysteines and can therefore be described as CX3C or SCYd (44).

Regulation of T helper responses by chemokines has been demonstrated. They are known to have several functions and exert chemotactic activity on cell types such as Th1, Th17 and Th2 cells (28). The selective recruitment of Th1 cells to inflamed tissue is usually independent of

Th2 cells, however, some chemokines appear to be able to influence the polarisation of Th1 or Th2 responses by direct interaction with these cells as precursors and/or favouring the production of Th1 or Th2 specific cytokines (28).

Specific chemokines and their ligands play a central role in the recruitment of inflammatory cells, Th1 lymphocytes are attracted to the site of inflammation by CXCL9, CXCL10 and CXCL11 which are all secreted by damaged cells (45). The Th1 lymphocytes that are recruited to the inflamed tissue will enhance production of IFN-γ and TNF-α from the tissue which in turn induces production of Th1 chemokines by different cells, causing an amplification loop (45).

In this thesis the role of the chemokine receptor CX3CR1 in the mouse model of uveitis is investigated. CX3CL1 (fractalkine) is a pro-inflammatory chemokine capable of inducing chemotaxis of circulating monocytes and inducing the selective recruitment of Th1 lymphocytes through interaction with the CX3CL1 receptor CX3CR1 (46). CX3CR1 has been further implicated in the recruitment of monocytes to sites of inflammation. Studies have illustrated a population of CX3CR1 positive monocytes patrolling the endothelium in its steady state but when signs of infection occur, this population are able to rapidly infiltrate the tissue (47).

B-cell antigen encounter takes place within the lymphoid follicles present in the compartments of lymphoid organs that are known to be rich in B cells (48). Chemokines can be considered organising factors of the immune system and co-ordinate microenvironmental architecture of primary and secondary lymphoid organs during physiological and pathological conditions (49).

1.6 Immune tolerance

Immunological tolerance describes a diverse range of host processes that can prevent potentially harmful immune responses from developing within the host tissue (50). Therefore the immune system is not normally activated by self-antigens (51). Tolerance is generated at an ‘upper’ level and a ‘lower’ level; the upper level is known as central tolerance and the lower level of peripheral tolerance, a faulty central tolerance and peripheral tolerance initiates an autoimmune disease (51).

Central tolerance is involved in the differentiation of immature thymocytes in primary lymphoid organs including the bone marrow and thymus. The major mechanisms involved in

central tolerance include clonal deletion and inactivation of clonal lymphocytes (52). Peripheral tolerance deals with mature B and T lymphocytes that have left the primary lymphoid tissues which are found in the secondary lymphoid tissue including lymph nodes and the blood (53). When mature lymphocytes have left the primary lymphoid tissues the antigen that would be of concern would be detected within the tissues instead of the primary lymphoid tissues (52). Positive selection is the process of maturation of immature double positive thymocytes that express T cell receptors with an intermediate affinity or avidity for self-peptide complexes by differentiation into single positive thymocytes (54), It further shapes the T cell repertoire. Negative selection or clonal deletion is the elimination of single or double positive expressing thymocytes within the thymus that express high affinity T cell receptors that are specific for self-antigen (54). Negative selection is efficient for deleting T cell precursors that have high avidity TCRs for self MHC complexes present on DCs. This suggests that peripheral tolerance mechanisms occur after central tolerance and are important for the control of mature T cells that bear a TCR with a lower avidity for self MHC molecules that have escaped central tolerance and are present in the periphery (55). Mechanisms of peripheral tolerance include deletion of cells, inducing anergy or by clonal ignorance (56)

To achieve tolerance there are a number of categories of adaptations that the immune system makes; firstly, newly differentiated T cells and B cells test their receptors for recognition of autoantigens. Strongly reactive T cells are censored by a deletional mechanism, these processes are termed ‘negative selection’ and ‘central tolerance’ (57) (Figure 1.2). A mature lymphocyte will move into the circulation and encounter new antigens, but the lymphocyte will require co-stimulation in addition to an antigen-specific response to make a positive response, without this response the cell will become hyporesponsive or die (57). In addition to this, natural T regulatory cells (nTregs) that have been selected for recognition of self-antigens can dampen early immune response. When a positive response from the lymphocyte against a self-antigen is made Tregs can modify this by inactivating further responses.

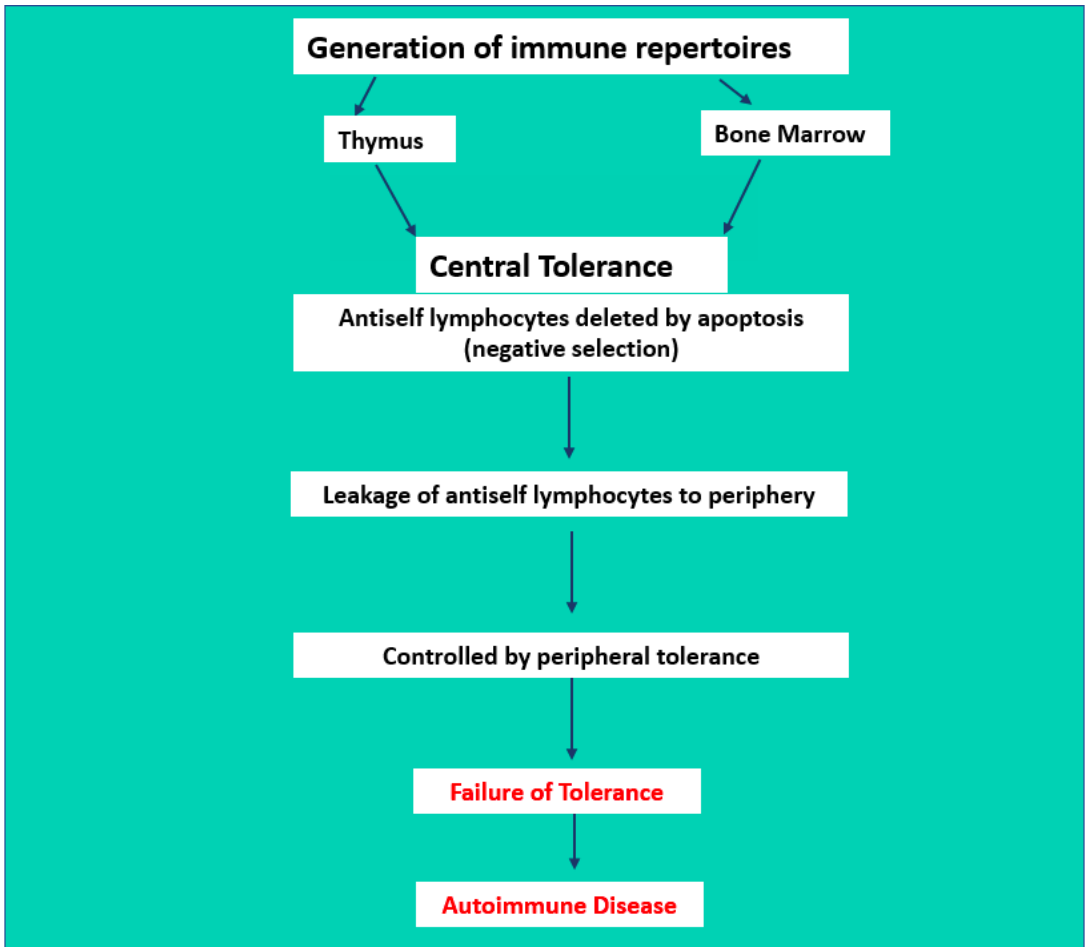

Figure 1.2: Overview of central tolerance. Induction of autoimmune disease due to failure of tolerance. Central tolerance is a censor mechanism to stop autoreactive T cells from entering the periphery to induce autoimmune disease, failure of tolerance combined with environmental and genetic effects leads to autoimmune disease. Figure adapted from Mackay (2000).

To prevent tissue destruction, induction of unresponsiveness or changes to the nature of the effector class involved in the response are made. New cells mediate immunoregulation by using cytokine release and bystander suppression to inhibit effector cell generation of a specific type (57).

The organism is known to be tolerant so long as the immune system does not cause any damage. By this definition of tolerance, an intact immune system does not react in a

destructive manner against the host, in this instance equilibrium is seen as a physiological state (57).

1.7 Autoimmunity

Autoimmune disease is a significant and growing clinical problem, it is chronic in nature leading to high healthcare costs, and is prevalent in the younger population effecting prime working and reproductive years (58).

Autoimmune disease can be defined as organ-specific or non-organ specific, several diseases fit into these two groups, but some diseases fall into the spectrum in between. Autoimmune disorders range from those in which antibodies and T cells react to self-antigens localised within a specific tissue, to systemic conditions which can be characterised by reactivity against a specific antigen or antigens spread throughout several tissues within the body (59). However, classification of autoimmune disease is complex and continues to evolve as our understanding of the underlying mechanisms increases, for example by the understanding of inflammatory conditions.

Current therapies to treat autoimmune disease include cytokine antagonists such as TNF antagonists. Most therapeutic interventions target the terminal phase of inflammation and don't address the problems causing initiation and progression of the disease (58). An immune response to a specific antigen involves the same components as an autoimmune response to an autoantigen, including APCs, B lymphocytes and T lymphocytes; messenger molecules including chemokines and cytokines and their corresponding receptors; and molecules present on the cell surface including signalling and costimulatory molecules (51).

All autoimmune diseases are thought to have three sequential phases of initiation, propagation and resolution (58) (Figure 1.3). Disruption of regulatory mechanisms are associated with each of the phases, the resolution phase occurs when the balance of effector and regulatory mechanisms has occurred this is normally a partial and short term ability (58). Significant parts of the disease process are clinically silent, making diagnosis of early disease difficult (Figure 1.3).

1.7.1 Initiation of autoimmune disease

Most patients will start showing symptoms after abnormal immune interactions have taken place, therefore it is often difficult to accurately depict which factors are responsible for the

initiation of disease in humans (58). Strong evidence shows that autoimmune disease arises from a combination of genetic and environmental factors. Environmental agents can trigger autoimmunity, but only in people with a permissive set of immune response genes go on to develop an autoimmune disease (51).

Environmental factors

Infection is strongly connected as it has the capability to breakdown cellular or vascular barriers to expose antigen to the immune system, induce bystander activation of T lymphocytes and macrophages to provide costimulatory signals and superantigen effects of bacterial products and induce cell death by necrosis instead of apoptosis, all these effects are capable of disrupting peripheral tolerance (51).

There is also the process of molecular (antigenic) mimicry, this involves an antigen of a microorganism that sufficiently resembles a self-molecule that can induce a cross-reactive autoreactive response (51). Other environmental initiators that can break tolerance act like infections to cause tissue damage (51).

Genetic factors

Many genome wide association studies (GWAS) have identified genetic polymorphisms that are associated with autoimmune disease. Most polymorphisms are in non-coding regions of genes, especially enhancers, but many associations are with genes that play a role in the immune response (51). Of all the genes associated with autoimmune disease, the strongest associations are with MHC alleles, however genes that are associated with autoimmune disease are often not specific to a single disease but are instead associated with multiple autoimmune diseases (60).

1.7.2 Propagation of autoimmune disease

Most patients present with clinical disease during the propagation phase characterised by progressive inflammation and tissue damage, as positive feedback amplifies the disease (58). Firstly the self-antigen that initiates autoimmunity often cannot be eliminated by the host, and the problem is intensified by the emergence of new autoantigenic epitopes as tissue damage and alterations in self-proteins occur, in a process that is known as epitope spreading (58) (Figure 1.3).

When newly generated antigenic epitopes activate different specificities of lymphocyte a recruitment of leukocytes to the site of inflammation occurs, this creates more damage to the tissue and gives rise to even more novel epitopes to be targeted by autoreactive lymphocytes

thus epitope spreading creates a vicious cycle that influences inflammation within the tissue (58). An inflammatory environment is created by the production of cytokines and cellular mediators by numerous immune cell types within an autoimmune reaction, these serve to amplify the reaction. However the driving force behind the autoimmune reaction could be due to the increase in the number of effector cells in comparison to the number of regulatory cells present (58). After the induction of a pathological immune reaction, there is increasing accumulation of effector T cells to the inflamed tissue that are driving the immune reaction, this is accompanied by a decrease in the number of Tregs or increased number of dysfunctional Tregs (58).

1.7.3 Resolution of autoimmunity

It is likely that the control of immune reactions involves the induction and activation of regulatory mechanisms that dampen the effector response to restore the effector cell/regulatory cell balance (58) (figure 1.3).

Autoimmune disorders are a result of the breakdown of immunological tolerance which leads to an immune response against the host's self-molecules (59).

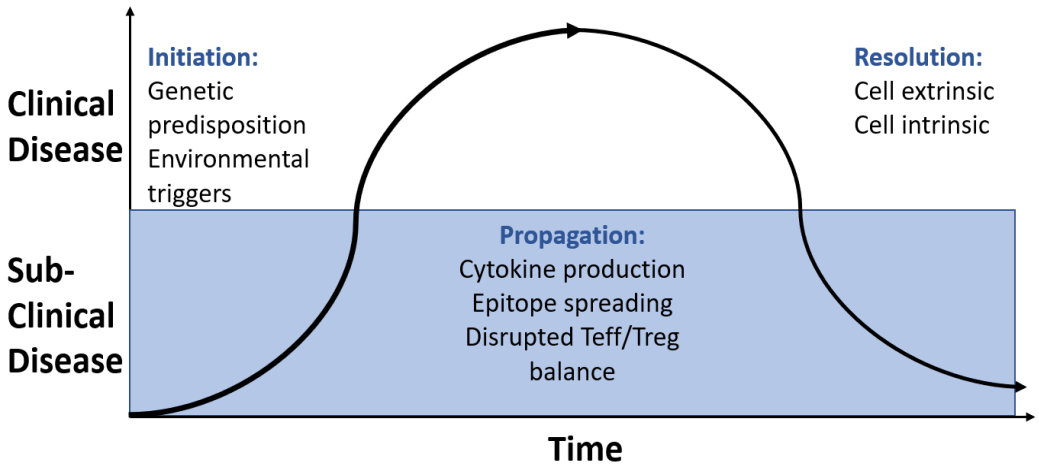

Figure 1.3: The sequential phases of autoimmune disease. Initiation includes the genetic predisposition of the individual combined with environmental triggers imitates clinical symptoms within patients. Propagation involves the immune response amplifying within the individual such as cytokine production and epitope spreading. These steps are then followed by regulatory mechanisms dampening the effector response to initiate resolution of the autoimmune disease. Figure adapted from Rosenblum et al (2015).

1.7.4 The role of CD4+ T cells in autoimmunity

In organ-specific autoimmunity, CD4+ T cells are essential to the autoimmune response. Pathogenic antigen-activated CD4+ T cells can adopt several different phenotypes depending on external cues and the transcription factors that they induce (61).

Th1 cells are predominantly involved in inducing macrophage activation to clear intracellular pathogens and inducing immunoglobulin class switching to complement-fixing antibodies through production of large quantities of IFN-γ (62). They are involved in cell-mediated and delayed-type hypersensitivity responses but have been implicated in the development of organ-specific autoimmune disease and more specifically in organ-specific T cell driven autoimmune diseases whereas Th2 cells reportedly exerted inhibitory effects (62).

However, the hypothesis that Th1 cells exclusively drive autoimmune tissue damage was challenged when blocking IFN-γ signalling did not protect mice from the induction of autoimmune disease and in fact caused a more severe disease phenotype (62).

The Th17 subset of T helper cells were discovered after the IL-17 family of cytokines was discovered. This was further supported by the finding of mediation of expansion of IL-17 producing cells by IL-23. Th17 cells require specific transcription factors and cytokine mediation to differentiate (63). Studies have shown that Th17 cells are generated from CD4+ T cells by stimulation from cytokines such as interleukin-6 (IL-6), transforming growth factor-β (TGF-β), interleukin-21 (IL-21) and interleukin-23 (IL-23) which all play an integral role in the induction of the autoimmune disease process (63).

Increased IL-17 was found in human autoimmune diseases such as multiple sclerosis and rheumatoid arthritis and in the corresponding mouse models of disease, which has caused much research to be focused on defining what role Th17 cells plays in the pathogenic process of tissue inflammation (62). The importance of Th17 cells in the pathogenesis of organ-specific autoimmunity has been demonstrated in several animal studies showing Th17 cells and Th1 cells are capable of inducing disease. These studies illustrate a role for both Th1 and Th17 cells in autoimmune disease.

1.8 Immune maintenance of the eye

The anatomy of the eye can be described as a fibrovascular sphere that contains an aqueous humor, lens, vitreous body and is lined with a retina (64). The cells of the retina are highly

diverse containing various neuronal cell types. It is considered to be a vital component for the production of nerve activation from light (64, 65). The retina is protected by a blood-retina barrier (BRB) and similarly to the brain and spinal cord is part of the central nervous system. It is made up of an intricate network of specialised cells that can be described as interconnected and heterozygous neuronal in nature such as bipolar cells, photoreceptors and ganglion cells (66). These cells present within the retina play an important role in creating neural impulses that are relayed to the brain by converting light from the outside environment that are then perceived as visual information by the individual. (66). To ensure regular neural conduction the neural retina is given support from glial cells including astrocytes and Müller cells (66).

Specialised members of the immune cell family of macrophages that reside within the retina are known as microglia, they are yolk sac derived and are found throughout the neural retina. The neural retina is a hemispherical sheet that curves towards the centre of the eye made up of neural tissue, it sits next to retinal pigment epithelium (RPE) and the retina. Tight junctions are important between vascular endothelial cells at retinal vessels and within the BRB between the RPE (66).

The layer that separates the choroid from the neural retina is known as the RPE, it is a monolayer of pigmented cells and is of neuroectoderm origin so is included as part of the retina (67).

The mammalian retina is made up of ~60 different cell types which all play a role in the processing of visual images (68), it is highly specialised with specific metabolic and physiological needs, to meet the demands of the extracellular environment and facilitate rapid neural conduction. The outer retina receives nourishment from the vascular choroid which receives its blood supply from the inner retina. The retinal blood supply is able to regulate the environment by excluding leukocytes (including, lymphocytes, granulocytes and myeloid derived cells) erythrocytes and large molecular weight proteins and therefore acts as a highly specialised blood barrier (66).

The normal retina is considered an immune privileged tissue due to the exclusion of immune cells, a property of a tissue to display highly attenuated responses to alloantigens (66).

1.8.1 Immune privilege

The term used to describe the relationship the eye has with the immune system is immune privilege, a term coined by Sir Peter Medawar in the 1940's who observed that foreign tissue

grafts placed in the anterior chamber of the eye were not rejected (69, 70). The concept of immune privilege may appear simple but research into this area has illustrated that multiple mechanisms are required to maintain the state of immune privilege within the ocular tissue (69). These mechanisms include; stopping the free movement of larger molecules into and out of the eye by the presence of the BRB and the absence of efferent lymphatics, the presence of cell-bound and soluble factors of an immunosuppressive nature to create an inhibitory ocular environment to stop the activity of immune-competent cells and the eye actively regulates systemic immune responses (69).

An unregulated innate immune response has potential to inflict significant damage to the eye, granulocytes and macrophages elaborate a variety of proteases and reactive oxygen species that can damage bystander cells (71).

The adaptive immune response is characterised by antigen specificity and memory, antibodies produced by B cells and T cells are both capable of inducing inflammation and injury to the eye (71). Membrane bound molecules that inhibit T cell proliferation or induce apoptosis of infiltrating immune cells are secreted by cells of the BRB that line the interior of the eye. In response to viral infections FasL is expressed throughout the ocular tissue to remove activated T cells and neutrophils (71, 72).

Sites considered to be of immune privilege such as the eye use membrane-bound and soluble molecules to reduce immune-mediated inflammation within the tissue, they also promote the dampening of the adaptive immune response by generating immunoregulatory processes (71). In the late 1970s studies performed by Streilein and colleagues introduced the paradigm of anterior chamber-associated immune deviation (ACAID) and described the concept of deflecting the adaptive immune response from effector type mechanisms that could impose severe injury to the tissue to sustain immune privilege (71). This was achieved by the injection of allogenic lymphoid cells into the anterior chamber of rat eyes and noted that alloantigens introduced into the eye were detected by the systemic immune apparatus and elicited an aberrant immune response characterised down regulation of cell-mediated alloimmunity by an antigen specific response and a concomitant activation of humoral antibody responses (73-75). Since the original experiments by Streilein and Kaplan, ACAID has further been demonstrated with a number of antigens including viruses, haptenated cells, tumour antigens, histocompatibility antigens and soluble proteins (75).

Multiple mechanisms contribute to ocular immune privilege including the inhibition of T cell proliferation by factors such as TGF-β2, VIP, Mueller cells and retinal epithelial cells, inhibition of Delayed-Type Hypersensitivity by ACAID, TGF-β, CGRP and α-MSH, deletion of infiltrating inflammatory cells by FasL, inhibition of NK cells by MIF, TGF-β2 and inhibition of complement by membrane bound regulatory proteins and soluble complement regulatory proteins (75).

Since these findings, the definition of ocular immune privilege has become broader to encompass induction of ACAID after antigenic induction and the capacity of the ocular tissue microenvironment to suppress immune effector responses and ocular inflammation (76).

1.8.2 Immune Surveillance

No organ is exempt from autoimmune disease, although immune privilege influences the nature and tempo of immune surveillance in the tissue (77). The main role of immune surveillance is to determine if the immune effector response is needed in order to address an invading pathogen, a cancerous cell or tissue injury (78).

Studies of human CSF obtained from healthy individuals allow further understanding of normal immunosurveilance of immune privileged tissue; mainly CD4+ T cells of the effector memory phenotype were detected (77, 79). Although anatomical and functional barriers protect the tissues of the brain and eye from the circulation in health, profound changes occur locally within the tissue when an immune response is triggered; the modification of the processes of immunosurveilance when local inflammation becomes established is still yet to be determined (77).

1.8.3 Immune mechanisms within the eye

The immune response appears to be customised to the organ in which it is initiated as well as being specialised for the region where it functions (80). There are also differences in responses based on route of antigen administration for example injection into the eye is used to induce tolerance but subcutaneous injection can be used to produce inflammation (80). The eye is filled with immunosuppressive factors such as neuropeptides, somatostatin, cytokines and complement inhibitors. There is also low expression of MHC class II molecules to limit antigen-presentation within the eye, furthermore stromal cells from the iris, ciliary body and retina within the eye have the capacity to convert immune T cells into regulatory T cells (Tregs) and RPE cells that line the borders of the eye can directly inhibit primed T cells. Lastly, death inducing molecules such as FasL are expressed by stromal cells within the eye to induce apoptosis of immune cells that pass the ocular boundary (80).

1.8.4 Endothelium within the eye

The cells that supply and drain the neural retina are the retinal endothelial cells, these cells line the microvasculature, anatomically and physiologically. The characteristics of these cells suit the nutritional requirements and protection of the tissues critical for vision (81). The endothelium allows the access of circulating cells and must ensure the oxygen supply to the metabolically active retina. This is necessary to maintain the vasculature and survey the retina for the presence of pathogens (81). The endothelium is considered a part of the blood-retina barrier that is involved in protection of the retina by excluding circulating molecular toxins, microorganism and pro-inflammatory leukocytes, thus the retinal endothelial cells are an important component in retinal ischemic vasculopathies and retinal inflammation such as posterior uveitis (81).

1.8.5 The endothelium during inflammation

When a tissue is injured or an infection occurs, endothelial cells are responsible for coordinating the recruitment of inflammatory cells. Endothelial cells produce communication signals, including cytokines and growth factors as well as a range of adhesion molecules and integrins to facilitate recruitment of inflammatory cells (82). Under stimulation with agents such as IL-1b and TNFα, the phenotype, morphology, and function of endothelial cells changes, to allow involvement in the immune response, this is known as endothelial activation.

The term was coined in the 1960's by investigators who observed that the endothelium became plump and leaky in DTH, with the term activated illustrating a change in function and morphology. The main changes of endothelial cell activation are loss of vascular integrity, expression of leukocyte adhesion molecules and cytokine production (83). Loss of vascular integrity can expose sub endothelium and permit the efflux of fluids from the intravascular space, upregulation of leukocyte adhesion molecules, including E-selectin, ICAM-1, and VCAM-1 allows leukocytes to adhere to the endothelium and move into the target tissues (83, 84).

Tethering and Rolling- Firstly, leukocytes adhere to the endothelium that lines the blood vessel walls in order to pass through to reach the inflamed tissue, the vascular leakage follows haemoconcentration in the early stages of the inflammatory response will slow the blood flow enough so leukocytes have the ability to make contact with the endothelium (85). The initial contact of leukocytes to the endothelium serve to tether, these interactions are mediated by

the selectin family which are found on both leukocytes and endothelial cells (82, 85). For cells to tether, interactions between adhesion molecules must form rapidly, in contrast, for cells to roll these interactions must break rapidly (86). Rolling adhesion is an important checkpoint for cells to encounter tissue-specific signals before entering a specific organ (86).

Arrest and Adhesion- In vivo, leukocytes will tether and roll along the endothelium. Both these processes are reversible and many of these leukocytes will not remain tethered to the vessel surface, they will instead re-enter the bloodstream all while still rolling throughout the entire process (86). Rolling of leukocytes can be stopped by high affinity adhesion of leukocytes to the surface of endothelial cells, which replaces the low affinity transient interactions that are made due to leukocyte rolling (85, 86). Chemokines and integrins can promote leukocytes to form a high affinity adhesion bond with the endothelium. ICAM-1 and -2 and VCAM-1 are receptors expressed on the endothelial cells that activated leukocytes can bind to using integrins, when no inflammation is present within the tissue these receptors are expressed at low levels particularly in the vascular beds, however inflammatory cytokines increase their expression drastically (85).

Migration on the Endothelial Surface- For a leukocyte to migrate into the tissue it must first adhere to the endothelium, the leukocyte may roll over several endothelial cells before arresting and forming a high affinity adhesion bond. To enter the tissue the leukocyte must then cross the border of the endothelial cell which it has adhered to (85).

1.9 Intraocular inflammation

Although inflammation of the eye is unusual, immune privilege within the eye can be overcome and allow the infiltration of proinflammatory immune cells including; T cells, B cells, macrophages/monocytes, natural killer cells, neutrophils and dendritic cells that invade the retina, choroid and vitreous along with anterior chambers of the eye (87).

1.9.1 Classification of Uveitis

Uveitis is a group of sight-threatening, intraocular inflammatory diseases (88). The term uveitis means inflammation of the uvea, in particular the choroid, ciliary body and iris but surrounding structures including the optic nerve, retina, and sclera are also effected (89). Uveitis encompasses a diverse group of ocular disorders classified as; anterior, intermediate, posterior or panuveitis based on the anatomical location within the eye (90). Classifying

uveitis into specific subgroups helps a clinical scientist to take a logical approach to diagnosis of the patient and management of disease (89). Anterior uveitis is the inflammation of the anterior chamber and is the most common form of uveitis, intermediate uveitis can be defined as the presence of inflammatory cells in the vitreous humor including; pars planitis, posterior cyclitis and hyalitis (90). Retinal and choroidal inflammation (choroiditis, chorioretinitis and hyalitis) is known as posterior uveitis, whereas panuveitis involves inflammation of all parts of the uvea i.e. retina, choroid, vitreous humor and the anterior chamber, (90). Uveitis can be classified based on anatomical involvement of the uveal tract but can also be classified by the etiology of inflammation (90).

The main causes of uveitis are infection, systemic immune-mediated disease, tissue-specific autoimmune disease and autoinflammatory disease, other causes include; post-traumatic, post-surgical and drug-induced uveitis (90).

1.9.2 Etiology of Uveitis

Infectious causes of uveitis can normally be treated with antimicrobials, with the remaining cases being of autoimmune origin or immune-mediated despite having different presentations within patients (91). Infectious agents, specifically viruses, have been proposed as one of the environmental triggers of autoimmune disease including uveitis through mechanisms that have not yet been fully characterised (91). There are instances when molecular mimicry can account for the development of autoimmune disease within the eye however potential bystander activation is thought to be limited due to the immunosuppressive nature of the eye but this kind of activation should not be ruled out (91).

1.9.3 Epidemiology of Uveitis

Uveitis accounts for 5-20% of legal blindness in both the United States and Europe and up to 25% of cases in the developing world (89, 92). The incidence of uveitis has been estimated to be between 17 to 52 cases per 100,000 per year with a prevalence of 38-714 cases per 100,000 population (93). Uveitis mostly has an equal gender distribution but in some studies a slight female predominance can be observed (93).

Uveitis can occur at any age, but the mean age incidence is between 30-40 years of age with 60-80% of uveitis cases occurring between the ages of 20-50 years (93). The prevalence of anterior uveitis is reported to be 24.5-52.3%, panuveitis 11.8-52.9%, posterior uveitis 7.1-46% and intermediate uveitis 6.3-19.3% observed in several studies (93-96).

1.9.4 Clinical features of Uveitis

Uveitis is a term that is used to describe a number of etiologies and disease phenotypes, in order to effectively manage the disease, correct anatomical location, assessment of disease activity, etiological diagnosis, identification of any potential complications and presence of any systemic disease associations are very important to identify (89, 97). Symptoms of acute forms of uveitis include ocular pain, photophobia, lacrimation and redness (98).

Uveitis is a disease that varies in phenotype and visual prognosis, inflammation can range from mild to severe (89). When a patient starts displaying symptoms, complications that could affect or threaten their sight may have already occurred. The severity of the symptoms displayed by the patient often effect the decision making in relation to determining the correct treatment as not all uveitic diseases require treatment. If the anterior chamber is involved in the disease process patients can be very symptomatic including vitritis with several floaters and macular edema. Patients who present with mild or intermediate uveitis may not require treatment as the risks associated with treatment outweigh the visual benefit for the patient (89).

Treatments are not curative, but suppress inflammation and need to be administered until the disease is observed to be in remission (89).

CLASSIFICATION OF UVEITIS		
INFECTIOUS CAUSES		
	Toxoplasmosis	
	Toxocariasis	
	Tuberculosis (TB)	
	Syphilis	
	Bartonella	
	Viral	(Including Herpes Simplex and Cytomegalovirus)
	Human immunodeficiency virus (HIV) related eye disease	
NON-INFECTIOUS CAUSES	Acute posterior multifocal placoid pigment epitheliopathy	(APMPPE)
	Multiple evanescent white dot syndrome	(MEWDS)
	Geographic helicoid peripapillary choroidopathy	(GHPC)
	Multifocal choroiditis	(MFC)
	Punctate inner choroidopathy	(PIC)
	Birdshot choroidopathy	
	Presumed ocular histoplasmosis syndrome	(POHS)
	Subretinal fibrosis and uveitis syndrome	(SFU)
	Diffuse unilateral and subacute neuroretinitis	(DUSN)
	Retinla pigment epithelitis (Krill's disease)	
	Sarcoidosis	
CLINICAL CHARACTERISTICS	Choroiditis	
	Retinochoroiditis/chorioretinitis	
	Retinitis	
	Neuroretinitis	
	Granuloma	

Table 1.1: Classification of Human Uveitis. Posterior uveitic disease can be classified based on both etiology and clinical characteristics. If the disease is caused by an infectious or non-infectious agent (Etiology) or the clinical characteristics of a lesion present within the eye. Table adapted from Sudharsham et al (2010).

1.9.5 Current treatments for Uveitis

Treating the systemic disease in patients that is associated with the presence of uveitis can sometimes control the uveitis, first line systemic treatments are usually based on corticosteroids and some patients being treated with steroids alone for posterior uveitis can control their symptoms (89, 99, 100).

Conventional second-line immunosuppressive agents have been used for several years, cytotoxic drugs such as chlorambucil (101) and cyclophosphamide (102) have been reported to be useful in treatment of uveitis, but the side effects associated with this course of treatment creates difficulties for patients when managing uveitis long-term, especially in cases of chronic uveitis in a young, healthy population (89).

These drugs although effective can take many weeks to months in order to be properly effective and can have severe side effects that can become intolerable so will therefore switch to a second-line immunosuppressant (89).

Efficacy of biological agents such as anti-tumour necrosis factor (anti-TNF) based drugs including; adalimumab, etanercept and infliximab, etanercept and have been reported in several studies (89). Most biologics are recombinant antibodies to or antagonists of specific cytokines or cell-surface receptors but they also include recombinant cytokines, they were first used to treat ocular inflammation in the early 1990's (103). Biologics are an attractive therapy to control the disease process by targeting individual molecules within the inflammatory process (103).

TNF is a key inflammatory cytokine that is involved in the pathogenesis of several inflammatory disorders which includes non-infectious uveitis; in the EAU model studies have shown a substantial role in the pathogenesis of non-infectious posterior uveitis and similarly in ocular fluids from patients with uveitis (103). There are a number of anti-TNF agents available including; etanercept, infliximab and adalimumab, both adalimumab and infliximab are capable of binding with soluble and transmembrane forms of TNF effectively, but in contrast etanercept is less capable of forming stable bonds with TNF, specifically the transmembrane form (103).

The experimental model of posterior uveitis (EAU) has implicated IL-1 and IL-2 in the pathophysiology, thus antiinterleukin therapies are also used for patient treatment (103, 104). Therefore, a recombinant version of human IL-1 receptor antagonist (IL-1RA) (a

naturally occurring inhibitor of IL-1) was developed into a biologic agent to be used as treatment (103).

Interferon-α (IFN-α) is a naturally occurring cytokine that is secreted by plasmacytoid dendritic cells during viral infections; IFN-α is proposed as the primary pathogenic cytokine in 'systemic' autoimmune disease, whereas TNF-α in organ-specific autoimmune disease is seen as a more pathogenic cytokine. The separation between TNF-α and IFN-α is not absolute due to cross reactivity to regulate each other, if either become unbalanced there is the potential for an autoimmune reaction (103). In vitro studies have illustrated reduced IFN-α expression in plasmacytoid dendritic cells in comparison to healthy controls, in addition to this, TNF-α reduces IFN-α levels by inhibiting the number of plasmacytoid dendritic cells along with the function (103). Recombinant human IFNα-2a and IFNα-2b have both been successful in treatment of posterior uveitis (103).

1.9.6 Breakdown of blood ocular barrier

Ocular disease is usually treated with a topical administration of drugs in the form of a solution but due to the many anatomical and physiological barriers present within the eye these treatments have limited ocular bioavailability (105). Due to the presence of the BRB other routes of drug administration such as intravenous, oral or subcutaneous are not often utilised because satisfactory drug concentration cannot enter the intraocular tissue (105-107). The blood-retinal barrier (BRB) and blood-aqueous barrier comprise the blood ocular barrier which ensures homeostatic control of the tissue by protecting from entry of toxic substances.

The blood-aqueous barrier is made up of endothelial and epithelial cells including; the endothelium of Schlemm's canal, the endothelium of the iris vessels with tight junctions of the leaky type, the posterior iris epithelium and the non-pigmented epithelium of the ciliary body (105). Similarly, the BRB is also made up of endothelial and epithelial cells that form an ocular barrier which is the retinal pigment epithelium and an inner barrier which is the endothelial membrane of the retinal vessels, both have nonleaky tight junctions (105).

Both functional barriers act to restrict movement of blood elements to the intraocular chambers which is what causes the drugs administered orally, subcutaneously and intravenously to only reach the tissue in low levels (105). In uveitis, immune mechanisms affect the integrity of the BRB and permit leukocyte infiltration into the eye. For this to occur,

changes are needed in both the leukocytes themselves and the cell that form the barrier (108).

1.10 Disease models of uveitis

1.10.1 Understanding disease processes

Uveitis is a heterogeneous disease with both polygenic and environmental influences (109). Most forms of immune-mediated uveitis are due to an imbalance in the regulatory mechanisms that inhibit the immune response and inflammatory mechanisms which can result in chronic disease if activated outside an infection (109). Further understanding of the pathogenesis of the disease will influence therapies and treatments (110). Human samples for study to explore the pathology of this complex human disease are largely unavailable, so instead experimental autoimmune uveitis (EAU) has been (87) established in vivo that shares many pathological features with human uveitis (88).

1.10.2 Experimental Autoimmune Uveitis

Experimental autoimmune uveitis (EAU) is a T-cell mediated, organ specific autoimmune disease model that targets the neural retina and related tissues, it is often induced by immunisation with ocular antigens or by the adoptive transfer of uveitogenic T cells (111-113). The model can be used to investigate a range of human uveitic diseases of an autoimmune or auto inflammatory etiology as it appears to share numerous immunological mechanisms with human uveitis. It can resemble the presentation of these diseases both clinically and histopathologically in a number of aspects (112) (114, 115).

The EAU model in particular is very useful for the study of posterior uveitis as many of the clinical signs in humans such as vasculitis and vitritis are found in the EAU model (116). The model has become an invaluable tool for aiding in the development of conventional therapeutic strategies and novel immunotherapies. The model is also useful for the study of basic mechanisms of organ-specific antigens in immunologically privileged tissue (such as the eye or the CNS) including tolerance and autoimmunity; thus the EAU model is a very useful model for both basic and clinical research into ocular and organ-specific autoimmune disease (117).

1.10.3 Experimental Autoimmune Uveitis (EAU) Induction

Peptides for Induction

EAU can be induced in susceptible animals by immunisation with uveitogenic peptides in adjuvant or by adoptive transfer of antigen specific lymphocytes (117-119). The uveitogenic proteins most commonly used are retinal soluble antigen (S-Ag), retinal binding protein-3 (RBP3, also known as Interphotoreceptor retinoid-binding protein (IRBP)), Rhodopsin, Recoverin and Phosducin (117).

Retinal soluble antigen is a 48 kDa intracellular photoreceptor protein found in rod outer segments and is involved in the photo-transduction cascade by binding to the photo-activated phosphorylated rhodopsin thereby preventing the transducin-mediated activation of phosphodi-esterase and is often used in rat models of EAU (120, 121).

Interphotoreceptor retinoid-binding protein (RBP3) is a large glycoliprotein that can be found in the inter-photoreceptor matrix (IPM) between the neural retina and retinal pigment epithelium, it is capable of binding retinoids and fatty acids with retinol bound in a light-dependent manner (121, 122). Based on these characteristics, transport between retinal photoreceptors and pigment epithelial cells, the protein can induce EAU in rats, monkeys, mice and may be involved in the induction of human uveitic conditions (123, 124).

Rhodopsin and opsin, this 40-kDa membrane protein is found in rods present in the retina, pathogenicity of the protein seems to be conformation dependent as rhodopsin is more pathogenic than opsin (121, 125).

Recoverin is a 23-kDa calcium-binding protein, it controls phosphorylation of the visual receptor rhodopsin by inhibition of rhodopsin kinase in photoreceptor cells (121, 126).

Phosducin is a 33-kDa soluble cytosolic photoreceptor protein and regulates the G-protein mediated signalling in the retina. From all the peptides mentioned above the most commonly used for EAU induction are S-Ag and RBP3 (121, 127).

Induction in animals

EAU can be induced by active immunisation or by adoptive transfer of uveitogenic leukocytes in several species of animal including mice and rats, guinea pigs, rabbits, monkeys, and horses, unfortunately no animal model fully represents the spectrum of human disease, but each model allows the study of a unique characteristic from human disease course. The rat, in particular is a useful model due to the detailed characterisation of the model both immune genetically and immunologically as well as being average in size (117). The most susceptible

strain in the mouse model is the B10.R111 followed by B10.A. However, the C57BL/6 mouse strain is a very useful model for studies into the basic mechanism of uveitis (121), and a strain where many genes have been targeted.

Inbred mouse strains have identical MHC complexes, and only a few mouse strains are susceptible to EAU, early studies have illustrated that for a mouse strain to be susceptible to EAU induction it has to have both a susceptible haplotype and a permissive background (121, 128). The haplotypes that have been identified range from highly to moderately susceptible; H-2r being the most susceptible such as a B10.R111 mouse, then H-2k from a B10.BR mouse followed by H-2b from a C57BL/6 background that is moderately susceptible to disease induction (121). If the uveitic response in mice involves T lymphocytes expressing specific V-gene elements, clonal deletion of such populations might result in resistance to disease in the corresponding background or MHC combinations (128). For all the EAU-susceptible haplotypes the most 'permissive' background was the B10 mouse which is not known to delete any TCR Vβ elements, however in some genetic backgrounds, factors controlling cytokine and hormonal responses could also be an important element in susceptibility (128).

Methods for Induction of EAU

The classic EAU model in mice was reported in 1988 and further modified for efficacy of induction, the protein used was RBP3 as S-Ag is poorly uveitogenic in mice (121, 129). RBP3 is emulsified in complete Freund's adjuvant (CFA) that consists of a suspension of tuberculosis bacteria in a mineral oil (121). CFA plays an integral part in disease induction in both mice and rats, many strains also require an additional inflammatory stimulus in the form of pertussis toxin (121, 129). Less susceptible strains to EAU induction can be rendered non-resistant by treatment with pertussis toxin (PTX) at the time of immunisation (117). This is thought to enhance vascular permeability disrupting the blood retina barrier to allow leukocytes to accumulate in the target organ (130). Subcutaneous injection of the (RBP3) peptide emulsified in CFA with a concurrent intraperitoneal injection of pertussis toxin induces uveitis in susceptible mouse strains within 2-3 weeks. The role of the adjuvant is to trigger a Th1 like response (121). Both Th1 and Th17 cells can initiate EAU, strains that are naturally high Th1 and Th17 responders tend to be susceptible to immunisation with uveitogenic peptides such as the C57BL/6 and B10.RIII mouse strains (117, 131).

An alternate method of EAU induction is known as adoptive transfer, this technique induces disease by inoculating animals with lymphocytes specific for retinal antigen, these cells are

taken from genetically compatible donors who had been immunised for EAU and are cultured in vitro with the same antigen (121, 132).

One of the advantages of using the adoptive transfer technique is that the recipients do not require adjuvant to induce disease and the disease resembles the clinical situation in a patient. It more effectively portrays a uveitic disease that arises because of circulating lymphocytes that have been exposed to retinal Ags (121). Specifically, knowing which cells within the recipient mice have been previously exposed to antigen and how the recipient's endogenous immune system interacts with these cells, with the added bonus of no adjuvant means controlled priming of the endogenous immune response apart from the presence of the antigen specific cells.

1.10.4 Other models of human uveitis

Humanised model of experimental autoimmune uveitis in human leukocyte antigen class II transgenic mice

This model uses mice that lack the murine MHC class II molecule I-A and are made transgenic (Tg) for the human leukocyte antigen HLA class II molecules HLA DR3, HLA DR4, HLA DQ6 or HLA DQ8, of these strains the HLA-DR3 mice develop the most severe disease when immunised with S-Ag (121, 133). Normally, several HLA class II molecules are expressed together, and it has been observed that transgenic mice expressing two HLA alleles are more susceptible than a single transgenic model; this is an indicator that different HLA molecules can influence each other for the development of the disease process (121, 133). Humanised EAU models show promise in helping identify the antigenic molecules that are responsible for human uveitis (121, 133).

Experimental melanin induced uveitis

To induce a disease that affects the uvea, melanin antigenic extracts are used. The disease presents as recurrent anterior uveitis (RAU) with choroiditis (121). Experimental autoimmune anterior uveitis (EAAU) and experimental melanin induced uveitis are induced by injecting crude fractions of bovine ciliary body, iris and RPE; EAAU is a well-established model of anterior uveitis that resembles the human disease both clinically and pathologically (121, 134, 135).

Endotoxin induced uveitis

Endotoxin-induced uveitis is a useful model of anterior uveitis, it is not an autoimmune based model but is triggered by the intravitreal, subcutaneous, or intraperitoneal injection of

bacterial endotoxin lipopolysaccharides (LPS) (121, 136). Breakdown of the blood-aqueous barrier occurs within 2 hours after LPS injection. By histology, leukocyte infiltration is observed in the iris and ciliary body from 8-12 hours after injection with cell numbers reaching their maximum by ~24 hours (136). Most cells are polymorphonuclear leukocytes but in addition to this a significant increase in the mononuclear cell component of the infiltrate (136). Leukocytes can also appear in the anterior chamber with eosinophilic material, very low levels of neutrophilic infiltrate is sometimes present within the conjunctiva (136). Although EIU is considered to be an inflammation predominantly of the anterior uvea, posterior segment inflammation such as choroiditis, vitritis, vitreous haemorrhage, retinal vasculitis, retinal haemorrhage and inflammatory cell infiltration of the retina with focal destruction of photoreceptor cells (136, 137) is also seen.

An alternate model of EAU induced with inter-photoreceptor retinoid-binding peptide presented by dendritic cells

Dendritic cells are the main antigen presenting cells that have the capabilities of stimulating naive T-cells. A model of EAU induced by the infusion of antigen loaded DCs has been developed by harvesting the spleens of mice injected with Flt3L DNA and which are later matured in vitro with LPS and anti CD40 antibody the cells are then pulsed with RBP3 peptide 161-180, this model differs from the classical EAU model immunologically, clinically and pathologically (121).

Spontaneous uveitis models

Human transgenic mice including the HLA-A29 Tg mouse developed by Szpak et al (138) spontaneously develop posterior uveitis that resembles birdshot choroidoretinopathy (121). Another model of spontaneous ocular inflammation is the R161H mouse that express a Tg T-cell receptor specific for RBP3 residues 161-180 that spontaneously develop ocular inflammation by 6 weeks of age (121, 139).

Autoimmune regulator (AIRE) knockout mice spontaneously develop ocular inflammation (140). AIRE-deficient mice fail to express many tissue antigens in the thymus, among them are RBP3, S-Ag and other retinal antigens, therefore over time AIRE deficient mice develop spontaneous antibodies to RBP3 and therefore uveitis (53, 128).

1.11 Immune mechanisms of EAU

1.11.1 EAU Disease mechanisms

Clinically, EAU is characterised by photoreceptor loss and the infiltration of lymphocytes and monocytes into the retinal tissue (141). The inflammatory process that occurs after disease induction involves the massive infiltration of lymphocytes along with mononuclear and polymorphonuclear cells and therefore causes a loss in vision (110). As seen in figure 1.4, it is useful to split EAU disease progression into 3 phases, a prodromal phase followed by a primary peak phase then a phase of secondary regulation (1). Histology in early disease has shown extensive large numbers of cellular infiltrate including T cells, macrophages, and neutrophils, within the choroid, anterior uvea, retina. This type of infiltration is also often associated with large exudative retinal detachments (116, 142, 143).

In mice, MHC and non-MHC gene control influences susceptibility to immunisation with RBP3. MHC control is suggested to be connected to the ability of the mouse strain to bind to and present uveitogenic epitopes whereas, it is assumed that non-MHC control is more complicated (117). Another important factor is the type of effector response that each strain of mouse is genetically programmed to mount towards the uveitogenic epitope.

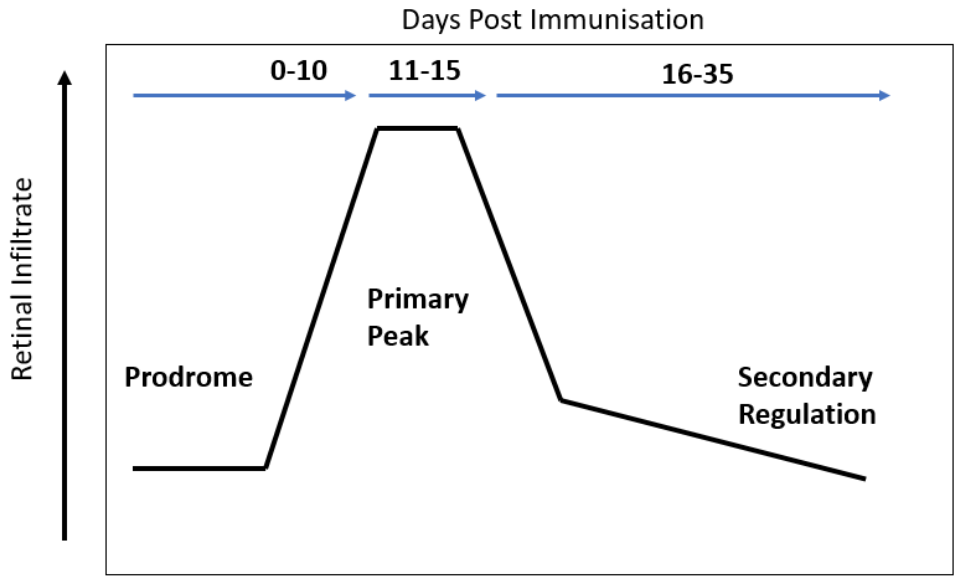

Figure 1.4: EAU disease progression seen in the mouse strain B10.RIII immunised with RBP 161-180. Illustrating leukocyte dynamics within the literature. Figure adapted from Kerr et al 2008. (1).

1.11.2 Cellular mechanisms in EAU

Autoreactive effector CD4+ T cells have been associated with the pathogenesis of a number of autoimmune disorders (144). A number of animal models have been used to transfer autoreactive T cells to illustrate induction of autoimmune disease such as EAU and the multiple sclerosis model (EAE), thus the pathogenic importance of autoreactive T cells can be formally demonstrated (145, 146).

EAU is a CD4 T-cell mediated disease model. It has been established in EAU models that immunisation with a peptide that is uveitogenic in nature triggers a peripheral immune response characterised by the activation and clonal expansion of pathogenic autoreactive CD4+ T cells (1). The activated T cell population are capable of crossing the BRB to interact with local APCs present within the tissue and induce a mixed population of leukocytes to localise within the eye and cause retinal disruption (1).

Autoreactive CD4+ T lymphocytes of a Th1 phenotype are critical in the pathogenesis of EAU alongside another CD4+ effector cell type known as Th17, which can be characterised by the secretion of IL-17 (147), Th17 cells have also been found to cause pathology in a number of other autoimmune diseases (1).

It is difficult to determine the individual roles of Th1 and Th17 cells when they are combined in the establishment and maintenance of EAU, as it appears that both cell types can independently promote disease onset and without the use of fate mapping we cannot be sure of the origin of the cells causing disease (148). Long lasting changes occur within the eye after inflammation in the retina due to EAU these include changes in the dynamics of leukocyte recruitment and phenotype. The breakdown of the BRB allows antigen specific T cells to enter the circulation but this is not the sole trigger to cause the recruitment of lymphocytes and leukocytes in high numbers to the target organ (1).

1.12 Thesis Objectives

EAU has provided information on lymphocyte subsets entering the tissue at different times during the inflammatory process of the disease. In order to study the role of pathogenic CD4+ T cells that initiate disease, the adoptive transfer model will be utilised in naive C57BL/6 animals not treated with adjuvant.

This model can be used to induce disease with uveitogenic T cell lines from an allelically marked donor animal into a naïve recipient, this enables the understanding of the relative contribution of endogenous and transferred cells in each eye by quantification by flow cytometry at various time points in disease progression and more generally, allows sensitive studies of pre-clinical disease. To track the transferred cells the mouse strains used will carry the allelic marker CD45.1 or CD45.2 so endogenous and transferred CD45+ cells can be separated.

Within this study several genetically modified mouse models on the C57BL/6 background are utilised as donors and recipients within the adoptive transfer protocol. Firstly, the C57BL/6B6.SJL-Ptprc^{a}Pepc^{b}/BoyJ which is allelically marked Ly5.1 (also known as CD45.1).

Using susceptible mouse strains, transgenic knock in mice have become very useful in vivo and in vitro research including the C57BL/6 CX3CR1 $^{+/GFP}$ for study of resident microglia cells within the eye and the brain (149). The C57BL/6 CX3CR1 $^{+/GFP}$ mouse is allelically marked with CD45.2, within this model one of the CX3CR1 alleles has been replaced with a green fluorescent protein (GFP) gene. Chemokines are small proteins that are chemoattractant and recruit inflammatory cells to the site of inflammation (150). CX3CL1 also known as fractalkine exists in two forms; a membrane bound form and a soluble form (150). CX3CR1 is the specific receptor for CX3CL1 which makes it an attractive possibility for therapeutic intervention (151). The high affinity interaction of CX3CL1 with CX3CR1 mediated leukocyte arrest under flow conditions (152, 153).

The third mouse model used is the RAG2$^{-/-}$ model allelically marked CD45.2. This model carries a germline mutation which results in a large portion of the RAG2 coding region being deleted. The homozygous mutant mice are viable but lack the ability to produce T and B lymphocytes (154). Therefore, this model has no endogenous adaptive lymphocyte cell compartment, so the only T cells present within the model will be the transferred uveitogenic T lymphocytes.

Another model used within this study is the TCR transgenic, C57BL/6 Ly5 OTII model allelically marked CD45.1. T cell receptor transgenic mouse models have had a big impact on the understanding of T cell biology and immunity (155). The OTII transgenic mouse have CD4+ T cells that express transgenic αβ-TCRs that recognise OVA (155). This mouse strain is useful for transferring activated non-antigen specific leukocytes into naïve recipients.

The final model used is the C57BL/6 IL27R^{-} (WSX-1$^{-/-}$) mouse allelically marked CD45.2. IL-27 is a member of the IL-12 family and is produced by antigen- presenting cells, it is important in the regulation of CD4+ T cell differentiation and immune response (156). There are now studies that highlight the inhibitory effects of IL-27 on differentiation of Th17 cells and Tregs but will promote the differentiation of Th1 cells (156, 157). IL-27R is a heterodimer composed of IL-27Rα also known as T- cell cytokine receptor (TCCR) or WSX-1 and a signal transducing chain glycoprotein 130 (gp130) (156). This model is useful to understand further the complicated biology underlying IL-27 and IL-27R within autoimmune diseases. It has been suggested in recent studies that IL-27/IL-27R could be a useful therapeutic target to suppress inflammatory diseases (158).

STRAIN	**CD45 ALLELIC MARKER**
C57BL/6 LY5	CD45.1
C57BL/6 CX3CR1$^{+/GFP}$	CD45.2
C57BL/6 CX3CR1 $^{GFP/GFP}$	CD45.2
C57BL/6 OTII LY5	CD45.1
C57BL/6 OTII LY5 CX3CR1$^{+/GFP}$	CD45.1 + .2
C57BL/6 RAG2$^{-/-}$	CD45.2
C57BL/6 IL-27RA$^{-/-}$	CD45.2

Table 1.2: C57BL/6 mouse strains with allelic marker used for tracking cells using the adoptive transfer technique.

In summary, interrelated hypotheses within this thesis relate to the tracking of antigen-specific disease-causing immune cells at different stages of clinical disease and using the retinal-antigen induced model of uveitis to look for potential targets for translatable treatments.

Allelically marked uveitogenic CD4+ T cells will initiate and drive clinical disease by recruitment to the ocular tissue. Do these cells concurrently stimulate an endogenous response causing infiltrate to be recruited to the ocular tissue throughout clinical disease from the endogenous compartment.

Uveitogenic transferred cells that are recruited to the ocular tissue by an antigen-specific mechanism initiate clinical disease which activates the endothelium. Investigate the role of non-specific T cell activation.

CX3CR1 is upregulated on CD4+ T cells in inflammatory disorders, suggesting a more long-lived phenotype that survives in the tissue throughout disease course and could therefore play a role on CD4+ T cells during EAU.

IL27R$\alpha^{-/-}$ CD4+ T cells will cause a more severe and persistent clinical disease phenotype using the adoptive transfer technique of CD4+ T cells from IL27R $\alpha^{-/-}$ donors.

In order to test these hypotheses, this thesis aimed to:

Optimise an adoptive transfer technique to induce disease, develop a standardised method of imaging using optical coherence tomography to compare between eyes and experiments, optimise a sensitive method of quantifying cellular infiltrate by flow cytometry (chapter 3 and 4)

Transfer allelically marked CD4+ T cells into naïve recipients to track pathogenic cells throughout disease course and assess the endogenous response to the pathogenic stimulus (chapter 4)

Investigate the recruitment of uveitogenic vs activated CD4+ T cells to the eye and disease initiation by the introduction of OVA antigen to the ocular tissue and track activated CD4+ T cells specific for that antigen within the recipient and the recruitment of these cells to the ocular tissue to induce disease (chapter 5)

Using CX3CR1$^{+/GFP}$ and CX3CR1$^{GFP/GFP}$ mice to look at the effect of loss of CX3CR1 in recipient tissue on clinical disease and the effect of CX3CR1 loss on transferred cells during clinical disease (chapter 6).

Analyse CX3CR1 expression on CD4+ T cells after adoptive transfer of EAU using the CX3CR1$^{+/GFP}$ mice as donors denoting CX3CR1 expression as GFP positive cells (chapter 6)

Using the IL27Rα$^{-/-}$ mice, look at the effect of the loss of the receptor on transferred cells and the effect on disease (chapter 7).

Characterise the effect on disease phenotype in both active immunisation and adoptive transfer and quantify immune infiltrate of naïve mice (chapter 7).

Chapter 2. Materials and Methods

Materials and Methods

2.1 Reagents

2.1.1 Immunising Peptides

RBP-3 peptide 629-643 (EAHYARPEIAQRARA) (159) was obtained from Severn Biotech Ltd (Worcestershire, UK). Peptide purity was determined by HPLC. Peptide was prepared with distilled water and aliquoted and stored at -80°C.

2.1.2 Peptides used for Intravitreal Injection

Chicken Ovalbumin peptide (OVA) (ISQAVHAAHAEINEAGR) (159) and L144/R147 (HSLGK**L**LGHPDKF) (160) was obtained from Severn Biotech Ltd (Worcestershire, UK).Peptide purity was determined by HPLC. Peptide was prepared with distilled water and aliquoted and stored at -80°C.

2.1.3 Recovery Anaesthetic

Mice were anaesthetised to perform experiments using an intraperitoneal (i.p.) injection of 90µl/10µg of body weight of a solution containing 6mg/ml ketamine (Ketavet, Zoetis Ireland Ltd. Dublin, Ireland) and 2mg/ml Xylazine (Rompun, Bayer plc. Newbury UK) mixed with sterile water.

2.1.4 Topical Eyedrops

In order to perform clinical imaging or intravitreal injections pupils were dilated using tropicamide 1% and phenylephrine 2.5% (Minims, Chauvin Pharmaceuticals. UK). For corneal anaesthesia oxybropucaine 0.4% (Minims) was administered and Viscotears (Novartis Pharmaceuticals. UK) were used as a further barrier of protection

2.2 Mouse Models

Several strains of C57BL/6 mice were utilised for this work including the CX3CR1 $^{GFP/GFP}$, CX3CR1 $^{+/GFP}$, Ly5, Ly5 OTII, Ly5 OTII CX3CR1$^{+/GFP}$, RAG2$^{-/-}$ and IL-27Rα$^{-/-}$.

STRAIN NAME	BACKGROUND	IN-HOUSE NAME	SUPPLIER
CX3CR1-GFP	C57BL/6J	CX3CR1$^{+/GFP}$/ CX3CR1$^{GFP/GFP}$	A gift from Heping Xu
B6.SJL-PTPRC^{B}PEPC^{B}/BOYJ (LY5 MICE; CD45.1)	B6/SJL (Ly5)	Ly5	JAX
B6.CG-TG (TCRATCRB)425CBN/J	B6/SJL (Ly5)	OT-II Ly5	JAX
B6.CG-THY1	C57BL/6J	RAG2$^{-/-}$	JAX
B6N.129P2-IL27RATM1MAK/J	C57BL/6J	IL-27Rα$^{-/-}$	JAX

Table 2.1: Mouse strains and backgrounds used in this thesis

Breeding colonies were established within the Animal Services Unit at University of Bristol, UK for experimentation. All mice were housed under specific pathogen-free conditions with continuous food and water available. Ear notches from CX3CR1$^{GFP/GFP}$ and CX3CR1$^{+/GFP}$ were genotyped using PCR to test the mice were of the correct genotype before experiments began. Blood was obtained from Ly5 OTII and Ly5 OTII CX3CR1$^{+/GFP}$ for phenotyping using flow cytometry to check the transgenic TCR before experimentation. Disease was induced in female mice aged between 6-8 weeks. Treatment of animals conformed to the ARVO statement for the use of animals in ophthalmic and vision research.

All procedures had local ethical approval and performed in accordance with home office project licence (30/139) and personal licence (I073AB938) under the United Kingdom Animals (Scientific Procedures) Act (1986).

Genetic variation has been detected in widely used C57BL/6 J CD45.2 model and the C57BL/6 SJL CD45.1 model based on the vendor source of the mouse strains (161), however the mice in these studies were all obtained from the same vendor and bred within the facilities at the University of Bristol.

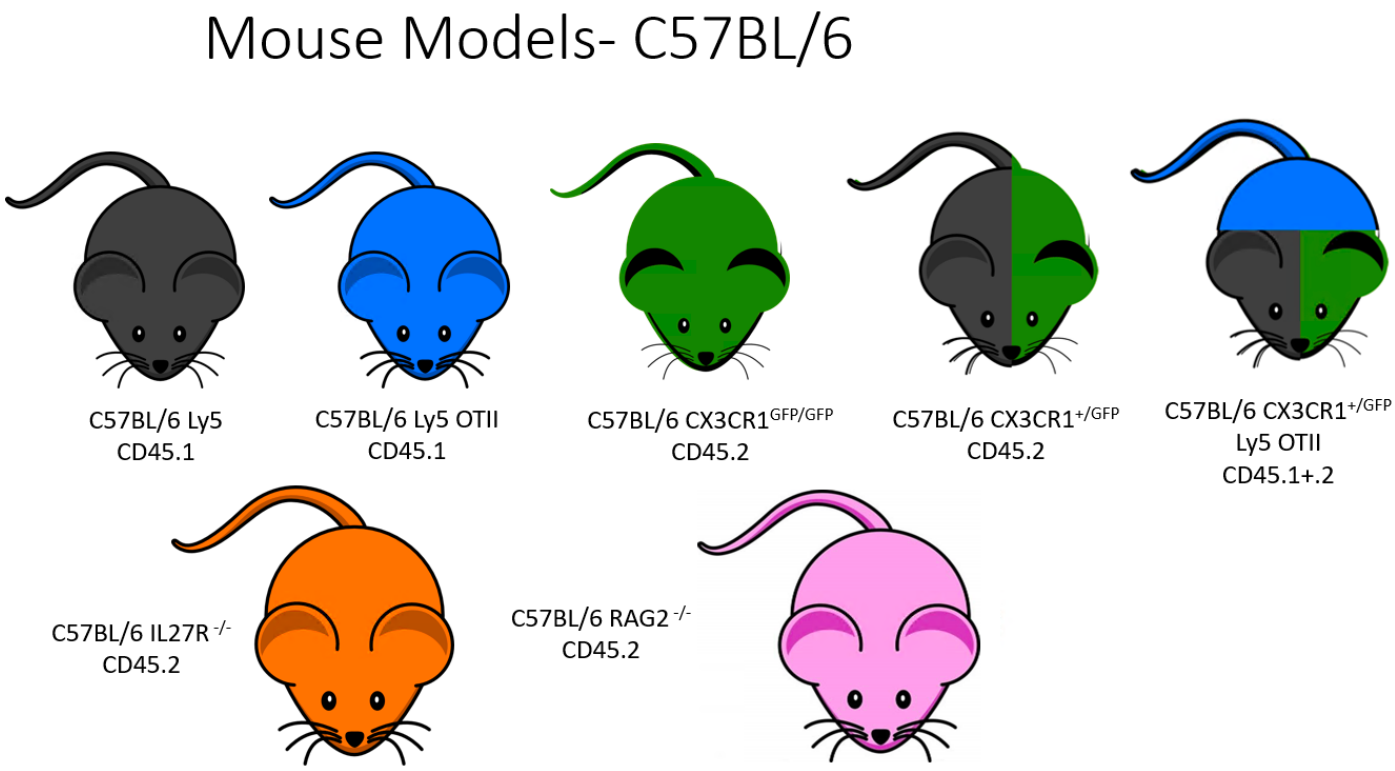

Figure 2.1: Overview of the mouse models and allelic markers utilised in this thesis

2.3 Induction of EAU

EAU was induced in a susceptible mouse strain (C57BL/6) using active immunisation or adoptive transfer of uveitogenic cells.

2.3.1 Active Immunisation

Female mice were immunised subcutaneously (s.c) in both flanks with 200µl of emulsion containing peptide immersed in CFA (*Mycobacterium Tuberculosis*) was injected subcutaneously into C57BL/6 mice to induce EAU. 400µg/mouse RBP-$3_{629-643}$ peptide in dH_20 was emulsified in Complete Freund's Adjuvant (CFA) (1mg/mL; 1:1 vol/vol) supplemented with *Mycobacterium tuberculosis* complete H37 Ra (BD Biosciences). *Bordetella pertussis* toxin (Sigma- Aldrich) was given intraperitoneally (i.p) at 1.5µg per mouse.

2.3.2 Adoptive Transfer of EAU

Mice were immunised using the protocol described for active immunisation, 11 days after immunisation mice were culled by schedule 1 and spleen and various lymph nodes harvested in Dulbecco's modified medium (DMEM).

After harvest spleen and lymph nodes were mashed in DMEM using the base of a 10ml syringe under sterile tissue culture conditions and filtered through a 70µm filter. Cells were then counted and plated down in $75cm^3$ flasks at 1-2x10^6 cells per $1cm^3$ in complete media.

Complete media was further supplemented with 10µg/ml RBP 629-643 peptide and 10ng/ml IL-23 (R&D Abingdon, UK). Cells were cultured in the incubator hydrated at 37°C and 4% CO_2. At 24 hours, cells were removed from the incubator and supplemented further with 10ng/ml IL-2 (Peprotech London, UK) in a further 10ml of complete medium. Then replaced in the incubator in the same conditions.

At 72 hours, flasks were removed from the incubator and washed using the medium containing the cells, then all media was removed from flasks. Supernatant was removed and the cell pellet washed in complete medium. Cells were then resuspended in 12ml of complete medium and split into two 15ml falcon tubes, 4ml of 1044 Histopaque (Sigma-Aldrich) was then layered underneath each cell suspension. The suspension was spun at 1800rpm for 20 minutes at 21°C with 1 acceleration and 0 brake to avoid the Histopaque and cells mixing when spun.

Cells were removed using a 5ml Pasteur pipette and washed in complete medium. Cells were then counted using a haemocytometer and transferred at $2x10^6$ per recipient in 100µl of PBS via intraperitoneal (i.p) injection.

2.3.3 Adoptive Transfer using MACS separated CD4+ T cells and other leukocytes

Leukocytes were stimulated as previously described for adoptive transfer. After isolation using Histopaque, leukocytes were then separated using MACS. Whole leukocyte populations were run through MACS columns (Miltenyi Biotec. Ltd. Surrey, UK) in MACS wash buffer (PBS supplemented with 10% BSA) selecting for a CD4 negative population.

After the column was run the CD4+ and CD4- population were both counted and transferred into naïve recipients at $2x10^6$ cells per mouse in 100µl of PBS.

2.3.4 Adoptive Transfer using MACS sorted cells followed by fluorescence sorting

Leukocytes were stimulated as previously described and separated using MACS columns. The CD4+ and CD4- population were then counted and stained using the protocol for flow cytometry staining (Described in 2.6). Specifically staining for CD4+ and CD8+ T cells, the leukocytes from the CD4+ and CD4- populations were then run through the BD Influx™ (BD Cytometry Systems. Oxford, UK) to sort for CD4+ T cells in the CD4+ MACS population and CD8+ T cells in the CD4- MACS population. CD4+ or CD8+ populations were then transferred into naïve recipients at ˜50,000 cells per recipient.

2.3.5 Adoptive Transfer using OTII TCR transgenic cells

Splenocytes from OTII TCR transgenic mice were cultured in the presence of 1µg/ml of the OVA peptide.

After the 72-hour cell culture, cells were prepared for transfer, in some experiments recipients were anaesthetised in order to perform an intravitreal injection of 2µl of OVA peptide at 1µg/ml. After the mice have recovered from the anaesthesia leukocytes isolated from cell cultures were transferred using i.p injection at $2x10^6$ cells per mouse in 100µl of PBS.

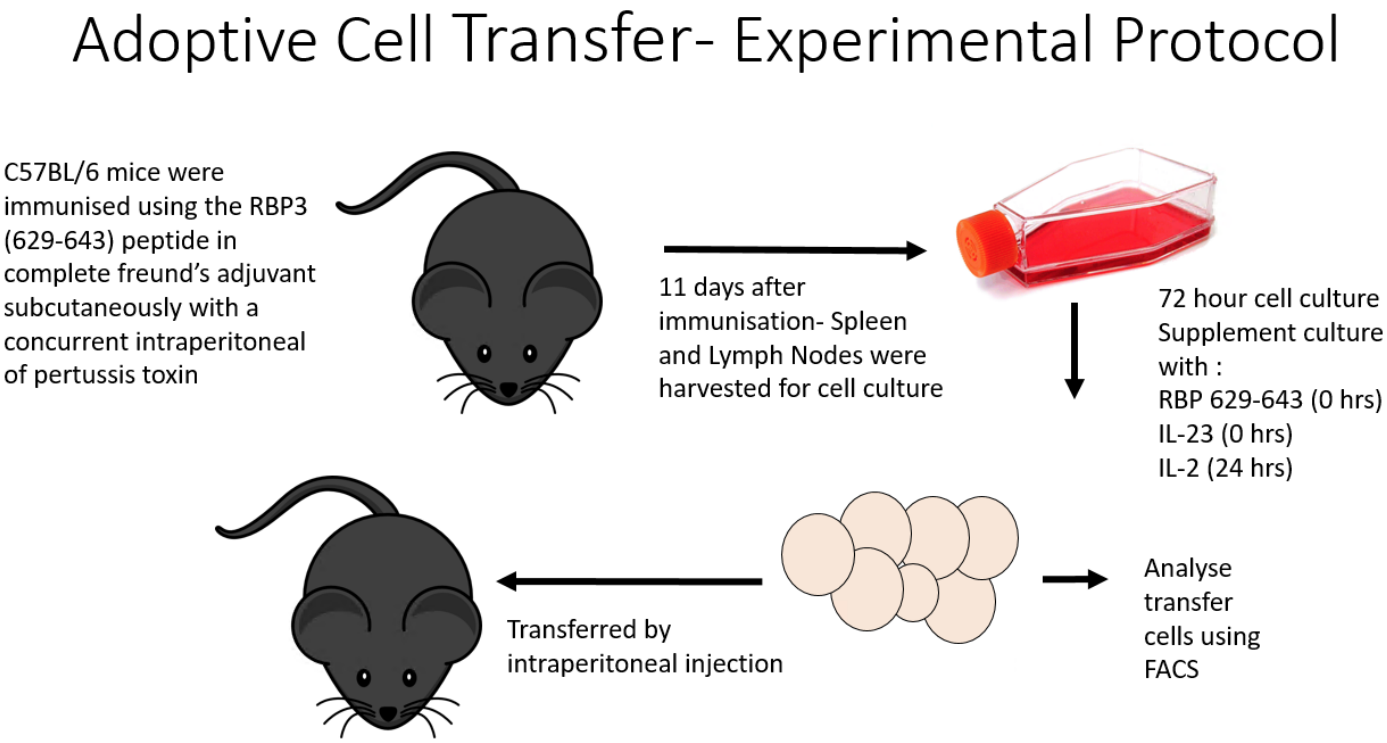

Figure 2.2: Adoptive transfer technique of uveitogenic leukocytes to induce EAU

2.4 Clinical Imaging

To monitor clinical disease course after disease induction two techniques were used: Topical Endoscopic Fundal Imaging (TEFI) and Optical Coherence Tomography (OCT).

2.4.1 Topical Endoscopic Fundal Imaging (TEFI)

Using a method previously developed in the lab (162), adapted from Paques et al,(163) an endoscope with a 5cm long telescope of 3mm outer diameter (1218AA; Karl Storz. Tuttlingen, Germany) was connected to a Nikon D80 digital camera with a 10-million-pixel charge-coupled device image sensor and Nikkor AF 85/F1.8 D (Nikon. Tokyo, Japan.), with an additional +4.00 dioptre magnifying lens. This system was used through pupils dilated by topical tropicamide 1% and phenylephrine 2.5% and topical oxybropucaine 0.4% and Viscotears were used for corneal anaesthesia.

Images were obtained by direct contact of the cornea to the endoscope. Images were then processed using Adobe Photoshop (Adobe Corporation. Mountain View, CA). Using an adapted clinical grading system fundal images were scored according to inflammatory changes to the optic disc and retinal vessels along with any retinal lesions and structural damage that has occurred. Scores were calculated using the clinical scoring criteria presented in Table 2.1.

2.4.2 Optical Coherence Tomography (OCT)

Mice were anaesthetised using recovery anaesthetic by intraperitoneal injection and pupils were dilated using tropicamide 1% and phenylephrine 2.5% to prepare for imaging.

Optical coherence tomography (OCT) scans and brightfield and fluorescence images were obtained using the Micron IV retinal imaging microscope (Phoenix Research Laboratories. Pleasanton, CA). Prior to beginning imaging the eyes the Micron IV CCD and OCT were fully calibrated according to the manufacturer's protocol. The gain was set to +4 dB and the frames per second (FPS) set to 15 for brightfield imaging and +15dB for green fluorescence imaging. For green fluorescence protein imaging a filter within the Micron IV system was utilised.

Settings for acquisition of the OCT scans were defined according to the manufacturers protocol, and scans were taken 30 times in rapid succession with the final image being an average from these images. Full-length B-scans were taken vertically and horizontally through the optic disc centred and one circle around the optic disc. A 3D cube scan is also taken

consisting of 512 images centred around the optic disc. All images were stored in TIFF file format, where cube images can be rendered into 3D cube videos using image processing techniques.

2.5 Analysis of EAU

2.5.1 Clinical Scoring of Disease

A scoring system obtained from (Table 2.2) previously published within the group (164) was used to accurately score the clinical disease in recipients using the TEFI fundal images acquired in *chapter 3* and the OCT fundus images. The single OCT line scans acquired with corresponding fundus imaging were scored independently by individuals experienced with scoring and masked to the origin of the data (Table 2.2).

Fundal images were scored for changes due to an inflammatory response effecting the optic disc, retinal vessels, retinal lesions, and causing structural damage. All scores were added together to give a total disease score which is then averaged for the number of criteria scored.

Score	Optic Disc	Retinal vessels	Retinal Tissue Infiltrate	Structural damage
1	Minimal inflammation	1-4 mild cuffings	1-4 small lesions or 1 linear lesion	Retinal lesions or retinal atrophy involving 1/4 to ¾ retina area
2	Mild inflammation	>4 mild cuffings or 1-3 moderate cuffings	5-10 small lesions or 2-3 linear lesions	Pan retinal atrophywith multiple small lesions (scars) or <3 linear lesions (scars)
3	Moderate inflammation	>3 moderate cuffings	>10 small lesions or >3 linear lesions	Pan-retinal atrophy with >3 linear lesions or confluent lesions (scars)
4	Severe inflammation	>1 severe cuffing	Linear lesion confluent	Retinal detachment with folding
5.	Not visible (white out or extreme detachment)	Not visible (white out or extreme detachment)	Not visible (white out or extreme detachment)	Not visible

Table 2.2: Clinical scoring overview for TEFI and OCT Fundal images. Table taken from Kerr et al 2008 (114).

2.5.2 Sample preparation for analysis

Retinal Preparation for Flow Cytometry

Retinal and vitreous infiltrating cells were isolated by dissection of retina and vitreous from enucleated eyes. The suspensions including the retina were then mechanically disrupted and passed through a 40-µm cell strainer to obtain a single cell suspension for staining for analysis by flow cytometry.

Retinal Preparation for Flatmounting and Lightsheet imaging

Enucleated eyes were pierced using a needle and left in fresh Cytofix™ (BD Biosciences. Franklin Lakes, NJ) for 2 hours at room temperature (RT). The anterior chamber was then removed, and the eyes were placed back into the Cytofix solution overnight at RT. Retinal

whole mounts were then prepared by peeling the retina from the choroid under a dissecting microscope ready for immunofluorescence staining.

Preparation of whole eyes for immunohistochemistry

Mice were sacrificed at pre-defined time points and eyes were enucleated and snap-frozen, oriented in optimal cutting temperature (OCT) compound (R. Lamb Ltd. East Sussex, UK). After they were prepared and stored at -80°C, serial 12-µm sections were prepared for antibody staining.

Preparation of whole organ samples for Flow Cytometry

To further analyse transferred cells during disease more tissues were obtained from each recipient. These tissues include spleen, lymph node, kidney, liver, and blood.

Spleen, kidney, and liver were prepared by mechanical dissociation of the tissue which is then filtered through a 70µm strainer before lysing red blood cells present within the suspension using ammonium-chloride-potassium buffer (ACK buffer). Cells were then resuspended in FACS buffer for staining. Blood samples were treated with the ACK buffer to lyse red blood cells and then resuspended in FACS buffer for staining.

2.6 Flow Cytometric Analysis

2.6.1 Cell surface staining of Flow Cytometry samples

Single cell suspensions were incubated with purified rat anti-mouse CD16/32 Fc block (Clone 2.4G2, BD Biosciences. Oxford UK) for 10 minutes at RT before incubation with fluorochrome-conjugated monoclonal antibodies (mAbs) against a panel of cell surface markers including: CD45.2, CD4, CD8 and CD11b with a biotin mAbs CD45.1 antibody. Cells were stained with the live dead marker 7AAD and the secondary streptavidin for 15 minutes before suspending in 200µl of FACS wash buffer to run samples.

Cell suspensions were acquired using a 4-laser BD^{TM} Fortessa X-20 flow cytometer (BD Cytometry systems. Oxford UK). Gating strategy is presented in figure 2.3 and analysis was performed using FlowJo software (Treestar. San Carlos, California). FMOs were used when necessary to help set gates for analysis and for confirmation of specificity of antibody staining.

2.6.2 Cell counting

Cell numbers were calculated by reference to a known cell-standard similarly to a previously published method from the group (114). Splenocyte suspensions of known concentration were acquired using a fixed and stable flow rate for 90 seconds per sample. Based on the number acquired using the known dilutions a standard curve was generated and from this the unknown total cell number from tissue samples can be interpolated if acquired at the same flow rate and time.

2.6.3 Intracellular cytokine staining

Single cell suspensions were incubated in complete medium supplemented with 25ng/ml PMA and 1µg/ml ionomycin (Sigma-Aldrich. Poole, UK) and 1µg/ml Golgi stop (BD Biosciences. UK) for 4 hours at 37°C in 5% CO_2.

Cells were resuspended in a fixable live dead 405 (ThermoFisher. UK) for 30 minutes at 4°C. The cells were then washed and stained using the previously described extracellular staining protocol. Stained cells were fixed using Cytofix for 15 minutes at RT and kept in the fridge for up to 7 days to run on the cytometer.

When the samples were to be run on the flow cytometer, the fixed cells were washed using 1x Perm wash for 15 minutes at 4°C and then stained using intracellular antibodies such as

IL-17, IFN-γ and FoxP3 for 30-45 minutes at 4°C. To run on the flow cytometer as previously described cells were resuspended in FACS buffer.

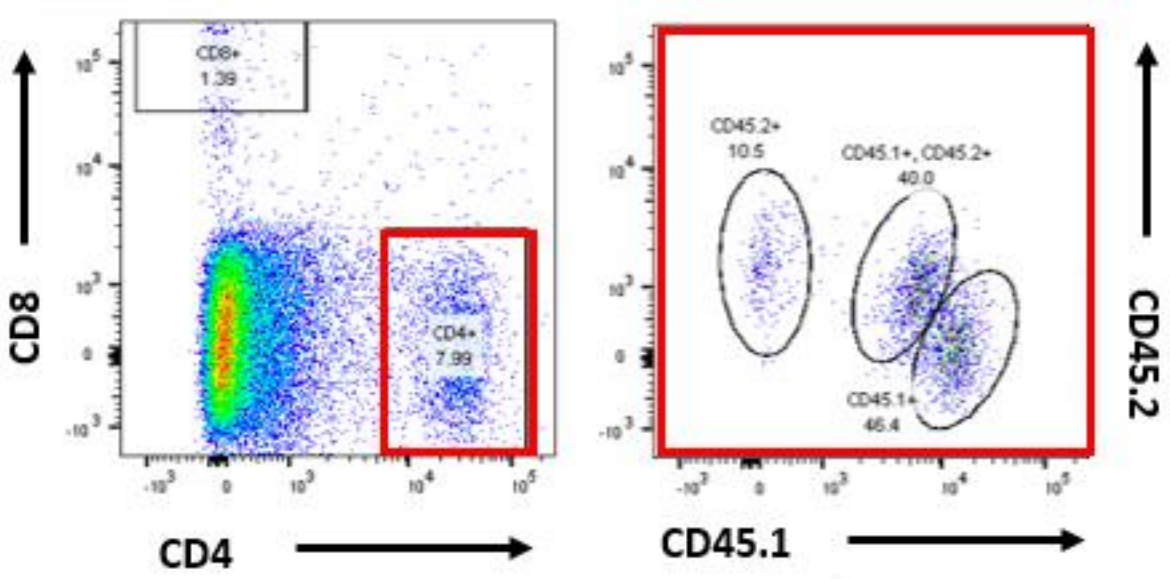

Figure 2.3: Flow cytometry gating analysing transferred and endogenous CD4+ populations. Allelically marked cells were transferred into naïve recipients, eyes were enucleated at pre-defined time points and a single cell suspension isolated using the retinal and vitreous cells and infiltrating leukocytes. Lymphocytes, single cells, and live cells were gated in to give the populations of interest. Live cells were then separated to give the CD4+ T cell population. Through the CD4+ gate the transferred and endogenous allelically marked populations are then distinguishable.

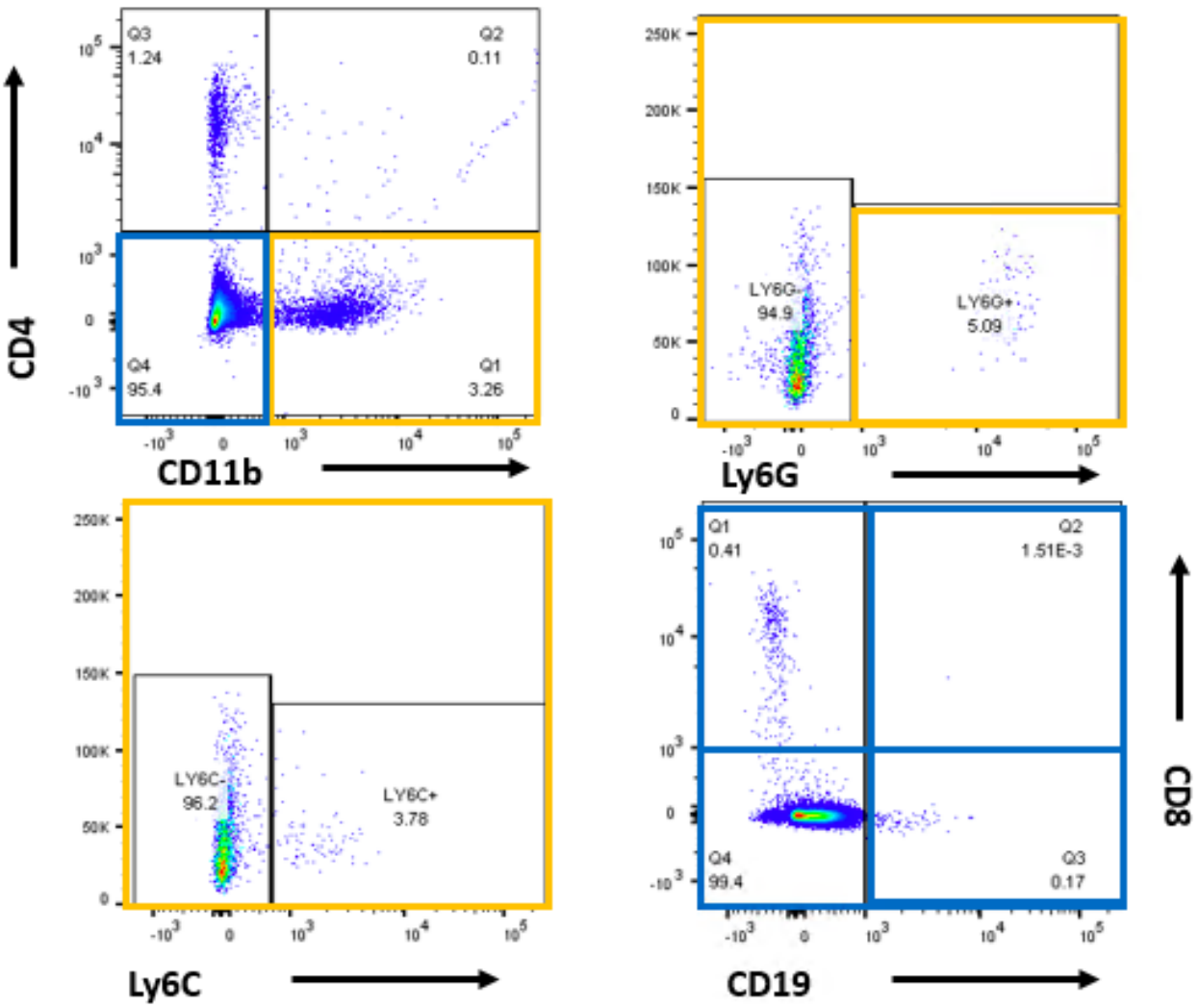

Figure 2.4: Further leukocyte gating for flow cytometry to identify different populations within the retinal infiltrate. Along with identification of endogenous and transferred populations specifically in the CD4+ T cell compartment within the retinal and vitreal infiltrate, analysis of a variety of other leukocytes present within the eye during clinical disease was also obtained. Lymphocytes, single cells, and live cells were gated in to give the populations of interest. Then from this population CD11b+ leukocytes can be isolated and further analysed using Ly6G and Ly6C markers. The CD4- and CD11b- population can also be further analysed by looking at markers such as CD8 and CD19.

2.7 Immunofluorescence techniques

2.7.1 Immunofluorescence whole eye sections staining

After sections were prepared (as previously described in section 2.5), sections were fixed in 4% PFA for 10 minutes at RT, washed and incubated in blocking buffer (5% bovine serum albumin/ normal goat serum) for 3 hours at RT. Sections were then stained with rat-anti mouse conjugated monoclonal CD3e (Alexa Fluor 647), CD4 (FITC) or CD8a (Alexa Fluor 594) antibodies (BioLegend. San Diego, California) overnight at 4°C.

Sections were then washed in PBS and stained with DAPI for 3 minutes before washing again and mounting using Vectashield to image on the EVOS fluorescence microscope (ThermoFisher. Waltham MA USA).

2.7.2 Ce3D media preparation

Ce3D media was prepared to clear and fix samples for both confocal microscopy and light sheet microscopy and to run the samples on the light sheet microscope. Firstly a ~29% N-methylacetamide solution was made by mixing 13.6ml N-methylacetamide (Sigma. Poole, UK) with 34ml PBS. N-methylacetamide is solid at room temperature so was warmed in a water bath for half an hour before use. To the N-methylacetamide 50g of Histodenz powder was added in small quantities while solution was being stirred and kept warm. The solution was then left overnight. The following day 0.1% v/v Triton X-100 and 0.5% v/v 1-thioglycerol were added and left to mix for 4 hours. The refractive index was then checked to be around 1.47. The media is based on protocol used in a study by Li et al (165).

2.7.3 Whole mount preparation and staining for Confocal Microscopy

After isolation, the whole retinal mounts were washed in 1x Perm Wash (BD Biosciences. Franklin Lakes, NJ) tissues were then incubated in Ce3D block (1% BSA + 1% NGS in 1x Perm Wash) for 5 hours at 4°C.

The Ce3D block was then replaced with the primary antibody stain composed of Ce3D block containing the CD3e, CD4 and CD8a antibodies previously described for section immunofluorescence staining and kept at 4°C for two days. The whole mounts were then washed using 1x Perm Wash four times over a 2-hour period. The whole mounts were then incubated in DAPI for 24 hours before mounting to image.

Retinas were spread on clean glass slides as flat as possible cutting into the tissue if necessary (vitreous side up), under coverslips with Ce3D media.

2.7.4 Preparation of retinal tissue for Lightsheet imaging

Whole retinas were washed in 1x Perm Wash and incubated in Ce3D block as previously described. The Ce3D block (1% BSA + 1% NGS in 1x Perm Wash) was then replaced with primary antibodies in Ce3D block including the previously described CD3e, CD4 and Cd8a antibodies with an additional primary unconjugated antibody for Isolectin B4 (IB4) (Sigma Aldrich) and kept at 4°C for two days. The whole mounts were washed using 1x Perm Wash four times over a 2-hour period and incubated in secondary antibody Alexa Fluor 405 (Molecular probes, ThermoFisher. Waltham MA USA) in Ce3D block for 3 hours at 4°C.
Retinas were washed in 1x Perm Wash before clearing using Ce3D media over the tip of a PCR microtube to maintain the shape. The tube with the tissue was placed into a 500µl Eppendorf tube filled with 200µl of the Ce3D media to keep the tissue hydrated before imaging.

2.7.5 Confocal Microscopy

Whole mounts described using the protocol in 2.7.2 were examined using confocal scanning laser imaging system fitted with krypton-argon lasers and a motorised XYZ stage to allow multiple site imaging (Leica TCS-SP2-AOBS, Leica Microsystems. Wetzlar, Germany). For 3D image preparation of tissues, the upper and lower limit of the tissues were determined before sequential z-scans at 1.5µm increments were taken through the whole thickness of the tissue using a 63x 1.4 aperture oil immersion lens.

2.7.6 Lightsheet Microscopy

Whole retinas obtained using the protocol in 2.7.3 were examined using Lightsheet fluorescence microscopy (Zeiss Z.1 Lightsheet 7. Germany). It is a multi-laser, turnkey system that can be used to image whole retinas suspended in Ce3D media within the tank in the system. Lightsheet images are collected using two high resolution sCMOS cameras using a range of filter modules and objectives including 20x and 40x. Automated imaging can be achieved to provide 3D and 4D rendering. When images were acquired the Zeiss Zen, software was used (Zeiss, Germany) but for further secondary analysis for 3D and 4D rendering the Arivis vision4D (Arivis. Munich, Germany) software was used.

2.8 In vitro assays

2.8.1 Complete medium

Complete medium used for in vitro assays such as the adoptive transfer cell culture consisted of Dulbecco's modified Eagle's medium (DMEM) supplemented with 10% heat inactivated fetal calf serum (TCS Cellworks. UK), 100U/ml penicillin-streptomycin, and 2mmol/L L-glutamine (Invitrogen. Paisley, UK).

2.8.2 Antigen specificity assay

Spleens and lymph nodes were collected from RBP3 629-643 immunised donors 11 days after immunisation and mechanically disrupted through a 70µm filter and red blood cells lysed. Cells were seeded into 96-well round bottom plates at $1x10^5$ cells/well and stimulated with different concentrations (100µg/ml, 10µg/ml, 1µg/ml and 0.1µg/ml) of OVA RBP3 1-20 or RBP 629-643.

After 72 hours, supernatant was removed and stored at -20°C until used for LegendPlex analysis.

2.8.3 Legendplex assay

Cytokine production in adoptive transfer cell culture supernatants and the antigen specificity assay were measured using a Legendplex™ kit (BioLegend. San Diego, CA). Briefly, the Legendplex is a bead-based immunoassay that uses the same principle as a sandwich-based immunoassay. Bead populations are distinguished from one another based on APC fluorescence and size with each bead set being conjugated to a specific antibody to serve as a specific capture bead for that analyte being present within the sample. After washing a biotinylated detection antibody is added to the sample to bind to the specific analyte bound to the capture beads, Streptavidin-phycoerythrin (SA-PE) was added to bind to the biotinylated detection antibody to provide a fluorescent signal with intensities that represents the proportion of analyte within the sample.

The PE signal can then be picked up by a flow cytometer (BD FACS Canto II (BD Biosciences)) and concentrations of each analyte quantified using a known standard curve using the Legendplex™ data analysis software provided.

2.9 Statistical analysis

Animal numbers are assessed such that the experiments are powered to a probability of 80% that a statistically significant result is observed. Statistical analysis was performed using GraphPad Prism software.

Where studies comprised of two experimental groups, for data that was not normally distributed a Mann- Whitney U- test was used to determine statistical significance.

To identify statistical significance between multiple groups a one-way ANOVA with Dunnett's multiple comparison test was used.

For OCT disease scoring, Area under the curve (AUC) was calculated and then tested using a Mann Whitney U- test to compare the calculated AUC numbers.

A $p<0.05$ was considered statistically significant. Graphs are presented as mean$\pm$ standard error of the mean (SEM) unless indicated otherwise.

2.10 Figure adaptation

Some figures from this thesis were adapted from previously published work using clipart images obtained from 'Smart servier medical art' (https://smart.servier.com/, France).

Table 2.3 Flow Cytometry Antibodies

Name	*Isotype*	*Format*	*Dilution*	*Supplier*	*Catalogue number*
CD45.1	**Mouse IgG2a**	**Unconjugated**	**1/200**	**Becton Dickinson**	**553774**
CD45.2	**Mouse IgG2a**	**BV605**	**1/200**	**BioLegend**	**109841**
CD45	**Rat IgG2b**	**AF700**	**1/200**	**BioLegend**	**103128**
CD3e	**IgG1**	**APC**	**1/200**	**Becton Dickinson**	**553066**
CD3e	**American Hamster IgG**	**BV786**	**1/200**	**BioLegend**	**100355**
CD4	**Rat IgG2a**	**APC**	**1/200**	**Becton Dickinson Pharmingen**	**553051**
CD4	**Rat IgG2b**	**BV421**	**1/200**	**BioLegend**	**100437**
CD8	**Rat IgG2b**	**PE-CY7**	**1/500**	**BioLegend**	**126616**
CD11b	**Rat IgG2b**	**APC-CY7**	**1/500**	**Becton Dickinson**	**557657**
LY6G	**Rat IgG2a**	**PE**	**1/200**	**BioLegend**	**127608**
LY6C	**Rat IgG2c**	**AF700**	**1/200**	**BioLegend**	**128024**
CD19	**Rat IgG2a**	**BV510**	**1/200**	**BioLegend**	**115545**
IFN-γ	**Rat IgG1**	**APC**	**1/200**	**Becton Dickinson**	**557735**
FoxP3	**RatIgG2b**	**PE**	**1/200**	**Becton Dickinson**	**560408**
IL-17	**Rat IgG1**	**BV605**	**1/200**	**Becton Dickinson**	**564169**
Vα2	**Rat IgG2a**	**PE**	**1/200**	**Becton Dickinson**	**127808**
Streptavidin		**V450**	**1/500**	**Becton Dickinson**	**560797**

Each dilution factor is used for samples of no more than $5x10^6$ cells

2.4 Immunofluorescence Antibodies

Name	*Isotype*	*Format*	*Dilution*	*Supplier*	*Catalogue number*
CD3	**Rat IgG2b**	**AF647**	**1/200**	**BioLegend**	**100209**
CD4	**Rat IgG2a**	**FITC**	**1/200**	**BioLegend**	**100532**
CD8a	**Rat IgG2a**	**AF594**	**1/200**	**BioLegend**	**100758**
CD19	**Rat IgG2a**	**AF594**	**1/200**	**BioLegend**	**115552**
IB4					

Chapter 3. Optimisation of adoptive transfer technique

3.1 Introduction

Animal models of uveitis have proven very useful for the study of the underlying mechanisms of intraocular inflammation and as a pre-clinical model for treatments of human uveitis (159). Retinal antigens can be used as targets to induce EAU, they are typically derived from retinal photoreceptor cells that can function in the visual cycle and are highly evolutionary conserved (166).

In the C57BL/6 model, mice are immunised with adjuvants (CFA and pertussis toxin) combined with interphotoreceptor retinoid binding protein (RBP3) derived peptides, specifically in this thesis using the 629-643 peptide sequence to induce EAU (159, 167).

Alternatively, EAU can be induced using the adoptive transfer technique by transfer of primed uveitogenic cells (159, 167, 168). RBP-3 is a key protein in establishing ocular tolerance, the transfer of uveitogenic T cells from RBP-3 knockout animals illustrates the importance of RBP-3 in the shaping of the T cell repertoire (159).

3.1.1 Adoptive Transfer Technique

Several animal models have successfully used the adoptive transfer of autoreactive T cells to induce autoimmune disease (146).

To induce autoimmune disease by using the adoptive transfer model, T cells isolated from spleen and lymph nodes of immunised animals, are stimulated in vitro with cognate antigen to produce an activated phenotype. Upon transfer these T cells have the capacity to proliferate, produce cytokines, interact with APCs and induce cytotoxicity (169). The transferred T cells use all these mechanisms to induce and control disease (169).

One of the advantages of the adoptive transfer technique is that T cells encounter the antigen for the first time before transfer into naïve recipients, thus the kinetics of responses of specific T cells to the self-antigen can be monitored from earliest encounter i.e. from point of transfer (170). Specifically in this study the main advantage of the adoptive transfer technique is the ability to track disease causing pathogenic cells throughout disease and compare it with the endogenous response throughout clinical disease.

3.1.2 Adoptive Transfer of EAU

Passive transfer was first demonstrated in EAU in 1971 by Aronson and McMaster using guinea pigs as the experimental model (171). The transfer technique was originally developed using guinea pigs with chronic uveitis as donors, cells were transferred intravenously (i.v) or intraperitoneally (i.p) with all recipients developing clinical disease by day 4 post transfer, determined by histology and uveal photography (172). This method used high numbers of donor cells to effectively induce disease in naïve recipients (173). When the adoptive transfer of lymphocytes was performed in rats, donors immunised with S-antigen were unable to induce EAU when injected at $x10^8$ or $x10^9$ per recipient, so the protocol was adapted to use an in vitro cell culture step to enhance the immunological capacities of lymphocytes, thus causing them to become highly uveitogenic by preincubating with the specific antigen required to induce disease. When subsets of T cells are purified to perform adoptive transfer, CD4+ T cells and T cell lines could induce EAU with an in vitro cell culture whereas CD8+ T cells alone were not capable of inducing the disease (173)

Current protocols for adoptive transfer in mice uses lymphocytes from animals immunised with uveitogenic antigen as donors, cells are isolated from spleen and lymph nodes and to transfer disease after cells are activated in vitro before transfer (174). The EAU model that is induced by RBP3 is a useful system to study migration and the fate of autoreactive T cells that mediate chronic EAU.(172). The addition of IL-23 has recently been used in both EAE (175) and EAU (176) adoptive transfer protocols to drive a highly pathogenic CD4+ T cell population that are highly essential for the induction of inflammation or autoimmune disease of the CNS (175). To yield the highest number of pathogenic CD4+ T cells I decided to further supplement the cultures with IL-2 to encourage cell expansion.

In this thesis, a more robust adoptive transfer technique was optimised for use in the C57BL/6 mouse model using the 629-643 RBP3 peptide to induce disease, which has not yet been used for disease induction by adoptive transfer.

Further to this, optimisation of the in vitro cell culture step such as the addition of IL-23 and IL-2 provides a pathogenic, expanded transfer population capable of inducing disease in lower numbers than found within the literature. The use of allelic markers in this study more easily allows tracking of uveitogenic T cells throughout clinical disease.

3.1.3 Distinguishing Transferred from Endogenous Cells

A major goal in study of the adaptive immune system and its responses is to understand the development and progression of antigen-specific T cells from naïve precursors to activated effector cells and long-lived memory cells (177, 178). In order to achieve this investigators need to track distinct populations of T cells with specificity to a single antigen (such as RBP3) throughout the course of an immune response (178). Discrimination of donor T cells from the endogenous T cells is dependent on donor T cells expressing a marker that is unique but doesn't provide a target that would cause the recipient mouse to reject the transferred cells (178).

A number of allelic variations of surface receptors have been bred into transgenic mice, the most common are CD45.1/2 and CD90.1/2 (177). T cells expressing the CD45.1 allele can be adoptively transferred into C57BL/6 mice which express the CD45.2 allele (177-179). Using antibodies specific to the different allelic forms of these markers can then be used to identify the donor and recipient populations (177). The flexibility of using the allelic markers CD45.1 and CD45.2 can be used to investigate both transferred and endogenous cells. This therefore allows for monitoring of antigen-specific transfer cells throughout disease course not only in the eye but in other organs within the recipient and how the recipient's own immune response interacts with the transferred cell population.

3.1.4 Analysis of Clinical Disease in vivo

Analysis of clinical disease in vivo is a very useful tool to understand clinical disease course in recipients. Retinal imaging has been revolutionised by the development of optical coherence tomography (OCT) in both mouse and humans (180). Quantification of changes within the retinal layers has relied upon histology but histology is labour intensive and does not allow for the same mouse to be monitored for disease over time (180).

OCT recognises structures in the retina based on the scatter of reflected light and reaches axial resolutions down to 4µm, advancing the prospect of observing histological detail in vivo throughout disease (181). One of the most important benefits of using OCT for clinical scoring of EAU similar to the detail of histology would permit the same staging of disease over time on the same eye, from this dynamic intraretinal changes can be monitored and defined in vivo (181).

To develop a scoring system for analysing disease, a standardised method would allow comparison of images not just through disease in one eye but comparison of eyes across experiments and between experiments.

This aim of this chapter is to on develop a robust adoptive transfer technique that allows in vivo clinical imaging to monitor clinical disease course and tracking of the transferred population.

3.2 Materials and Methods

3.2.1 Adoptive Transfer Technique

Pathogenic polyclonal antigen specific cells were produced by immunising different donor strains with RBP3 peptide, these donor cells were then transferred using i.p injection into C57BL/6 recipients at variable cell concentrations to determine the optimum number of cells needed to induce a disease.

C57BL/6 Ly5 (CD45.1) were immunised and cells transferred into RAG2 deficient mice as a leukocyte population or sorted cells.

3.2.2 Flow Cytometry Analysis

Flow cytometry was used to identify subsets of cells within the transferred cell population and retinal infiltrate using extracellular and intracellular staining.

Within transferred recipients' allelic markers CD45.1 and CD45.2 were used to identify endogenous and transferred populations of cells within the retina.

3.2.3 MACS Sorting and Fluorescent Associated Cell Sorting

CD4- MACS sorting was used to isolate a CD4+ population from a total leukocyte cell population from WT C57BL/6 mice, the CD4+ and CD4- population were then transferred into $RAG2^{-/-}$ mice. A purer population was required after MACS sorting so additional FACS was used to obtain a purer population of CD4+ and CD8+ T cells for transfer into $RAG2^{-/-}$ recipients.

3.2.4 Legendplex

Legendplex analysis is a bead-based immunoassay that utilises the same principles of sandwich immunoassays, where a soluble analyte is captured between two antibodies (Biolegend,2019).

Legendplex analysis was used on supernatant from splenocyte cultures taken from immunised donors stimulated with different peptides to identify and quantify cytokines expressed by cells present within the culture supernatant.

Supernatant from cultures of transferred cells were also analysed using LegendPlex and compared across recipient genotype.

3.2.5 Clinical Imaging

TEFI was used to study onset of disease and disease severity without anaesthetising the animal, this was then followed by OCT scans and fundus images standardised across recipients during transfer optimisation to study disease course at each cell concentration transferred.

3.3 Results

3.3.1 Optimisation of cell culture for use in adoptive transfer protocol to induce EAU

Useful information about immunopathogenic mechanisms of autoimmune disease have been obtained from studies of the adoptive transfer of serum or lymphoid cells from immunised donors (132). More reproducible attempts to induce EAU have been made by transferring lymphoid cells (132, 171, 182). The efficacy of the transfer of disease by lymphoid cells was increased greatly by preculturing the cells with the organ-specific antigen such as RBP3, a number of studies demonstrated this in models of EAE using the pMOG peptide but this effect has also been shown in the EAU transfer model (132).

Cells were transferred as total leukocyte populations, to determine optimal cell density, the concentration of cells was then compared with the cell yield (Figure 3.1a) for transfer, that concurrently can provide the greatest percentage of CD45+ CD3+ (Figure 3.1b) and CD4+ cell numbers (Figure 3.1c) to allow more transfers to be performed. The density most suited in terms of yield from cells plated down and highest percentage of CD4+ T cells yielded from the culture is at $1x10^6$ cells plated down per $1cm^3$ (figure 3.1a and figure 3.1c).

To further increase the efficacy of the cell culture conditions, the T cell growth factor IL-2 to maximise cell viability and the cytokine IL-23 was used to select a pathogenic cell population of IL-17 and IFN-γ producing phenotype. Therefore, experiments investigating the time point of cytokine addition of IL-23 and IL-2 to cultures can affect percentage yield of CD45+ CD3+ (Figure 3.1d) and CD4+ and CD8+ (Figure 3.1e). Yield also changed with the concentration of the cytokine IL-23 (Figure 3.2a) and origin of the IL-2 (mouse or human) (Figure 3.2b). Further analysis considered the percentage of CD4+, CD8+ and CD11b+ cells present within the cultures using different IL-23 concentrations and species origin of IL-2 (Figure 3.2e and 3.2f). The highest percentage yield of CD4+ T cells was addition of IL-23 at 0 hours followed by IL-2 at 24 hours (figure 3.1e). Study of the species origin of the IL-2 highlighted a greater total cell yield per flask and a greater disease incidence when using murine IL-2 when compared to human IL-2. The addition of 10ng/ml IL-23 gave a high enough cell yield that cells could be used at and a good disease incidence and severity when transferred into recipients, whereas the 20ng/ml gave a doubled cell yield compared to the 10ng/ml of IL-23 but a similar disease

incidence suggesting no added effect on pathogenicity was caused by doubling IL-23 concentration in the cell cultures.

After analysis of cell culture and analysis of disease in recipients comparing cell cultures (Figure 3.2c and 3.2d) it was identified which conditions will give the most robust disease across recipients. This analysis is useful as reliable disease incidence and severity allows the use of the adoptive transfer protocol.

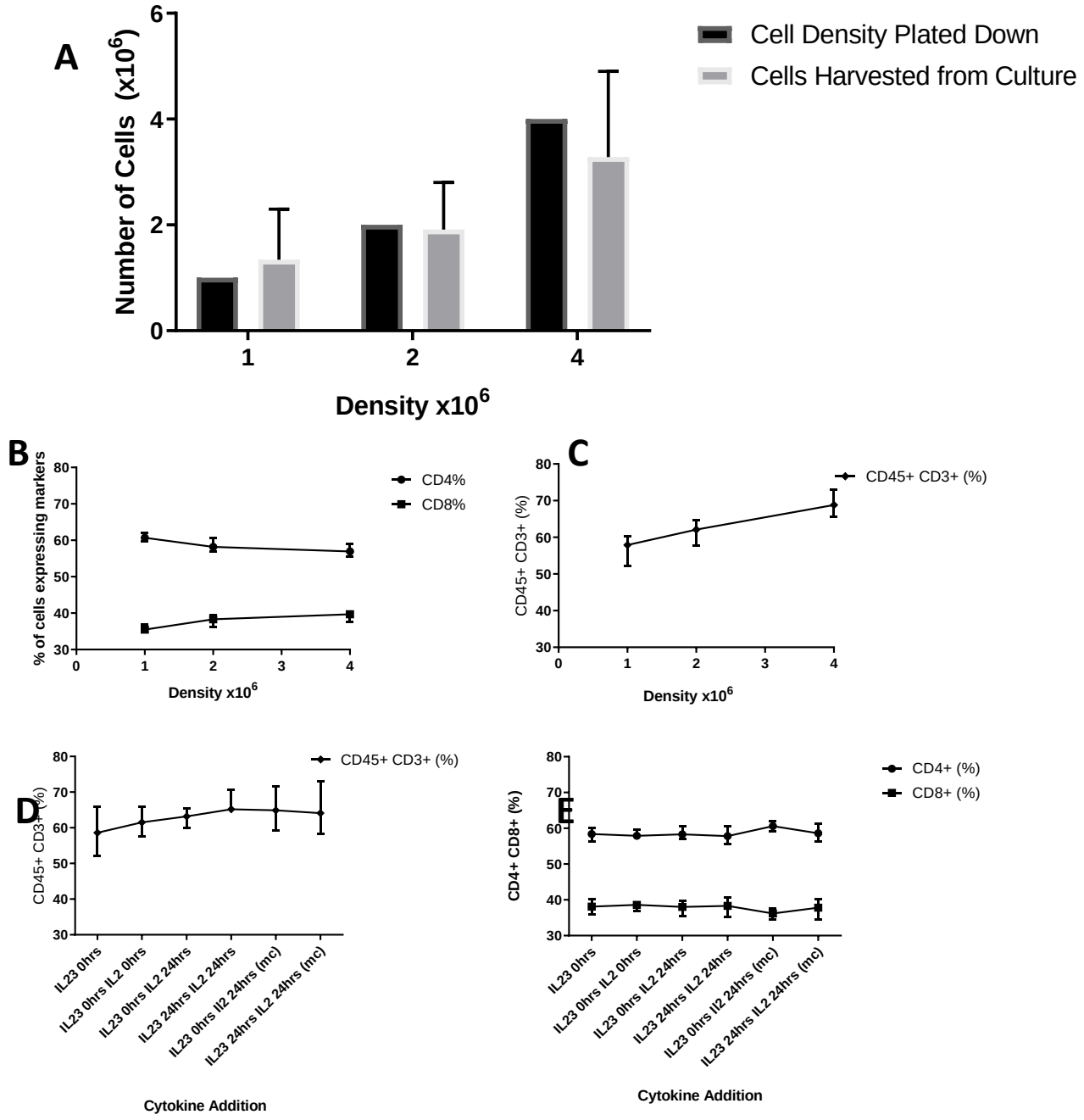

Figure 3.1: Optimisation of culture conditions analysis for in vitro step of adoptive transfer protocol. (A) Cell yield from culture based on cell density plated down at $1x10^6$, $2x10^6$ and $4x10^6$ (Mean ± SEM) (B) Percentage of CD45+ CD3+ cells obtained from cell cultures at densities $1x10^6$, $2x10^6$ and $4x10^6$ (Mean ± SEM) (C) Percentage of CD4+ and CD8+ cells obtained from cell cultures at densities $1x10^6$, $2x10^6$ and $4x10^6$ (Mean ± SEM) (D) Percentage of CD45+ CD3+ cells obtained from cell cultures with different time points for addition of IL-23 and IL-2 (Mean ± SEM) (E) Percentage of CD4+ and CD8+ cells obtained from cultures with different time points for addition of IL-23 and IL-2 (Mean ± SEM). Cell cultures performed in 3-6 replicates.

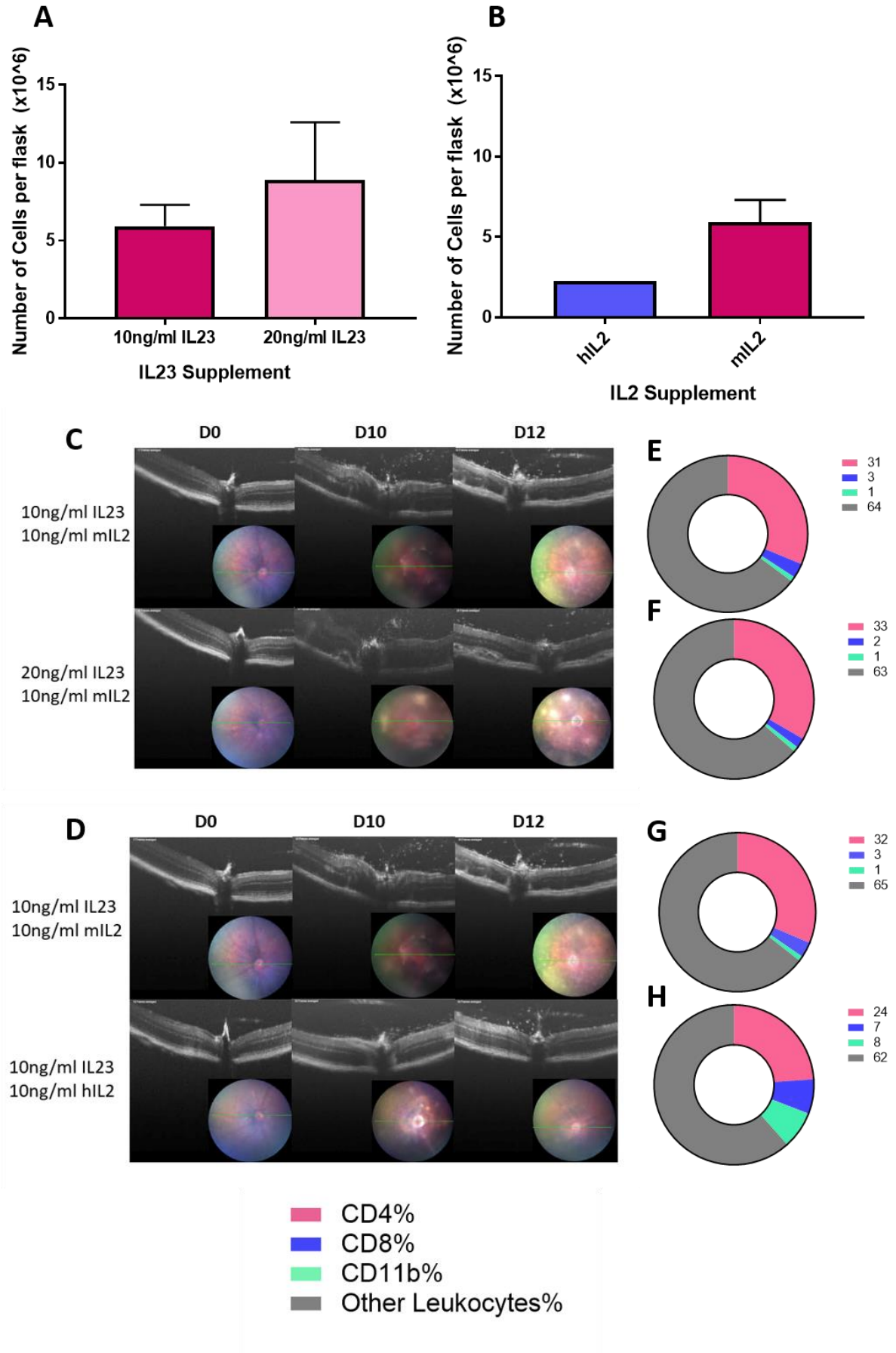
A
Number of Cells per flask (x10^6)
15
10
5
0
10ng/ml IL23
20ng/ml IL23
IL23 Supplement
B
Number of Cells per flask (x10^6)
15
10
5
0
hIL2
mIL2
IL2 Supplement
C
D0
D10
D12
10ng/ml IL23
10ng/ml mIL2
20ng/ml IL23
10ng/ml mIL2
D
D0
D10
D12
10ng/ml IL23
10ng/ml mIL2
10ng/ml IL23
10ng/ml hIL2
E
31
3
1
64
F
33
2
1
63
G
32
3
1
65
H
24
7
8
62
CD4%
CD8%
CD11b%
Other Leukocytes%

Figure 3.2: Effects of cytokines added to the in vitro step of adoptive transfer protocol

(A) Quantification of cells recovered from cultures with varying concentrations of IL-23 (10ng/ml and 20ng/ml) (Mean ± SEM) (B) Quantification of cells from cultures with murine or human IL-2 species origin (10ng/ml) (Mean ± SEM) (C) Representative OCT time course of clinical disease in recipients that received cell transfers from cultures primed with varying concentrations of IL-23 (10ng/ml or 20ng/ml) $2x10^6$ transferred per recipient. OCT image acquired through optic disc (green line on fundal image) (D) Representative OCT time course of clinical disease in recipients that received cell transfers from cultures primed with murine or human IL-2 at 10ng/ml $2x10^6$ transferred per recipient. OCT image acquired through optic disc (green line on fundal image) (E-H) Corresponding cell culture analysis of cells transferred into naïve recipients from cultures used to optimise cytokine addition, percentage of CD4+ T cells, CD8+ T cells, CD11b+ cells and other leukocytes from the transferred population.
Cell cultures and transfers performed in 3-6 replicate.

3.3.2 Analysis of clinical disease using OCT

OCT is very useful in monitoring clinical disease progression in recipients and matching disease severity across recipients.

In order to compare disease across recipients in one experiment and compare recipients across experiments, a standardised way of acquiring OCT needed to be developed.

Firstly, day 0 OCT was acquired before inducing disease to check if recipients are normal before cell transfer. At this stage the retinal layers are clearly visible and easily distinguished (Figure 3.3). The corresponding fundal imaging shows by the green scanning line where the OCT is taken and a clear fundus before disease induction (Figure 3.3). In the OCT image (Figure 3.3) the vitreous has no infiltrate and the optic disc is not swollen.

OCT was taken from each mouse at exactly the same points in each experiment for each eye which include a 0° horizontal line through the optic disc, a 90° vertical line through the optic disc, a circle around the optic disc and a volume scan around the optic disc (Figure 3.4b, Figure 3.5a).

In comparsion to the day 0 OCT (Figure 3.3), a diseased OCT (Figure 3.4a) shows lots of retinal infiltrate and a swollen optic disc along with a fundal image containing vitreal haze (Figure 3.4b). The line scans allow acquisition of a 2D image through the optic disc but in order to obtain more information for quantification of disease a 3D cube around the optic disc allows a more complete assessment of the inifltrate within diseased retinas.

A 3D volume scan was taken around the optic disc of the recipients at each time point to quantify disease course between different disease groups and at different time points, each cube was then made into a 3D video showing retinal infiltrate (Figure 3.5a-b).

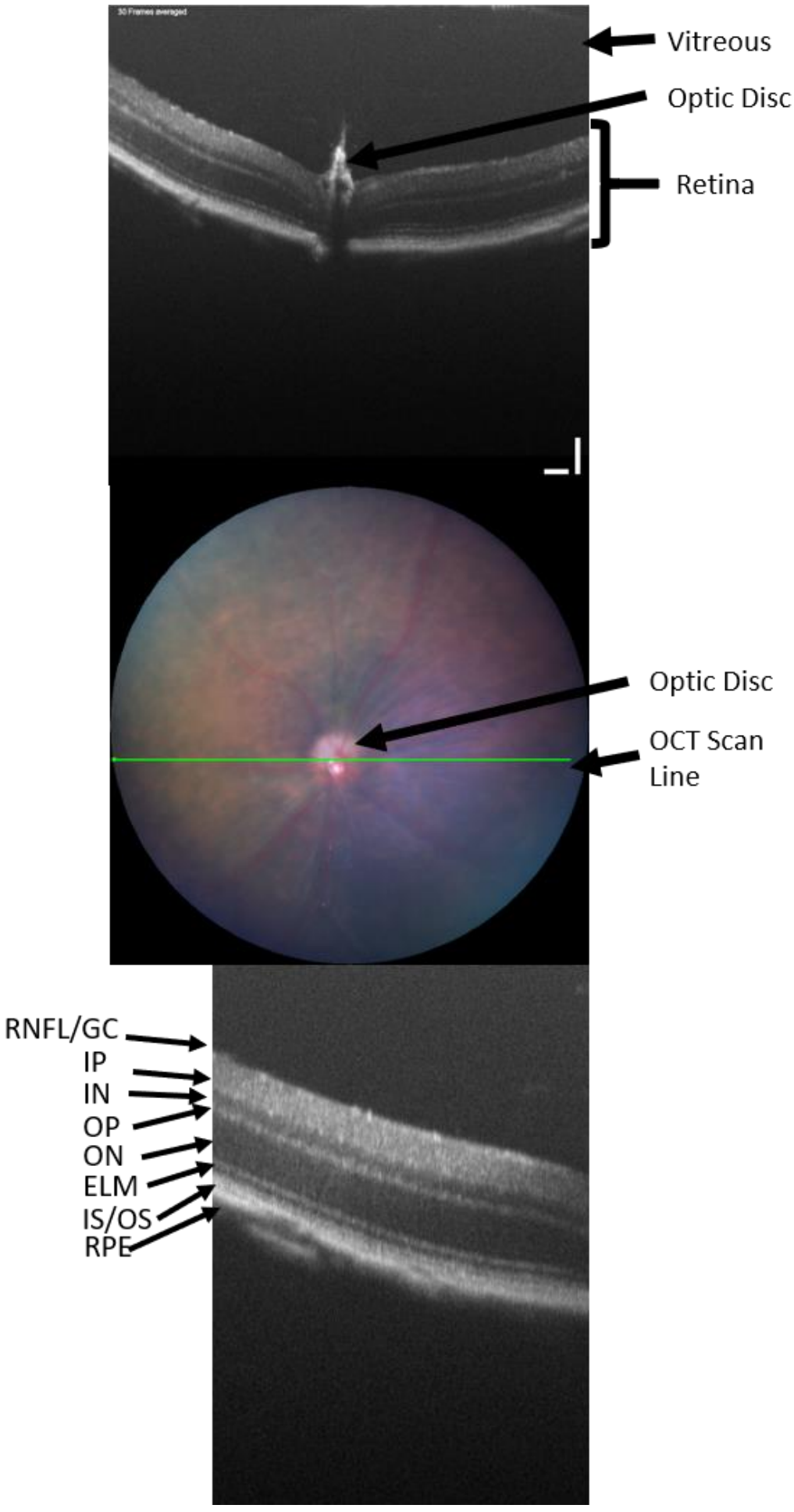
30 Frames averaged
Vitreous
Optic Disc
Retina
Optic Disc
OCT Scan Line
RNFL/GC
IP
IN
OP
ON
ELM
IS/OS
RPE

Figure 3.3: Baseline OCT images for standardisation throughout and across experiments. Baseline normal OCT taken at day 0 (A), corresponding fundus imaging taken with OCT image, the green line denotes where the OCT is taken from (B). Full description of retinal layers observed within the OCT image (C).

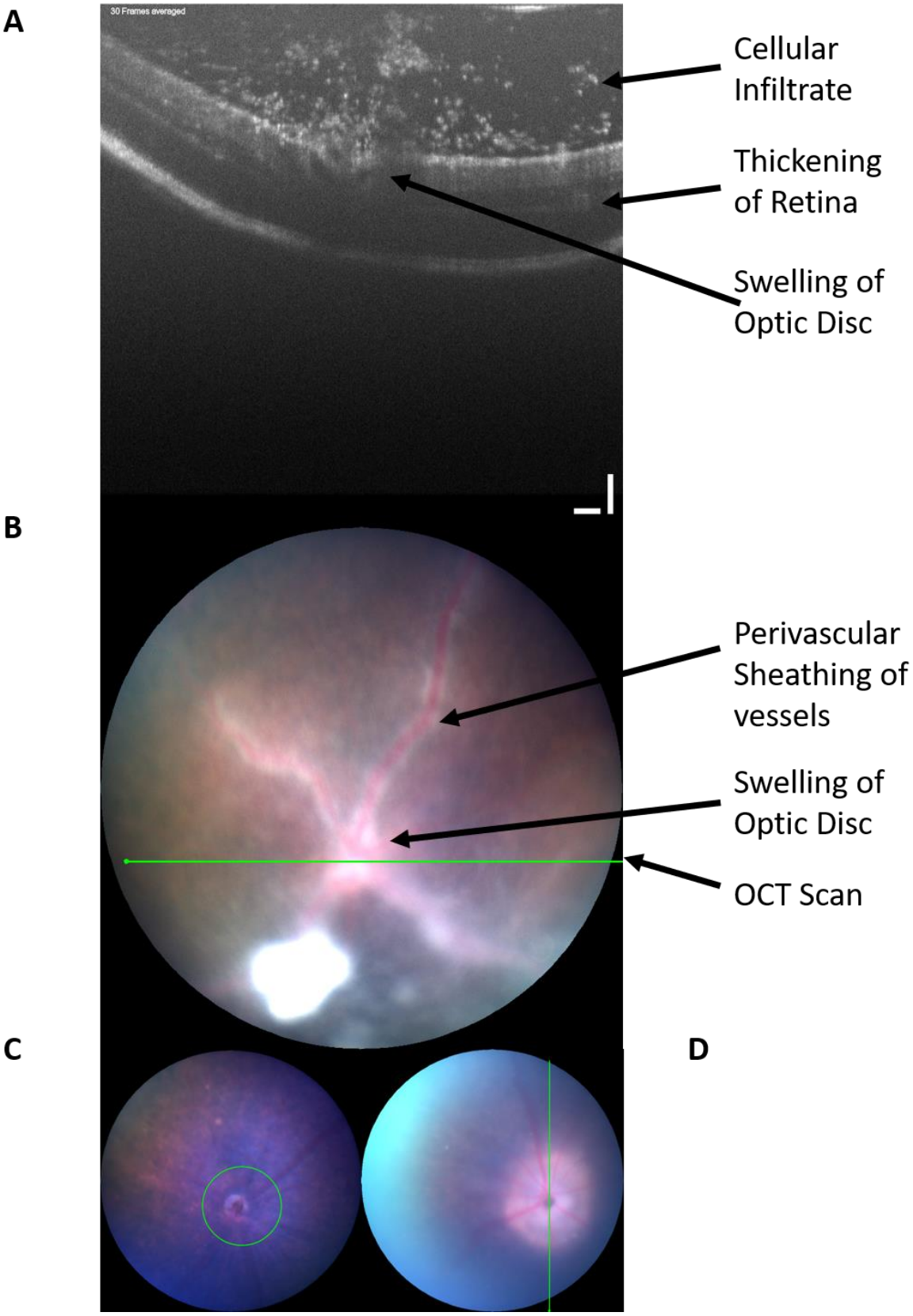
A
30 Frames averaged
Cellular Infiltrate
Thickening of Retina
Swelling of Optic Disc
B
Perivascular Sheathing of vessels
Swelling of Optic Disc
OCT Scan
C
D

Figure 3.4: Diseased OCT of adoptive transfer recipients illustrating full OCT acquisition method. Retinal infiltrate is observed within the vitreous corresponding with a thickening retina and swollen optic disc with corresponding fundus image showing a vitreous haze and sheathing of immune infiltrate along vessels (A-B). Along with a 0° line scan a 90°-line scan and a circle around the optic disc are also taken at each time point (C-D).

A

B

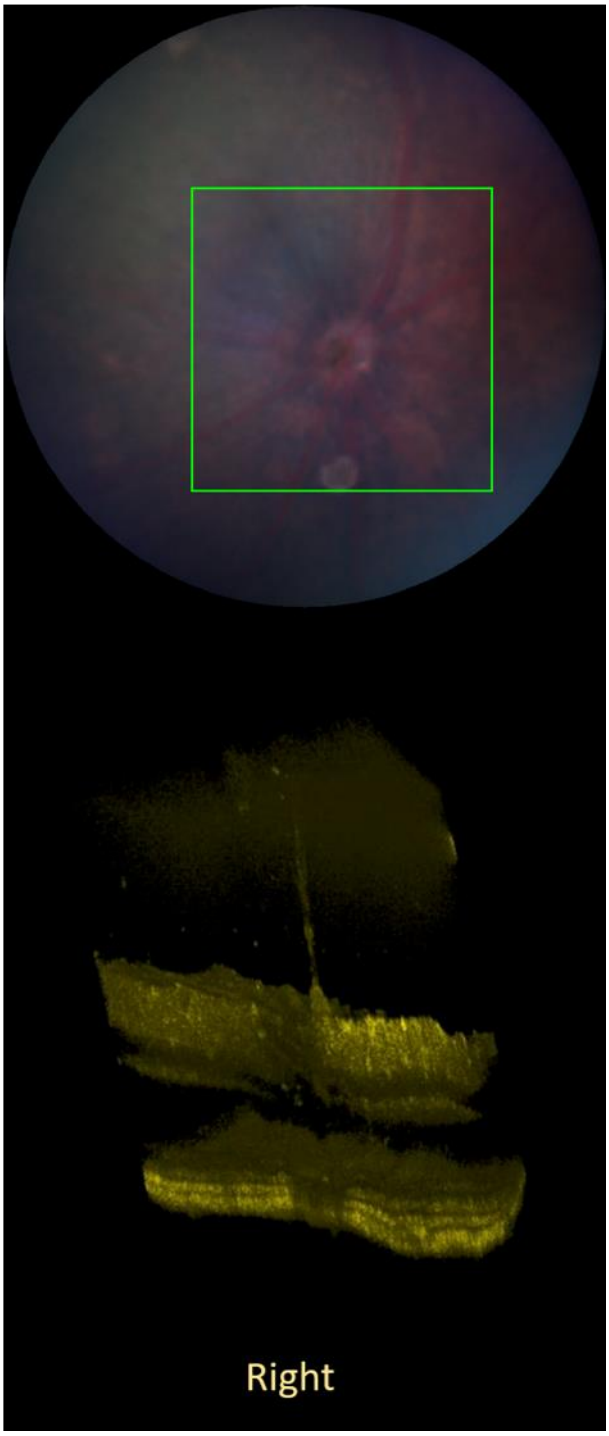

Figure 3.5: 3D volume OCT acquisition and video. To acquire a 3D volume the optic disc is once again used as a reference point to acquire around a fundus image was also taken to illustrate cube placement on each eye (A). The cube is the acquired by the OCT made up of 512 individual slices which can be made into a video of a 3D model and eyes compared (B).

3.3.3 Preliminary analysis of clinical disease produced by using the optimised adoptive transfer model

Optimisation of the cell culture step in the adoptive transfer protocol produced disease with an incidence and severity that allowed preliminary analysis of the disease induced in naïve recipients. In previous studies, induction of disease using adoptive transfer in C57BL/6 mice needed a cell transfer of ~50-100x10^6 total leukocytes to cause disease that developed at day 7 by fundal imaging and histopathology (117, 183).

Using the conditions optimised from figure 1 and 2, preliminary analysis of disease induced by adoptive transfer could be done using techniques such as TEFI, OCT, Flow Cytometry and Immunohistochemistry (Figures 3.6-3.8).

Cells were transferred as total leukocyte populations into naïve C57BL/6 mice at different cell numbers intraperitoneally, resuspended in PBS ranging from 5x10^4 – 4x10^6 cells per recipient (figure 3.6a-i). The cell number that gave a high disease incidence and a moderate clinical disease phenotype was 2x10^6 per recipient (figure 3.6b and figure 3.6j and 3.6k).

Flow cytometric analysis of recipients at peak disease (day 7 and day 14) using allelic markers illustrated the ability to track cells in the endogenous and transferred cells using the markers (Figure 3.8a).

The percentages of CD4+ and CD8+ T cells that are endogenous and transferred at each of the time points during clinical disease (Figure 3.8b-3.8e) can be calculated using the gating strategy in figure 3.8a.

Further analysis of sections of whole eyes can be achieved using immunohistochemistry staining for CD3, CD4 and CD8 to analyse where in the tissue the cells reside (Figure 3.7a and 3.7b)

All methods combined can allow for in vivo analysis of clinical disease by imaging followed by quantitative analysis of endogenous and transferred cells at specific time points as well as frozen sections taken from OCT embedded whole eyes or whole mounts to analyse location of cells within the tissue.

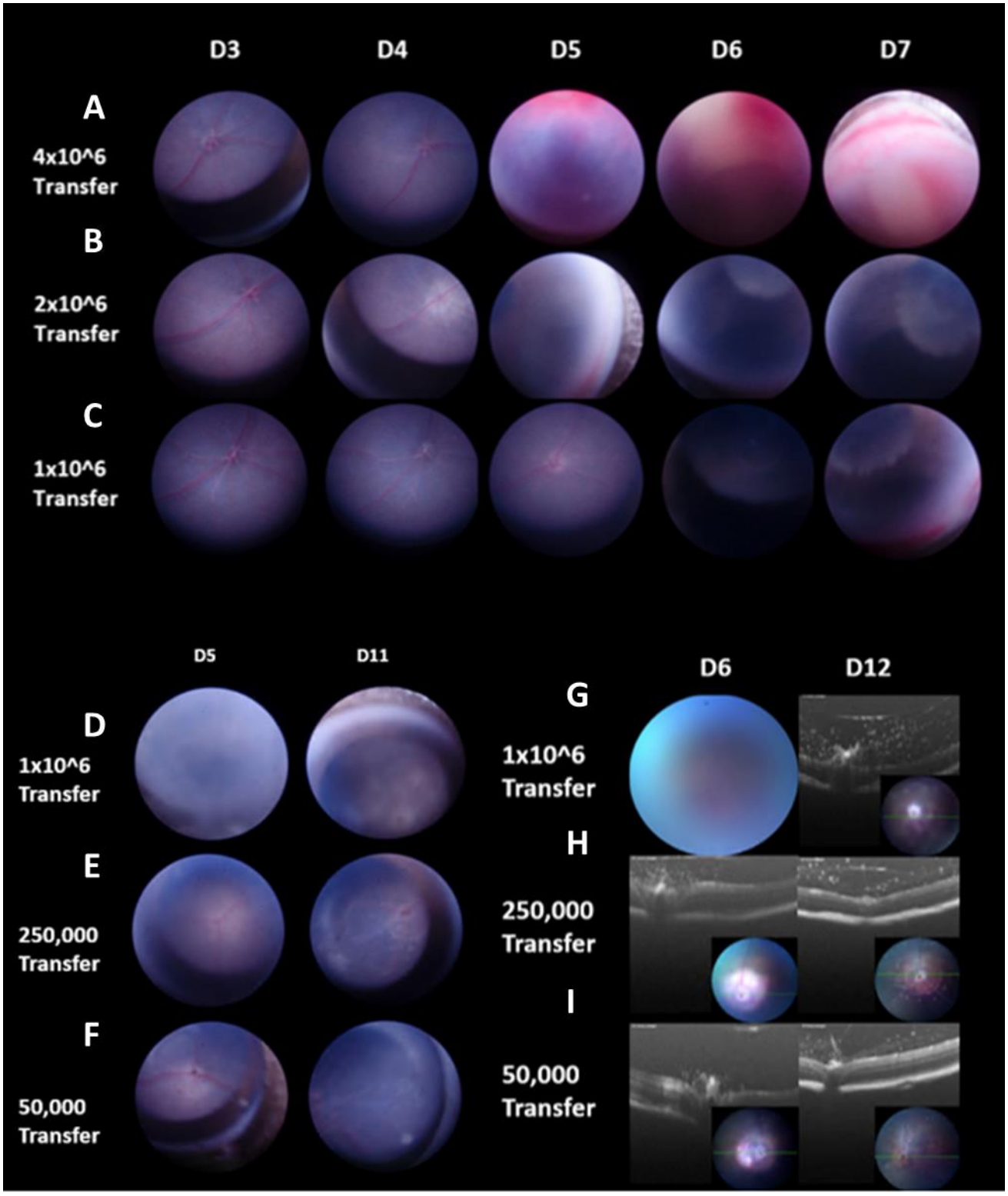
D3
D4
D5
D6
D7
A
4x10^6
Transfer
B
2x10^6
Transfer
C
1x10^6
Transfer
D5
D11
D
1x10^6
Transfer
E
250,000
Transfer
F
50,000
Transfer
D6
D12
G
1x10^6
Transfer
H
250,000
Transfer
I
50,000
Transfer

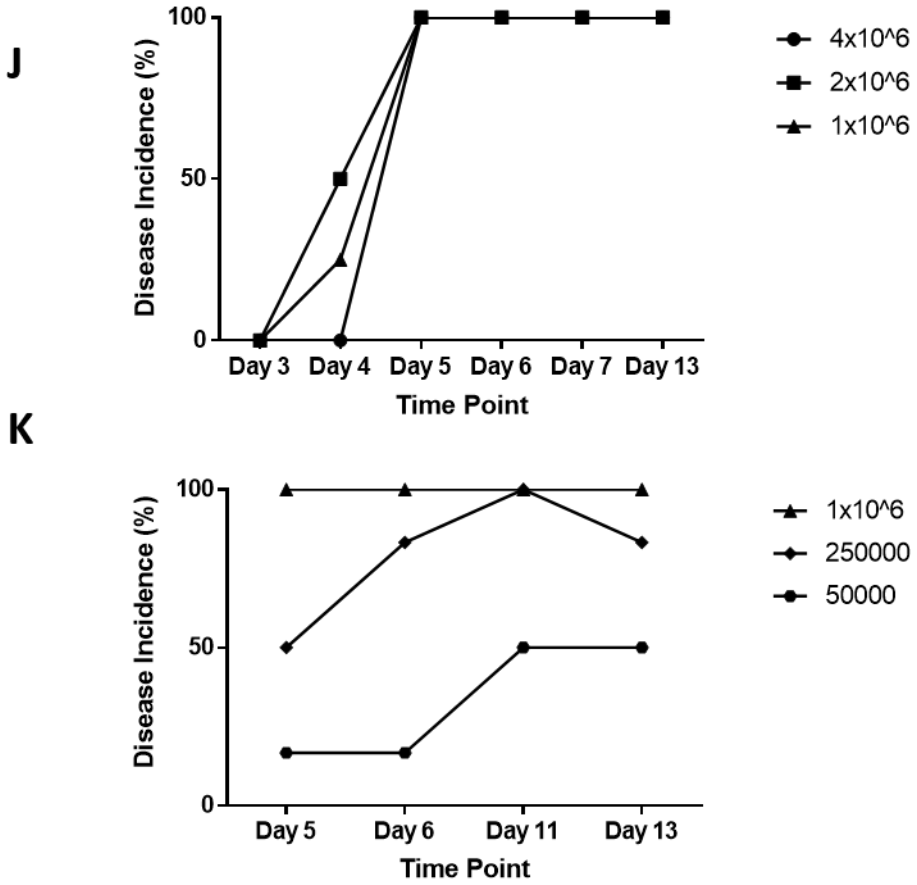

Figure 3.6: Analysis of disease severity and incidence using TEFI and OCT after adoptive cell transfer of primed uveitogenic cells into naïve recipients. (A-C) Representative TEFI time course from day 3 to day 7 after transfer of uveitogenic cells into naïve recipients, cells are transferred as total leukocytes at $4x10^6$, $2x10^6$ or $1x10^6$ per recipient. (D-F) Representative TEFI time course from day 5 to day 11 after transfer of uveitogenic cells into naïve recipients, cells are transferred at $1x10^6$, 250,000 or 50,000 per recipient. (G-I) Corresponding OCT time course of clinical disease illustrating clinical features of disease using OCT imaging alongside fundal imaging. (J) Percentage of disease incidence in recipients that received $4x10^6$, $2x10^6$ or $1x10^6$ transferred uveitogenic cells calculated using TEFI imaging throughout clinical disease. (K) Percentage of disease incidence in recipients that received $1x10^6$, 250,000 or 50,000 transferred uveitogenic cells.

Transfer recipients >3 per group.

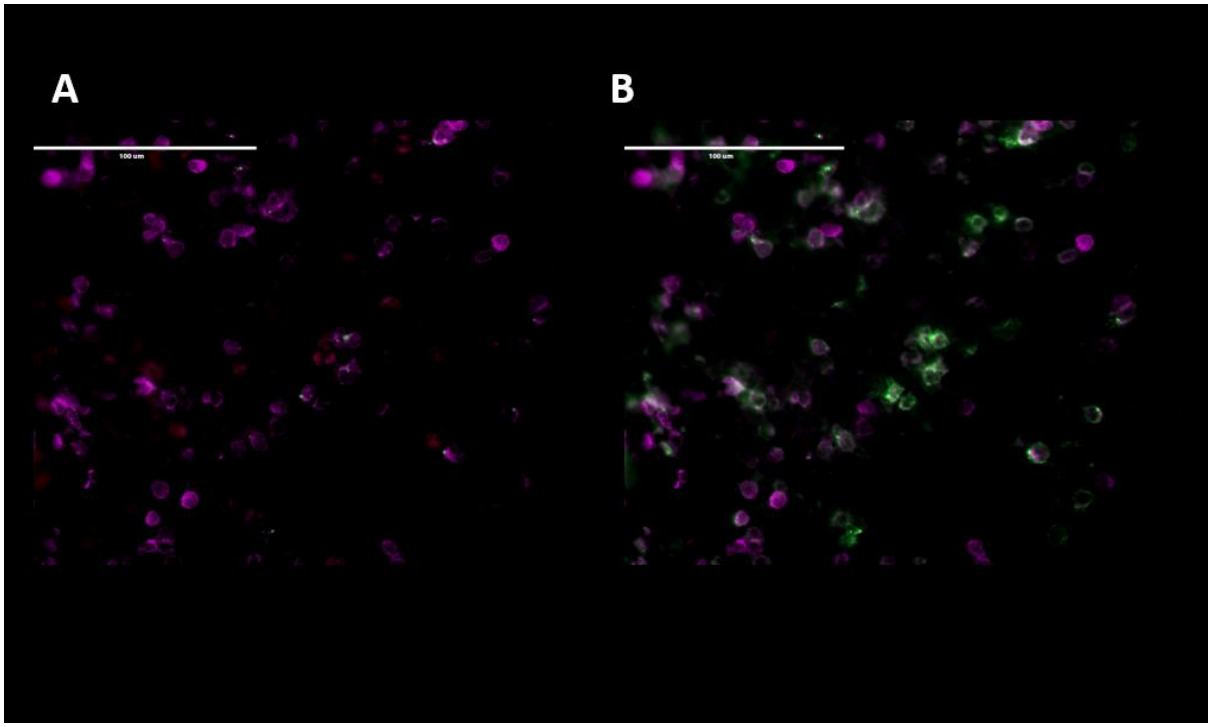

Figure 3.7: Immunohistochemistry allows detection of CD3+ CD4+ and CD3+ CD8+ T cells within sections of whole tissue. (A) Co-staining of CD3+ CD8+ T cells within sections of eyes from recipients of adoptive transfer of uveitogenic cells at day 7 (Magenta-CD3, Red-CD8) (B) Co-staining of CD3+ CD4+ T cells within sections of eyes from recipients of adoptive transfer of uveitogenic cells at day 7 (Magenta-CD3, Green-CD4). (100µm scale bars).

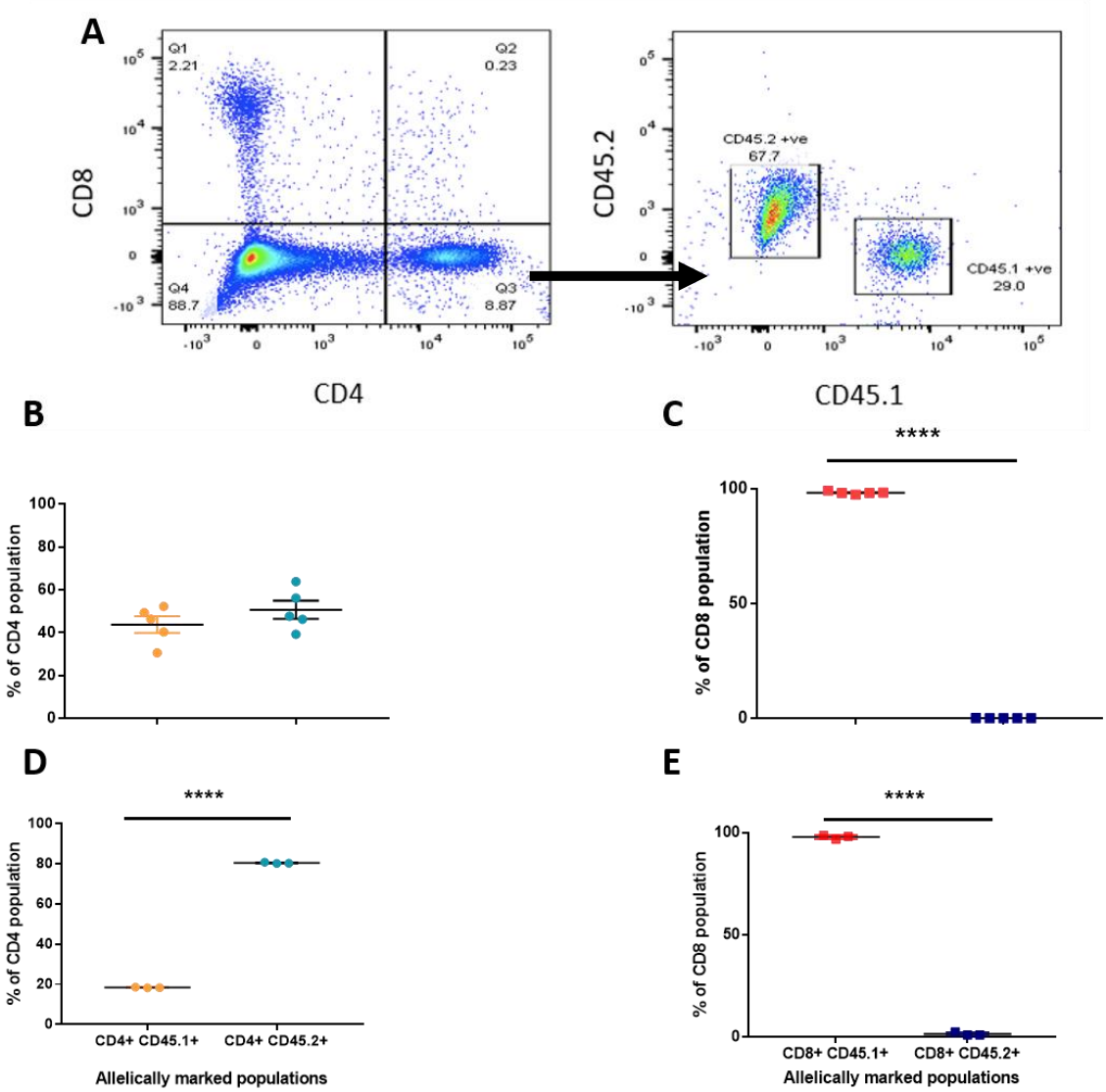

Figure 3.8: Preliminary analysis of disease induced using adoptive transfer using flow cytometry. (A) Exemplar gating strategy used for flow cytometry analysis, firstly gate for CD4+ and CD8+ cells then gate using allelic markers CD45.1+ and CD45.2+ to detect endogenous and transferred CD4+ and CD8+ T cells. (B-C) Percentage of total CD4+ and CD8+ T cells that express CD45.1 (Endogenous) or CD45.2+ (Transferred) at day 7. (D-E) Percentage of total CD4+ and CD8+ T cells that express CD45.1+ (Endogenous) or CD45.2+ (Transferred) at day 14.

3.3.4 Characterisation of transferred cells using extracellular and intracellular staining

When cells were transferred into naïve recipients using the optimised cell culture conditions disease was induced with as few as 50,000 cells but the most robust cell number for disease incidence and severity was $2x10^6$ cells transferred per recipient.

A more detailed analysis of transferred cells (Figure 3.9) and supernatant from the cell cultures (Figure 3.10) allowed further study of the phenotype of disease-causing cells that were being injected into the recipients.

As EAU is mediated by CD4+ T cells specific for retinal antigens that secrete cytokines and chemokines within the eye during disease (184), analysing the concentration of cytokines that are secreted within the supernatant of the cultures before transfer (Figure 3.9) specifically that are involved in polarising the culture especially CD4+ T cells to a Th1 and Th17 phenotype such as IFN-γ and IL-17 are valuable for understanding what cells are being transferred in the total leukocyte population.

Flow cytometric analysis of cells from different donor mice using extracellular staining to look for markers such as CD4, CD8 and CD11b alongside intracellular cytokine staining to analyse CD4 T cell phenotype for cytokines such as IFN-γ, IL17 and FoxP3 was used to investigate transferred T cell phenotypes (Th1, Th17 or Treg).

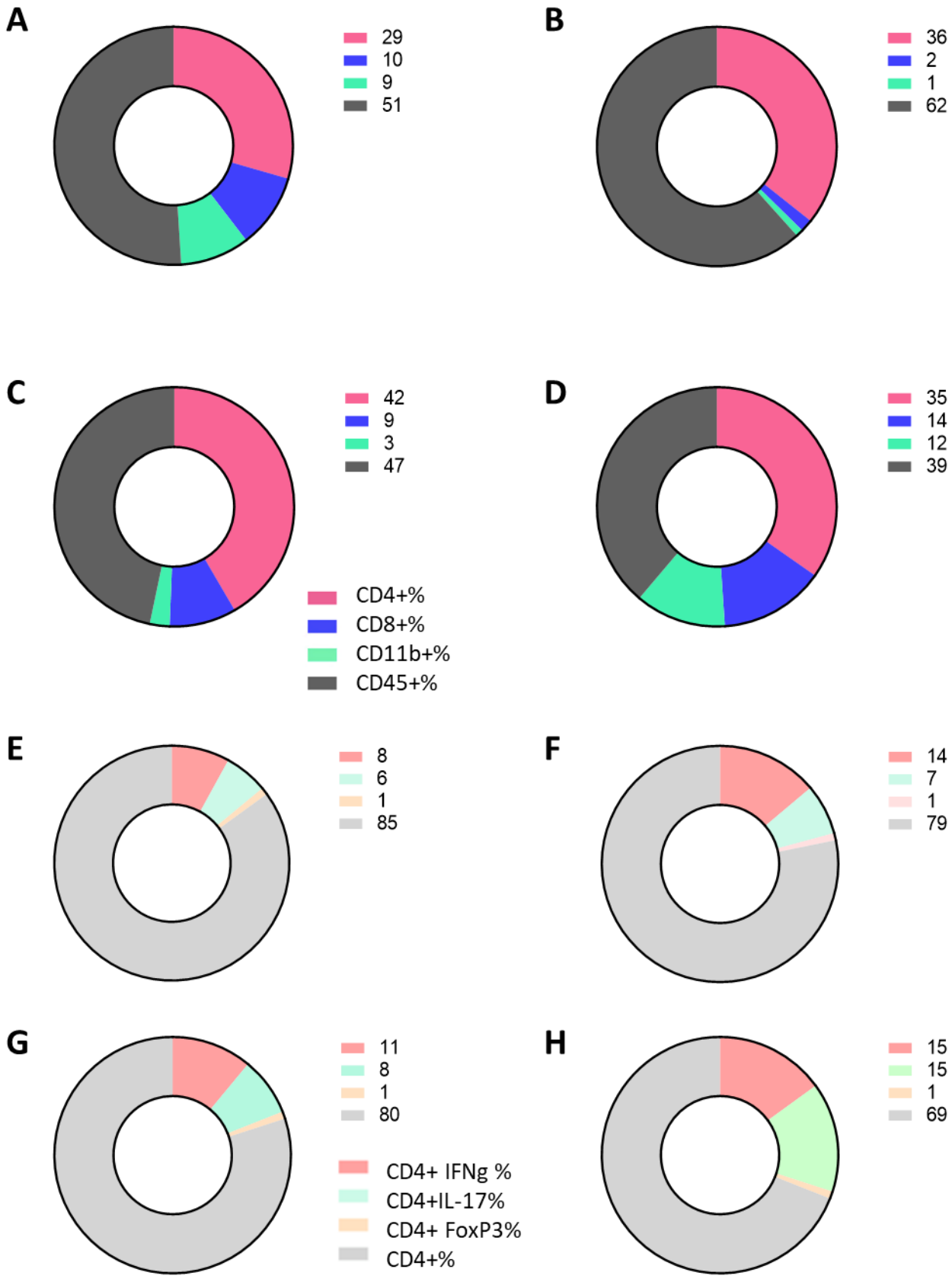
A
29
10
9
51
B
36
2
1
62
C
42
9
3
47
CD4+%
CD8+%
CD11b+%
CD45+%
D
35
14
12
39
E
8
6
1
85
F
14
7
1
79
G
11
8
1
80
CD4+ IFNg %
CD4+IL-17%
CD4+ FoxP3%
CD4+%
H
15
15
1
69

Figure 3.9: Extracellular and intracellular analysis of adoptive transfer cell cultures from different donor mice. (A-D) Extracellular staining of cultures obtained spleen and lymph nodes from different donor mice at day 11 after immunisation and 72 hours in vitro culture. (A) Donor cells obtained from a CX3CR1 heterozygous knockout (B) Donor cells obtained from a CX3CR1 knockout (C) Donor cells obtained from OTII TCR transgenic mouse (D) Donor cells obtained from Ly5 (WT). (E-H) Intracellular staining of cultures obtained from spleen and lymph nodes from different donor mice at day 11 after immunisation and 72 hours in culture, cells were re-stimulated with PMA and Ionomycin for 4 hours at 37°C before extracellular staining was performed then cells were fixed and intracellular staining performed for FACS analysis. Populations shown include, CD4+, CD4+ IL-17+, CD4+ IFN-γ+ and CD4+ FoxP3+. (E) Donor cells obtained from CX3CR1 heterozygous knockout (F) Donor cells obtained from CX3CR1 knockout (G) Donor cells obtained from OTII TCR transgenic mouse (H) Donor cells obtained from Ly5 (WT).
Cells obtained from >5 cell cultures per strain.

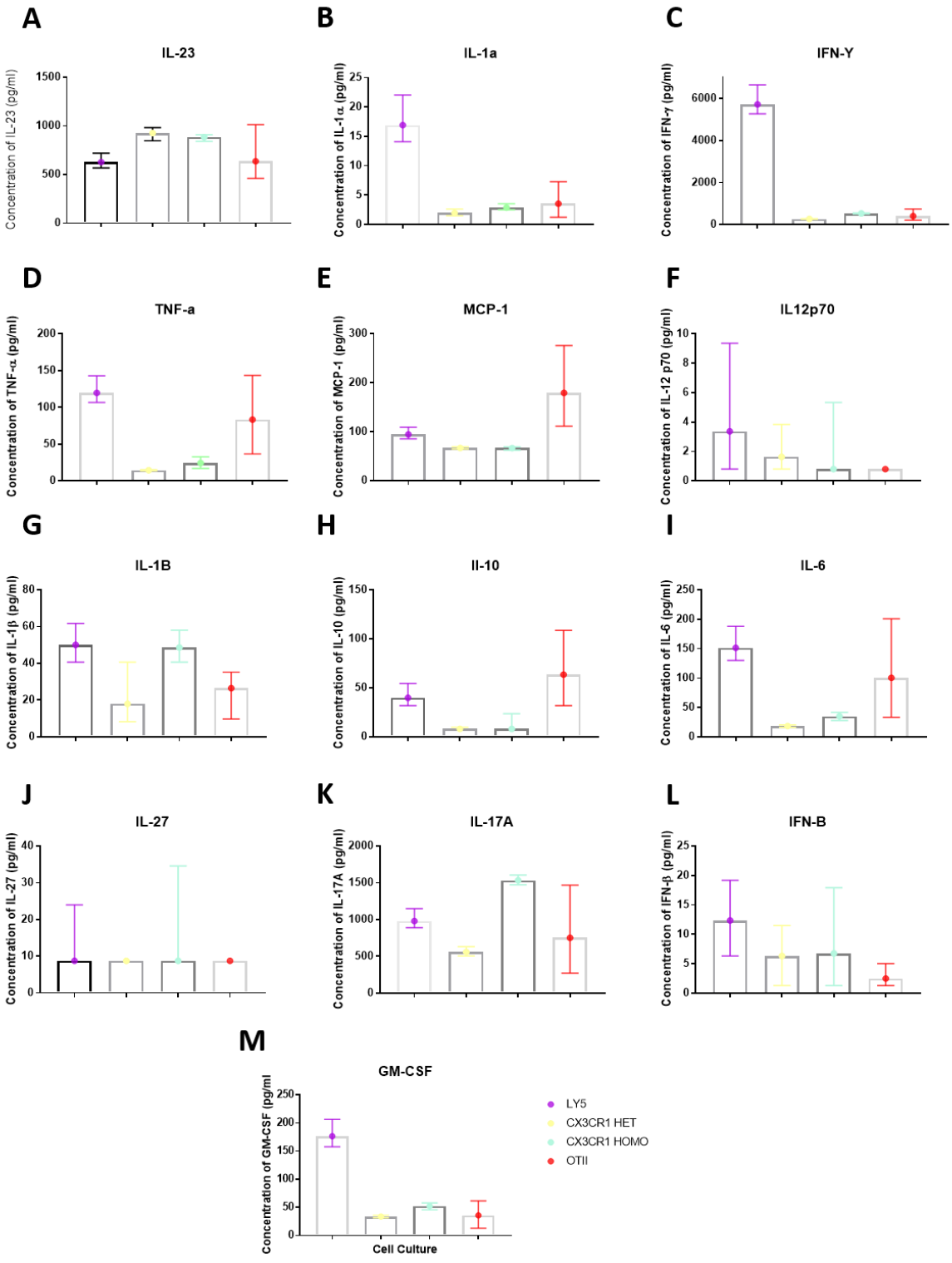
A
IL-23
Concentration of IL-23 (pg/ml)
1500
1000
500
0
B
IL-1a
Concentration of IL-1α (pg/ml)
25
20
15
10
5
0
C
IFN-Y
Concentration of IFN-γ (pg/ml)
6000
4000
2000
0
D
TNF-a
Concentration of TNF-α (pg/ml)
200
150
100
50
0
E
MCP-1
Concentration of MCP-1 (pg/ml)
300
200
100
0
F
IL12p70
Concentration of IL-12 p70 (pg/ml)
10
8
6
4
2
0
G
IL-1B
Concentration of IL-1β (pg/ml)
80
60
40
20
0
H
Il-10
Concentration of IL-10 (pg/ml)
150
100
50
0
I
IL-6
Concentration of IL-6 (pg/ml)
250
200
150
100
50
0
J
IL-27
Concentration of IL-27 (pg/ml)
40
30
20
10
0
K
IL-17A
Concentration of IL-17A (pg/ml)
2000
1500
1000
500
0
L
IFN-B
Concentration of IFN-β (pg/ml)
25
20
15
10
5
0
M
GM-CSF
Concentration of GM-CSF (pg/ml)
250
200
150
100
50
0
Cell Culture
LY5
CX3CR1 HET
CX3CR1 HOMO
OTII

Figure 3.10: Legend Plex analysis of culture supernatant from donor cells. (A-M) Supernatant acquired from cell cultures from different donors: Ly5 (WT), CX3CR1 heterozygous knockout, CX3CR1 knockout which were pathogenic on transfer and OTII (TCR transgenic) cells which are activated used for adoptive transfer to induce EAU and analysed using 13-plex Legend Plex assay. (A) Concentration of IL-23 in supernatant of donor cell cultures (pg/ml) (B) Concentration of IL-1α in supernatant of donor cell cultures (pg/ml) (C) Concentration of IFN-γ in supernatant of donor cell cultures (pg/ml) (D) Concentration of TNF-α in the supernatant of donor cell cultures (pg/ml) (E) Concentration of MCP-1 in supernatant of donor cell cultures (pg/ml) (F) Concentration of IL-12p70 in supernatant of donor cell cultures (pg/ml) (G) Concentration of IL-1β in supernatant of donor cell cultures (pg/ml) (H) Concentration of IL-10 in supernatant of donor cell cultures (pg/ml) (I) Concentration of IL-6 in supernatant of donor cell cultures (pg/ml) (J) Concentration of IL-27 in donor cell cultures (pg/ml) (K) Concentration of IL-17A in donor cell cultures (pg/ml) (L) Concentration of IFN-β in donor cell cultures (pg/ml) (M) Concentration of GM-CSF in donor cell cultures (pg/ml).
Supernatant analysed from 3 cultures of each mouse strain.

3.3.5 Analysis of cross reactivity between peptides causing upregulation of cytokines in splenocytes in vitro after immunisation

The diversification of the immune response that is induced by a tissue to a new T cell and/or antibody specificities during an autoimmune disease is known as epitope spreading (185). Epitope spreading can be defined as the development of immune responses to endogenous epitopes after the release of antigens during an autoimmune response. Evidence has been found to support a major role of epitope spreading in the pathogenesis of chronic EAE (186). Multiple factors are involved in the induction of epitope spreading including enhanced display of previously cryptic determinants under the local inflammatory and cytokine environment. These follow tissue damage alongside differences in the size of the epitope specific T cell subsets (185). Evidence from studies in autoimmune disease shows that disease progression may be due to an activation of autoreactive lymphocytes, regardless of the event that initiated them (186, 187). These autoreactive lymphocytes are specific to epitopes that are distinct from and non-cross-reactive with disease inducing epitopes that result in chronic tissue damage (186, 187). The broadening of the immune response can target epitopes either within the same antigen known as intramolecular spreading or another antigen known as intermolecular spreading (185).

Mice were immunised with RBP3 peptide and spleens isolated at day 11, all cultures were stimulated in culture with IL-23 (10ng/ml) at 0 hours and IL-2 (10ng/ml) at 24 hours. At this stage it may be considered too early to observe epitope spreading as the immunised mice have not reached peak clinical disease. The cultures were split at 0 hours and one of 3 peptides were added OVA, RBP3 629-643 or RBP3 1-20 at varied concentrations of 0.1µg/ml, 1µg/ml, 10µg/ml or 100µg/ml. This data shows no evidence of epitope spreading at the time of adoptive transfer but further experimentation into the transferred and endogenous CD4+ populations present in the eyes of recipients during peak disease could be used to further look into epitope spreading when using the adoptive transfer technique.

Overall, stimulation in vitro with RBP3 629-643 gives an increase in secretion of IFN-γ and IL-17 compared to OVA and RBP3 1-20. There is also a correlation between increase of concentration of peptide causing increase in secretion of IFN-γ and IL-17 suggesting an increase of Th1 and Th17 CD4+ T cells within the culture (Figure 3.11a and 3.11b). The same response is observed in several cytokines not associated with CD4+ T cell phenotype (Figure 3.11).

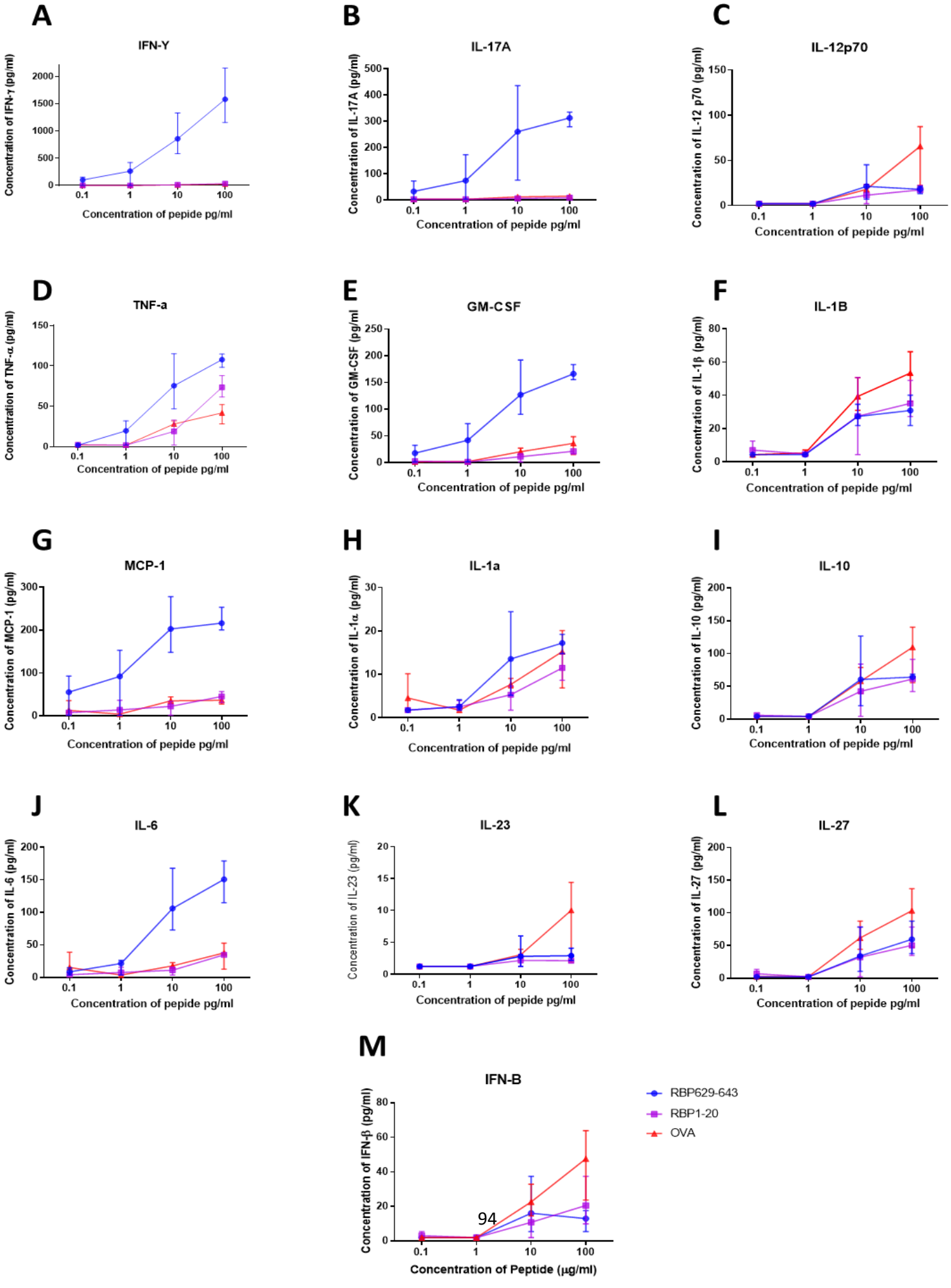
A
IFN-Y
Concentration of IFN-γ (pg/ml)
Concentration of pepide pg/ml
B
IL-17A
Concentration of IL-17A (pg/ml)
Concentration of pepide pg/ml
C
IL-12p70
Concentration of IL-12 p70 (pg/ml)
Concentration of pepide pg/ml
D
TNF-a
Concentration of TNF-α (pg/ml)
Concentration of pepide pg/ml
E
GM-CSF
Concentration of GM-CSF (pg/ml
Concentration of pepide pg/ml
F
IL-1B
Concentration of IL-1β (pg/ml)
Concentration of pepide pg/ml
G
MCP-1
Concentration of MCP-1 (pg/ml)
Concentration of pepide pg/ml
H
IL-1a
Concentration of IL-1α (pg/ml)
Concentration of pepide pg/ml
I
IL-10
Concentration of IL-10 (pg/ml)
Concentration of pepide pg/ml
J
IL-6
Concentration of IL-6 (pg/ml)
Concentration of pepide pg/ml
K
IL-23
Concentration of IL-23 (pg/ml)
Concentration of pepide pg/ml
L
IL-27
Concentration of IL-27 (pg/ml)
Concentration of pepide pg/ml
M
IFN-B
Concentration of IFN-β (pg/ml)
Concentration of Peptide (μg/ml)
RBP629-643
RBP1-20
OVA

Figure 3.11: Analysis of antigen specificity in splenocytes obtained from C57BL/6 mice 11 days after immunisation with RBP3 (629-643) peptide using 13-plex Legend Plex analysis. (A-M) Supernatant obtained from 72 hour splenocyte culture from mice immunised with RBP3 (629-643) at day 11, supplemented with 10ng/ml IL-23 and 10ng/ml IL-2 and either RBP3 (629-643) (blue) RBP 1-20 (purple) or OVA (red) peptide. (A) Concentration of IFN-γ in splenocyte cultures supplemented with each peptide (pg/ml) (B) Concentration of IL-17A in splenocyte cultures supplemented with each peptide (pg/ml) (C) Concentration of IL-12p70 in splenocyte cultures with each peptide (pg/ml) (D) Concentration of TNF-α in splenocyte cultures with each peptide (pg/ml) (E) Concentration of GM-CSF in splenocyte cultures with each peptide (pg/ml) (F) Concentration of IL-1β in splenocyte cultures with each peptide (pg/ml) (G) Concentration of MCP-1 in splenocytes in cultures with each peptide (pg/ml) (H) Concentration of IL-1α in splenocyte cultures with each peptide (pg/ml) (I) Concentration of IL-10 in splenocyte cultures with each peptide (pg/ml) (J) Concentration of IL-6 in splenocyte cultures with each peptide (pg/ml) (K) Concentration of IL-23 in splenocyte cultures with each peptide (pg/ml) (L) Concentration of IL-27 in splenocyte cultures with each peptide (pg/ml) (M) Concentration of IFN-β in splenocyte cultures with each peptide (pg/ml).
Supernatant obtained from 3 separate samples for each peptide concentration.

3.3.6 Transfer of pathogenic cells into immunocompromised mice causes severe clinical disease

When uveitogenic T cells are transferred into wildtype mice, the recipients develop clinical disease that peaks at day 7-10 (Figure 3.6). Analysis of retinal infiltrate by flow cytometry illustrates a recruitment of both endogenous and transferred CD4+ T cells in similar numbers to the eye during peak clinical disease (Figure 3.8). But in the CD8+ compartment a large number of endogenous cells are recruited but transferred cells do not appear to survive or proliferate and recruit to the eye during active clinical disease (Figure 3.8).

To understand if the transferred cells alone are sufficient to cause clinical disease without recruiment of endogenous T cells, a pathogenic transfer into immunocomprimised mice was undertaken.

RAG2$^{-/-}$ mice lack mature T and B cells so will not have an endogenous repsonse to the transfer of pathogenic T cells.

When a whole leukocyte population of pathogenic wildtype cells are transferred into RAG2$^{-/-}$ mice, clinical disease is induced by day 7 similar to the previous transfers (Figure 3.6) but by day 14 a more severe disease is observed in the RAG2$^{-/-}$ recipients in comparison to the wildtype recipients. When retinal infiltrate was analysed by flow cytometry, an increase of CD4+ T cells is observed between day 7 and day 14. In the CD8+ T cell compartment an expansion and recruitment of transferred cells is observed at day 7 and day 14 within the retinal infiltrate, showing that CD8+ T cells survive within recipients that are immunocompromised and may play a part in the disease process, but this is not the case within wildtype recipients (Figure 3.12).

Due to the expansion of CD8+ T cells within RAG2$^{-/-}$ recipients, to assess if CD4+ T cells alone were sufficient to induce disease, a pure population of CD4+ T cells were transferred to these mice. A CD4 negative MACS isolation was used to isolate CD4+ T cells, when the population was analysed by flow cytometry a small population of other leukocytes such as CD8+ cells was detected within the transferred cell population (Figure 3.13) the CD4+ population was >65% compared to previous cultures with no MACS isolation where the percentage of CD4+ cells was ~35% (Figure 3.6). After transfer, clinical disease incidence and severity was analysed using in vivo imaging. By day 7 both the CD4+ and CD4- transfers developed clinical disease (Figure 3.13h), at day 22 eyes were analysed by flow cytometry to quantify leukocyte populations within the retina (Figure 3.13i-k).

Due to the RAG2$^{-/-}$ recipients developing clinical disease after MACS isolation of a CD4- leukocyte population (Figure 3.13), a purer CD4- CD8+ cell population was prepared using a CD4- MACS seperation that was then sorted using fluorescent associated cell sorting to isolate a CD8+ population for adoptive transfer. Recipients were monitored using clinical imaging to day 28, the CD4+ transferred population caused clinical disease to occur by day 7 after transfer with disease continuing through to day 28. Whereas, the CD8+ transfer did not induce clinical disease observed by clinical imaging fom day 7 through to day 28 (Figure 3.14a-h) when retinal infiltrate was analysed by flow cytometry at day 28 a small CD4+ population could be detected in the CD8+ transfer suggesting an expansion of the small CD4+ population that after MACS isolation and FACS sorting still was present in the CD4- CD8+ population transferred into RAG2$^{-/-}$ recipients (Figure 3.14i-k).

Finally to study, leukocyte trafficking of CD4+ T cells within the eyes of recipients in RAG2$^{-/-}$ mice intravitreal injections of MACS isolated CD4+ T cells were injected into the left eye of recipients. The recipients were then monitored using the micron IV with fluorescent filters to track transferred CAG GFP expressing cells from the left eye to the right eye over time (Figure 3.15a-i). Clinical disease was not observed through clinical imaging to day 28 (Figure 3.15a-i), at day 28 analysis of retinal infiltrate illustrated a small population of CD4+ T cells was present in both eyes along with blood, spleen and lymph node (Figure 3.15j-n) but an increased number of CD4+ T cells were found in the eye that received the CD4+ population transfer in comparison to the contra lateral eye as expected.

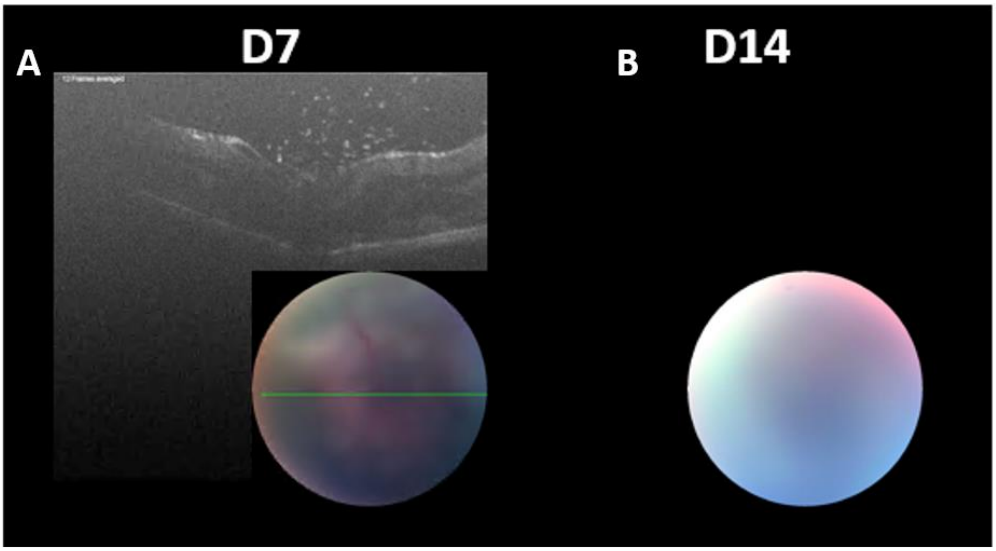
A
D7
B
D14

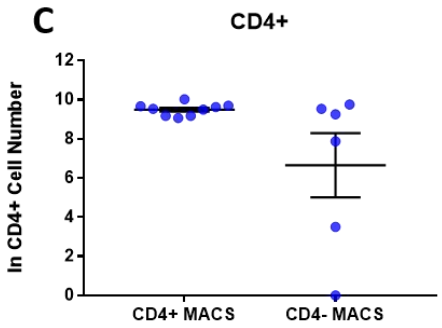
C
CD4+
ln CD4+ Cell Number
12
10
8
6
4
2
0
CD4+ MACS
CD4- MACS

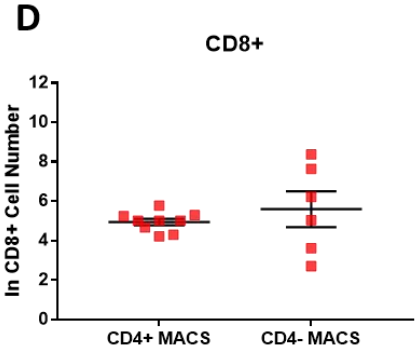
D
CD8+
ln CD8+ Cell Number
12
10
8
6
4
2
0
CD4+ MACS
CD4- MACS

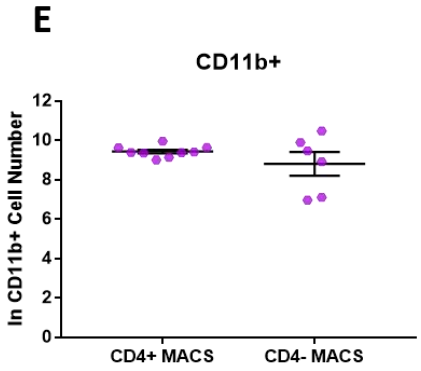
E
CD11b+
ln CD11b+ Cell Number
12
10
8
6
4
2
0
CD4+ MACS
CD4- MACS

AVERAGE CELL NUMBER

	Day 7	Day 14
CD4	11000	25033
CD8	172	835
CD11B	57720	56339

Figure 3.12: Analysis of transfer of 2x10^{6} Ly5 uveitogenic cells as a whole population of leukocytes isolated using Ficoll density centrifugation into RAG2$^{-/-}$ mice at day 7 and day 14. (A) OCT and fundus imaging of RAG2$^{-/-}$ recipients at day 7 after transfer of uveitogenic cells (B) Fundus imaging of RAG2$^{-/-}$ recipients at day 14 after transfer of uveitogenic cells (C-E) Analysis of eyes taken from RAG2$^{-/-}$ recipients at day 7 and day 14 after transfer using flow cytometry to identify immune cell infiltrate using extracellular markers and absolute numbers to quantify infiltrate. (C) Total number of CD4+ T cells present within the eyes of recipients at day 7 and day 14 after transfer using extracellular staining and absolute numbers protocol (D) Total number of CD8+ T cells present within the eyes of recipients at day 7 and day 14 after transfer using extracellular staining and absolute numbers protocol (E) Total number of CD11b+ cells present in retinal infiltrate of recipients at day 7 and day 14.

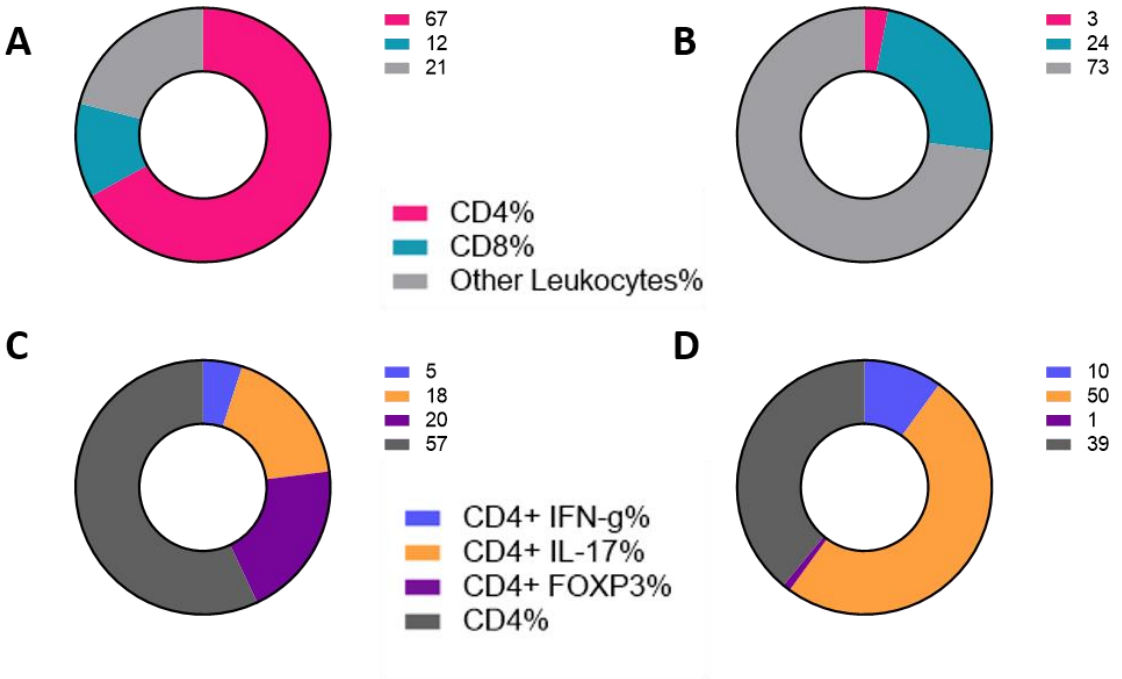
A
67
12
21
CD4%
CD8%
Other Leukocytes%
B
3
24
73
C
5
18
20
57
CD4+ IFN-g%
CD4+ IL-17%
CD4+ FOXP3%
CD4%
D
10
50
1
39

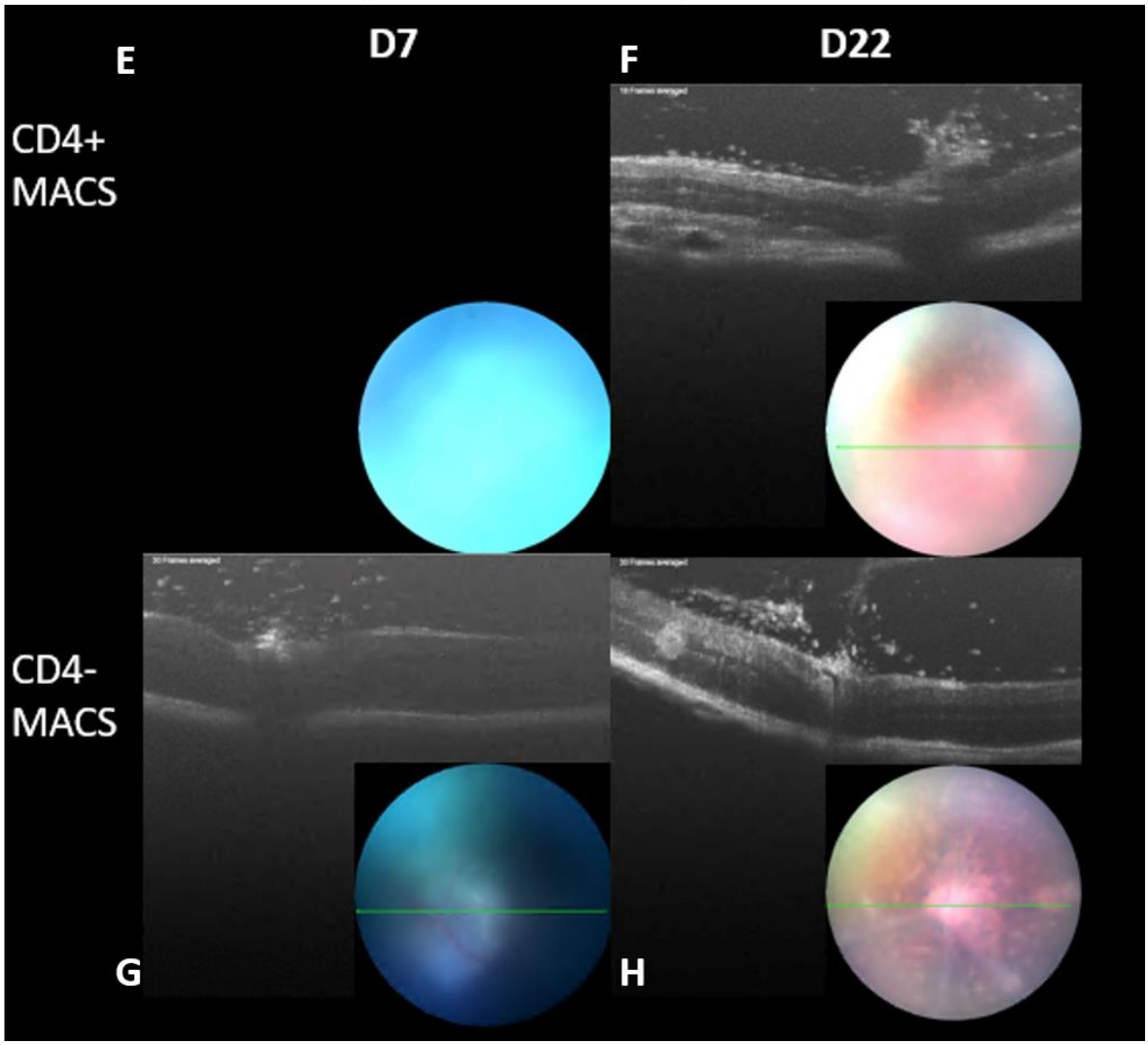
E
D7
F
D22
CD4+
MACS
CD4-
MACS
G
H

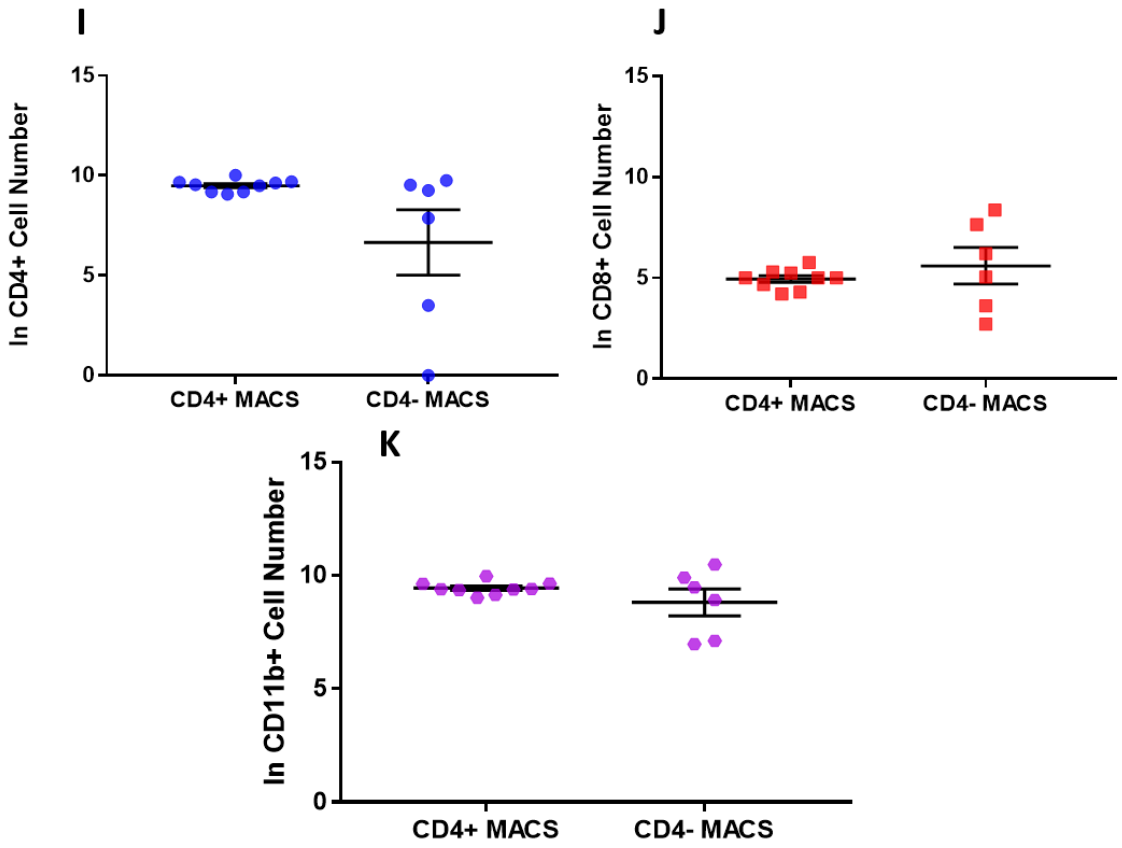
I
ln CD4+ Cell Number
15
10
5
0
CD4+ MACS
CD4- MACS
J
ln CD8+ Cell Number
15
10
5
0
CD4+ MACS
CD4- MACS
K
ln CD11b+ Cell Number
15
10
5
0
CD4+ MACS
CD4- MACS

AVERAGE CELL NUMBER

	CD4+ MACS	CD4- MACS
CD4	**13864**	**5926**
CD8	**155**	**1329**
CD11B	**13036**	**13001**

Figure 3.13: Adoptive transfer of MACS isolated leukocytes using a CD4 negative MACS isolation into RAG2$^{-/-}$ recipients at 2x10^{6} CD4+ or 2x10^{6} CD4- cells per mouse. (A-D) Analysis of cells transferred into RAG2$^{-/-}$ mice (A) Extracellular analysis of CD4+ cells isolated by CD4 negative MACS isolation for cell transfer (B) Extracellular analysis of CD4- cells isolated by CD4 negative MACS isolation for cell transfer (C) Intracellular analysis of CD4+ T cells isolated for transfer by CD4 negative MACS isolation (D) Intracellular analysis of CD4+ population present within the CD4- population obtained using CD4 negative MACS isolation. (E-H) OCT and fundus imaging following clinical disease in both CD4+ and CD4- groups of recipients (E) Fundus imaging of CD4+ transfer at day 7 after cell transfer at 2x10^{6} cells transferred per mouse, no OCT is shown due to severity of cellular infiltrate (F) OCT and fundus imaging of CD4+ transfer at day 22 after transfer (G) OCT and fundus imaging of CD4- transfer at day 7 after cell transfer at 2x10^{6} cells transferred per mouse (H) OCT and fundus imaging of CD4- transfer at day 22 after transfer (I-K) Flow Cytometry analysis of eyes from RAG2$^{-/-}$ recipients at day 22 after transfer of CD4+ or CD4- populations. (I) CD4+ populations present within the eyes of the groups of CD4+ and CD4- transfer recipients at day 22 (J) CD8+ populations present within the eyes of the groups of the groups of CD4+ and CD4- transfer recipients at day 22 (K) CD11b+ populations present within the eyes of the groups of CD4+ and CD4- transfer recipients at day 22 after transfer.

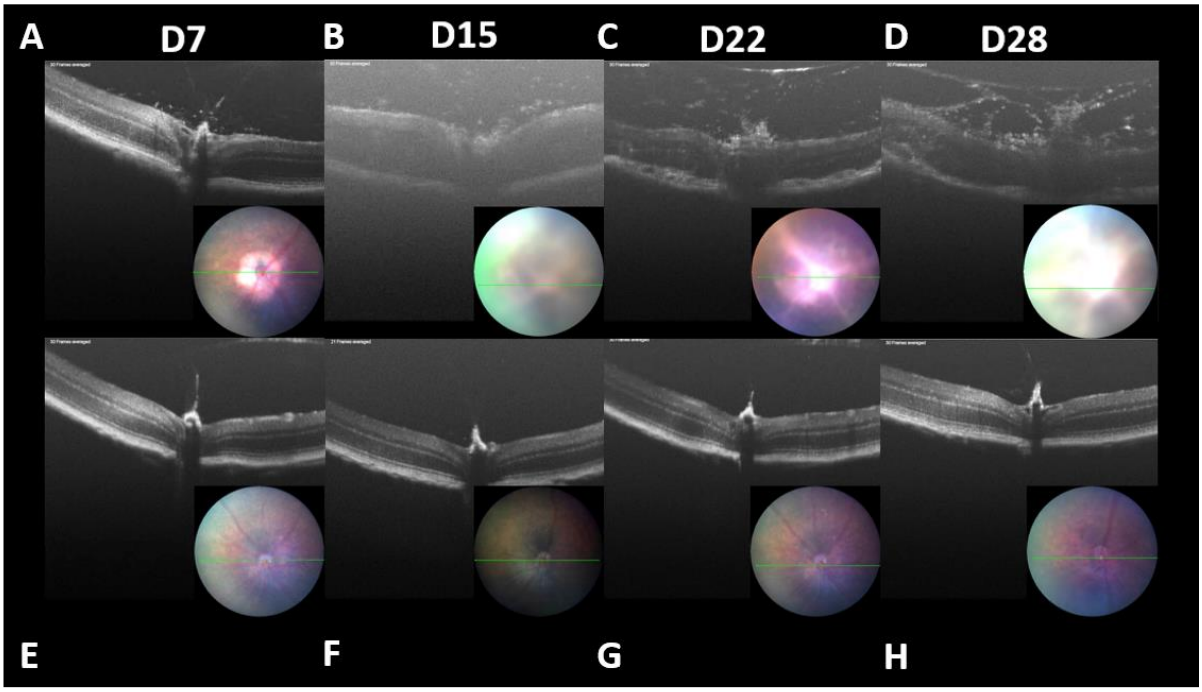
A
D7
B
D15
C
D22
D
D28
E
F
G
H

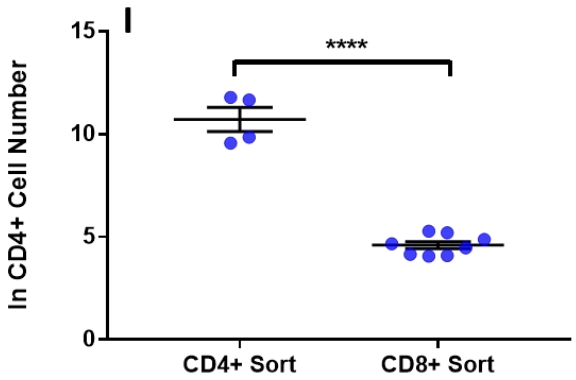
I
****
ln CD4+ Cell Number
15
10
5
0
CD4+ Sort
CD8+ Sort

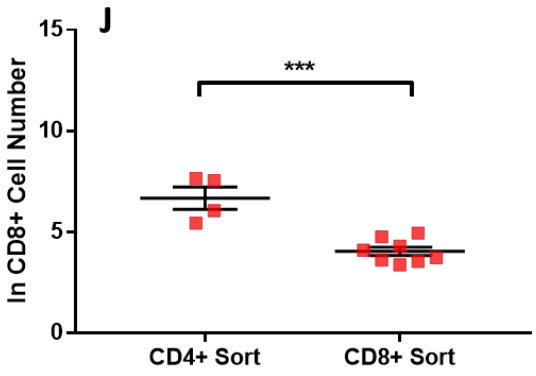
J
***
ln CD8+ Cell Number
15
10
5
0
CD4+ Sort
CD8+ Sort

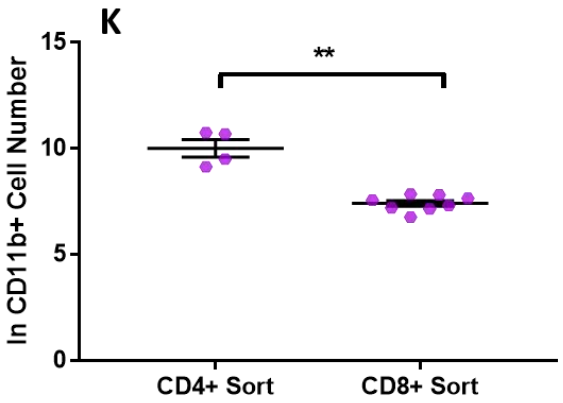
K
**
ln CD11b+ Cell Number
15
10
5
0
CD4+ Sort
CD8+ Sort

AVERAGE CELL NUMBER

	CD4+ Sort	CD8+ Sort
CD4	70566	111
CD8	1157	66
CD11B	28374	1762

Figure 3.14: OCT and flow cytometry analysis of transfers of MACS isolated CD4+ and CD4- leukocytes. Populations are stained using flow cytometry antibodies and sorted using a fluorescence cell sorter to obtain a purer population of CD4+ and a purer population of CD8+ T cells which are then transferred at 500,000 cells per mouse into $RAG2^{-/-}$ recipients. (A-H) OCT and fundus imaging of CD4+ and CD8+ transfer following disease course from day 7 to day 28. (A) Representative clinical imaging at day 7 by fundus and OCT of recipients that received a CD4+ T cell transfer (B) Representative clinical imaging at day 15 by fundus and OCT imaging of recipients that received a CD4+ T cell transfer (C) Representative clinical imaging at day 22 fundus and OCT of recipients that received a CD4+ T cell transfer (D) Representative clinical imaging at day 28 by fundus and OCT of recipients that received a CD4+ T cell transfer (E) Representative clinical imaging at day 7 by fundus and OCT of recipients that received a CD8+ T cell transfer (F) Representative clinical imaging at day 15 by fundus and OCT of recipients that received a CD8+ T cell transfer (G) Representative clinical imaging at day 22 by fundus and OCT of recipients that received a CD8+ T cell transfer (H) Representative clinical imaging by fundus and OCT of recipients that received a CD8+ T cell transfer. (I-K) Analysis by flow cytometry of eyes from CD4+ and CD8+ transfer recipients at day 28 using extracellular staining and absolute numbers to quantify immune infiltrate.

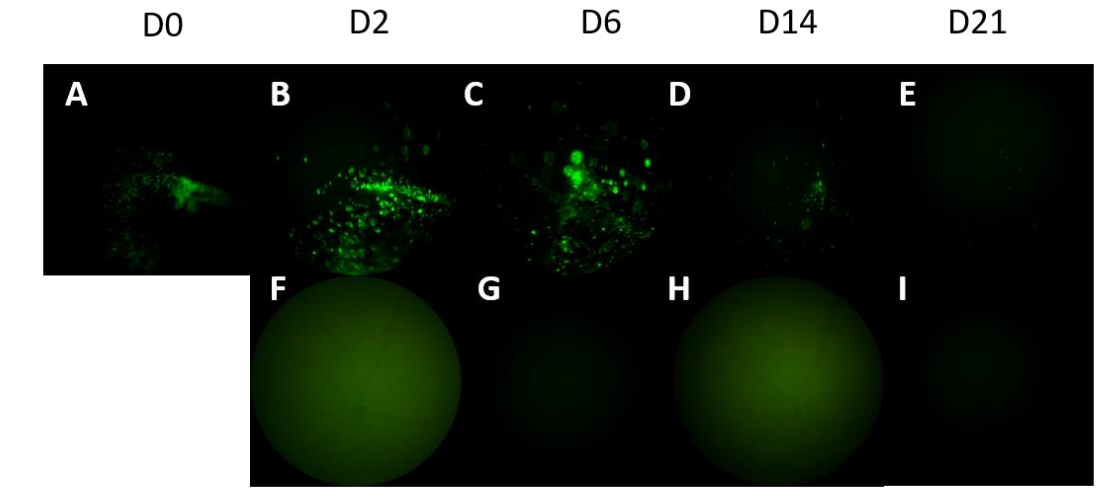
D0
D2
D6
D14
D21
A
B
C
D
E
F
G
H
I

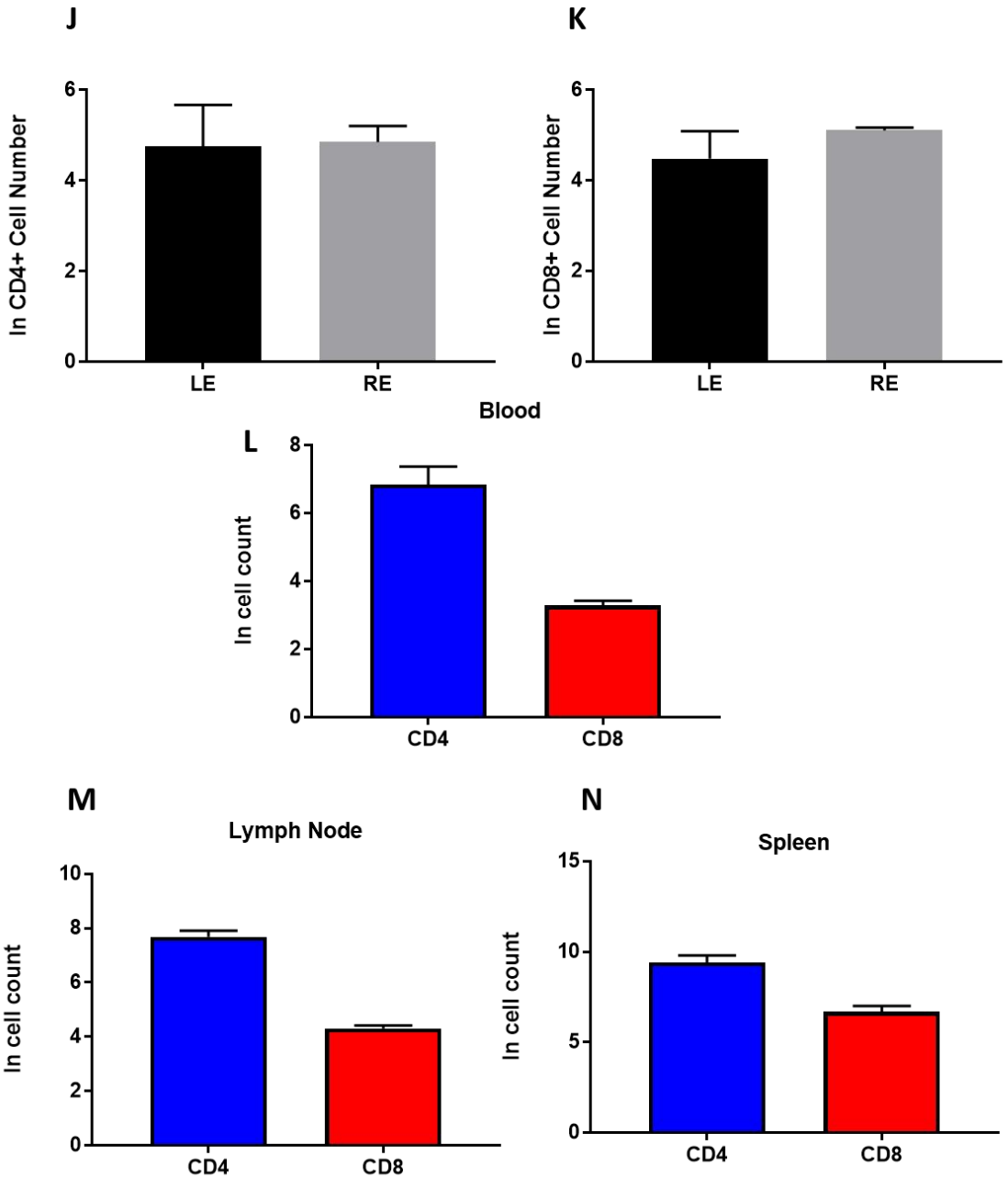
J
ln CD4+ Cell Number
6
4
2
0
LE
RE
K
ln CD8+ Cell Number
6
4
2
0
LE
RE
Blood
L
ln cell count
8
6
4
2
0
CD4
CD8
M
Lymph Node
ln cell count
10
8
6
4
2
0
CD4
CD8
N
Spleen
ln cell count
15
10
5
0
CD4
CD8

AVERAGE CELL NUMBER

	Blood	Lymph Node	Spleen	Invit eye (LE)	RE
CD4	1223	2289	14194	151	132
CD8	26	74	887	117	166

Figure 3.15: OCT and flow cytometry analysis of RAG2$^{-/-}$ recipients of CD4+ and CD8+ MACS then FACS sorted populations. CD4+ or CD8+ cell populations were isolated from cell cultures of CAG GFP tagged donor cells firstly using a CD4- MACS isolation, then after antibody stains for CD4 or CD8 cells are sorted using fluorescent associated cell sorting for pure populations of CD4+ or CD8+ T cells. Recipients then received an intravitreal injection of 50,000 CD4+ or CD8+ T cells into the left eye. RAG2$^{-/-}$ recipients were monitored using the micron IV camera with fluorescent filters to track GFP tagged cells in the left and right eyes (A-I).

At day 28, retinal infiltrate was analysed in all recipient eyes and CD4+ and CD8+ numbers quantified (J-K). To analyse leukocyte migration from the eye to the blood (L) and lymphoid organs such as spleen(N) and lymph node(M) CD4+ and CD8+ were also quantified to look at expansion of T cell populations.

3.4 Discussion

This chapter outlines a robust adoptive transfer technique using total leukocyte populations to induce EAU along with preliminary analysis of recipients at peak disease after transfer and of the cell populations transferred. It also illustrates the use of allelic markers to track transferred and endogenous cells throughout disease using allelic markers.

Before proceeding with full analysis of clinical disease course after adoptive transfer, I characterised a transfer technique using a novel RBP3 peptide to induce disease for analysis. This involved inducing a phenotype that could be easily monitored using clinical imaging, the protocol was adopted from the method developed by the Caspi group (176). The first step of the protocol is immunisation with RBP3 peptide which has already been optimised within our group (188) followed by a 72 hour cell culture which was optimised in terms of addition of antigen and cytokines. The addition of the immunising antigen to the cell culture is used to re-stimulate the CD4+ T cells in vitro, the cells may also be propagated in vitro using the addition of IL-2 (189). The addition of IL-23 has been demonstrated to play a pivotal role in establishment and maintenance of organ-specific inflammatory autoimmune disease (175). It has also been shown in vitro that IL-23 promotes a T cell population characterised by production of IL-17A, IL-17F, TNF and IL-6, when these cells are used for adoptive transfer into naïve recipient mice IL-23 dependent T cell subsets invade the target organ and can promote the development of organ-specific autoimmune inflammation (175). So, the optimisation of the addition of IL-23 and IL-2 to the transfer cell cultures to give the most effective leukocyte population for cell transfer was a necessary step in the adoptive transfer protocol. Each culture was then analysed for percentage of cell populations specifically CD4+ T cells, cytokines expressed by CD4+ T cells and cytokines within the culture supernatant. Future chapters will discuss the sole surviving population of the total leukocyte cell transfers to be CD4+ T cells.

Secondly, the number of cells needed to induce disease was optimised to allow full analysis of disease in vivo and in vitro, using cell titration experiments the optimum cell number to use to induce consistent disease across all recipients was $2x10^6$ of which ~20% are CD4+, which is significantly lower than the paper by the Caspi group originally published which was $50x10^6$-$100x10^6$ total cells which has been reduced to $5x10^6$ total cells but still uses

significantly more cells than this optimised adoptive transfer technique to induce clinical disease (117, 176).

After the cell number for transfer was optimised, the identification of transferred cells within recipients during clinical disease could be validated. Congenic mouse strains with allelic variants of CD45, including CD45.1 and CD45.2 can be differentiated using flow cytometry and are used routinely in experiments to track populations of immune cells (190). Allelic markers can be used to track where transferred cell populations have been recruited not only to the target tissue but also to lymphoid and non-lymphoid tissue and blood. Disease is defined by increased number of cells infiltrating the eye, thickening of the retina, swelling of the optic disc by OCT imaging and large numbers of leukocytes present in flow cytometric and histological analysis.

During clinical disease, a large percentage of the CD4+ T cells present within the eye are from the transferred population based on allelic markers, thus suggesting that the antigen specific transferred cells are driving the disease process and being recruited to the eye. Although the transferred cells make up a large compartment of the CD4+ T cells present within the eye, endogenous CD4+ T cells from the recipient are also recruited during clinical disease and contribute to the disease progression as the percentage of endogenous cells are present in the eye increase at day 14 compared to day 7.

Due to this recruitment of endogenous CD4+ T cells, the question stood of whether transferred cells alone are enough to drive clinical disease with no recruitment of lymphocytes from the endogenous compartment of the recipients. Therefore, experiments were carried out using $RAG2^{-/-}$ mice that lacked mature T and B cells so the only CD4+ T cells present within the recipient were the transferred cells. By day 7, clinical disease can be observed by increased cell infiltrate and increased presence of hyperintense regions in the retina as measured by OCT which persists through to day 14 with no resolution, this illustrates that transferred pathogenic cells are able to drive disease without recruitment of endogenous T cells.

In summary, this chapter describes the optimisation of an adoptive transfer technique and preliminary analysis to study the recruitment of pathogenic T cells to the target tissue and induction of clinical disease. At the time of transfer there is a mixed Th1 and Th17 CD4+ phenotype present in the cell cultures based on cytokines present in the supernatant and intracellular cytokine staining. The main difference in CD4+ phenotype is observed within the

supernatant of the transferred cell cultures where an increase in IFN-γ is observed in the C57BL/6 Ly5 cultures in comparison to the OTII, CX3CR1 heterozygous and the CX3CR1 knockout suggesting an increased Th1 phenotype is present in these cultures. The FoxP3 staining illustrates a limited number of Tregs is present when cells are transferred. Further to this there is no evidence of epitope spreading to the RBP3 1-20 peptide when transfer donors are culled for cell culture which can be seen later and has been published previously by the group (159). This approach utilising allelic markers allows tracking of transferred cells throughout clinical disease and to study the role of antigen-specific transferred cells in clinical disease induction and disease course that will be used in further chapters throughout this thesis.

.

Chapter 4. Recruitment of transferred and endogenous cell populations during EAU

4.1 Introduction

Autoimmune diseases are a result of a breakdown in immunological tolerance against self-molecules creating an adaptive immune response against a self-antigen (59, 61). Three major mechanisms are offered to explain the development and progression of autoimmunity: molecular mimicry, bystander activation and dysfunctional Tregs (191). The majority of autoimmune diseases develop through complex mechanisms due to a number of factors including genetic, molecular, cellular and environmental elements (192). This results in alterations at many checkpoints that combine to cause a breakdown in immune tolerance, and manifests as harmful inflammatory responses in peripheral tissues amplified by an innate immune response and self-antigen specific T and B cells (192). Research suggests that T cells play the central role in organ specific autoimmune disease both in initiation of disease and persistence (193). It is believed that the immune privilege can leave the eye susceptible to an attack by primed lymphocytes of an autoimmune nature from elsewhere within the body by a random or chance encounter with a self-antigen or a mimic antigen (194).

4.1.1 Immune tolerance

Central tolerance is sometimes inefficient therefore another mechanism known as peripheral tolerance to regulate potentially harmful autoreactive T and B cells that have been released into the periphery (192). Tissue specific autoimmune disease is the main consequence of the activation of a population of self-reactive T cells that cause destruction of single or multiple target tissues (170). Identifying the target antigens that are recognised by autoreactive T cells in autoimmune disease would allow further studies of the mechanisms involved in tolerance and autoimmunity. These are currently considered a challenge and therefore allow further study of specific lymphocyte responses to these autoantigens (170).

Autoreactive T lymphocytes can act as both regulatory and effector cells, playing a key role in autoimmune diseases (146). Autoreactive memory T cells mediate autoimmune diseases of the CNS including multiple sclerosis where the cells recognise the myelin sheath and uveitis where the cells recognise the retinal tissues, in contrast to memory T cells which are known to be associated with a protective immunity (172). T lymphocytes can be divided into two major subsets based on their function, CD4+ T helper cells and CD8+ cytotoxic T cells (173). Peripheral blood responses against autoantigens in CD4+ and CD8+ T cells has been

demonstrated, using technologies such as ELISPOT and MHC-tetramer to demonstrate in vitro CD4+ T cell reactivities against self-antigens (195). The coexistence of both autoreactive and protective T cells is supported by multi-organ autoimmunity when naïve CD4+ T cells are transferred into immune deficient mouse strains (196).

CD4+ T cells are involved in the adaptive immune response and play the key role in development of autoimmunity (61), they can be subdivided into subsets based on a network of transcriptional regulators and unique cytokine profiles (197). As highlighted in chapter 1, most organ-specific autoimmune diseases including multiple sclerosis and uveitis are mediated by autoreactive CD4+ T cells and can be characterised by unpredictable, explosive inflammatory responses which become less active with clinical features of disease subsiding spontaneously without treatment, but then return with repetitive attacks. It is known that between attacks reduced inflammation can be detected in the target tissue (172). Understanding the mechanisms by which autoimmunity evolves and its links to tolerance is a great challenge (170).

Transgenic mouse models have become valuable tools to understand mechanisms involved in the pathogenesis of autoimmune disease as they provide both defined, tissue specific cognate antigens along with well characterised T cell receptors that recognises these antigens, two major approaches utilise transgenic mouse models, one of which is the adoptive transfer of T cells into naïve recipients (170).

4.1.2 Tolerance to retinal antigens

Central tolerance to retinal antigens is similar to the central tolerance of other tissue specific antigens (194). Retinal antigens such as RBP3 have been detected in the thymus to produce central tolerance and are under the control of the AIRE transcription factor (53, 194). Different mouse strains express different amounts of RBP3 in the thymus, the amount of RBP3 expressed is linked to the susceptibility of the mouse strain to EAU induction which is inversely correlated (167, 194).

As mentioned previously, within the thymus negative selection occurs to eliminate all autoreactive T cells, unfortunately this process is not 100% effective that is where the peripheral tolerance aids by controlling the autoreactive thymic migrants that have escaped thymic negative selection (194). Resident retinal antigens within the healthy eye are isolated

behind the blood-retina barrier and are not readily available to circulating lymphocytes, whereas during ocular inflammation when the blood ocular barrier is compromised can lead to exposure of retinal antigens to circulating lymphocytes in the periphery (194).

4.1.3 Bystander CD4+ T cell activation

Antigen specific CD4+ T cell clonal expansion plays an important role in both organ-specific and systemic autoimmune disease (198). Studies of T cell responses to several antigens illustrate that all variable components of the αβ TCR contribute to the binding of conventional peptide antigens with products of the MHC. Further work coined the term super antigen for a second group of antigens that stimulates T cells at very high frequencies, the group encompasses self-antigens (199). T cell clones that accumulate within the eye during clinical disease are qualitatively different depending on what stage of disease they are recruited, for example, T cells that have accumulated within the eye at early disease will be different from those that are found within the eye during the advanced phase of disease. Therefore, the T cells that are found within the eye at each disease phase are involved in disease pathogenesis in different ways (198).

The first description of bystander activation was by Tough et al in 1996, it was used to attempt to understand in the context of cytokine secretion the large clonal CD8+ T cell expansion after viral infection (191). Non-antigen specific lymphocytes are activated in a heterologous manner to mediate the signals that indirectly favour an inflammatory milieu including chemokines, cytokines, extracellular vesicles, ligands of co-signalling receptors, PAMPs and microbial particles (191, 200).

Classical T cell activation is mediated mainly through engagement of TCR and costimulatory signalling pathways which promote signalling cascades that induce cytokine production, proliferation, differentiation and/or apoptosis (191).

4.1.4 Bystander T cell accumulation in autoimmune disease

The development of autoimmunity is potentially due to the mechanism of bystander effects, this mechanism is different from the mechanisms of molecular mimicry and microbial agents (191, 201, 202). The notion of bystander activation can be described as the disturbance of self-tolerance due to an encounter with a pathogen, this causes the activation of resting autoreactive T cells that are then recruited to the tissue to cause inflammation, these cells

are antigen specific, however not all cells recruited to the tissue will be antigen specific some are known to be recruited non-specifically (202). The immunological pathways associated with bystander effects are not antigen-specific whether they be by effects of activation or suppression. The recruitment of non-specific cells can be induced by the initiation of cell death to cause the release of cellular antigens, perturbing of the cytokine balance or by increasing the antigen abundance or visibility (202).

4.1.5 Bystander activation and recruitment after adoptive transfer

A study conducted by Arata et al (202) using the adoptive transfer model of experimental autoimmune thyroiditis illustrated using GFP+ transferred T cells to study the fate of these cells during the development of thyroiditis (202). Immunohistochemistry staining of the thyroid tissue of recipient mice showed the development of thyroiditis after adoptive transfer of Tg-primed GFP+ cells, this was demonstrated by intrathyroidal accumulation of GFP+ T cells (202). GFP+ cells are also observed in the periphery of recipients such as blood, bone marrow and spleen but these cells are not present early within disease (202). However, a rapid disappearance of GFP+ T cells was observed, this may have been due to a secondary immune response potentially to the transgene product (202). The presence of activated GFP+ transferred T cells within the thyroid was observed along with the presence of infiltration from the host, which can be assumed to be initiated by the recruitment of transferred T cells. This study suggests that in this model of adoptive transfer the activated GFP+ cells may have initiated bystander activation of the host's immune response by TCR-mediated activation such as; increasing the effect and attraction of host APCs and by causing cell death to induce cellular antigens to be released, or by non TCR mediated activation such as; disruption of the cytokine balance within the host (202). Using depletion of CD8+ cells the disease severity decreased, showing a necessity for the endogenous compartment to drive disease course (202).

The adoptive transfer technique is a useful tool for EAU disease induction. Using allelically marked cells (as shown in chapter 3) allows tracking of uveitogenic primed CD4+ T cells after transfer including during the pre-clinical phase of disease, peak clinical disease and as disease resolves. Cell counts are normalised to eyes from naïve animals.

The aims of this chapter are to quantify total retinal cellular infiltrate after adoptive transfer of leukocytes before clinical disease, during and post disease. Further to this, analyse

endogenous and transferred cells within each leukocyte population at each time point during EAU. Transferred cells were also quantified within the periphery of each recipient to determine tissue specific recruitment to the ocular tissue and any non-specific recruitment in lymphoid and non-lymphoid tissues.

4.2 Materials and Methods

4.2.1 Adoptive transfer technique

EAU was induced in C57BL/6 CX3CR1$^{+/GFP}$ (CD45.2) using RBP3 peptide 629-643, after a 72-hour cell culture these donor cells were then transferred using i.p injection into C57BL/6 ly5 (CD45.1) recipients at 2x10^6 total leukocytes per recipient.

4.2.2 Flow cytometry analysis

Flow cytometry was used to identify and quantify subsets of cells within the transferred cell population and retinal infiltrate using extracellular staining.

Within transferred recipients' allelic markers CD45.1 and CD45.2 were used to identify endogenous and transferred populations of cells within the retina.

4.2.3 Clinical imaging

OCT scans and fundus images standardised across recipients during transfer optimisation to study disease course at each cell concentration transferred.

4.3 Results

4.3.1 Flow cytometric analysis of naïve eyes

An important aspect of Immune surveillance is local recruitment and retention of immune cells within healthy tissue (203). Peripheral tissue immune surveillance compartments are composed of cells from both the innate and adaptive immune system, the diversity of their composition reflects the specialised need for immune surveillance tailored to distinct locations within the body (203).

Therefore, healthy mice will have a population of CD4+ T cells present within the eye without any disease induction due to maintenance of the tissue by immune surveillance. Studies have suggested that T cells present in a healthy or steady-state in peripheral tissues do not simply mirror the image of circulating T cells (203).

Pre-clinical changes in CD4+ T cell number can be an early sign of disease initiation, therefore quantification of the CD4+ T cell population present within the eye before disease induction is a useful measure of the small to moderate increase in CD4+ T cells within the eye before disease is observed by clinical imaging. Baseline numbers also set a threshold for distinguishing, after active disease has resolved, if the number of leukocytes present within the retina and vitreous remain persistently elevated.

Total CD4+ T cells, CD8+ T cells, CD11b+. LY6G+ and LY6C+ cells (figure 4.1) were quantified as described in the methods in naïve C57BL/6 mice to give a baseline to compare with pre- and post-clinical disease leukocyte numbers.

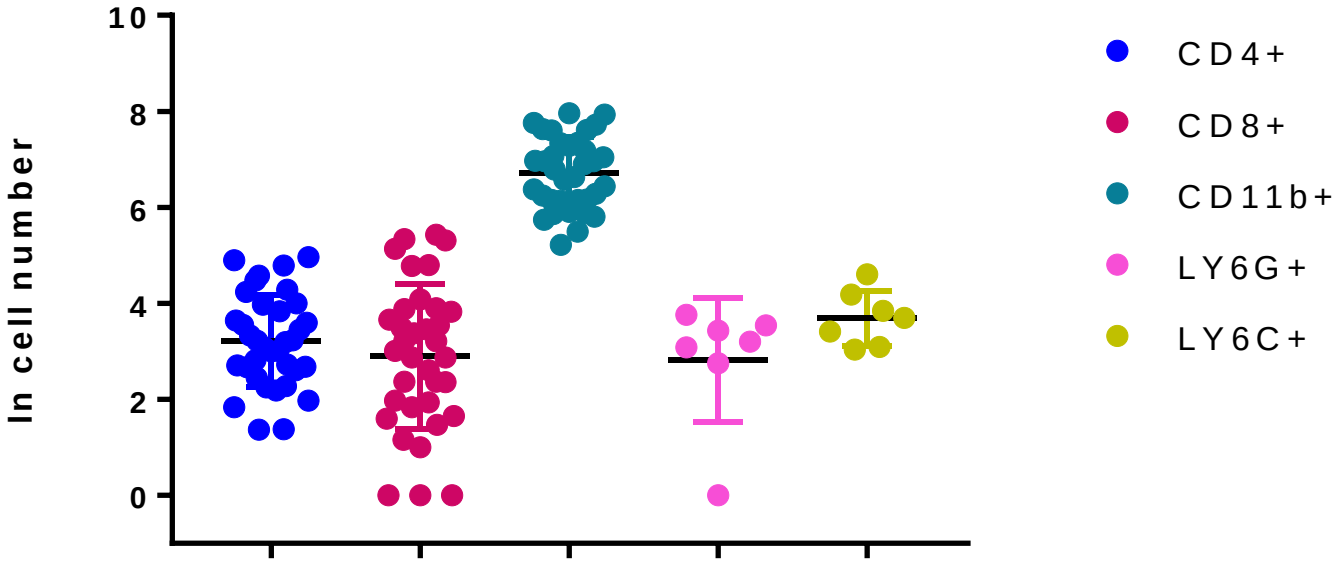

	LOWEST VALUE	HIGHEST VALUE	MEAN
CD4	3	68	22
CD8	0	58	18
CD11B	184	2251	791
LY6G+	0	42	24
LY6C+	20	99	46

Figure 4.1: Quantified leukocyte infiltrate present in the retina and vitreous in naïve mice before manipulation or disease induction. Retinas were dissected and vitreous flushed to prepare for quantification of leukocytes. Using a standard curve of known cell number CD4+, CD8+, CD11b+, LY6G+ and LY6C+ cell numbers were calculated. Data expressed as Mean ±SEM. Table shows range and mean of data presented. Data obtained from 7-30 eyes.

4.3.2 Disease course within the adoptive transfer model of EAU

After transfer of uveitogenic leukocytes clinical disease was monitored using optical coherence tomography and compared with studies from the literature where disease was produced by active immunisation. Clinical disease follows a sequential pattern of prodrome, primary peak, then secondary regulation (1). The RBP-3 subunit 3 (629-643 peptide sequence) induces clinical disease in ~90% of C57BL/6 mice immunised (188). Peak disease is observed between days 21-27 where there is the largest number of CD45+ cells present within the retina and vitreal infiltrate, at day 40-45 CD45+ cell number has decreased but remains increased in comparison to naïve animals and is accompanied by an increase in the percentage of CD8+ T cells at this time point (188).

To understand disease course more fully in the adoptive transfer model recipients were monitored by OCT to assess severity and disease kinetics. Figure 4.2a shows a naïve eye in a Ly5 recipient. The fundus is clear, and the optic disc and vessels show no signs of inflammation within the fundal image. In the OCT image the retinal layers are well demarcated, no swelling is present around the optic disc and no retinal infiltrate is detectable.

At day 2, the fundal image remains clear of any signs of clinical disease. In the OCT image the retinal layers are visible and there is no obvious swelling of the optic disc. However, early signs of retinal infiltrate appear around the optic disc within the vitreous (figure 4.2b).

By day 6, obvious signs of clinical disease manifestation are present within the fundal and OCT imaging (figure 4.2c). In the fundal image a vitreal haze is present and swelling around the optic disc is observed. The OCT image further confirms the onset of clinical disease, thickening of the retina and swelling of the optic disc and obvious cellular infiltrate within the vitreous is present (figure 4.2c).

At day 13, clinical disease is still active in the eyes of the transfer recipients but is less severe than at day 6. The reduction in disease severity suggests that peak disease occurs between day 6- 12. In the fundal image, the inflammation is reduced around the optic disc and the vitreal haze has reduced. The OCT image shows a reduction in thickness of the retina and swelling of the optic disc and the infiltrate within the vitreous has reduced (figure 4.2d).

By day 21, disease is active but has mostly resolved with minimal cell infiltrate observed, although the eye looks similar to day 0 in retinal thickness and optic disc thickness (figure 4.2a and 4.3a). The layers of the retina are visible, and the optic disc has returned to a normal

state. Vitreal infiltrate has further reduced, although some cells appear to persist within the vitreous (figure 4.3a).

Disease continues to resolve from an active phase dominated by infiltration to a persistent phase characterised by retinal thinning and degenerative lesions from day 21 to day 67. Retinal infiltrate is not present within the OCT image at day 35 and clear retinal layers are present (figure 4.3b). This is reflected also in the fundal image, with no vitreal haze or swelling around the optic disc or sheathing of the vessels. At day 51 and 67, the OCT remains clear of vitreal infiltrate, but a thinning of the retina is observed. In the fundal image loss of definition of vessels is observed and haziness with distinct colour changes are present (figure 4.3c and 4.3d).

This full-time course of disease and corresponding disease scores (figure 4.4) illustrates a primary peak of disease at day 6-12 followed by a resolution of active clinical disease from day 21, that persists to day 67.

D0

D2

D6

D13

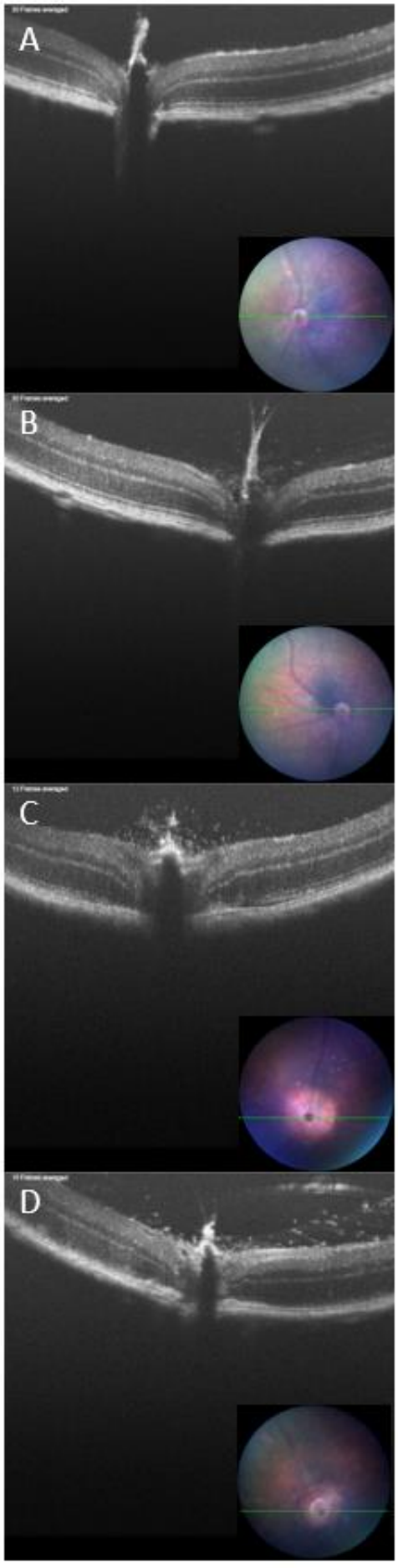

Figure 4.2: OCT clinical imaging throughout peak disease, day 0-13 after adoptive transfer of uveitogenic leukocytes. Baseline imaging was taken at day 0 before manipulation of Ly5 (wildtype) recipients (A). 2 days after transfer of uveitogenic leukocytes recipients were imaged at a pre-clinical disease timepoint (B). At day 6, peak disease occurs, and recipients had maximal infiltrate and retinal and optic disc swelling when imaged using OCT (C). By day 13, disease is still active but has reduced in severity. Reduced vitreal infiltrate is present and swelling of the retina and optic disc has begun resolving (D). (Images taken from different eyes throughout the time course due to quality and length of experiments).

D21

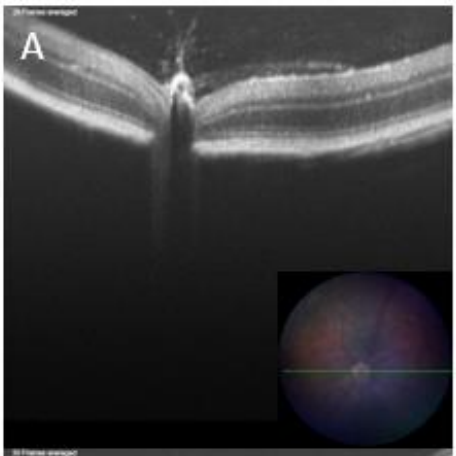

D35

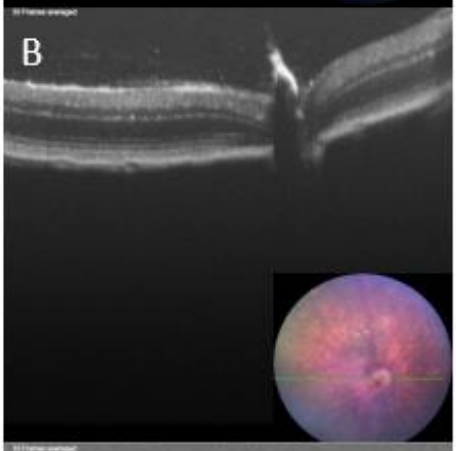

D51

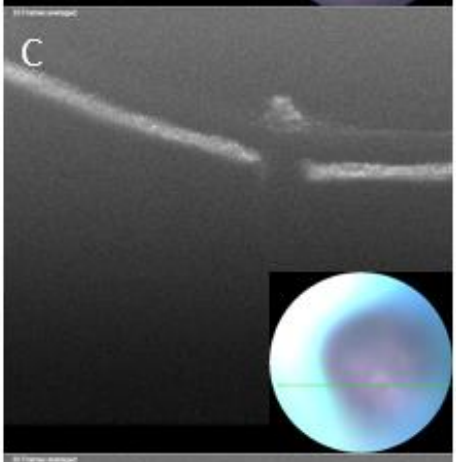

D67

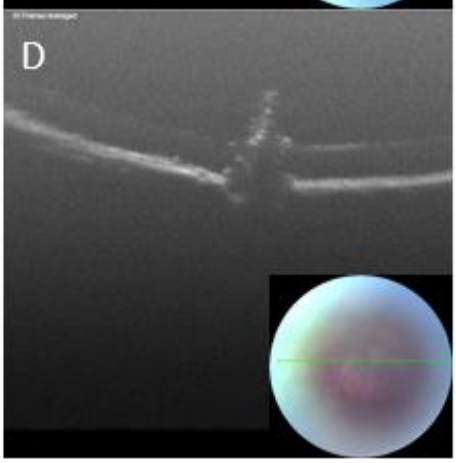

Figure 4.3: OCT clinical imaging throughout post-peak clinical disease, days 21-67 after adoptive transfer of uveitogenic leukocytes. After peak clinical disease, recipients are still monitored for signs of a relapse of active disease. (A) Day 21 after disease induction recipients no longer have active disease, the retina has reduced to a thickness similar to day 0 and the vitreal infiltrate has reduced but is still visible by OCT. At day 35 after transfer, there are no longer signs of active clinical disease (B). At days 51 and 67 post transfer, signs of active clinical disease have gone but the retina remains scarred from disease progression (C+D). (Images taken from different eyes throughout the time course due to quality and length of experiments).

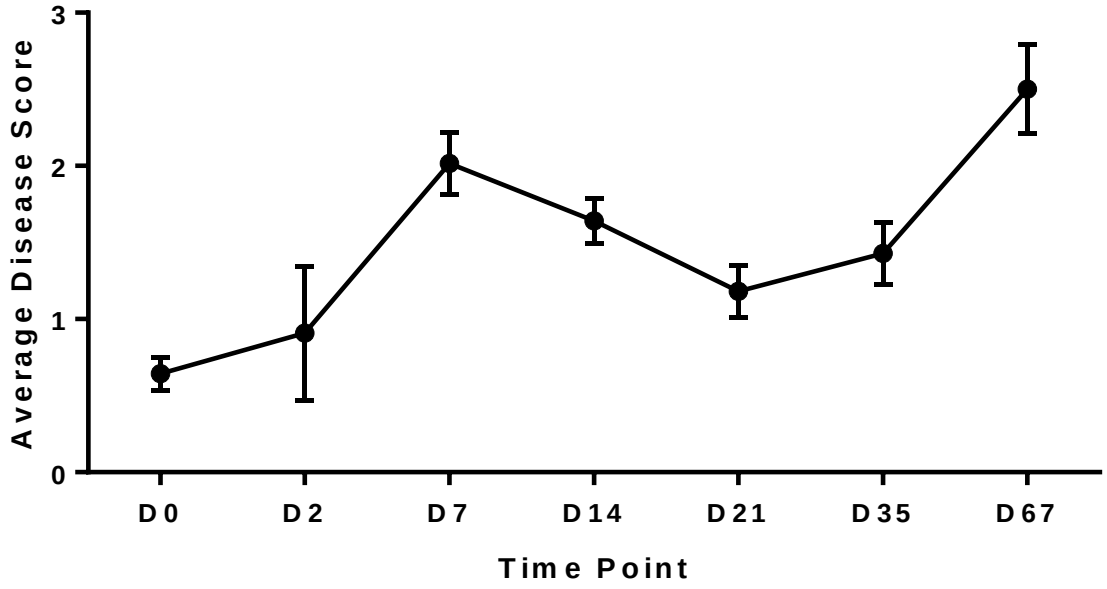

Figure 4.4: Average clinical scores of recipients over full disease course. OCT imaging was used to acquire corresponding fundal images throughout disease course. The images were then scored blind using the criteria described in *chapter 2* and the average score taken from each eye at each time point. Data expressed as Mean ±SEM. Data obtained from 8-78 eyes per time point.

4.3.3 Flow cytometric analysis of CD4+ T cell populations present within the eyes of recipients

Recipients were monitored using clinical imaging to establish the disease course, and at different points retina and vitreous were isolated from recipient's eyes for flow cytometric analysis to quantify leukocyte infiltrate at several time points throughout the disease.

In the first part of the analysis, the aim is to quantify endogenous and transferred CD4+ T cell number at each time point through pre-clinical disease to active disease and through post active clinical disease, to assess total cell number and the ratio of endogenous and transferred CD4+ T cells present within the retina and vitreous of the eyes of the recipients.

Day 0 is the baseline CD4+ T cell number quantified previously and shown in figure 4.1. This population allows comparison with pre-clinical disease. At day 2, transferred CD4+ T cells can be detected within the eye (figure 4.5) and there is increased recruitment of endogenous CD4+ T cells in comparison to the day 0 baseline CD4 cell number.

By day 7, when peak disease is detected by clinical imaging (figure 4.2c), eyes were taken for analysis by flow cytometry. Quantified cell number illustrate an increase from an average of 97 at day 2 to an average of 3967 at day 7 in the endogenous CD4+ compartment and an increase from an average of 62 at day 2 to an average of 822 at day 7 in the transferred CD4+ compartment present within the isolated retina and vitreous (figure 4.5). The ratio of endogenous to transferred CD4+ cells is close to 1:1 in some recipients (figure 4.5).

At day 14, active disease is still present within the eyes of the recipients when using clinical imaging to assess disease progression (figure 4.2d). At this time point, the mean transferred CD4+ T cell number has increased in some recipients in comparison to day 7 (822-817) , whereas the endogenous CD4+ T cell number remains constant and has decreased in some recipients (3967-1384) (figure 4.5).

Active disease is still observed at day 21, although it has mostly resolved, cellular infiltrate is still present within the vitreous when the eyes are clinically imaged (figure 4.3a). When vitreous and retina from recipient animals was analysed by flow cytometry a decrease in both the endogenous (1384-128) and transferred (817-115) CD4+ T cell populations was observed. Transferred CD4 cells have become the largest of the CD4+ populations in many recipients (figure 4.5).

By day 35, active disease has resolved by clinical imaging and no cellular infiltrate is detected within the vitreous of the recipients (figure 4.3c). The transferred CD4+ T cell population has persisted in the eyes of the recipients as a smaller portion of the CD4+ T cell population present in the eye. Endogenous CD4+ T cells are still increased in comparison to the population of CD4+ T cells present at baseline day 0 (figure 4.5).

Clinical disease continues to exhibit features of secondary regulation by OCT at day 51 (figure 4.3c) and day 67 (figure 4.3d). The retina has thinned, but there is no obvious infiltrate observed. When recipients' eyes were analysed by flow cytometry at day 67 (figure 4.5), transferred cells are still present within the retinas of the recipients. Also, in comparison to baseline at day 0, the endogenous CD4+ T cell number remains increased in the recipient's eyes at day 67 and have not returned to baseline that is observed in a 6-8-week old C57BL/6 mouse.

The data was log transformed to achieve a normal distribution and statistical analysis performed using one-way ANOVA (Fig 4.5). Multiple comparisons were made between endogenous and transferred populations throughout the time course using a Dunnett's test. When the test is performed across time points throughout disease course all endogenous CD4+ populations are statistically significantly increased ($P<0.01$**-$P<0.0001$****). Comparisons between the day 2 transferred population and the transferred population present within the eye at day 7 and day 14 by one way ANOVA are also statistically significant ($P<0.0001$****).

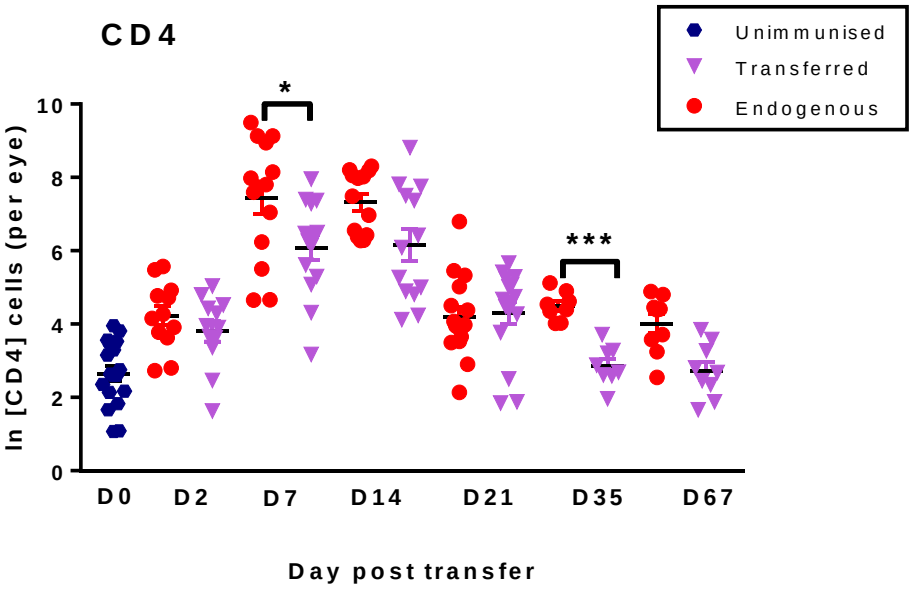

ENDOGENOUS

CD4	Lowest Value	Highest Value	Mean
D0	3	68	22
D2	15	241	97
D7	105	13320	3967
D14	74	4034	1384
D21	34	891	128
D35	55	166	95
D67	12	132	68

TRANSFER

CD4	Lowest Value	Highest Value	Mean
D0	n/a	n/a	n/a
D2	5	154	62
D7	24	3165	822
D14	69	6727	817
D21	6	287	115
D35	6	40	19
D67	4	46	18

Figure 4.5: Total endogenous and transferred CD4+ T cells present within the retina and vitreous at each clinical imaging time point. Quantified CD4+ T cell infiltrate in recipients' eyes throughout clinical disease in both the endogenous and transferred compartment. Baseline day 0 CD4+ T cell number allows detection of subtle pre-active clinical disease and post-active clinical disease. At day 2, (pre-active clinical disease) endogenous and transferred CD4+ cell number was quantified to compare to the day 0 baseline. Day 7 and Day 14 illustrate endogenous and transferred CD4+ T cell recruitment during peak disease. Day 21, active clinical disease has begun to resolve but infiltrate is still observed by OCT. Active clinical disease has resolved at time points day 35 to day 67, endogenous and transferred CD4+ T cells are quantified in this post active clinical disease stage to detect differences to the baseline day 0 data. Data expressed as mean $\pm$ SEM. All endogenous populations are statistically significantly different to the normal baseline. Statistical analysis performed: One-Way ANOVA multiple comparisons of against naïve for the endogenous cell compartment and Mann-Whitney non-parametric test between each endogenous and transferred population *$p<0.05$, ***$p<0.001$.

Table shows range and mean of data presented.

4.3.4 Flow cytometric analysis of leukocyte populations present within the eyes of recipients during clinical disease

EAU is a CD4+ T cell mediated disease model, but throughout disease course other leukocytes are recruited to the eye and are involved in the disease process.

As seen in figure 4.1, baseline leukocyte number was quantified from naïve unmanipulated eyes to establish the sensitivity of the analysis to small changes in cell number and therefore pre-clinical disease and post-clinical disease changes in leukocyte number.

At day 2, unlike endogenous CD4+ T cell number, there was no increase in other endogenous leukocyte numbers quantified by flow cytometry, including CD11b+ cell number, Ly6G+ cell number, Ly6C+ cell number and Ly6C- cell number (figure 4.6a-e).

Transferred cells from each leukocyte compartment are detected within the ocular tissue by day 2, similarly to the transferred CD4+ T cells (figure 4.6a-e).

As previously described in figure 4.2, 4.3 and 4.4, peak clinical disease occurs at day 7 after transfer of uveitogenic leukocytes. As seen in figure 4.5, a large increase in recruitment of CD4+ T cells occurs. Similarly, to this, the endogenous compartment of other leukocytes also reaches peak at day 7. In contrast to the CD4+ T cell data presented in figure 4.5, transferred cell recruitment to the eye during peak disease does not increase from day 2 in the CD11b+ cell compartment, Ly6G+ and Ly6C- compartments (figure 4.6b 4.6c and 4.6e). An increase in transferred cell number is observed in the CD8+ T cell compartment and the Ly6C+ compartment (figure 4.6a, 4.6b, 4.6d). Although a small increase was observed in transferred cell number in some leukocyte compartments, overall transfer cell number remains low in all leukocytes in comparison to CD4+ T cells. The transferred leukocytes are also not found in other lymphoid organs such as spleen and lymph node, and non-lymphoid organs such as kidney and liver along with blood suggesting the transferred leukocytes that are not CD4+ do not survive long term in the recipients after adoptive transfer.

At day 14, transferred cell numbers within all leukocyte compartments remain constant from day 7. Within most leukocyte compartments bar CD11b+ (figure 4.6b), the endogenous cell number similarly remains constant from day 7 to day 14. This is due to a continuation of active disease from day 7 to day 14.

At day 21, a minimal number of transferred leukocytes are still present within the eye in similar numbers at day 2 through to day 14. Whereas in the endogenous compartment

leukocyte number decreases (figure 4.6) due to resolution of active disease, a similar effect that is observed in the CD4+ T cell number (figure 4.5). Minimal transferred leukocytes persist within the ocular tissue after active disease has resolved at day 35 and day 67.

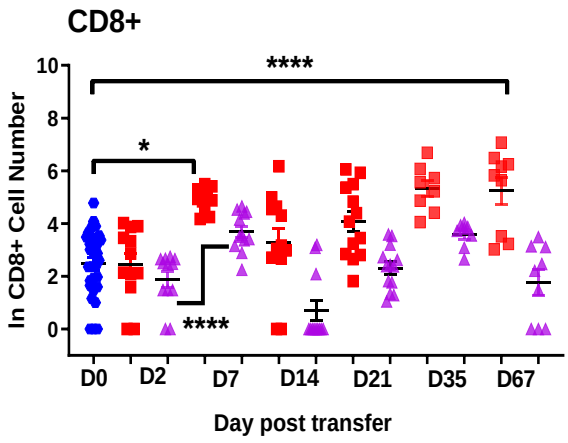
CD8+
ln CD8+ Cell Number
10
8
6
4
2
0
****
*
****
D0
D2
D7
D14
D21
D35
D67
Day post transfer

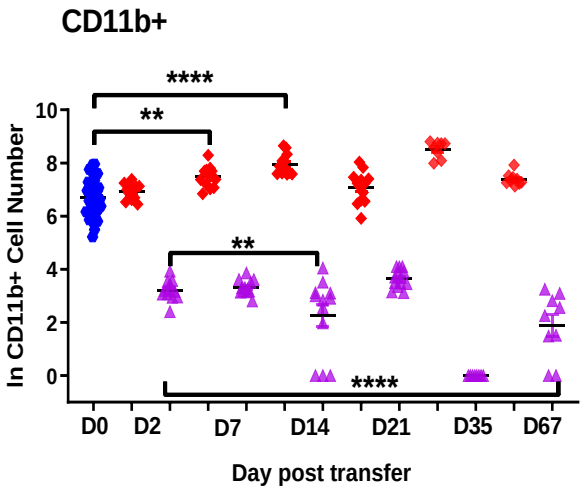
CD11b+
ln CD11b+ Cell Number
10
8
6
4
2
0
****
**
**
****
D0
D2
D7
D14
D21
D35
D67
Day post transfer

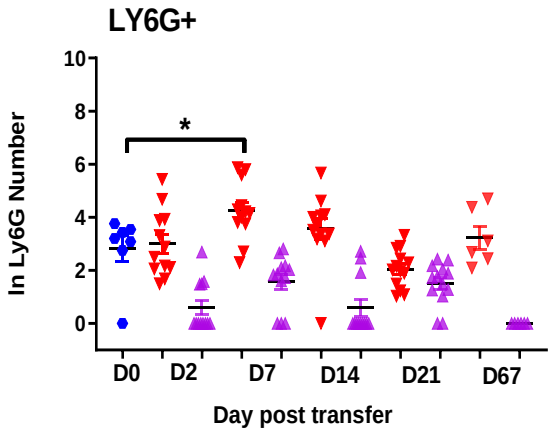
LY6G+
ln Ly6G Number
10
8
6
4
2
0
*
D0
D2
D7
D14
D21
D67
Day post transfer

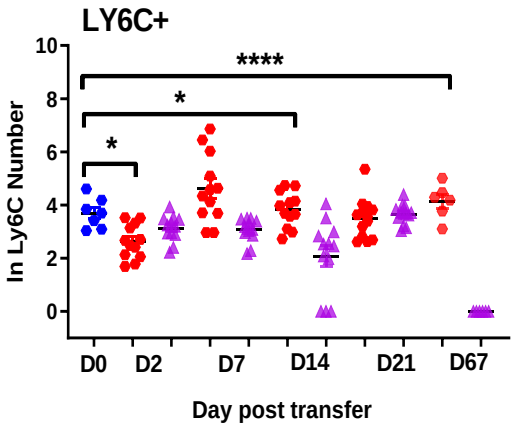
LY6C+
ln Ly6C Number
10
8
6
4
2
0
****
*
*
D0
D2
D7
D14
D21
D67
Day post transfer

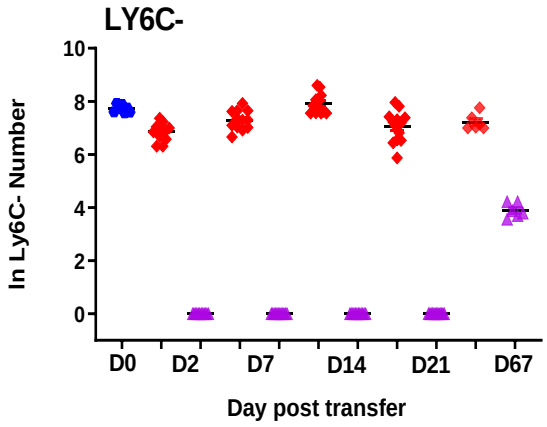
LY6C-
ln Ly6C- Number
10
8
6
4
2
0
D0
D2
D7
D14
D21
D67
Day post transfer

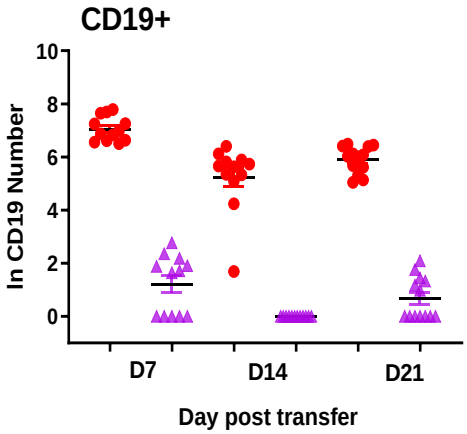
CD19+
ln CD19 Number
10
8
6
4
2
0
D7
D14
D21
Day post transfer

ENDOGENOUS				TRANSFER			
CD8	Lowest Value	Highest Value	Mean	CD8	Lowest Value	Highest Value	Mean
D0	0	58	18	D0	n/a	n/a	n/a
D2	0	176	81	D2	0	205	50
D7	29	5094	1554	D7	0	222	23
D14	2	6129	1027	D14	0	30	8
D21	3	488	183	D21	0	26	11
ENDOGENOUS				TRANSFER			
CD11B	Lowest Value	Highest Value	Mean	CD11b	Lowest Value	Highest Value	Mean
D0	184	2251	791	D0	n/a	n/a	n/a
D2	286	2750	1239	D2	0	134	34
D7	1766	73685	27429	D7	0	192	21
D14	76	24042	7412	D14	2	313	132
D21	340	8552	2083	D21	3	185	68
ENDOGENOUS				TRANSFER			
LY6G	Lowest Value	Highest Value	Mean	Ly6G	Lowest Value	Highest Value	Mean
D0	0	42	24	D0	n/a	n/a	n/a
D2	4	228	43	D2	0	14	2
D7	9	353	116	D7	0	16	6
D14	0	290	61	D14	0	14	3
D21	2	27	9	D21	0	10	5

ENDOGENOUS				TRANSFER			
LY6C	Lowest Value	Highest Value	Mean	Ly6C	Lowest Value	Highest Value	Mean
D0	20	99	46	D0	n/a	n/a	n/a
D2	4	33	16	D2	8	50	24
D7	18	952	217	D7	8	32	22
D14	14	113	55	D14	0	56	14
D21	13	209	44	D21	20	80	40

ENDOGENOUS				TRANSFER			
LY6C-	Lowest Value	Highest Value	Mean	Ly6C-	Lowest Value	Highest Value	Mean
D0	1936	2762	2279	D0	n/a	n/a	n/a
D2	550	1583	989	D2	0	0	0
D7	779	2758	1561	D7	0	0	0
D14	1919	5455	2930	D14	0	0	0
D21	354	2876	1330	D21	0	0	0

ENDOGENOUS				TRANSFER			
CD19	Lowest Value	Highest Value	Mean	CD19	Lowest Value	Highest Value	Mean
D7	701	2395	1278	D7	0	15	4
D14	4	600	273	D14	0	0	0
D21	155	652	407	D21	0	7	2

Figure 4.6: Total endogenous and transferred leukocytes present within the retina and vitreous at each clinical imaging time point. Quantified leukocyte numbers present within the retina and vitreous at each clinical imaging time point during clinical disease. In the endogenous and transferred compartment. Full time course of CD8+ T cell number present within the eye during disease (A). Full time course of CD11b+ cell number present within the eye during disease (B). Full time course of Ly6G+ (neutrophil) cell number present within the eye during disease (C). Full time course of Ly6C+ (inflammatory monocytes) cell number present within the eye during disease (D). Full time course of Ly6C- cell number present within the eye during disease (E). Full time course of CD19+; B cell number present within the eye during disease (F). Data expressed as mean $\pm$ SEM. One-Way ANOVA multiple comparisons of against naïve for the endogenous cell compartment and against day 2 for transferred cells *p<0.1, **p<0.01, ***p<0.001, p<0.0001. Stats not performed for day 35 as only one experiment, data shown to represent time course.

Tables shows range and mean of data presented.

4.3.5 Adoptive transfer of CX3CR1 heterozygous cells into RAG2$^{-/-}$ recipients causes recruitment of antigen-specific CD4+ T cells to ocular tissue by day 2

As illustrated previously (figure 4.5), the recruitment of uveitogenic transferred CD4+ T cells to the ocular tissue is detectable by day 2 after transfer this is associated with an increased number of endogenous CD4+ T cells that accumulate in the eye at this time point. To analyse if the endogenous T cell compartment is needed for the retention of transferred cells to occur, this compartment was eliminated from the experiment by using RAG2$^{-/-}$ mice as recipients of uveitogenic cell transfer.

Cells were transferred into Ly5 recipients or RAG2$^{-/-}$ recipients. When the two groups are compared (figure 4.7) recruitment of transferred CD4+ and CD8+ T cells to the eye two days after adoptive transfer is comparable.

Recruitment of transferred CD4+ T cells is observed in both groups at day 2 after adoptive transfer is shown in figure 4.7a. There is no significant difference between recruitment of transferred cells within the two recipient groups. The same affect is also present within the CD8+ compartment (figure 4.7b).

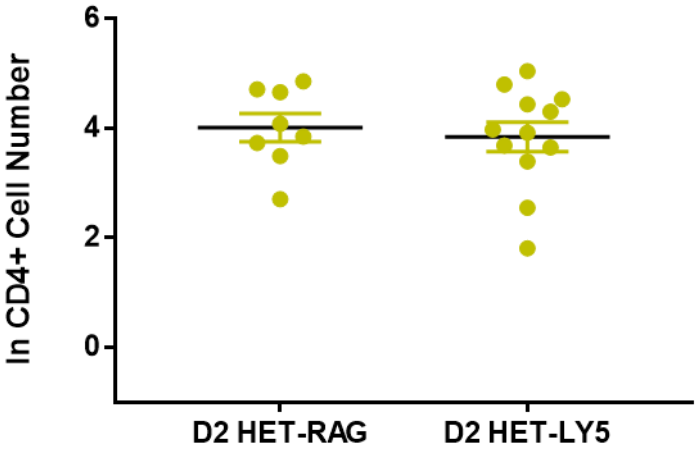

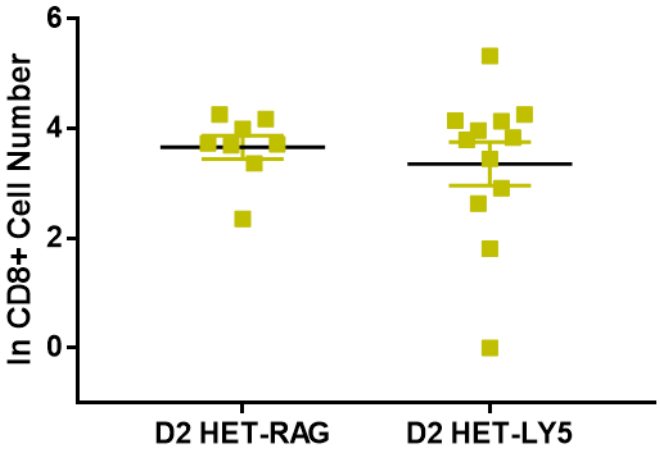

	LOWEST VALUE	HIGHEST VALUE	MEAN
CD4 HET-RAG	14	128	67
CD4 HET-LY5	5	154	62
CD8 HET-RAG	10	70	43
CD8 HET-LY5	0	205	50

Figure 4.7: Total endogenous and transferred leukocytes present within the retina and vitreous at each clinical imaging time point. Leukocytes were transferred into Ly5 (wildtype) mice and RAG2$^{-/-}$mice. Two days after adoptive transfer vitreous and retinas were assessed by flow cytometry. CD4+ (A) and CD8+ (B) transferred cell populations present within the eye were quantified and comparisons across the two groups made. Data expressed as mean $\pm$ SEM.

Table shows range and mean of data presented.

4.3.6 Selective recruitment of CD4+ T cells to the ocular tissue during active clinical disease

Recruitment of transferred CD4+ T cells to the ocular tissue during active clinical disease was illustrated in figure 4.5. To determine if this is a selective recruitment to the ocular tissue, other organs were analysed and endogenous and transferred CD4+ T cells quantified.

Within the eye (figure 4.8), transferred cells are detected by day 2 after adoptive transfer (highlighted in figure 4.5), by day 7 this population has increased due to peak disease. The transferred population then persists through active clinical disease to day 14 and continues to persist through to day 21 when active disease has resolved. The transferred cells further persist through to day 67 where disease can be considered to be quiescent.

In contrast within recipient's blood (figure 4.8), transferred CD4+ T cells are detected at day 2 but by day 7 (peak disease) the frequency of transferred CD4+ T cells detected within the blood has decreased. This effect is further seen at day 14 and day 21 with transferred cells making up a smaller frequency of the total CD4+ populations.

In a sample taken from a whole liver at each time point (figure 4.8), transferred CD4+ T cells are detected at day 2, the ratio of transferred and endogenous CD4+ T cells remains consistent throughout disease course but in contrast to the blood the frequency of CD4+ transferred cells present within the liver at day 7 increases in comparison to day 2 this increase in the frequency of transferred CD4+ T cells coincides with peak clinical disease in the eye. At day 14 and day 21, the frequency of transferred cells continues to decrease as active disease resolves which is also seen in the blood.

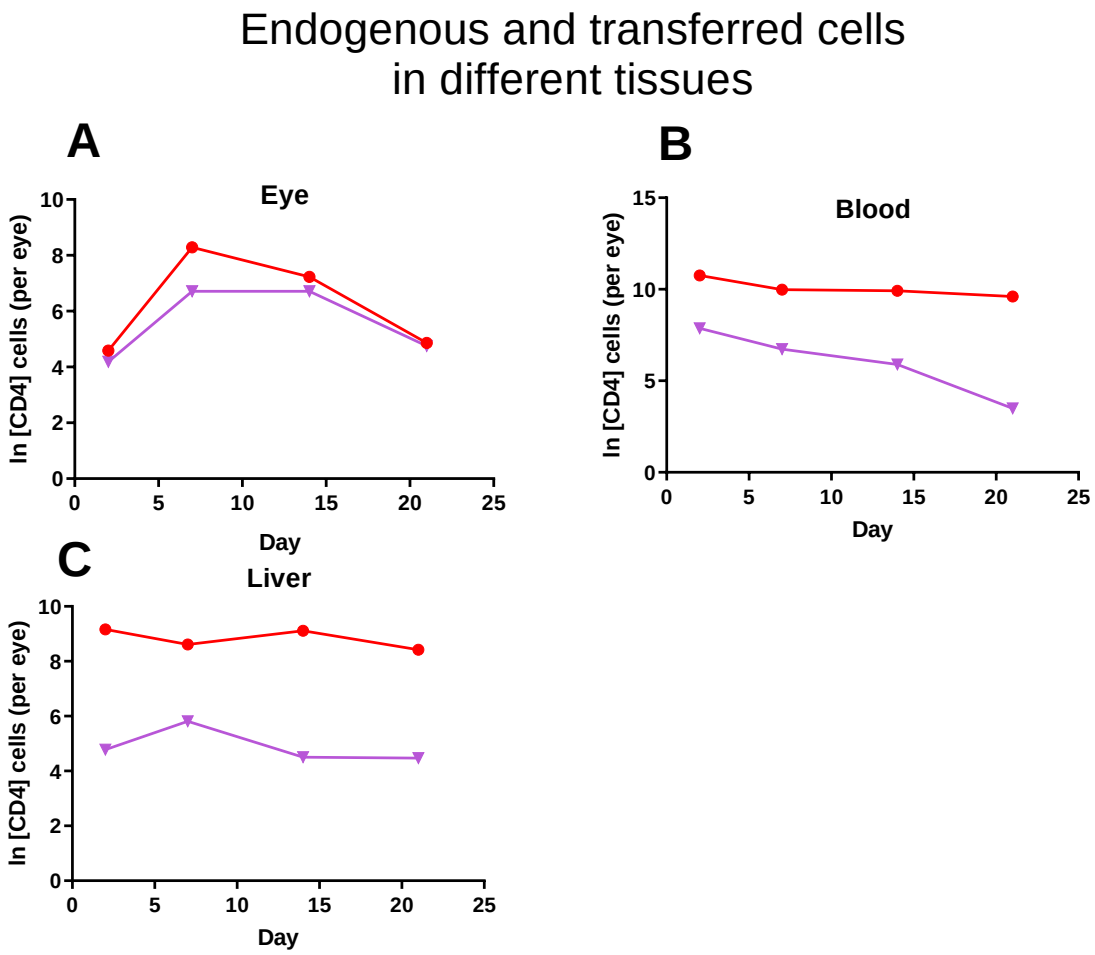

Figure 4.8: Frequency of transferred CD4+ T cells in the periphery of recipients during EAU. To determine if the recruitment of transferred CD4+ T cells to the eye to cause clinical disease is a selective recruitment, transferred populations within non-lymphoid tissues such as blood and liver were quantified. (A) Recruitment of endogenous and transferred CD4+ T cells present within the eye during clinical disease. (B) Recruitment of endogenous and transferred CD4+ T cells present within the blood during clinical disease. (C)) Recruitment of endogenous and transferred CD4+ T cells present within the liver during clinical disease. Data expressed as Mean cell number.

4.4 Discussion

This chapter uses the adoptive transfer technique developed in chapter 3 to induce EAU and interrogate disease course.

In order to understand disease, eyes were monitored using an optimised OCT clinical imaging technique following disease progression from day 2 to day 67. At different time points vitreous and retinas were isolated and analysed to quantify leukocyte infiltrate, specifically endogenous and transferred CD4+ T cells.

To establish pre-clinical changes of leukocyte number, leukocytes present within the eyes of naïve non-manipulated mice were quantified to give a baseline. 2 days after adoptive transfer recipients' eyes were imaged, where no clinical changes can be identified by OCT. When the retina and vitreous is isolated and leukocytes quantified using flow cytometry transferred cells are detected within the tissue (figure 4.4 and 4.5). Disease scoring was obtained by analysing fundal images at each time point. The mean score is obtained from the set of criteria described in *chapter 2* (Table 2.2), hence why increased scores are observed at peak disease due to the high levels of infiltrate and at late disease where minimal infiltrate is present but structural damage is greatest. Peak active clinical disease is observed at day 7 to 10 within the recipients and persists in an active phenotype through to day 14. Resolution of the active stage of disease occurs from day 21 and disease remains in a quiescent state from this time point. Although minimal retinal infiltrate is observed, due to the severity of the active disease stage the eye remains scarred and the structure damaged.

This chapter presents the kinetics of disease in comparison to naïve control eyes, however in future chapters mice that have received a PBS intraperitoneal injection are used as the baseline control for comparison.

In the CD4+ T cell compartment at day 2, a small population of transferred CD4+ T cells were detected, along with an increase within the endogenous CD4+ T cell compartment. This observation suggests an increased recruitment of endogenous CD4+ T cells after adoptive transfer of uveitogenic antigen specific leukocytes. Whether they are sticking in the eye due to non-specific tissue activation or whether an antigen-specific response is required is addressed within the next chapter. To understand if the recruitment of transferred cells to the eye at day 2 required an endogenous T cell response within the recipient, uveitogenic leukocytes were transferred into RAG2$^{-/-}$ mice that have no endogenous T or B cells. Retinas

and vitreous were isolated from recipients from the RAG2$^{-/-}$ group. CD4+ transferred T cells were quantified to analyse differences in transferred cell recruitment (figure 4.6). No difference in transferred CD4+ T cells was observed between the two groups at day 2 after adoptive transfer, demonstrating that endogenous lymphocytes are not required for the recruitment of transferred cells to be recruited and retained in the eye at this time point. We conclude that the transferred cells are sufficient to cause disease.

In wild type recipients, throughout active clinical disease course (day 7-21), recruitment of both endogenous and transferred CD4+ T cells increases within the retinal and vitreous infiltrate in comparison to day 2 infiltrate (figure 4.4). As seen at the day 2 time point transferred CD4+ T cells are recruited to the eye accompanied by increased endogenous CD4+ T cells, this is followed by further increased recruitment of both endogenous and transferred CD4+ T cells to obtain a peak in clinical disease at day 7 (figure 4.4). The ratio of endogenous and transferred CD4+ T cells at this time point is at roughly 1:1, but in some recipients a slightly larger endogenous population is observed.

At day 14, the endogenous and transferred populations have persisted to continue active disease. The ratio of endogenous to transfer CD4+ T cells remains at 1:1 in most recipients. This highlights the persistence of a large, transferred population within the tissue during active clinical disease. However, the larger population in some recipients continues to be the endogenous population due to activation within the inflammatory environment of the ocular tissue. When T cells encounter antigen within the eye they have to capabilities to become anergic or undergo apoptosis, secrete TGF-β and release soluble regulatory factors including the TCR α chain (204). Antigen taken up by cells originating from the eye, escape the tissue and are recruited to the spleen to activate a population of antigen-specific B and T cells (204). Anergic cells can be differentiated from naive and activated cells by CTLA4 and PD-1 staining (205).

By day 21, active disease has begun to resolve, and overall infiltrate has reduced when the eyes are imaged using OCT (figure 4.3). This is mirrored in the CD4+ T cell number an overall reduction in total CD4+ T cells is observed by flow cytometry.

Overall, following the induction of clinical disease, the ratio of transferred to endogenous cells remains ~1:1 through the duration of the experiment. Therefore, the disease process sustains the original pathogenic cells and their progeny indefinitely. Also, using clinical scoring alone disease does not appear to resolve, this is due to increased tissue damage after the high levels

of retinal infiltrate present throughout active clinical disease. When correlating flow cytometry data with OCT clinical scoring it is obvious the differences in disease activity and tissue damage, however with the imaging data alone this is not easily distinguishable.

At day 35 through to day 67, active clinical disease has resolved but transferred CD4+ T cells persist within the eye. The persistence of the original uveitogenic transferred CD4+ T cells within the eye throughout clinical disease suggest these cells are long lived and although may not be driving active disease they are persisting within the eye after active disease has resolved. The persistent increase in endogenous CD4+ T cells within the eye after active clinical disease suggests that changes in the tissue due to disease course have resulted in the increased retention of endogenous CD4+ T cells patrolling the tissue. In studies previously undertaken within the group a change in the nature of immune surveillance of the retina was observed following inflammation suggesting it is more likely a relapse of autoimmune disease is triggered by intercurrent activation of the immune system (114).

In comparison, CD8+, CD11b+ and CD19+ cells, which are components of the cell line, do not survive in the long term after adoptive transfer in the recipients and minimal cell numbers are detected within the eye. However, in the CD8+ transfer population an increase in the transferred population was observed at peak disease (day 7) but decreases in numbers and does not persist within the tissue throughout disease. The endogenous compartment does contribute cells from these lineages during active clinical disease where the changes in their cell numbers parallel those of the CD4+ infiltrate.

To further interrogate the behaviour of the transferred CD4+ population within the recipients, lymphoid and non-lymphoid organs were also analysed by flow cytometry through clinical disease to calculate the frequency of transferred CD4+ T cells within lymphoid and non-lymphoid tissue. In the blood, transferred CD4+ T cells are detected in the largest frequency at day 2 and as clinical disease develops the frequency is reduced (4.8). In the liver although a small increase in transferred CD4+ cells is observed at day 7 this could be due to the cells proliferating within the tissue. The frequency of transferred cells reduces from this timepoint (figure 4.8). BrdU staining could be used to understand if the cells are proliferating within the tissue between day 2 and day 7 or if the cells are being recruited from the periphery between these time points. The reduction in frequency of transferred CD4+ T cells in non-lymphoid tissue through clinical disease is in contrast to the eye where the transferred CD4+ population

increases through active clinical disease and persists through post-clinical disease suggesting a selective recruitment of the RBP3 specific transferred CD4+ T cells.

In conclusion, adoptive transfer of antigen specific pathogenic cells induces EAU in naïve recipients. Transferred CD4+ cells are detectable within the eye at day 2 after transfer concurrently with an increase of endogenous CD4+ T cells. The recruitment of transferred CD4+ T cells by day 2 to the eye is not reliant on the presence of endogenous CD4+ T cell recruitment. Endogenous and transferred CD4+ T cell recruitment increases by day 7 when peak disease is observed by OCT and quantification of leukocyte infiltrate. At this time point, endogenous and transferred CD4+ T cells are at a ratio of ~1:1 in some recipients but with a slightly larger endogenous population present within the eyes of other recipients. Active clinical disease persists to day 14 and endogenous and transfer populations persist within the eye. By day 21, active disease has resolved so total CD4+ T cell number reduces. Elevated endogenous CD4+ T cell population persists within the eye. By this time point transferred CD4+ T cells are now the larger population within the eye and have persisted throughout active clinical disease. By day 35 through to day 67 clinical disease has resolved but elevated endogenous CD4+ T cells in comparison to the naïve baseline remain present within the eye. Transferred CD4+ T cells persist in the eye through to day 67 in a small population even with no active disease present. Suggesting that the tissue never returns to its original state and immune surveillance of the tissue is permanently altered after active clinical disease.

Chapter 5. Antigen specific and non-antigen specific recruitment of CD4+ T cells during EAU

5.1 Introduction

The structure of the vasculature and lymphatic system are lined with endothelium, which is a single layer in thickness, this semipermeable layer lies between the vessel walls and the circulation. The endothelium acts as a barrier between vessels present in the blood and lymph and the tissues that surround them (206). The endothelium is essential in a number of physiological processes. It is considered a highly dynamic organ spread throughout the body to perform highly specialised functions. In total, in humans there are roughly 1-6x10^{13} endothelial cells that make up the endothelium with a total surface area of more than 1000 square metres (206). The heterogeneity of endothelial cells enables them to adapt their functions in different vascular sites (206).

5.1.1 Functions of the endothelium

The endothelium was once thought to have no specific functions other than the wrapping of the vasculature allowing selective permeability to water and electrolytes (207). But now it is understood that endothelial cells are paramount to vascular biology. The main functions of the endothelium are thrombosis and thrombolysis, coagulant mechanisms, regulation of vascular tone and growth, cell proliferation and angiogenesis and platelet and leukocyte interaction (207).

5.1.2 The resting endothelium and how it becomes activated in inflammation

The main site of leukocyte trafficking from the blood into non-inflamed tissues are the vascular endothelial cells, these cells are also responsible for maintaining the fluidity of blood and regulation of blood flow, and are capable of controlling the permeability of vessel walls (208). Interactions between leukocytes and endothelial cells influence immune surveillance and mediate wound repair and acute and chronic inflammation. Leukocytes accumulate within the tissue due to excessive adhesive interactions between the endothelium and patrolling leukocytes (209). Weibel-Palade bodies are secretory vesicles used by resting endothelial cells to accumulate leukocyte interactive proteins including P-selectin and chemokines to stop any interactions with patrolling leukocytes. Transcription of adhesion molecules is also suppressed by resting endothelial cells including vascular cell-adhesion

molecules (VCAM1), intracellular adhesion molecule (ICAM1) and E-selectin (208-211). Vascular endothelial cells will then change their phenotypes depending on the phase of the inflammatory process (208).

During non-infectious posterior uveitis, activated T cells recruited to the eye contributing to the inflammatory response produce cytokines and chemokines that are capable of activating retinal vessels (212). Activation of the retinal vessels induces a change in the phenotype of the endothelial cells present within the eye, upregulation of adhesion molecules including P-selectin, ICAM-1 and VCAM-1 concurrently with a downregulation of tight junction protein (212). This response leads to recruitment of a wide range of leukocytes that are directly responsible for damage to the tissue, this causes the BRB to become increasingly permeable to allow more immune infiltrate into the eye to create an amplification loop of the pathogenic process (212).

In studies of EAU in the B10 RII mouse, Heping et al described the sequence of events after EAU induction to be the focal adhesion of leukocytes on postcapillary venules in discrete sites followed by upregulation of adhesion molecules that induces breakdown of the blood retina barrier (213).

Activation of endothelial cells consists of two stages, endothelial cell activation type I and endothelial cell activation type II. Endothelial cell activation type I is rapidly occurring and stimulates endothelial cells without the need for gene upregulation or de novo protein synthesis, however endothelial cell activation type II takes time to have an effect on endothelial cells by gene transcription or protein synthesis as the stimulating agent needs time to take effect (83). The effects of endothelial cell activation type I are the expression of P selectin, the release of von Willebrand factor and the retraction of endothelial cells. the genes that are involved are those for adhesion molecules, cytokines and tissue factor (83). In order to migrate through the endothelium into the circulation, leukocytes first must adhere to the endothelium at preferential sites with specialised functions to undergo transendothelial migration within blood vessels. In non-lymphoid tissues these specialised sites are found at post capillary sites and in lymphoid tissue at high endothelial venules. Leukocytes moving through the blood will make contact with the wall of the vessel to interact with the endothelium, the cells will then slow and begin to roll along the endothelium and either disengage and re-enter flow of blood or will stop and remain stuck on the endothelium (84).

5.1.3 The endothelium as an antigen-presenting cell

It has been demonstrated both in vitro and in vivo that T cells can recognise antigen on the surface of endothelial cells (214). In vitro, it has been demonstrated that IFN-γ induces expression of MHC class II molecules on endothelial cells which results in T-cell activation and proliferation after interaction (214). In vivo, circulating T cells have also been observed to recognise antigens on the surface of endothelial cells which trigger endothelial cell activation causing a release of mediators (214, 215).

In rat models studying the endothelium presenting antigen within the eye during EAU, antigen was detected within the retinal vessels when early signs of retinal infiltrate was observed (216). Further to this, studies have also shown gamma interferon expression within the eye induce vascular endothelium to express class II antigens at comparable levels to a macrophage (217).

5.1.4 Antigen specific T cell recruitment during disease

When using the adoptive transfer model that is discussed in *chapter 4*, T cells are stimulated in vitro with the cognate antigen to give an activated phenotype. Thus, when the cells are transferred into the recipient and enters the ocular tissue the T cell has the capacity to proliferate, produce cytokines, interact with APCs and induce cytotoxicity to promote inflammation (169).

From data collected and presented in *chapter 4*, an increased recruitment of endogenous CD4+ T cells is observed at day 2 after transfer. From this observation the hypothesis that the endothelium is becoming activated by the transferred pathogenic CD4+ T cells, causing endogenous cells to tether to the endothelium to initiate clinical disease was considered. The aim of this chapter is to understand if the activation of the endothelium depends on an antigen specific response initiated by the pathogenic transferred T cells or a non-antigen specific response caused by the activation status of the transferred T cells.

5.2 Materials and Methods

5.2.1 Activation of OTII TCR Transgenic splenocytes

Splenocytes were isolated from OTII CD45.1 TCR transgenic mice or OTII CX3CR1$^{+/GFP}$ CD45.1.2 mice and activated in cell culture with 1µg/ml OVA peptide antigen, 10ng/ml IL-23 and 10ng/ml IL-2 (added at 24 hours). Leukocytes were isolated after 72 hours of culture using Ficoll centrifugation and transferred by intraperitoneal injection at 2x10^6 total leukocytes per recipient.

5.2.2 Generation of uveitogenic leukocytes for adoptive transfer

C57BL/6 CX3CR1$^{+/GFP}$ CD45.2 mice were immunised with RBP3 peptide 629-643, spleen and lymph nodes were isolated at day 11 and cultured for 72 hours supplemented with RBP3, 10 no/ml IL-23 and 10ng/ml IL-2 (added at 24 hours). Leukocytes were then isolated using Ficoll centrifugation and transferred into naïve CD45.1 Ly5 WT recipients by intraperitoneal injection at 2x10^6 cells per mouse.

5.2.3 Clinical imaging

OCT was used to acquire clinical imaging for a disease time course from day 0 to day 25 using the standardised method developed and described in data chapter 3.

5.2.4 Flow cytometry

At predefined time points after adoptive transfer, retinas were analysed by flow cytometry to quantify total cell number for each leukocyte population. Allelic markers were used as seen previously to identify transferred and endogenous populations including CD45.1, CD45.2 and CD45.1.2.

5.2.5 Statistical Analysis

Cell numbers were calculated from the standard curve (n) and were log transformed (ln(n+1) and expressed as Mean $\pm$ SEM. Statistical analysis such as a Mann Whitney test (for 2 sample groups) or a one-way ANOVA for sample groups of more than two was performed.

5.3 Results

5.3.1 Intraperitoneal injection of PBS causes an increase in endogenous cells present within the eye

In order to establish the sensitivity of the analysis to small changes between total CD4+ and CD8+ T cells in naïve unmanipulated recipients and changes in cell number before clinical disease is observed, cell numbers in the eye were quantified using standard methods previously used in the group (data first shown in *chapter 4*) (114).

The optimised adoptive transfer technique uses an intraperitoneal injection to transfer the cells into the recipients. To account for the trauma from any injection, a baseline analysis of the effect this might have on cell numbers is useful when studying small differences in CD4+ and CD8+ cell numbers between naïve animals, animals receiving PBS only and those receiving PBS plus an aliquot of cells.

Naïve mice received an intraperitoneal injection of 200µl of PBS alone but with no cell transfer. At day 2 after injection retinas were analysed to quantify CD4+ cell numbers and CD8+ cell numbers.

A statistically significant increase in CD4+ T cell number within the eye is observed at day 2 after intraperitoneal injection of PBS (Figure 5.1) compared with naïve cell numbers, this shows that injection trauma effects the number of CD4+ T cells that adhere in the eye.

In contrast, the procedure does not appear to influence the CD8+ T cell number due to the larger dynamic range in the naïve CD8+ dataset therefore no change in cell number can be detected (Figure 5.1).

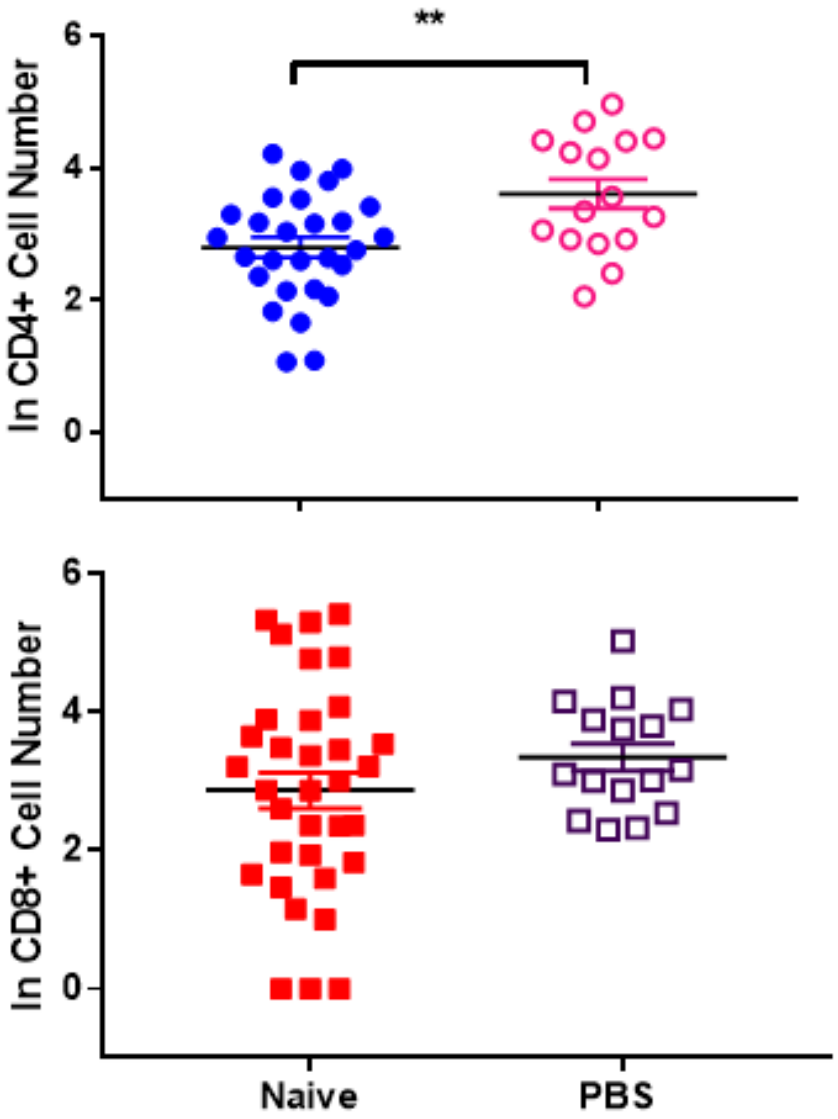

Figure 5.1: Intraperitoneal injection of PBS causes a statistically significant increase in CD4+ T cells sticking in the eye. Mice were age-match naïve or were given a 200µl intraperitoneal injection of tissue culture grade PBS. At day 2, eyes were dissected and total CD4+ and CD8+ numbers quantified. Data are expressed as Mean ±SEM. Statistical analysis performed: unpaired non-parametric Mann-Whitney Test **p<0.01.

5.3.2 Activated and non-activated OTII cells do not activate the endothelium and remain in the eye after adoptive transfer

To investigate whether the recruitment of endogenous cells at day 2 after pathogenic adoptive transfer requires an antigen specific response to activate the endothelium or is solely due to a non-specific accumulation of activated transferred cells induced by the intraperitoneal injection, OVA specific activated cells were transferred into naïve recipients and leukocytes quantified to determine changes in endogenous and transferred leukocyte cell number retained within the eye after transfer.

Antigen presentation by the endothelium leads to recruitment of specific T cells. Interactions between circulating T cells and the endothelium could influence the development of a local immune response. Due to the continuous interaction of circulating T cells with endothelial cells full competency of the endothelium as an APC could create problems in the regulation of autoimmune reactivity (218). The possibility that antigen presentation by the endothelium can directly influence the extent of lymphocyte recruitment at the site of inflammation has been demonstrated in EAE (218).

TCR transgenic OTII cells were activated in vitro with OVA antigen and then transferred into naïve recipients (figure 5.2) because as seen in figure 5.1, i.p injection increases ocular CD4+ cell numbers, analysis were carried out using i.p injections as a baseline.

At day 2 after transfer of $2x10^6$ activated or non-activated OTII cells, there is no significant increase in endogenous CD4+ T cell recruitment to the eye in comparison to a PBS intraperitoneal injection (data originally shown in figure 5.1) whereas at day 7 the CD4+ T cell number had dropped to similar numbers to a naïve unmanipulated mouse (Figure 5.2a). Although the number of endogenous CD4+ T cells increases at day 2 after transfer the number of transferred cells remaining within the eye is low and not activation state dependent, this continues to day 7 when the endogenous cell number decreases to the level seen in samples from naïve animals (Figure 5.2b) activated and non-activated OTII cells do not reach statistical significance.

Whereas in the CD8+ T cell compartment there is no significant increase in the endogenous cell number and very few transferred cells stick in the eye at day 2 and day 7 (Figure 5.2c and 5.2d).

At day 2 after transfer of $5x10^6$ activated cells an increased number of CD4+ transferred cells can be seen in the eyes of recipients in comparison to the transfer of $2x10^6$ cells (Figure 5.2b and 5.3b). The number of activated transferred cells that stick in the eye is statistically significantly increased in comparison to the non-activated transferred cells after transfer.

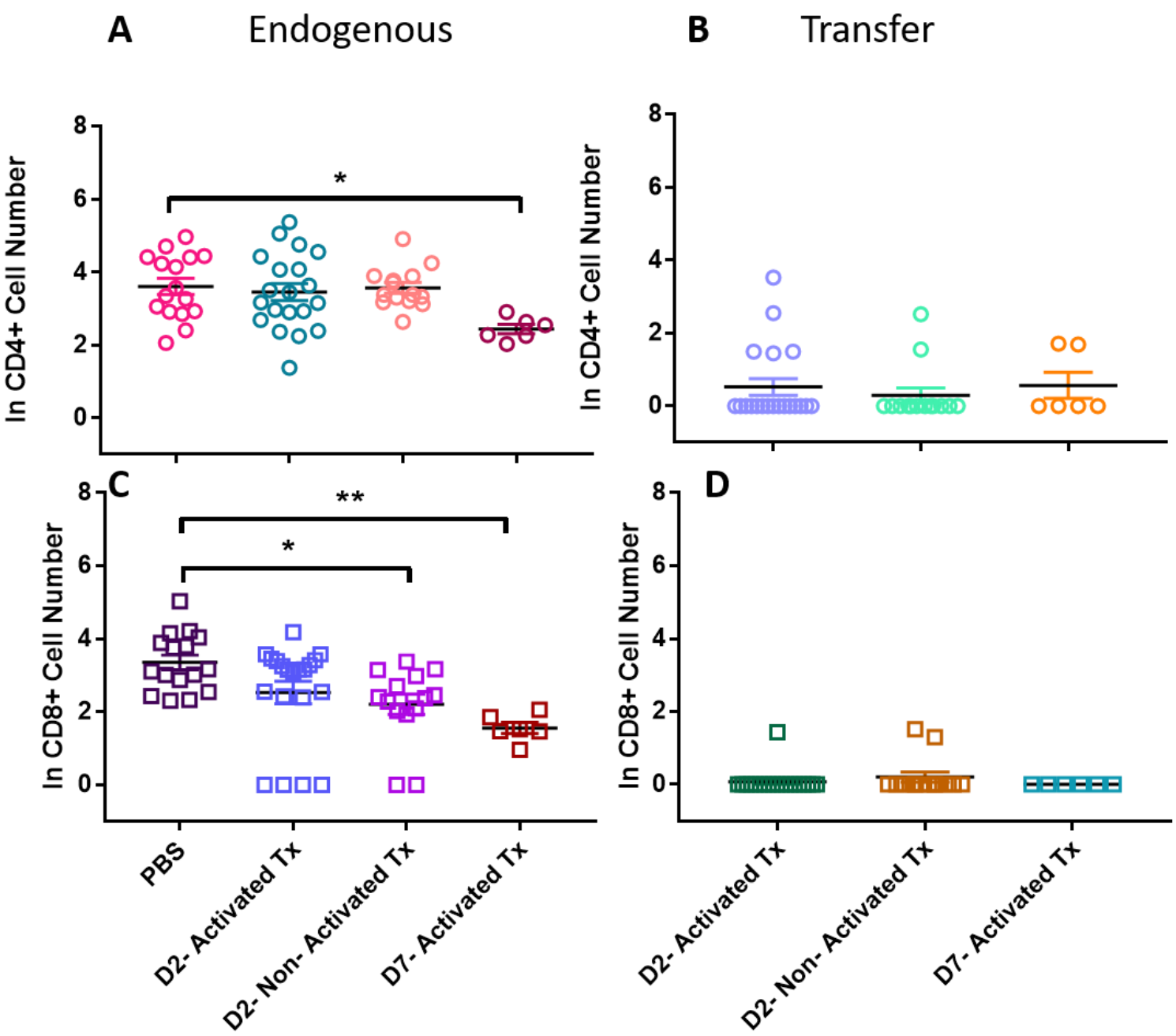
A
Endogenous
B
Transfer
ln CD4+ Cell Number
ln CD4+ Cell Number
*
C
D
ln CD8+ Cell Number
ln CD8+ Cell Number
**
*
PBS
D2- Activated Tx
D2- Non- Activated Tx
D7- Activated Tx
D2- Activated Tx
D2- Non- Activated Tx
D7- Activated Tx

Figure 5.2: Adoptive transfer of activated or non-activated $2x10^6$ TCR transgenic cells into naïve recipients. Naïve recipients received an intraperitoneal injection of activated or non-activated OTII cells at $2x10^6$ cells per mouse. Retinas were dissected and analysed using flow cytometry at day 2 or day 7 to quantify the endogenous and transferred CD4+ and CD8+ T cell populations present within the eye. (A+C) Endogenous CD4+ or CD8+ T cell number present within the eye in naïve recipients, recipients that received a PBS intraperitoneal injection (data originally shown in figure 5.1), recipients that received a $2x10^6$ activated cell transfer analysed at day 2, recipients that received a $2x10^6$ non-activated cell transfer analysed at day 2 or recipients that received a $2x10^6$ activated cell transfer analysed at day 7. (B+D) Corresponding analysis of transferred CD4+ or CD8+ OTII TCR transgenic cells present within the eyes of recipients after activated or non-activated transfer at day 2 or day 7. Data are expressed Mean $\pm$SEM. Statistical analysis performed: One-Way ANOVA multiple comparisons against PBS (A+C) or against D2 activated (B+D). *$p<0.05$

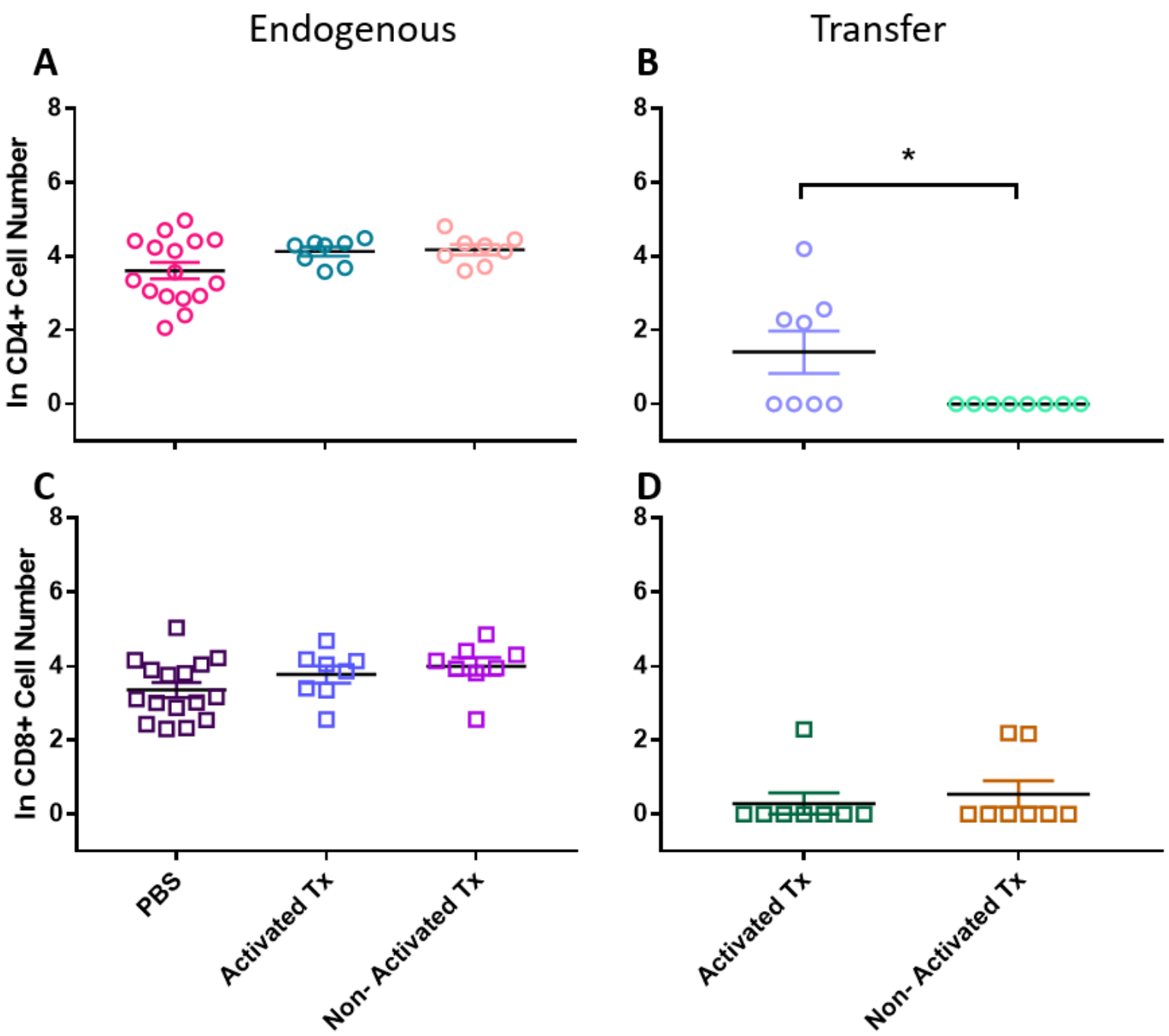
Endogenous
Transfer
A
B
C
D
ln CD4+ Cell Number
ln CD8+ Cell Number
8
6
4
2
0
*
PBS
Activated Tx
Non- Activated Tx
Activated Tx
Non- Activated Tx

Figure 5.3: Adoptive transfer of activated or non-activated 5x10^6 TCR transgenic cells into naïve recipients. Naïve recipients received a transfer of 5x10^6 activated or non-activated OTII cells. Retinas were dissected and endogenous and transferred CD4+ and CD8+ T cells were quantified at day 2. (A+B) Endogenous and transferred CD4+ T cells present within the eye. (C+D) Endogenous and transferred CD8+ T cells present within the eye. Data are expressed as Mean ±SEM. Statistical analysis performed: One-Way ANOVA multiple comparisons against PBS (A+C). Statistical analysis performed: unpaired non-parametric Mann-Whitney Test (B+D) *$p<0.05$.

5.3.3 Intravitreal injection of OVA with OTII cell transfer causes large amounts of retinal infiltrate

As seen in figure 5.2, transfer of activated or non-activated OTII TCR transgenic cells does not initiate clinical ocular disease or recruitment of transferred and endogenous cells. Suggesting that the recruitment of endogenous cells by day 2 after pathogenic transfer is due to an antigen-specific response.

To further investigate if the introduction of antigen would lead to the recruitment of OTII cells to the eye, OVA antigen was injected intravitreally into one eye. Activated OTII cells were then transferred by intraperitoneal injection.

At day 2, there is no difference by clinical imaging of retinal infiltrate within the OVA injected and PBS injected eyes (Figure 5.4a and 5.4b). Flow cytometry demonstrated that transferred CD4+ T cells can be detected in both eyes in similar numbers as the activated cell transfer alone (Figure 5.2b) (Figure 5.6b). However, when the eye receives the OVA intravitreal injection (figure 5.6b) active disease develops after day 2, whereas when OVA specific cells are transferred with no intravitreal injection, at day 7 no active disease is present and minimal transferred cells are present in the eye.

The increase in endogenous CD4+ cell number in both eyes is within the range seen in CD4+ cell numbers after PBS intraperitoneal injection (Figure 5.6a). A similar response can also be seen in the CD8+ and CD11b+ compartments (Figure 5.7a-d and Figure 5.8a-d). In contrast within the Ly6G+ and Ly6C+ cell compartment the greatest number of cells is observed at day 2 due to the injection trauma (Figure 5.9a-d and Figure 5.10a-d). Transferred Ly6C+ cell number is the highest number of transferred cells recruited to the eye by that time point (Figure 5.10b and 5.10d).

Whereas, at day 4 by OCT obvious retinal infiltrate was observed around the optic disc in both eyes of the recipients (Figure 5.4c and 5.4d) corresponding flow cytometry analysis illustrated a recruitment of transferred CD4+ cells to the left eye that received OVA and some non-specific sticking of the transferred CD4+ T cells in the right eye that received the control injection (Figure 5.7b and 5.7d). Whereas, in the endogenous compartment the CD4+ cell number in both eyes remains the same as day 2 (Figure 5.6a and 5.6c). In the CD8+ and CD11b+ cell compartment endogenous recruitment is within the same limits as day 2, and

transferred cells are recruited in low cell number which corresponds with the CD4+ compartment (Figure 5.7a-d and 5.8a-d).

At day 8, OCT shows peak clinical disease characterised by severe retinal infiltrate within the vitreous, thickening of the retina and swelling of the optic disc by OCT and vitreal haze and perivascular sheathing within the fundus (Figure 5.4e) in the left eye which received the OVA antigen in comparison to the right eye which received PBS which continues to look normal (figure 5.4f).

At day 15, clinical disease continued although retinal infiltrate is visibly reduced within the vitreous and the retina and optic disc have thinned (Figure 5.6g) suggesting that at this time point the disease is past peak. In contrast the right eye still shows no clinical signs of disease by OCT and remains normal (Figure 5.4h). When retinal infiltrate is analysed by flow cytometry recruitment of endogenous to transferred CD4+ T cells is occurring at a ~1:1 ratio in large cell numbers (in the left eye that received the OVA antigen Figure 5.6a-b). Whereas, in the right eye endogenous recruitment remains constant from day 4 (Figure 5.6c), in the transferred compartment some CD4+ T cells stick non-specifically in the eye but this is not statistically significantly higher than day 2 before induction of clinical disease (Figure 5.6d). Recruitment of CD8+ T cells to the left eye are significantly higher than seen at day 2 in the left eye illustrating a recruitment of endogenous CD8+ T cells to the eye with clinical disease (Figure 5.7a) whereas in the right eye where no clinical disease is seen by OCT there is no increased recruitment of CD8+ cells (Figure 5.7c). In the transferred compartment cells are not recruited to either eye irrespective of clinical disease status, this effect is similarly seen in the recruitment of CD11b+ cells (Figure 5.8a-d). In contrast, the increase seen in the Ly6G+ cell number at day 2 persists in the inflamed eye (left eye) but does not increase (Figure 5.9a) in the non-inflamed eye (right eye) the Ly6G+ cell number decreases significantly by day 15 (Figure 5.9c). Ly6G+ transferred cells are not recruited to the eye during clinical disease (Figure 5.9b and 5.9d). Both endogenous and transferred Ly6C+ cell number decreases by day 15 (Figure 5.10a-d).

Clinical disease persists through to day 25 in the left eye after transfer but shows signs of resolving by OCT such as reduced cellular infiltrate within the vitreous, and the retinal thickness and optic disc have returned to pre disease thickness, in the fundal image the vitreous haze has resolved and the perivascular sheathing is no longer visible (Figure 5.4i and 5.4j). In the left eye, total CD4+ cell number reduces between day 15 and day 25, subsequently

the transferred and endogenous populations have also decreased (Figure 5.6a 5.6b). Endogenous CD8+ T cell number persists in both eyes, but increased cell numbers were seen in the left eye of the recipients in comparison to the right eyes (Figure 5.7a-d). In the CD11b+, Ly6G+ and Ly6C+ compartment transferred cells are not recruited to the eye, but endogenous cells persist throughout disease, in the left eye that received the OVA peptide there is a more severe clinical disease thus cell numbers are increased across all leukocyte populations in comparison to the right eye (Figures 5.8a-d, 5.9a-d and 5.10a-d).

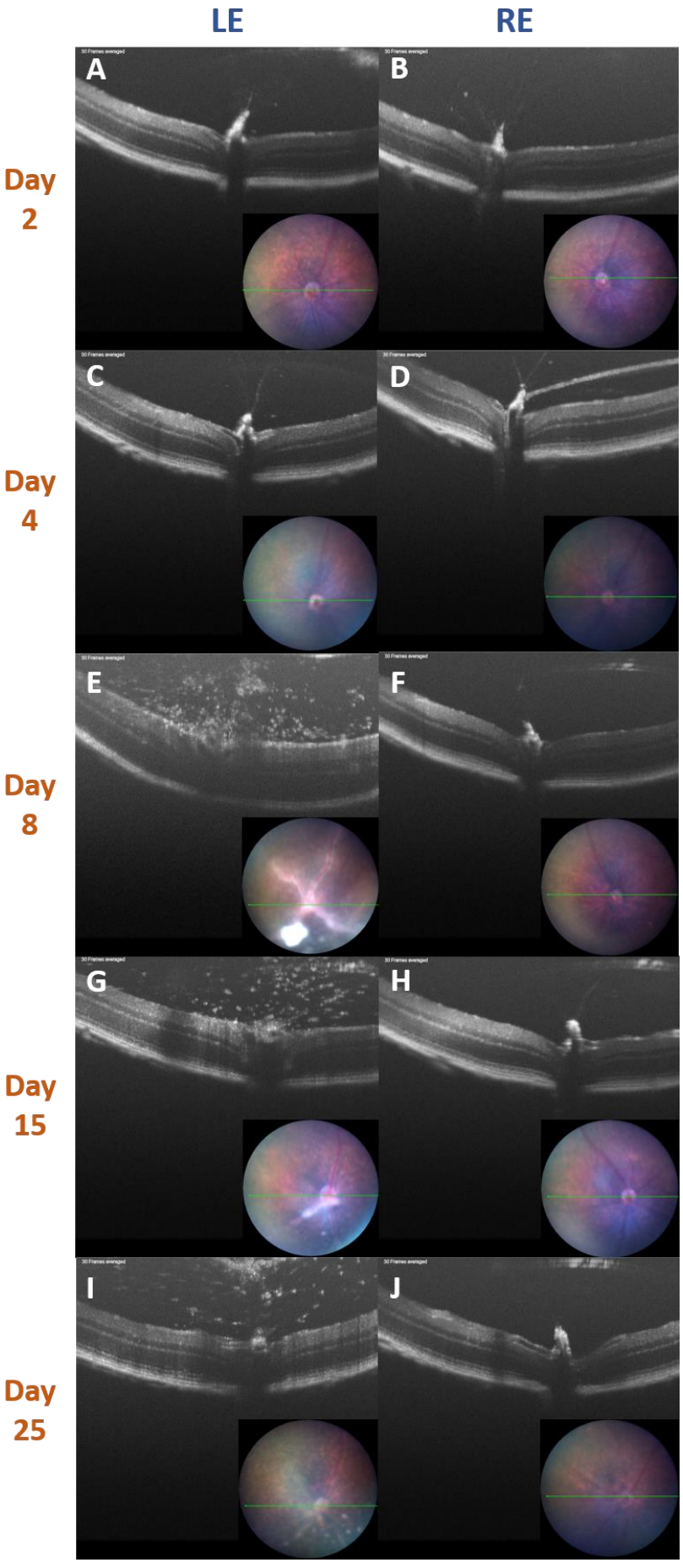
LE
RE
Day 2
Day 4
Day 8
Day 15
Day 25
A
B
C
D
E
F
G
H
I
J

Figure 5.4: OCT imaging after intravitreal injection of OVA or PBS to day 25. Time course from day 2 after intravitreal OVA injection with concurrent intraperitoneal transfer of activated OTII cells at $2x10^6$ cells per mouse. Left eye received an intravitreal injection of OVA antigen, Right eye received an intravitreal injection of PBS. (A-J) Representative OCT images with concurrent fundal imaging from day 2 and day 25. Clinical disease is characterised by retinal infiltrate within the vitreous, swelling of the optic disc and thickening of the retina on the OCT image and vascular sheathing and vitreal haze on the fundal image.

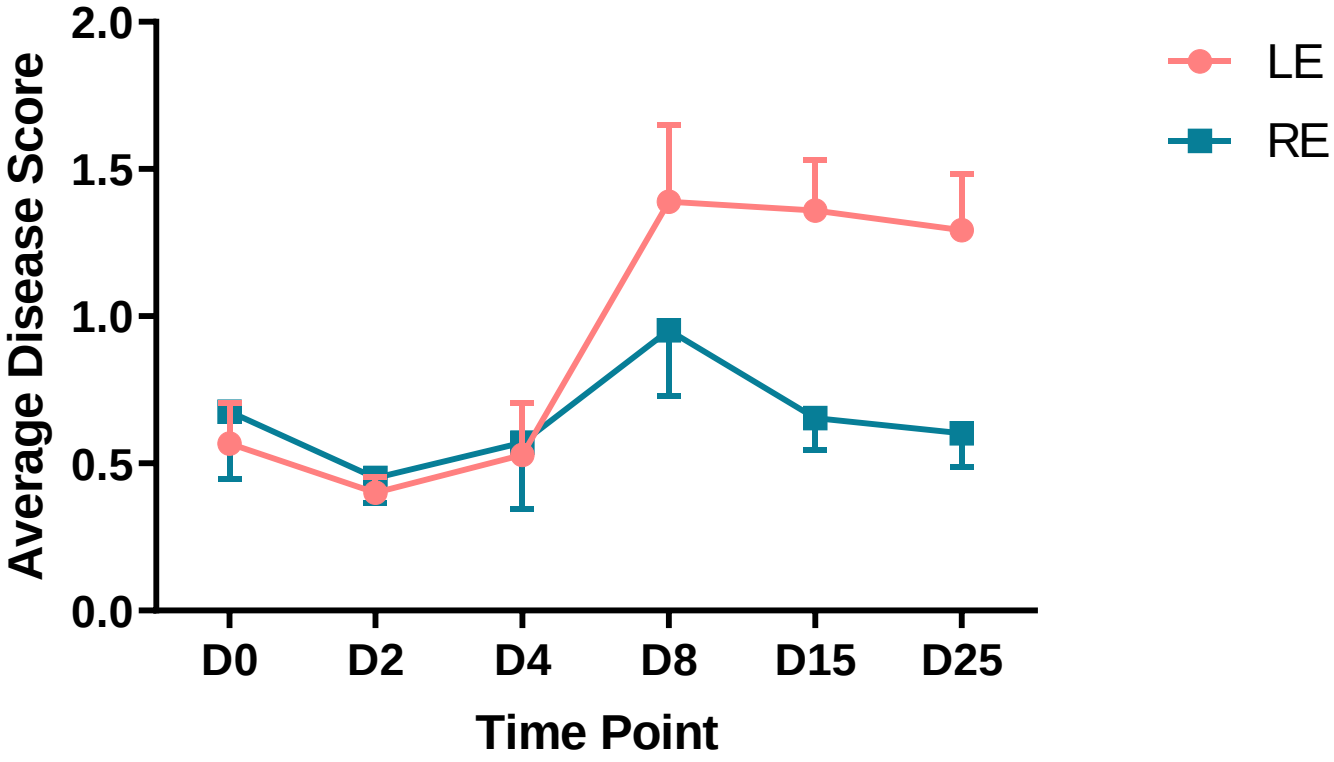

Figure 5.5: Average OCT disease scores throughout clinical disease course. Fundal images acquired concurrently with OCT images at each time point were scored blind using the criteria detailled In *chapter 2*. Average score was calculated for each eye, data expressed as mean ± SEM. Left eye received OVA intravitreal injection, right eye received control (PBS/L144) intravitreal injcetion.

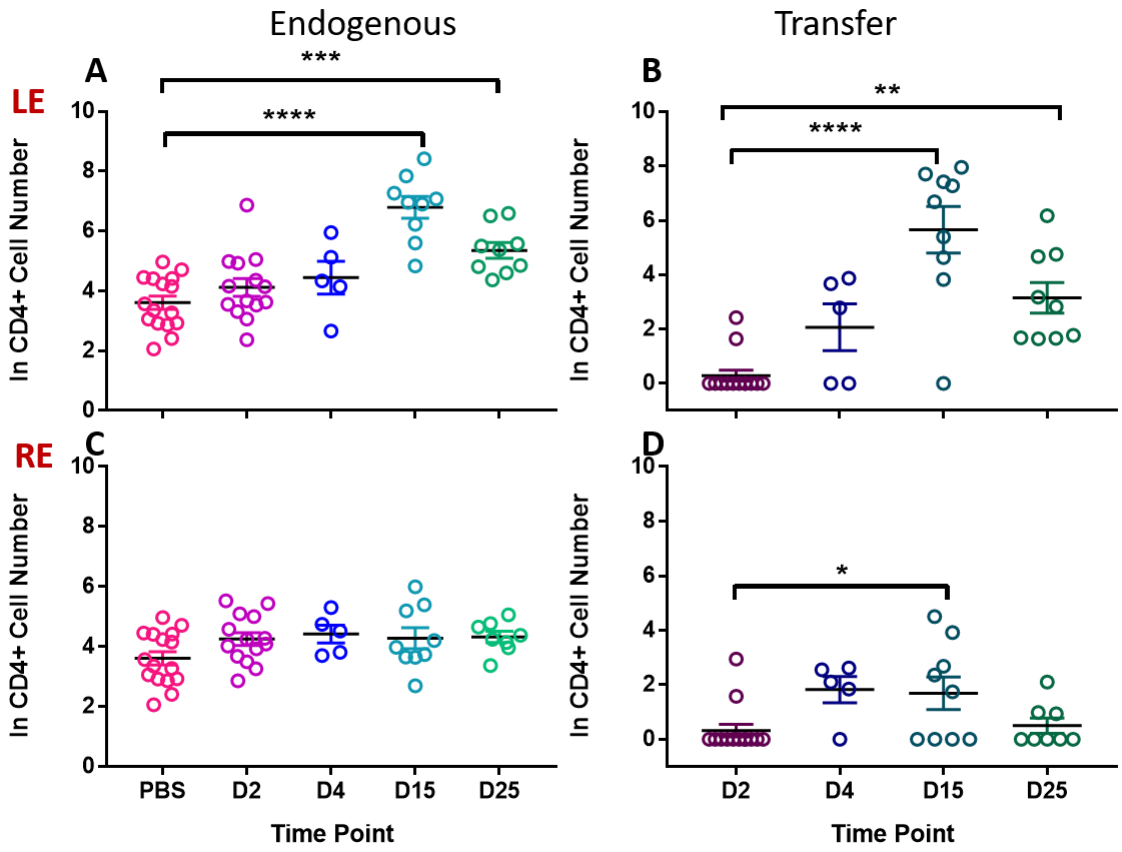

Figure 5.6: Flow cytometric quantification of CD4+ retinal infiltrate. Retinas were dissected and prepared for flow cytometry at pre-defined time points. Total CD4+ cell numbers were quantified and then endogenous and transferred cell populations calculated. (A) Total endogenous CD4+ T cells present within the left eye of recipients at each time point (B) Total transferred CD4+ T cells present within the left eye of recipients at each time point (C) Total endogenous CD4+ T cells present within the right eye of recipients at each time point (D) Total transfer CD4+ T cells present within the right eye of recipients at each time point. Data are expressed as Mean ±SEM. Statistical analysis performed: One-Way ANOVA multiple comparisons against PBS (previously shown in figure 5.2) (A+C), comparisons against day 2 (B+D). *p<0.05, **p<0.01, ***p<0.001, ****p<0.0001.

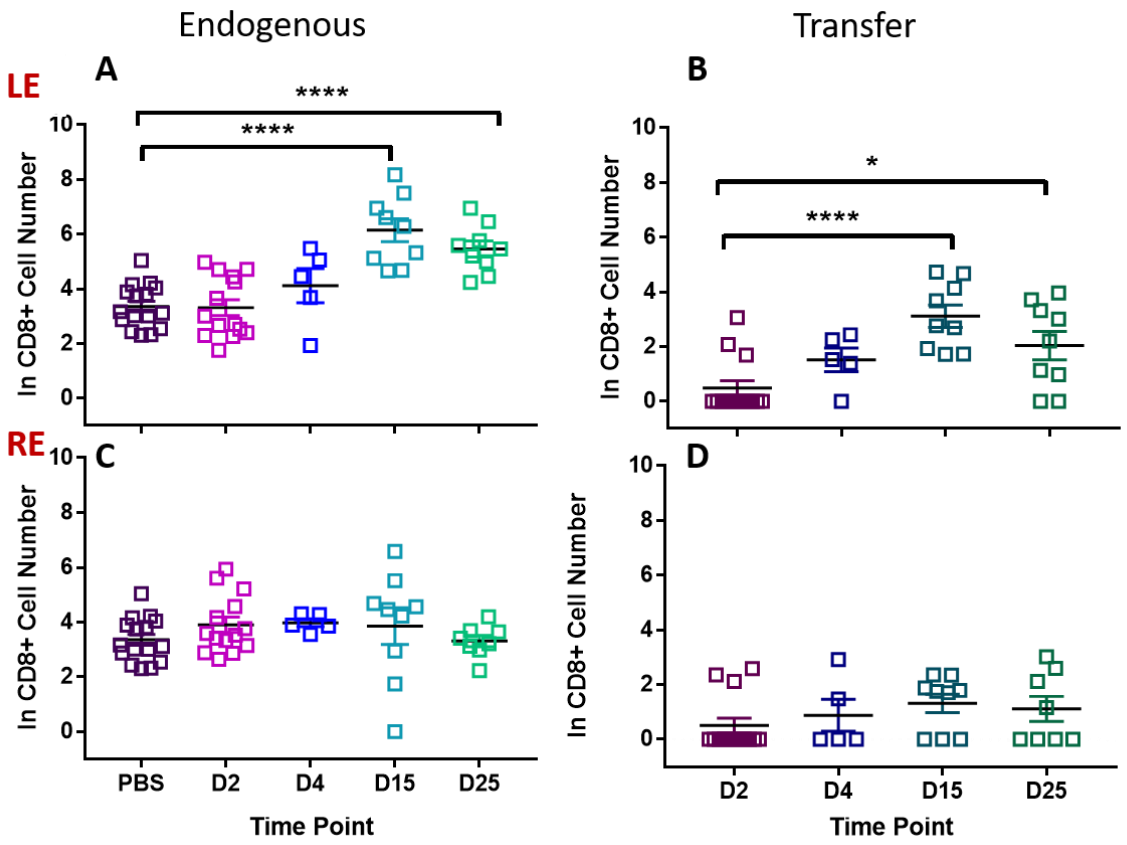

Figure 5.7: Flow cytometric quantification of CD8+ retinal infiltrate. Retinas were dissected and prepared for flow cytometry at pre-defined time points. Total CD8+ cell numbers were quantified and then endogenous and transferred cell populations calculated. (A) Total endogenous CD8+ T cells present within the left eye of recipients at each time point (B) Total transferred CD8+ T cells present within the left eye of recipients at each time point (C) Total endogenous CD8+ T cells present within the right eye of recipients at each time point (D) Total transfer CD8+ T cells present within the right eye of recipients at each time point. Data are expressed as Mean ±SEM. Statistical analysis performed: One-Way ANOVA multiple comparisons against PBS (previously shown in figure 5.2) (A+C), comparisons against day 2 (B+D). *p<0.05, ****p<0.0001.

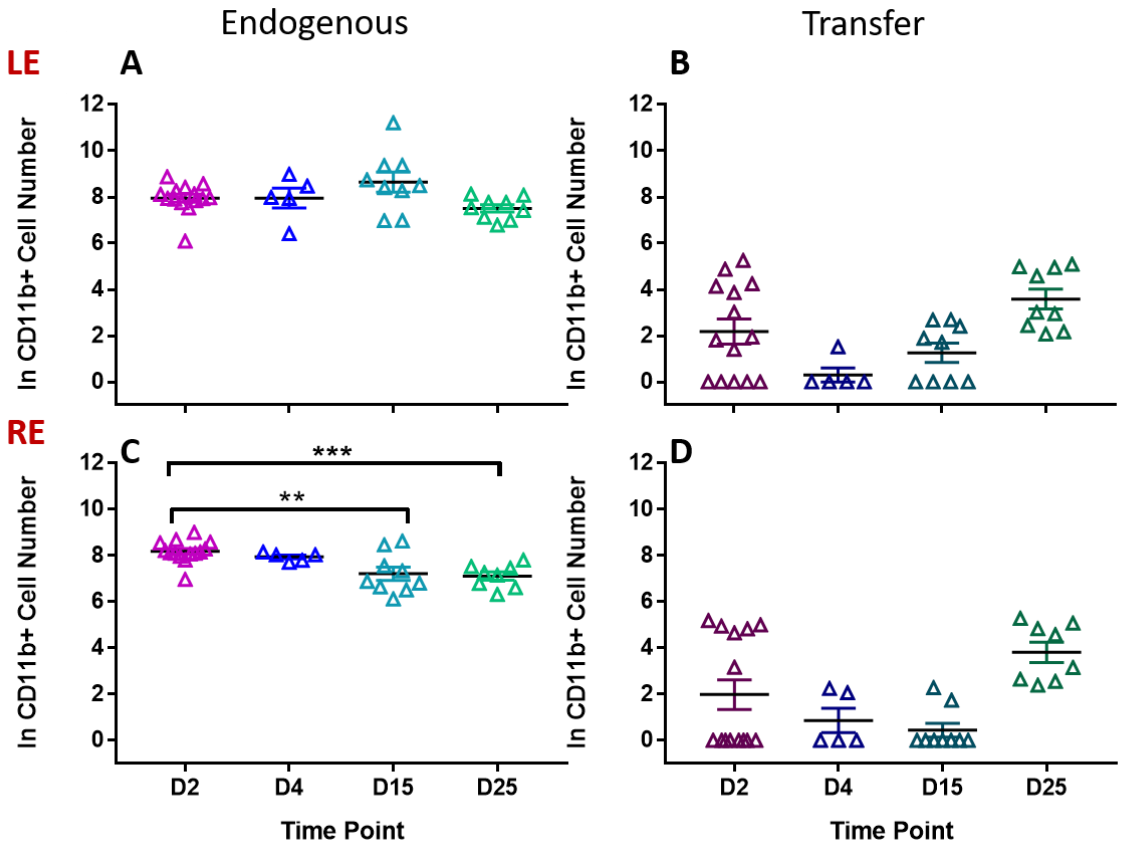

Figure 5.8: Flow cytometric quantification of CD11b+ retinal infiltrate. Retinas were dissected and prepared for flow cytometry at pre-defined time points. Total CD11b+ cell numbers were quantified and then endogenous and transferred cell populations calculated. (A) Total endogenous CD11b+ cells present within the left eye of recipients at each time point (B) Total transferred CD11b+ cells present within the left eye of recipients at each time point (C) Total endogenous CD11b+ cells present within the right eye of recipients at each time point (D) Total transfer CD11b+ cells present within the right eye of recipients at each time point. Data are expressed as Mean ±SEM. Statistical analysis performed: One-Way ANOVA multiple comparisons against day 2 (A-D). **p<0.01, ***p<0.001

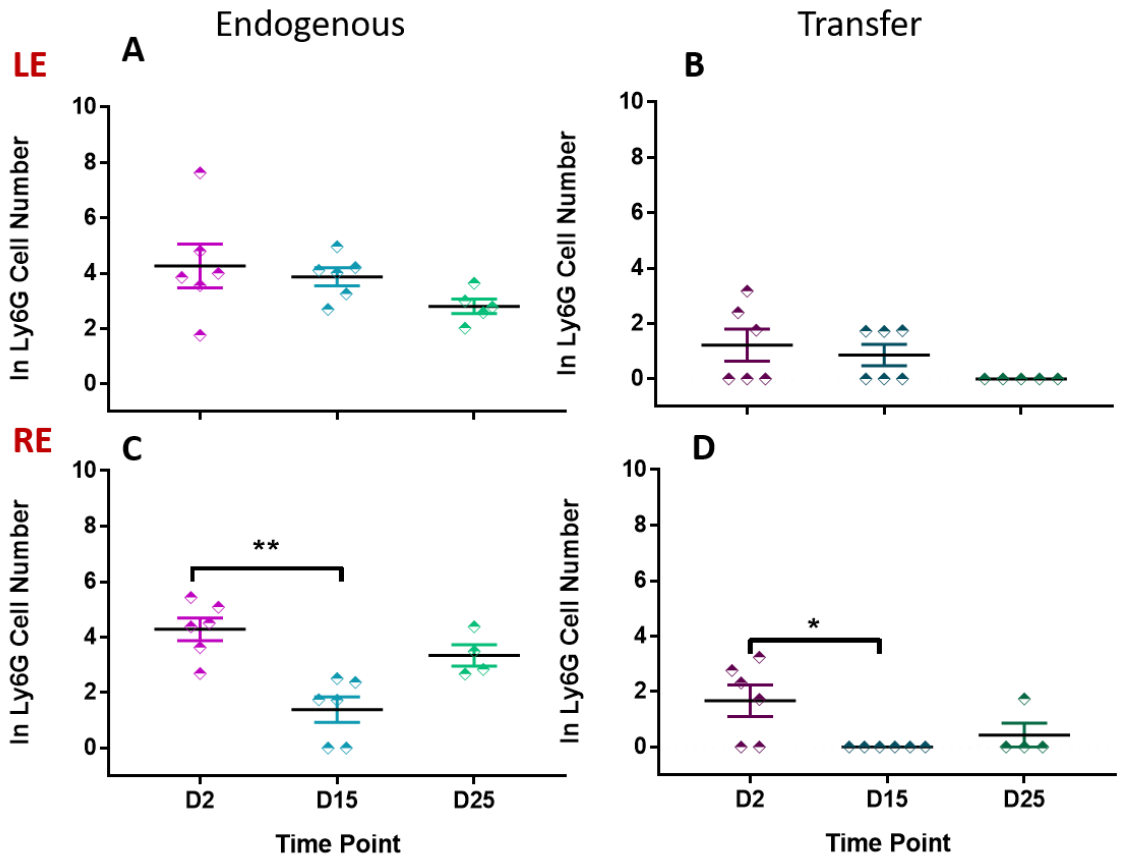

Figure 5.9: Flow cytometric quantification of Ly6G+ retinal infiltrate. Retinas were dissected and prepared for flow cytometry at pre-defined time points. Total Ly6G+ cell numbers were quantified and then endogenous and transferred cell populations calculated. (A) Total endogenous Ly6G+ cells present within the left eye of recipients at each time point (B) Total transferred Ly6G+ cells present within the left eye of recipients at each time point (C) Total endogenous Ly6G+ cells present within the right eye of recipients at each time point (D) Total transfer Ly6G+ cells present within the right eye of recipients at each time point. Data are expressed as Mean ±SEM. Statistical analysis performed: One-Way ANOVA multiple comparisons against day 2 (A-D). *p<0.05, **p<0.01, ***p<0.001, ****p<0.0001.

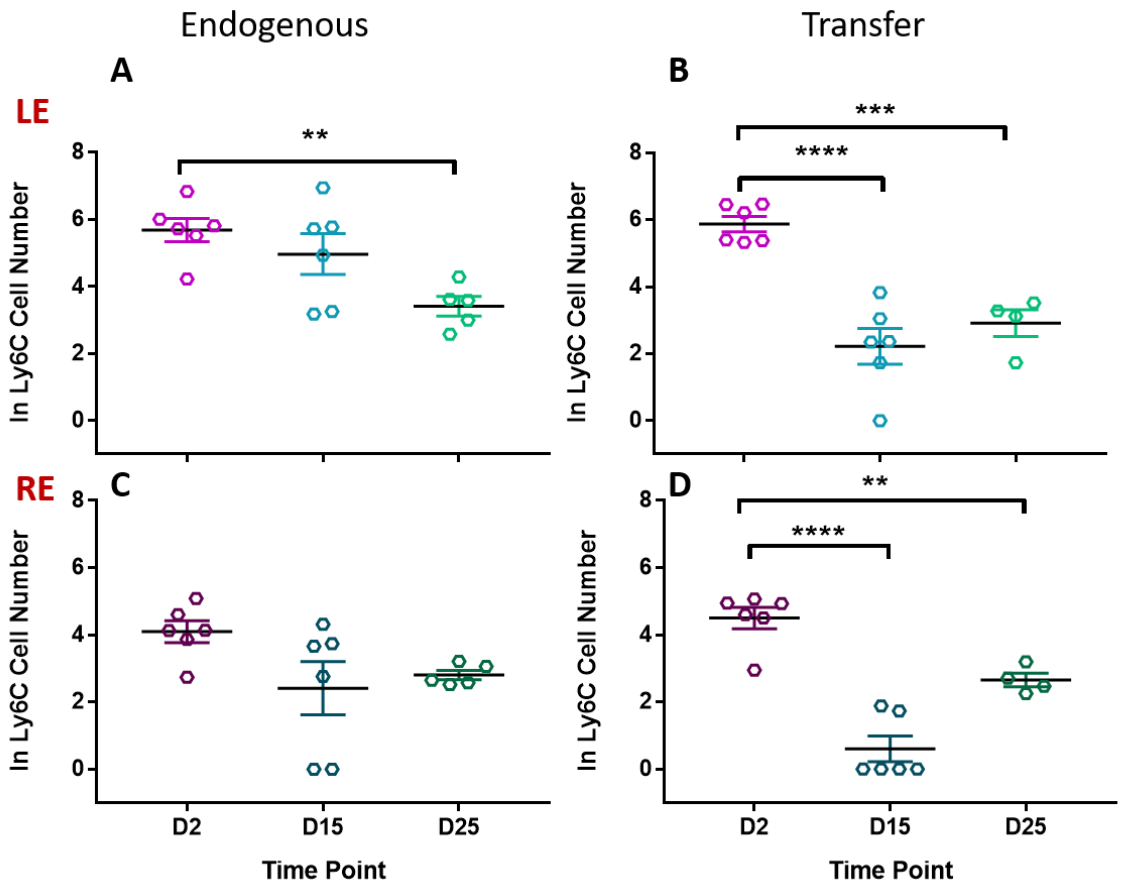

Figure 5.10: Flow cytometric quantification of Ly6C+ retinal infiltrate. Retinas were dissected and prepared for flow cytometry at pre-defined time points. Total Ly6C+ cell numbers were quantified and then endogenous and transferred cell populations calculated. (A) Total endogenous Ly6C+ cells present within the left eye of recipients at each time point (B) Total transferred Ly6C+ cells present within the left eye of recipients at each time point (C) Total endogenous Ly6C+ cells present within the right eye of recipients at each time point (D) Total transfer Ly6C+ cells present within the right eye of recipients at each time point. Data are expressed as Mean ±SEM. Statistical analysis performed: One-Way ANOVA multiple comparisons against day 2 (A-D). *p<0.05, **p<0.01, ***p<0.001, ****p<0.0001.

5.3.4 Selective recruitment of transferred cells to the retinal tissue throughout clinical disease

The recruitment of transferred activated CD4+ T cells to the eye is due to an antigen-specific response. As OVA is not present within the ocular tissue naturally, an intravitreal injection of the OVA peptide allows local presentation of that antigen to the OTII TCR carried by the transferred activated OTII T cells.

When OVA antigen is present within the ocular tissue (similarly to the uveitogenic cell transfer where the antigen the leukocytes have been primed to recognise is present within the ocular tissue) a large number of cells are recruited to the tissue of both a transferred and endogenous phenotype which is not observed when the antigen is not present.

At day 15, clinical disease is observed (Figure 5.5g and 5.5h) and the ratio of endogenous to transferred CD4+ T cells within the eye is ~1:1 (Figure 5.6a and 5.6b). At this time point within lymphoid and non-lymphoid tissues and blood transferred cells were also seen in comparable populations to the eye (Figure 5.11b).

The transferred cell population persists within the lymphoid and non-lymphoid tissue through to day 25 (figure 5.11d) but transferred cell number within the left eyes (that received the OVA peptide) of recipients has begun to decrease as clinical disease by OCT is resolving (Figure5.5i) (Figure 5.11d).

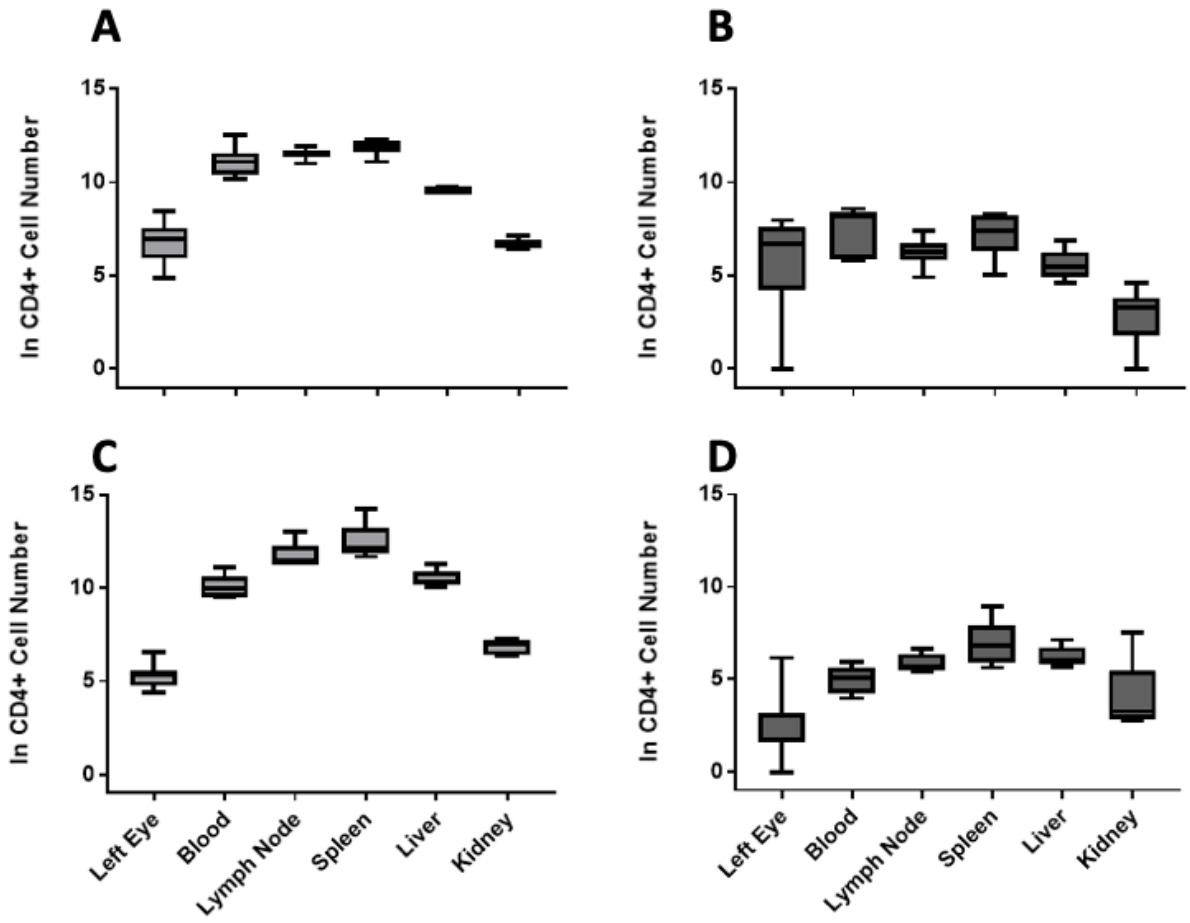

Figure 5.11: Recruitment of OVA specific cells to lymphoid and non-lymphoid tissue. After intravitreal injection of OVA transferred CD4+ T cells were tracked in eyes, blood, lymphoid tissue (spleen and lymph node) and non-lymphoid tissue (liver and kidney). A) endogenous CD4+ T cells present within each tissue at day 15 B) transferred CD4+ T cells present within each tissue at day 15. C) endogenous CD4+ T cells present within the tissues at day 25 D) transferred CD4+ T cells present within the tissues at day 25.

Data expressed as ln (1+ cell number) with error bars illustrating minimum and maximum cell number within data set.

5.3.5 Non-specific recruitment of non-antigen specific activated cells during clinical disease

Cellular infiltrate is a distinctive feature of infection, in many types of inflammation the role T cells have to play has been well documented but the specific impact of the accumulation of other effector cells and migration of T cells to the tissue due to antigen recognition is still needing to be investigated (219). In a study carried out by Ghani et al 2009, a model driven by an inflammatory effector phase using TCR transgenic T cells found that, (i) increased recruitment of effector T cells and other leukocytes was due to antigen specific T cells playing a critical role as 'pioneer cells' to prepare the tissue, (II) infiltration of T cells is not reliant upon antigen specificity (219). It was further demonstrated that a minimal number of antigen-specific cells recruited to the tissue are capable of inducing a large number of cells to migrate to the antigen-loaded site (219). Accumulation of T cells is independent of T cell reactivity to antigen during the early stages of inflammation despite it being a process driven by antigen later on in disease course, after initial arrival both transgenic and wild-type T effector cells show levels of increased recruitment to the site of antigen challenge and further activation of antigen-specific pioneer cells (219). This study further suggests that bystander activation of non-specific effector/memory T cells is a general feature of inflammation (219).

As illustrated in previous chapters, adoptive transfer of uveitogenic cells induces EAU (figure 4.5). By day 2, antigen-specific transferred cells can be detected in the eye, by day 7 as peak disease is reached a selective accumulation of antigen-specific transferred cells are present within the eye (figure 4.5). This continues through to day 14. In contrast, adoptive transfer of non-antigen specific activated cells causes limited CD4+ T cells stick in the ocular tissue (Figure 5.3a and 5.3b), if the antigen is then added to the tissue using an intravitreal injection a recruitment of transferred CD4+ T cells occurs and clinical disease ensues (Figure 5.6a and 5.6b) including recruitment of endogenous cells in large numbers to the eye containing the antigen (Figure 5.6c).

Further to these observations the adoptive transfer of antigen-specific leukocytes and non-antigen specific OT-II activated leukocytes at a 1:1 ratio was performed. Clinical disease course followed the same pattern as the previous antigen-specific transfers (figure 4.4 and 4.5). Clinical imaging was used to monitor recipients (Figure 5.12) from day 0 to day 14, eyes were then analysed by flow cytometry at ay 2, day 7/8 and day 14 to analyse cellular infiltrate

and using allelic markers detect the endogenous CD4+, CD8+ and CD11b+ cells (Figure 5.13a, 5.14a and 5.15a), transferred antigen-specific CD4+, CD8+ and CD11b+ cells (Figure 5.13b, 5.14b and 5.15b) and transferred activated OTII CD4+, CD8+ and CD11b+ cells that are non-antigen specific (Figure 5.13c, 5.14c and 5.15c).

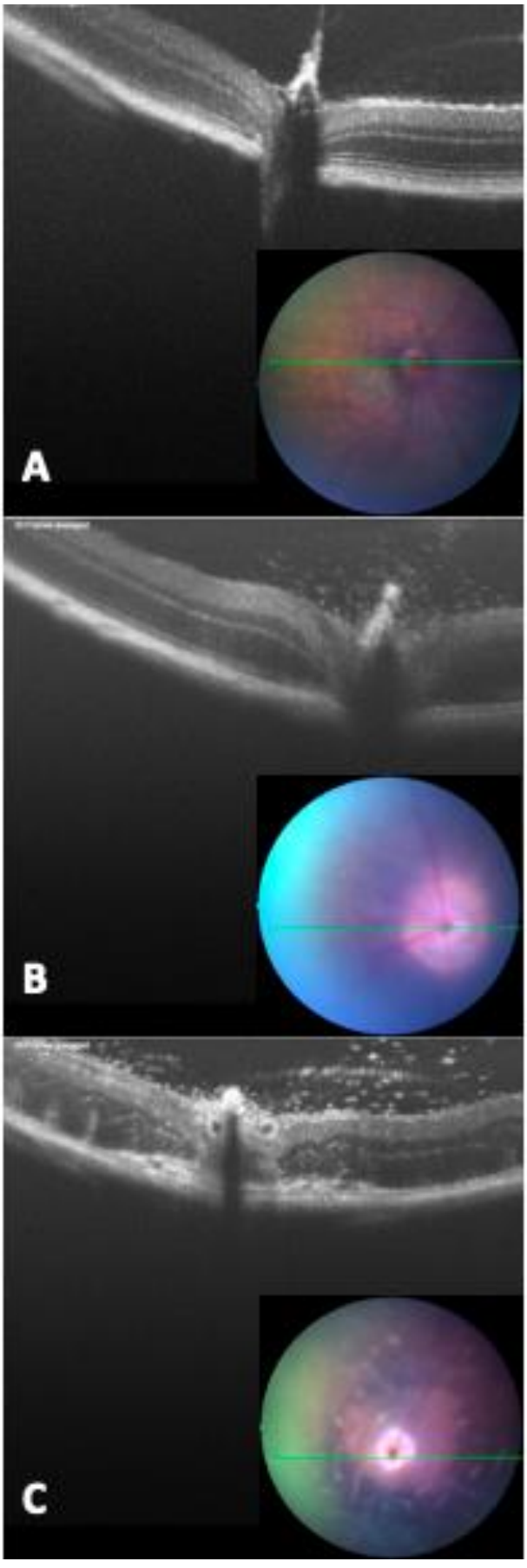
D0
A
D5
B
D14
C

Figure 5.12: OCT imaging of recipients from day 0 (baseline) to day 14 after transfer. (A) Baseline fundal and OCT imaging of recipients before manipulation. (B) Fundus and OCT at day 5 after adoptive transfer; increased levels of cellular infiltrate is observed within the vitreous, thickening of the retina and swelling of the optic disc in the OCT image, within the fundal image a vitreal haze has formed due to cellular infiltrate and whitening around the optic disc. (C) Fundus and OCT imaging at day 14 after adoptive transfer; traits observed are still observed but disease is past peak and clinical signs of diseases have started to resolve.

(A) Endogenous

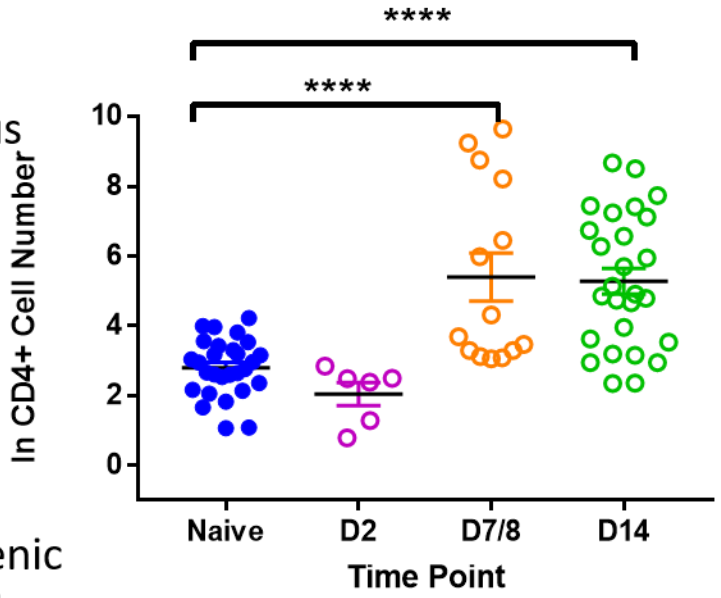

(B) Pathogenic Transferred

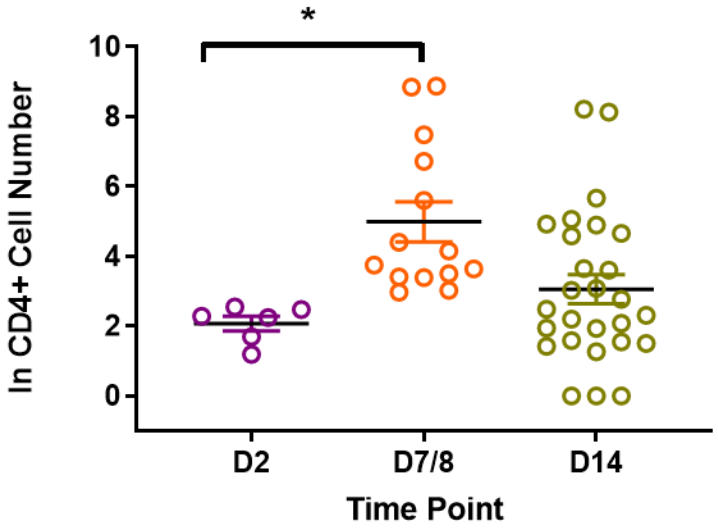

(C) OTII Transferred

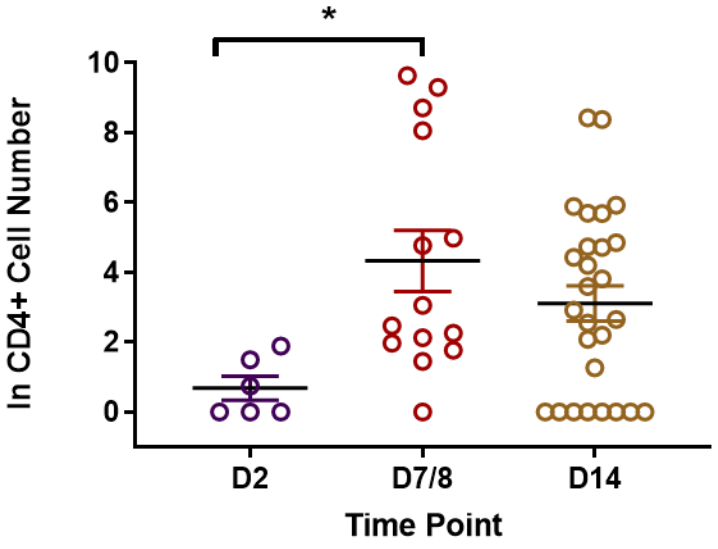

Figure 5.13: Flow cytometry quantification of allelically marked CD4+ T cells. Allelic markers allow detection and quantification of different populations of CD4+ T cells. (A) Total endogenous CD4+ T cells quantified using flow cytometry at different time points throughout clinical disease. (B) Total transferred antigen specific CD4+ T cells quantified using flow cytometry at each time point throughout clinical disease. (C) Total transferred OTII non-antigen specific activated CD4+ T cells quantified using flow cytometry at different time points throughout clinical disease.

Data are expressed as Mean ±SEM. Statistical analysis performed: One-Way ANOVA multiple comparisons against naive (A), comparisons against day 2 (B+C). *$p<0.05$, ****$p<0.0001$.

(B) Pathogenic Transferred

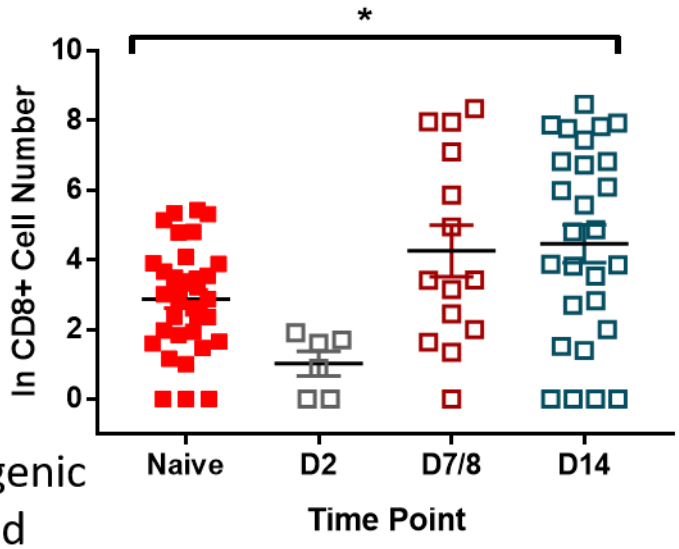

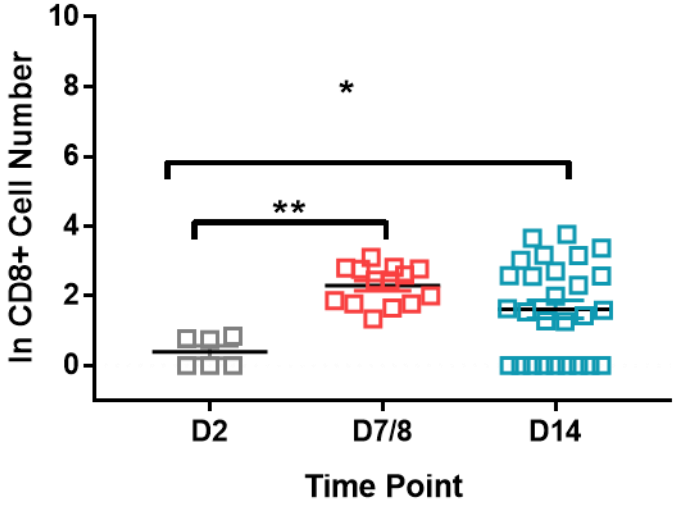

(C) OTII Transferred

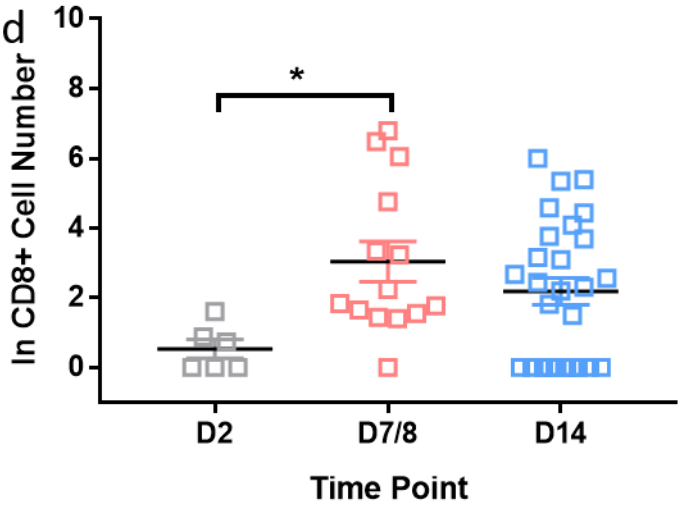

Figure 5.14: Flow cytometry quantification of allelically marked CD8+ T cells. Allelic markers allow detection and quantification of different populations of CD8+ T cells. (A) Total endogenous CD8+ T cells quantified using flow cytometry at different time points throughout clinical disease. (B) Total transferred antigen specific CD8+ T cells quantified using flow cytometry at each time point throughout clinical disease. (C) Total transferred OTII non-antigen specific activated CD8+ T cells quantified using flow cytometry at different time points throughout clinical disease.

Data are expressed as Mean $\pm$SEM. Statistical analysis performed: One-Way ANOVA multiple comparisons against naive (A), comparisons against day 2 (B+C). *$p<0.05$, ****$p<0.0001$.

(A) Endogenous

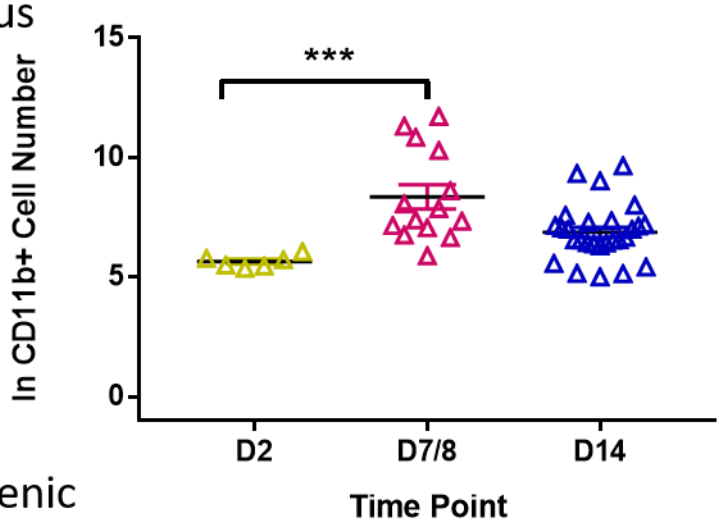

(B) Pathogenic Transferred

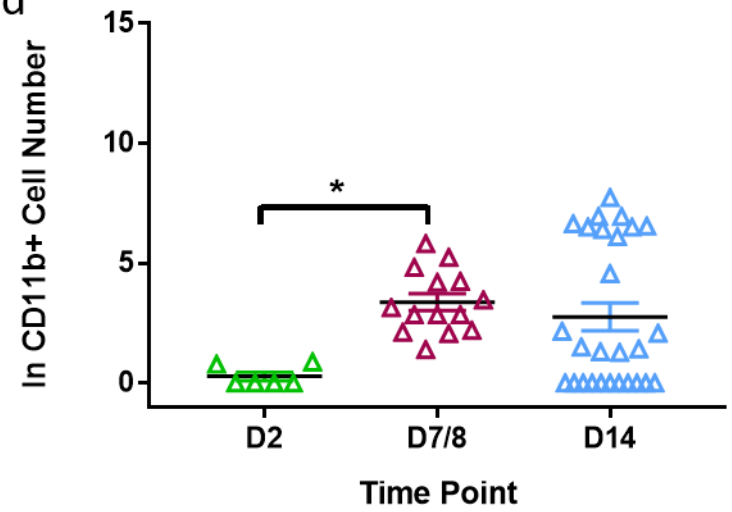

(C) OTII Transferred

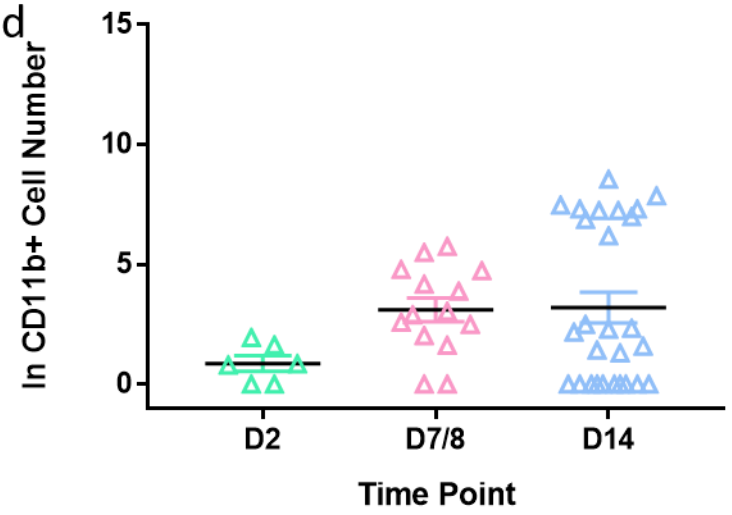

Figure 5.15: Flow cytometry quantification of allelically marked CD11b+ cells. Allelic markers allow detection and quantification of different populations of CD4+ T cells. (A) Total endogenous CD11b+ cells quantified using flow cytometry at different time points throughout clinical disease. (B) Total transferred antigen specific CD11b+ cells quantified using flow cytometry at each time point throughout clinical disease. (C) Total transferred non-antigen specific activated CD11b+ cells quantified using flow cytometry at different time points throughout clinical disease.

Data are expressed as Mean ±SEM. Statistical analysis performed: One-Way ANOVA multiple comparisons against naive (A), comparisons against day 2 (B+C). *p<0.05, ****p<0.0001.

5.4 Discussion

The work presented in this chapter demonstrates that both non-antigen specific and antigen specific stimuli induce recruitment of CD4+ T cells to the ocular tissue, although to very different levels.

Intraperitoneal injection of PBS initiated a change in the numbers of endogenous CD4+ T cells to the eyes of recipients, compared with age matched naïve mice at day 2 after injection (Figure 5.2). This procedure provides a baseline for recipients after cell transfer. This increase in CD4+ T cells within the ocular tissue could be due to endotoxin release from the injection site activating endothelial cells within the eye encouraging retention of CD4+ T cells.

In the endotoxin induced uveitis model, LPS is injected directly into the ocular tissue to initiate a cascade of signalling reactions, increased expression of inflammatory markers results in the breakdown of the blood-ocular barrier and the infiltration of leukocytes into ocular tissue causing clinical disease (220).

Toll like receptor 4 (TLR4) recognises the bacterial component LPS and is ubiquitously expressed in the vasculature (221). The small release of endotoxin from the injection site induces a lesser effect and recruitment of cells in comparison to EIU induction by intravitreal injection of LPS. Endothelial cells can be involved in the coordination of the recruitment of inflammatory cells to the tissue after injury or infection to produce and release cytokines and growth factors to communicate with immune cells entering the tissue. The activation of endothelial cells through TLRs can be direct through interaction with ligand molecules or may require a prior inflammatory stimulus such as IFN-γ, LPS or TNF-α (221). It has been observed in various models of inflammation that LPS leads to cell arrest in the tissue. On the other hand, TLR4 activation has been demonstrated to enhance survival and proliferation of CD4+ T cells (222).

To assess if the recruitment of endogenous cells observed at day 2 in the pathogenic transfer is due to more than a non-antigen specific response stimulating endothelial activation, adoptive transfer of antigen specific activated cells was contrasted with non-antigen specific activated OTII cells and non-antigen specific non activated OTII cells that were transferred into naïve recipients. Analysed by flow cytometry at day 2 and day 7 (Figure 5.3 and 5.4) the increase in endogenous CD4+ T cells in the non-antigen specific OTII cell transfer is indistinguishable from the PBS intraperitoneal injection alone at day 2 and declines by day 7.

In the transferred CD4+ T cell compartment, very small numbers of cells are recovered from the eye, showing that without an antigen specific response in the eye, T cell activation alone leads to very low levels of cell retention at day 2.

As the OVA-specific T cells are not recruited to the eye of recipients when no local stimulus is present, two experiments were carried out. Firstly, a transfer of OVA-specific T cells concurrently with an intravitreal injection of OVA into one eye and a control intravitreal injection into the other eye of each recipient showed selective recruitment to the OVA injected eye. Several studies have described the disappearance of antigen-specific effector/memory T cells from the periphery and their accumulation within antigen-challenged sites (219, 223). Accumulation of autoantigen specific T cells was observed in these studies in lymphoid organs that specifically expressed the autoantigen (219). It has been further demonstrated that antigen-specific CD4 T cells also migrate to non-lymphoid organs in large numbers after systemic exposure to antigen (224, 225) but here it was not possible to determine whether T cells migrated preferentially to the antigen-containing organs (225). Data presented in *chapter 4* supports the accumulation of CD4+ T cells to non-lymphoid organs and suggests that the transferred auto-antigen specific T cells were selectively recruited to the eye which contains the target antigen, as well as being retained in lymphoid tissues such as the spleen and lymph nodes.

In a study by Reinhardt et al (225) the group were able to confirm by confining antigen to a local site injection of OVA peptide/IFA subcutaneously to mouse tails with a concurrent transfer of OVA specific T cells, that by day 5 after subcutaneous injection of OVA peptide large numbers of OTII cells were present within the tail tissue (225). In the data presented in this chapter, at day 4 after adoptive transfer of OTII cells with an intravitreal injection of OVA, transferred OTII cells can be detected within the eyes of recipients providing evidence that the local site of antigen deposition is the major non-lymphoid tissue in which activated antigen-specific CD4 T cells accumulate during a primary response. A small population of transferred OTII cells is also observed in lymphoid and non-lymphoid tissues such as spleen, lymph node, liver and kidney suggesting that local antigen presentation is not the only factor that determines the distribution of antigen-specific T cells in lymphoid and non-lymphoid tissue, also in agreement with the results of the Reinhardt study (225).

When activated TCR transgenic OVA specific OTII cells are transferred into recipients with no pathogenic stimulus, endogenous cells do not stick in the eye in greater numbers than just a

PBS injection alone and very low levels of transferred cells stick non-specifically in the eye 2 days after transfer. When OVA antigen is then injected into one eye of each recipient an antigen-specific recruitment was observed to the OVA injected eye over the control injected eye, inducing an increase in the endogenous compartment and clinical disease by OCT. Within the control eye, no increase in endogenous cells compared to a PBS intraperitoneal injection is observed, increased numbers of transferred OTII cells stick non-specifically in the eye in comparison to the activated OTII cell transfer. This non-specific sticking of OTII cells within the eye that received no antigen could be due to cells recirculating after encountering the OVA antigen within the contralateral eye.

The recruitment of endogenous cells to the eyes of pathogenic transfer recipients at day 2 is not significantly increased in comparison to the mice that received an OTII cell transfer or OTII transfer with intravitreal OVA injection. However, the recruitment of pathogenic transferred cells to the eyes of recipients by day 2 is significantly increased ($p<0.001$****) in comparison to the OTII transfer and the OTII transfer with intravitreal OVA injection. Thus, suggesting that the retinal antigen present in the eye is facilitating the recruitment of the transferred population and by injecting OVA into the eye does not induce transferred cell recruitment this early after cell transfer which could be due to the APCs not presenting the antigen to the CD4+ T cells by this time point.

The adoptive transfer of a mixture of pathogenic and non-pathogenic activated T cells at a ratio of 1:1 allowed further assessment of the recruitment of these cells to the eye. Several studies have shown that T cells were recruited irrespective of their antigen-specificity, into acute T-cell dependent inflammatory sites (219, 226, 227). Activated OTII cells behave differently in tissues that are ‘vulnerable’ due to an ongoing antigen specific response, which could have the effect of focussing recently activated cells to a target tissue increasing the likelihood of them catching the infection.

The data presented in this chapter illustrates a recruitment of antigen-specific pathogenic cells to the eye to initiate clinical disease, when non-pathogenic (OVA specific) activated cells are transferred with no OVA peptide injection there is low levels of recruitment in the endogenous compartment but not significantly different from recipients who received a PBS intraperitoneal injection along with minimal numbers of transferred cells are detected within the eye. Therefore, the recruitment of large numbers of OVA specific cells to the eye occurs

when a pathogenic stimulus is present or if the antigen has been introduced into the ocular tissue.

In conclusion, intraperitoneal injection alone causes changes in the number of CD4+ T cells retained in ocular tissue, this number is not significantly increased if the injection includes activated non-ocular-antigen specific T cells. The data that co-transfer of pathogenic and non-pathogenic cells together leads to much greater retention of both populations suggests that an antigen specific signal from the pathogenic cell transfer induces a qualitatively different activation of the endothelium than intraperitoneal injection alone.

Chapter 6. The role of CX3CR1 in EAU

6.1 Introduction

Leukocyte trafficking is a thoroughly regulated process, the breakdown of the fundamental control mechanisms can contribute to conditions such as immunodeficiency and autoimmune disease (228). Migration profiles can greatly vary between types of leukocytes and are known to have a direct effect on leukocyte retention at sites of immune defence and inflammatory diseases, it is now recognised that chemokines and chemokine receptors working alongside adhesion molecules are the main controllers of leukocyte migration and are critical to fundamental biological processes including embryonic development early in life, immune surveillance, host defence and wound repair throughout life (228, 229).

6.1.1 Chemokines

Chemokines are a family of small, highly conserved proteins involved in numerous biological processes including chemotaxis, leukocyte degranulation, haematopoiesis and angiogenesis and are the largest family of cytokines in human immunophysiology (230-235). The proteins are sized roughly 8 to 12 kDa, and are able to induce chemotaxis in a variety of cell types including, neutrophils, monocytes, lymphocytes, eosinophils, fibroblasts and keratinocytes (236). Chemokines provide a wide range of functions and can be naturally inclined to create a homeostatic environment. They are produced constitutively and secreted to mediate lymphocyte trafficking to lymphoid tissues, and are also known to play a role in immunosurveillance (237). The role chemokines play in immunosurveillance involves T and B cell localisation with APCs from the lymphatic system presenting antigen, however not all chemokines are produced in a resting state some chemokines are considered to be inflammatory in nature and are only secreted when infection is present or due to a pro-inflammatory stimulus (237). In order to mount an immune response chemokines induce leukocytes to migrate to the site of inflammation where injury or infection is present and inflammatory cytokines are aiding in mounting an immune response by activating cells (237).

6.1.2 Chemokine receptors

Chemokines are secreted proteins that travel in the circulation, they move through the parenchyma and extracellular matrix of tissues and bind to and activate the extracellular

domain of their cognate receptors present on individual cell types (237, 238), they act on leukocytes by interactions with seven-transmembrane G protein-coupled receptors which are localised on target cells (239). Chemokine activity is initiated by the binding of the chemokine against the specific corresponding G protein-coupled receptor, in order to activate a chemokine receptor two steps need to be undertaken, firstly binding of the receptor to the specific chemokine agonist it recognises, followed by the flexibility of the N terminus allowing a conformational change to take place. This change is necessary to allow the N terminus to form interactions with the specific chemokine receptor to induce activation (240). After the receptor has been activated, GDP bound to the α sub-unit of the G proteins is changed for GTP (240). Chemokines interact with both chemokine receptors and with glycosaminoglycans to promote migration and impact directionality to cell movement (241).

Ten CC-receptors and six CXC-receptors have been identified, single XCR1 and CX3CR1 receptors have also been described (239). Most chemokine receptors recognise several ligands and multiple chemokines are able to bind to more than one receptor, additionally, some chemokines act as natural antagonists of specific receptors (239).

The functions of chemokine receptors are vast but they can be grouped depending on if they are predominantly involved in response to infection and inflammation or maintaining homeostasis within the host (242). By inducing chemotaxis and therefore directing cells to the source of chemokine gradients, allows chemokines to control the position and trafficking of leukocyte within the host. Specifically, mobilisation of leukocytes to the site of inflammation in response to chemokine secretion is due to the significant role inflammatory chemokine receptors play in the hosts defence and their ability to trigger leukocyte movement (242).

6.1.3 Chemokine interactions with chemokine receptors

Mechanisms affecting the chemokine or chemokine receptor modulate a leukocytes ability to respond to chemokines. Modulation of levels of the receptor molecules on a cellular basis or functionally active receptors being presented at the cell surface are methods of control exerted on the chemokine receptor (242). By affecting the activation state, cellular location or signalling ability of a functional chemokine receptor at the cell surface tight control is

achieved, an essential method of rapid control in response to cross-talk from other receptors or due to ligand binding (242).

6.1.4 Fractalkine (CX3CL1)

CX3CL1 also known as fractalkine is the only known member of the CX3C chemokine subclass (150, 243). Fractalkine is unique within the chemokine family due to its synthesis as a transmembrane molecule, it is made up of 373 total amino acids including: at residues 1-76 an extracellular terminal domain, 77-317 a mucin like stalk, 318-336 a transmembrane helix and at 337-373 a short cytoplasmic tail (150). Fractalkine can exist in a membrane bound or soluble form. The soluble form of fractalkine has chemoattractive functions that act on T cells, NK cells and monocytes, it is generated by disintergrin-like metalloproteinases ADAM 10 and ADAM 17/TACE, and is made up of a and extracellular mucin-like stalk and the chemokine domain. The membrane bound form acts as an adhesion molecule and assists integrin-independent adhesion induced by IL-1, IFN-γ and TNF-α on primary endothelial cells (150, 243). The membrane bound form of CX3CL1 also promotes the friction and interlocking of CX3CL1 leukocytes (150).

6.1.5 CX3CR1

The highly specialised receptor for CX3CL1 and CCL26 in humans is known as CX3CR1 (244). CX3CR1 can be found on the surface of cytotoxic effector lymphocytes including CD8 T cells, NK cells and γδ cells as a marker due to the expression of large amounts of granzyme B and perforin no matter what the mode of target recognition or cell lineage (150).

During inflammation fractalkine is expressed by monocytes within the peripheral blood, it can also be expressed on endothelial cells, fibroblasts, dendritic cells, and macrophages during autoimmune inflammation such as during the autoimmune disease rheumatoid arthritis (150, 245). A role for interactions between fractalkine and its specific receptor have been suggested in immune-related inflammatory disease due to their presence on lymphocytes and increased cellular expression during inflammatory conditions (150). In both humans and mice CX3CR1 is expressed on monocytes, macrophages, mucosal dendritic cells , natural killer cells, mast cells, CD8+ T cells and a subset of CD4+ T cells (151).

6.1.6 CX3CR1 expression on CD4+ T cells

Chemokine receptors expressed on lymphocytes can vary based on different subtypes and specific development stage so as to facilitate chemotaxis to different tissues (246). Studies have illustrated in humans that expression of CX3CR1 is predominantly seen in Th1 cells that respond chemotactically to fractalkine (246), CX3CL1 upregulation during inflammation is suggested to be a contributing factor of inflammatory disease by the promotion of transmigration of CX3CR1 expressing cells to sites of inflammation (151).

In a study by Mionnet et al (151), CX3CR1-associated survival was observed on Th1 cells upon airway inflammation but not under homeostatic conditions or peripheral inflammation (151). In vitro, differentiated Th1 cells did not express CX3CR1 unless incubated with lung cells or injected into sensitised mice exposed to aerosols of their cognate antigens, therefore CX3CR1 expression in T helper cells is inducible under specific conditions in vivo and in vitro (151). It was also shown that CX3CR1 does not play an integral role in T cell migration to the lung but is instead required for maintenance and survival within inflamed airways (151). Whereas in a study by Staumont-Sallé (247) in an adoptive transfer model of atopic dermatitis CX3CR1 Th1 cells are established as a key regulator of CD4+ T cells retention at the inflamed site, which indicates a new function for the fractalkine ligand and receptor (247).

6.1.7 CX3CR1 in EAU

The role of CX3CR1 in EAU is not yet defined. Dagkalis et al has suggested CX3CR1 deficiency generates a more severe EAU disease phenotype (47). To understand the role of CX3CR1 in regulating function of monocytes and microglia, using CX3CR1 deficient mice (47) it was found that in comparison to CX3CR1 positive mice, CX3CR1 negative mice had a more severe disease phenotype 23 days post immunisation, based on increased cellular infiltrate and increased monocyte/macrophage clustering (47).

In contrast, Kezic et al (248), reported no impact on the pathogenesis of EAU when comparing CX3CR1 positive and CX3CR1 negative mice, demonstrating the lack of a significant role for CX3CR1 in this particular study compared to previous studies suggesting a role in other retinal and neurodegenerative conditions (248). This perhaps may reflect a differential role for CX3CR1 expression on different cell types such as T cells versus macrophages. These studies

highlight a need to investigate soluble mediators in various disease states and tissue microenvironments (248).

6.1.8 CX3CR1 Knockout mice

CX3CR1$^{+/GFP}$ mice were produced by targeted inactivation of the *CX3CR1* gene with cDNA encoding EGFP (Clontech) (152). In the construct (and mutant locus) the EGFP gene replaces the first 390 bp of the second CX3CR1 exon encoding the N-terminus of the seven-transmembrane receptor specific for CX3CL1 (152). Germ line transition of the mutant allele yielded heterozygous CX3CR1$^{+/GFP}$ mice, which were inter-crossed to generate CX3CR1$^{GFP/GFP}$ mice (152) on a C57BL/6 background screened for rd8 mutations.

CX3CR1$^{+/GFP}$ mice can serve as a source of unmanipulated, in vivo labelled cell populations that could be instrumental in high-resolution studies on the development and dynamic properties of CX3CR1 (152), whereas CX3CR1$^{GFP/GFP}$ mice are usual to understand what effect deleting CX3CR1 has on disease course.

This chapter focuses on utilising the adoptive transfer technique to induce EAU using C57BL/6 CX3CR1$^{+/GFP}$ (CD45.2) or CX3CR1$^{GFP/GFP}$ (CD45.2) as donors or recipients to analyse the role CX3CR1 plays on disease pathogenesis in donor CD4+ T cells and within recipient tissue.

Secondly, the use of CX3CR1$^{+/GFP}$ mice allows tracking of the transferred population and using GFP expression to monitor CX3CR1 expression on CD4+ T cells throughout clinical disease. In the early sets of experiments presented in this chapter minimal effects of CX3CR1 on disease course is observed but work later in the chapter marks an important phenotype change of cells in an autoimmune environment.

6.2 Materials and Methods

6.2.1 Adoptive transfer technique

EAU was induced in C57BL/6 CX3CR1$^{+/GFP}$ (CD45.2) or C57BL/6 CX3CR1$^{GFP/GFP}$ (CD45.2) using RBP3 peptide, these donor cells were then transferred using i.p injection into C57BL/6 RAG2$^{-/-}$ to analyse differences in disease through donor cells.

C57BL/6 Ly5 (CD45.1) were immunised and donor cells were then transferred using i.p injection into C57BL/6 CX3CR1$^{+/GFP}$ (CD45.2) or C57BL/6 CX3CR1$^{GFP/GFP}$ (CD45.2) mice to analyse differences in disease in recipient tissue.

C57BL/6 CX3CR1$^{+/GFP}$ (CD45.2) were immunised and donor cells were then transferred using i.p injection into or C57BL/6 Ly5 (CD45.1) mice to analyse expression of CX3CR1 on CD4+ T cells during clinical disease.

6.2.2 Clinical imaging

OCT was used to acquire clinical imaging for a disease time course from day 0 to day 25 using the standardised method developed during data chapter 3.

6.2.3 Flow cytometry

At predefined time points after adoptive transfer, retinas were analysed by flow cytometry to quantify total cell number for each leukocyte population. Allelic markers were used as seen previously to identify transferred and endogenous populations including CD45.1, CD45.2 and expression of GFP denoting CX3CR1 expression.

6.2.4 Absolute numbers quantification

Splenocytes were counted to form a 7-fold serial dilution from 20x10^6-312,500. All samples including the standard curve are resuspended in the same volume and acquired at the same speed for the same amount of time. Unknown sample numbers were then interpolated from the standard curve drawn using the known serial dilution samples.

6.2.5 Statistical analysis

Data is presented as log transformed to normalise the data(ln (1+)) and expressed as Mean ± SEM. Statistical analysis such as a Mann Whitney test (for 2 sample groups) or a one-way ANOVA for sample groups of more than two was performed.

6.3 Results

6.3.1 CX3CR1 deficiency on donor cells affects initiation of disease in RAG2$^{-/-}$ mice

In order to investigate the effect of CX3CR1 on donor T cells on EAU disease course, we used the adoptive transfer technique to transfer uveitogenic T cells into RAG2$^{-/-}$ recipients using cells with different CX3CR1 expression.

Cells were transferred from either Ly5 (Wild type mice), CX3CR1$^{+/GFP}$ (CX3CR1 heterozygous) or CX3CR1$^{GFP/GFP}$ (CX3Cr1 Knockout) into RAG2$^{-/-}$ (CX3CR1 WT) recipients. RAG2$^{-/-}$ recipients do not have endogenous T or B cells so the effect of changing CX3CR1 expression on the donor T cells on the recipient, can be analysed based on disease initiation, disease severity and quantification of retinal infiltrate.

Ly5 CD4+ transferred cells induced disease at day 7, as seen by OCT imaging (Figure 6.1) in comparison to the CX3CR1 heterozygous and CX3CR1 knockout transfers (Figure 6.1c and 6.1g). By day 13 all cell transfer groups have clinical disease by OCT at reasonably consistent severity across the three groups (Figure 6.1b, 6.1d and 6.1h).

In the CX3CR1 heterozygous and CX3CR1 knockout group, disease was monitored through to day 28, both groups appeared by OCT to have similar clinical disease phenotype (Figure 6.1f and 6.1j).

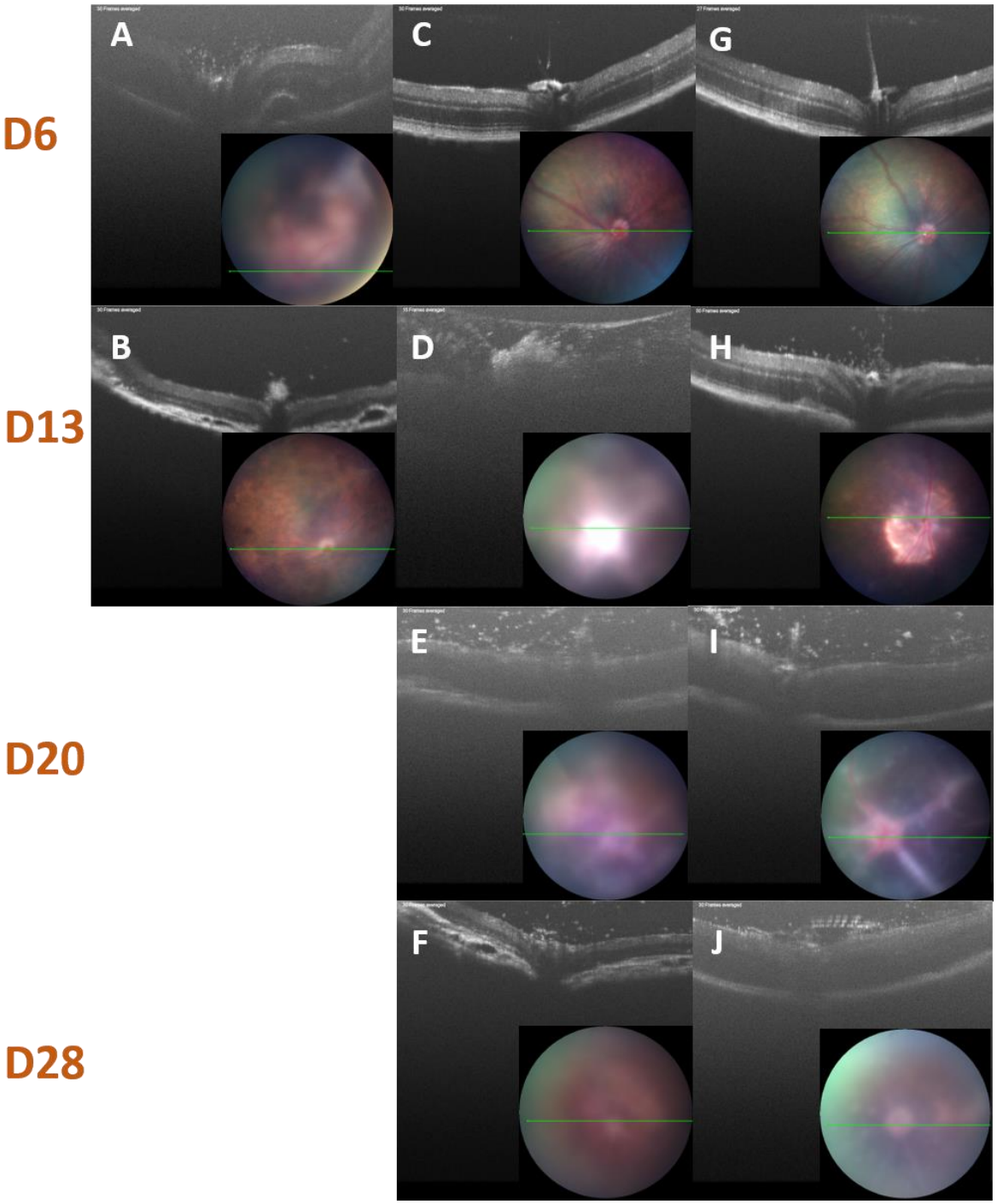
Ly5
Wildtype
CX3CR1
Heterozygous
CX3CR1
Knockout
D6
D13
D20
D28
A
B
C
D
E
F
G
H
I
J

Figure 6.1: OCT clinical imaging of disease of each group of recipients Ly5, CX3CR1 heterozygous and CX3CR1 knockout. A+B Disease course from day 6 to day 14 in RAG2$^{-/-}$ mice that received a Ly5 wildtype transfer of uveitogenic cells. C-F Disease course from day 0 to day 28 in RAG2$^{-/-}$ mice that received a CX3CR1 heterozygous transfer of uveitogenic cells. G-J Disease course from day 6 to day 28 in RAG2$^{-/-}$ mice that received a CX3CR1 knockout transfer of uveitogenic cells.

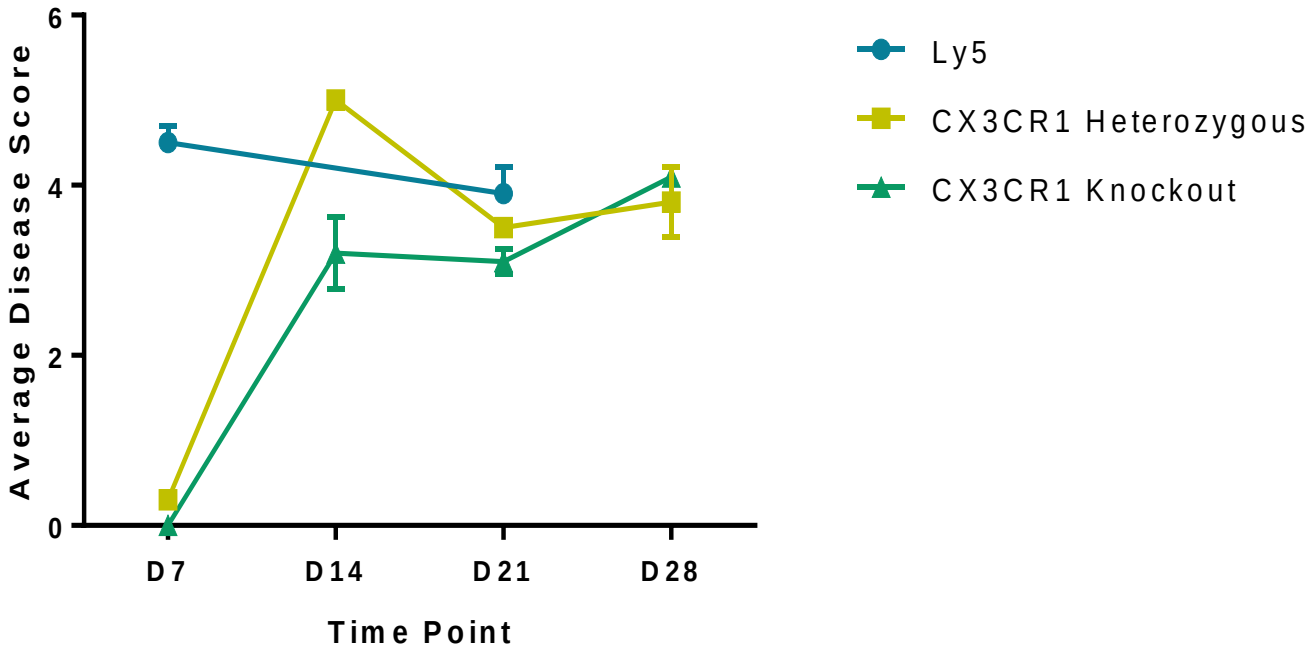

Figure 6.2: Average OCT disease scoring across all three recipient groups during active disease. Fundal images were acquired with OCT at various time points throughout disease course. The images were then collated and scored blind using the clinical disease scoring criteria presented in *chapter 2*. Averages for each were then calculated. Data expressed as Mean ± SEM.

6.3.2 CX3CR1 deficiency on donor cells does not affect disease phenotype after disease initiation

Analysis of retinas during clinical disease allowed quantification of retinal infiltrate. Due to the lack of endogenous B and T cells, the cells driving the disease are from the transferred population.

At day 7 after adoptive transfer (as highlighted previously in figure 6.1), severe clinical disease is present in the imaging of the wildtype Ly5 transfer eyes of the RAG2$^{-/-}$ mice. This is confirmed by the flow cytometry quantification of CD4+ T cells (figure 6.3a). There is a statistically significant difference between the total CD4+ T cells present in the retinas of the Ly5 wildtype transfer and the retinas of the two other groups; CX3CR1 heterozygous and CX3CR1 knockout (Figure 6.3a). In the CD8 compartment, the transferred cells have survived and been recruited to the retinas of all groups of animals (figure 6.4a) and in similar numbers across the groups. The CD11b+ endogenous infiltrate illustrated a statistically significant (****$p<0.0001$) increase between the Ly5 wildtype RAG2$^{-/-}$ recipients and the RAG2$^{-/-}$ recipients that received a CX3CR1 heterozygous or CX3CR1 knockout groups (figure 6.5a).

By day 14, the total number of CD4+ T cells in the retinas of each group has reached similar levels (figure 6.3b), similarly observed in the OCT imaging at day 13 in figure 6.1. This pattern is also observed within the CD8+ and CD11b+ cell numbers (figure 6.4b and 6.5b)

At day 21, only the CX3CR1 heterozygous and CX3CR1 knockout RAG2$^{-/-}$ recipients remain and disease between the two groups is still comparable (figure 6.1), this observation is backed up by the retinal infiltrate in CD4, CD8 and CD11b cell number (figure 6.3c, 6.4c and 6.5c).

Disease still has not resolved by day 28 the pattern follows from day 21 with equal disease severity and retinal infiltrate observed across the two groups (figure 6.1, 6.3d, 6.4d and 6.5d).

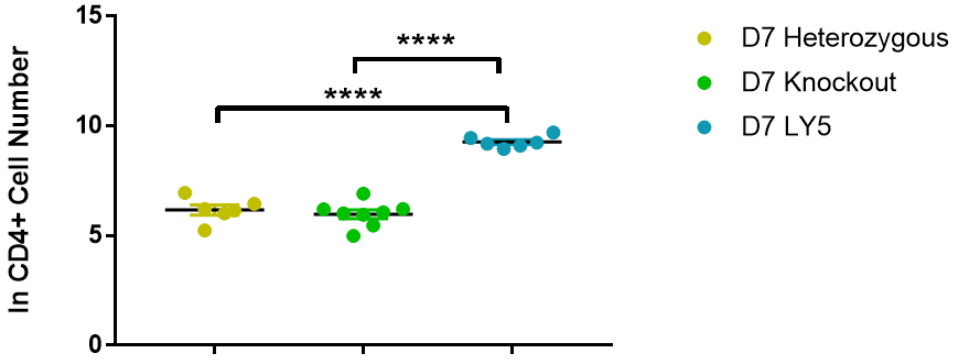
ln CD4+ Cell Number
15
10
5
0
****
****
D7 Heterozygous
D7 Knockout
D7 LY5

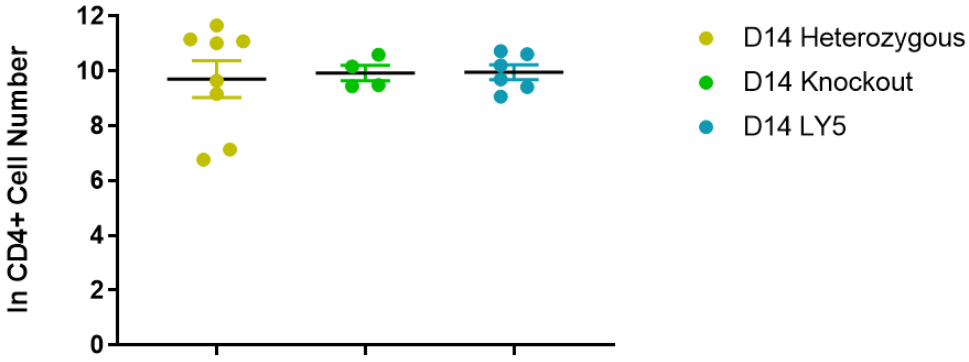
ln CD4+ Cell Number
12
10
8
6
4
2
0
D14 Heterozygous
D14 Knockout
D14 LY5

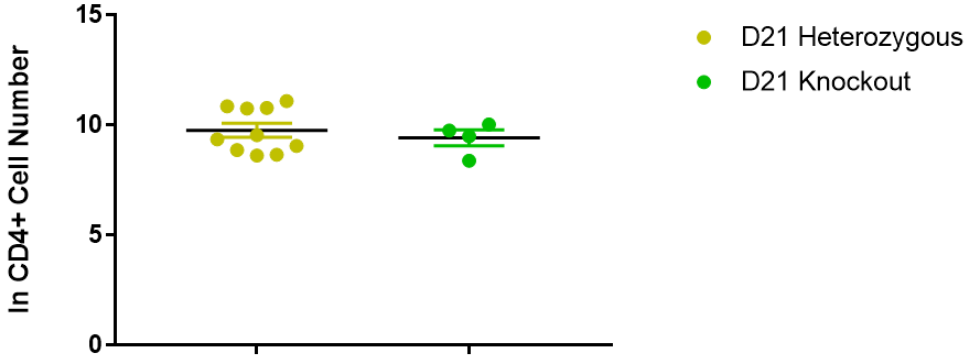
ln CD4+ Cell Number
15
10
5
0
D21 Heterozygous
D21 Knockout

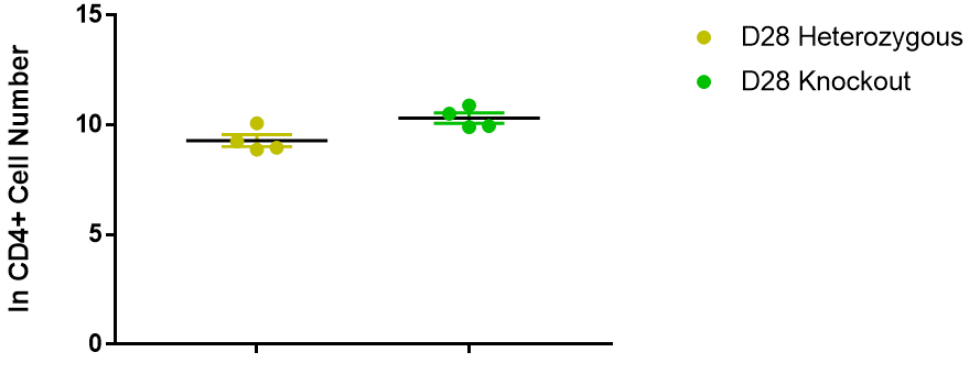
ln CD4+ Cell Number
15
10
5
0
D28 Heterozygous
D28 Knockout

AVERAGE

CELL NUMBER

	Ly5	CX3CR1 Heterozygous	CX3CR1 Homozygous
D7	**11000**	**543**	**452**
D14	**25033**	**23967**	**22972**
D21		**31333**	**14596**
D28		**12337**	**33086**

Figure 6.3: Analysis of total CD4+ T cell number within the retinal infiltrate at different time points throughout clinical disease. $RAG2^{-/-}$ recipients received an intraperitoneal transfer of uveitogenic cells from one of three donor types Ly5, CX3CR1 heterozygous or CX3CR1 knockout. As seen in figure 6.1 clinical disease was monitored using OCT clinical imaging throughout clinical disease. To correlate with the clinical imaging at each time point retinas were dissected and prepared for flow cytometric analysis and CD4+ T cells numbers were quantified. Data expressed as Mean $\pm$SEM. Statistical analysis performed: One-Way ANOVA multiple comparisons compared to wildtype transfer (A+B) unpaired non-parametric Mann-Whitney Test (C+D) ****$p<0.0001$.

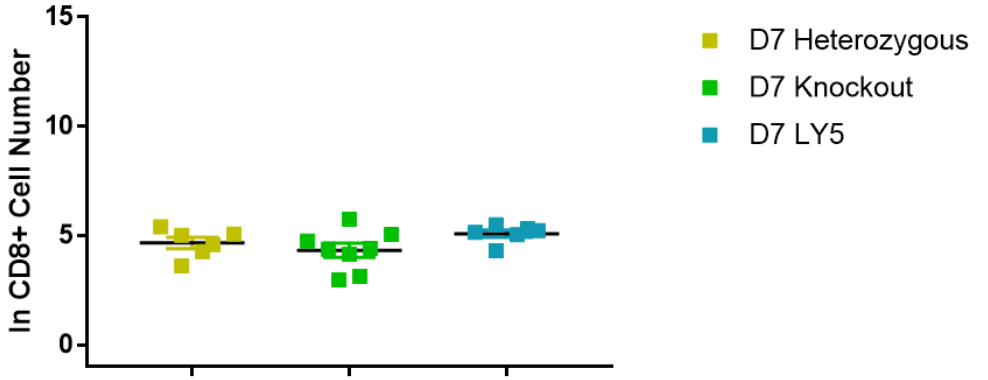
15
10
5
0
ln CD8+ Cell Number
D7 Heterozygous
D7 Knockout
D7 LY5

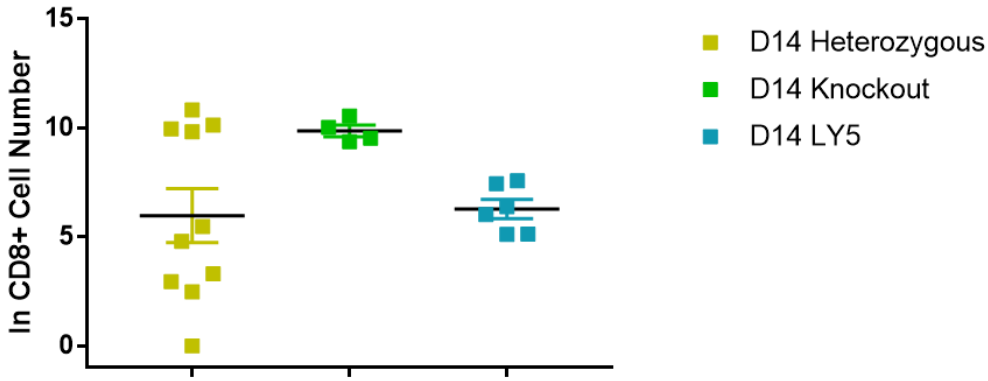
15
10
5
0
ln CD8+ Cell Number
D14 Heterozygous
D14 Knockout
D14 LY5

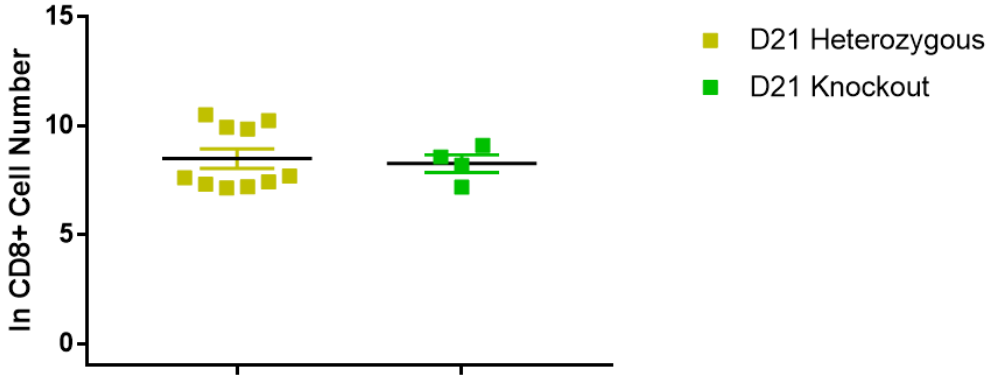
15
10
5
0
ln CD8+ Cell Number
D21 Heterozygous
D21 Knockout

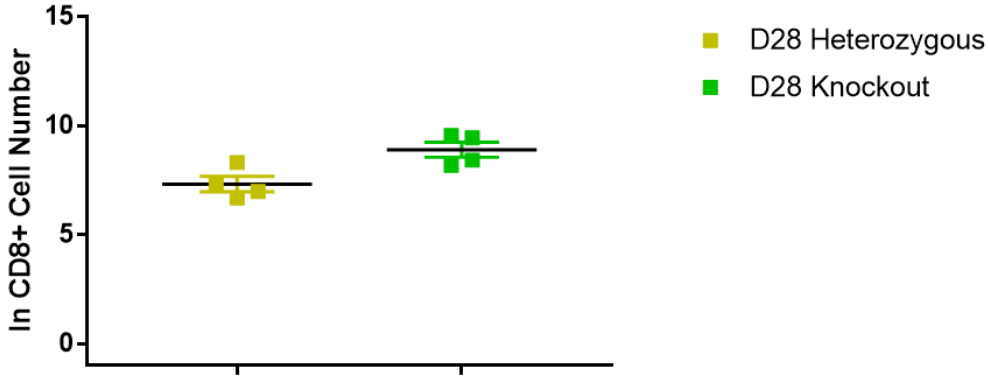
15
10
5
0
ln CD8+ Cell Number
D28 Heterozygous
D28 Knockout

AVERAGE CELL NUMBER			
	Ly5	**CX3CR1 Heterozygous**	**CX3CR1 Homozygous**
D7	**172**	**123**	**106**
D14	**835**	**14583**	**21688**
D21		**13977**	**4841**
D28		**1883**	**8831**

Figure 6.4: Analysis of total CD8+ T cell number within the retinal infiltrate at different time points throughout clinical disease. $RAG2^{-/-}$ recipients received an intraperitoneal transfer of uveitogenic cells from one of three donor types Ly5, CX3CR1 heterozygous or CX3CR1 knockout. To correlate with the clinical imaging at each time point retinas were dissected and prepared for flow cytometric analysis and CD8+ T cells numbers were quantified. Data expressed as Mean $\pm$SEM. Statistical analysis performed: One-Way ANOVA multiple comparisons compared to wildtype transfer (A+B) unpaired non-parametric Mann-Whitney Test (C+D).

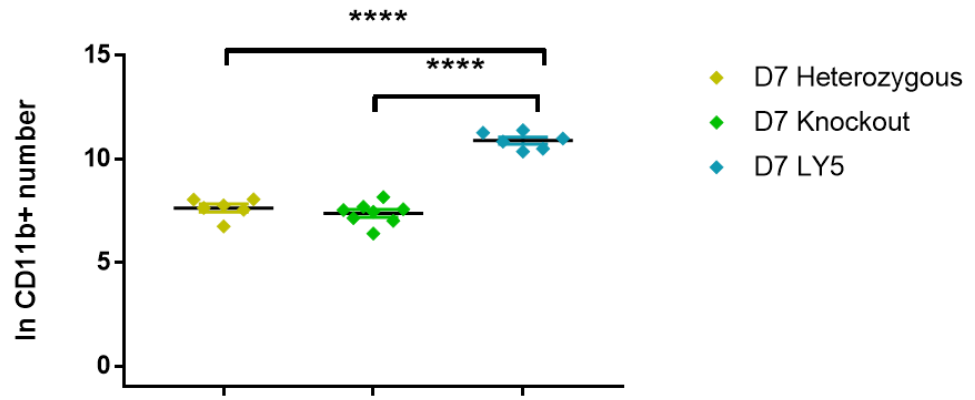
****
****
15
10
5
0
ln CD11b+ number
D7 Heterozygous
D7 Knockout
D7 LY5

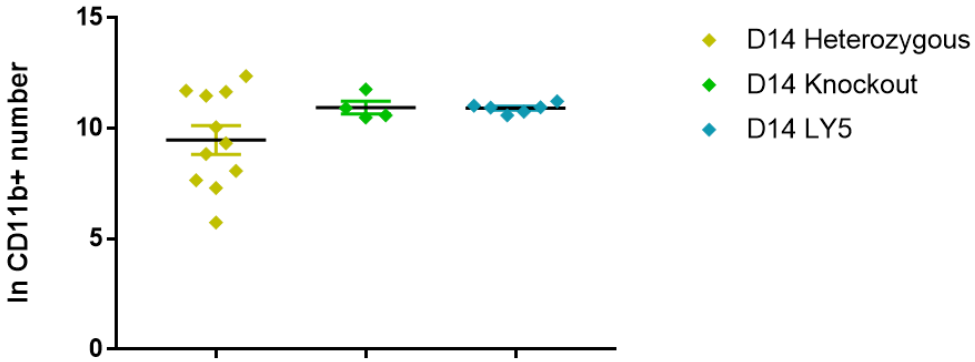
15
10
5
0
ln CD11b+ number
D14 Heterozygous
D14 Knockout
D14 LY5

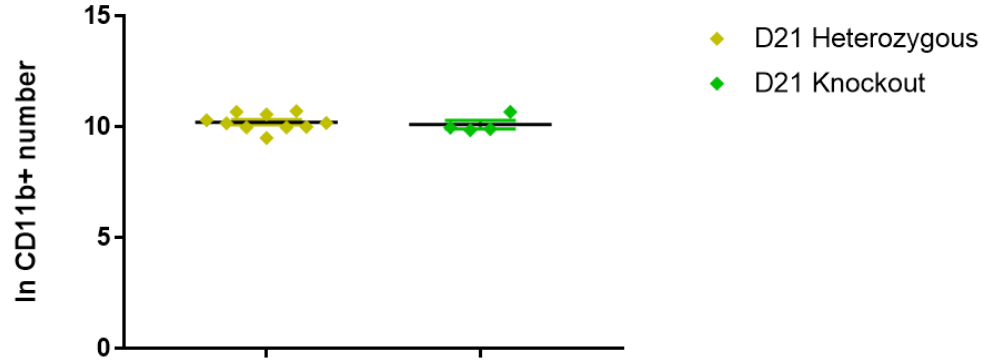
15
10
5
0
ln CD11b+ number
D21 Heterozygous
D21 Knockout

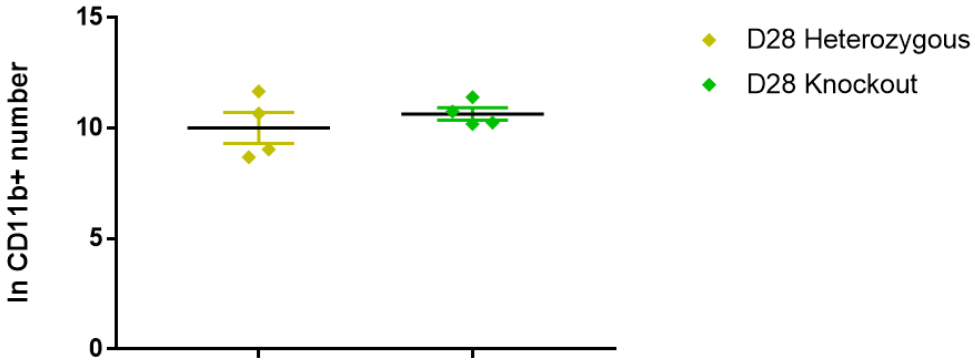
15
10
5
0
ln CD11b+ number
D28 Heterozygous
D28 Knockout

AVERAGE CELL NUMBER

	Ly5	CX3CR1 Heterozygous	CX3CR1 Homozygous
D7	**57720**	**2244**	**1788**
D14	**56339**	**74716**	**64884**
D21		**31030**	**26325**
D28		**47830**	**43620**

Figure 6.5: Analysis of total CD11b+ cell number within the retinal infiltrate at different time points throughout clinical disease. RAG2$^{-/-}$ recipients received an intraperitoneal transfer of uveitogenic cells from one of three donor types Ly5, CX3CR1 heterozygous or CX3CR1 knockout. To correlate with the clinical imaging at each time point retinas were dissected and prepared for flow cytometric analysis and CD11b+ cell numbers were quantified. Data expressed as Mean ±SEM. Statistical analysis performed: One-Way ANOVA multiple comparisons compared to wildtype transfer (A+B) unpaired non-parametric Mann-Whitney Test (C+D). ****p<0.0001.

6.3.3 CX3CR1 deficiency in recipient tissue does not affect EAU disease onset

The transfer of CX3CR1 deficient cells into RAG2$^{-/-}$ recipients saw a late onset of EAU in comparison to wildtype transfers (figure 6.1 and 6.3).

From this we wanted to understand if CX3CR1 deficiency within recipients had a similar effect. In order to investigate the affect CX3CR1 deficiency within the recipient tissue has on disease initiation, wildtype (Ly5) cells were transferred into CX3CR1 heterozygous (CX3CR1$^{+/GFP}$) or CX3CR1 (CX3CR1$^{GFP/GFP}$) knockout recipients. In previous studies using active immunisation of CX3CR1 heterozygous mice or CX3CR1 knockout mice, CX3CR1 was found to not have an effect on disease onset (248).

At day 0, the fundus and OCT images are both similar and normal before disease induction (figure 6.6a and 6.6f). At day 2, clinical disease cannot be observed by OCT imaging in both groups of recipients (figure 6.6b and 6.6g).

By day 7, severe clinical disease can be seen in both groups by OCT (figure 6.6c and 6.6h), severe retinal infiltrate (vitritis) is present within the vitreous of the animals in both groups. Obvious swelling of the retina and optic disc is also observed within the OCT image and a vitreal haze is present within the fundus image with obvious swelling around the optic disc.

At day 14, active clinical disease has begun to resolve (figure 6.6d and 6.6i). In the OCT image swelling of the retina and optic disc has resolved but retinal infiltrate is still seen within the vitreous. The fundus images still show a swelling around the optic disc and some perivascular sheathing but the vitreal haze has subsided.

At day 21, active disease has further resolved with minimal retinal infiltrate present within the OCT. Although active disease appears to be resolving within the OCT image in the fundal imaging retinal scarring remains and mild inflammation is observed around the optic disc (figure 6.6e and 6.6j).

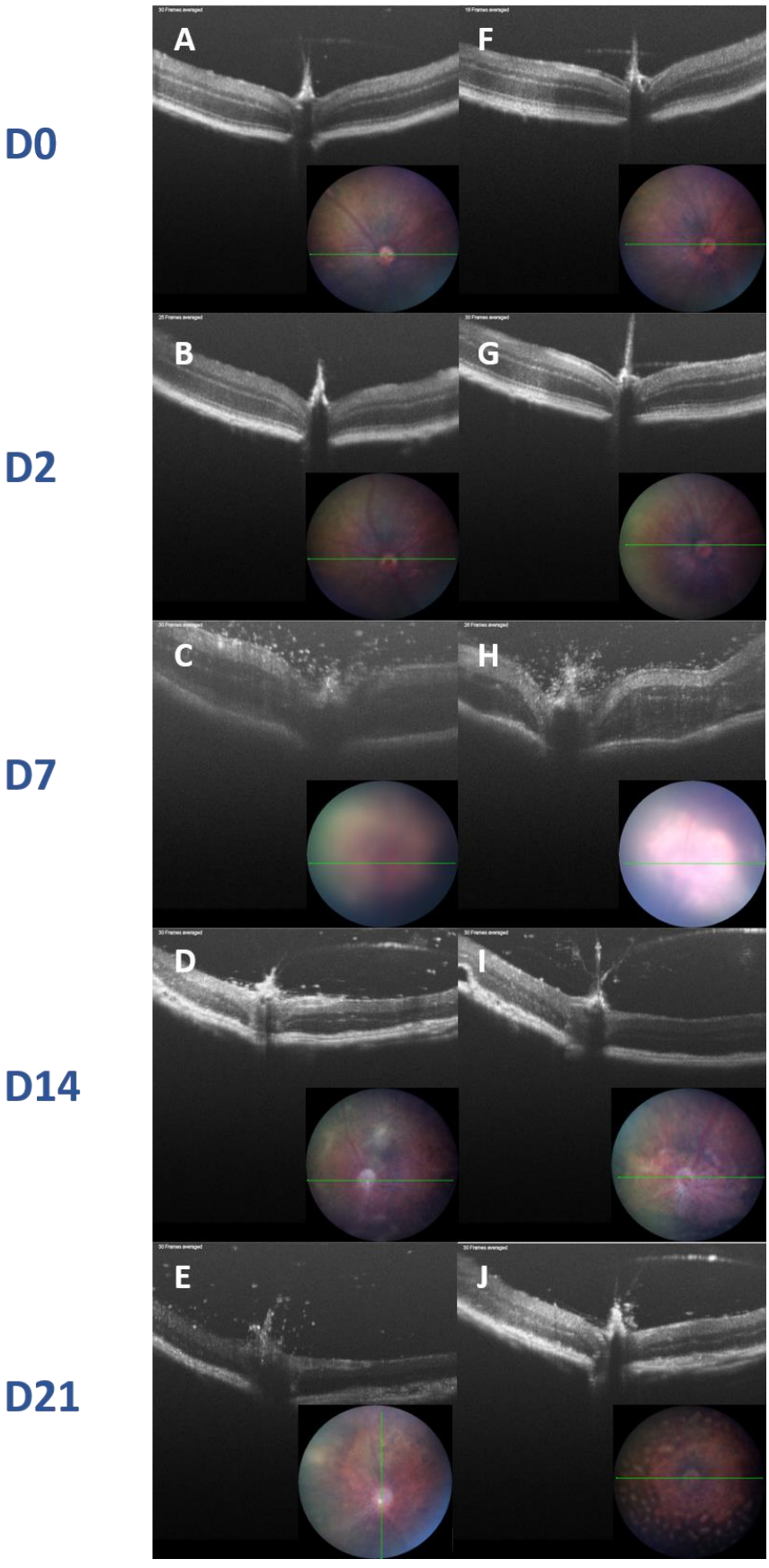
CX3CR1
Heterozygous
CX3CR1
Knockout
D0
D2
D7
D14
D21
A
F
B
G
C
H
D
I
E
J

Figure 6.6: OCT imaging of clinical disease course using a Ly5 transfer of uveitogenic cells into CX3CR1 heterozygous or CX3CR1 knockout mice. Clinical imaging was taken throughout clinical disease to observe disease initiation and progression within the two groups. Day 0 baseline illustrates the two groups of recipients have similar characteristics as other wildtype naives (A+F). At day 2, clinical disease is not observed, and the OCT and fundus imaging is comparable to the baseline at day 0 (B+G). From day 7, clinical disease is observed in both the fundal images and OCT (C+H). By day 14, inflammation has begun to resolve (D+I) this resolution continues through to day 21 (E+J).

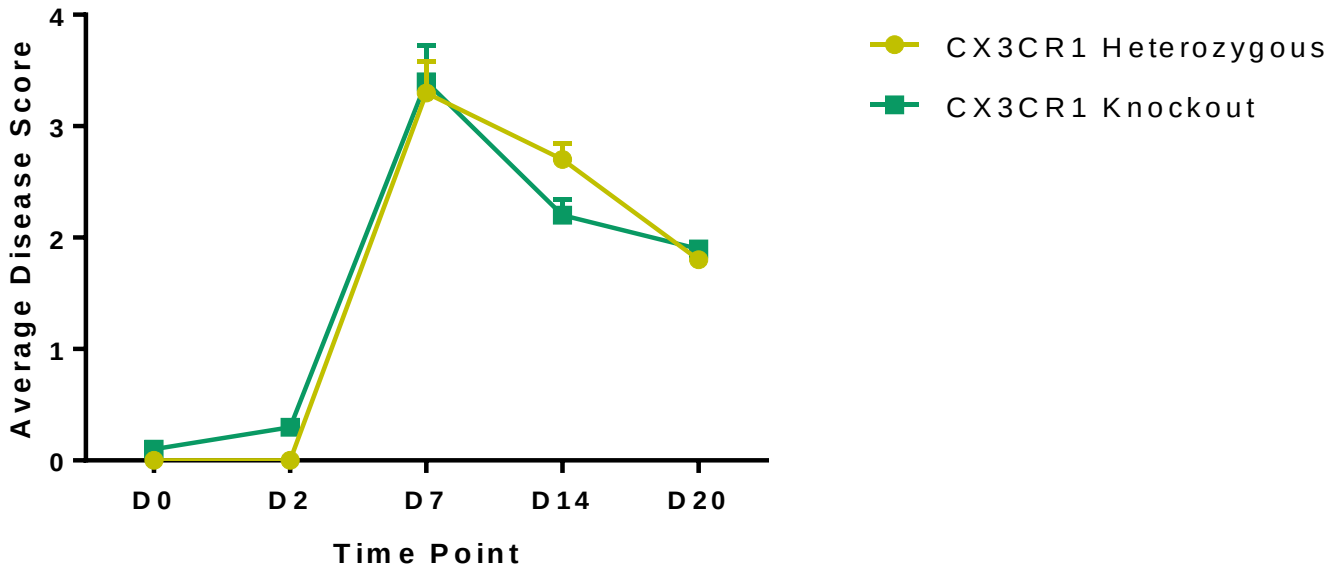

Figure 6.7: Average OCT scores of CX3CR1 heterozygous and CX3CR1 knockout recipients after adoptive transfer. Fundal images were obtained throughout clinical disease from both recipient groups. Images were then scored blind using the criteria described in *chapter 2*. Average scores were calculated for each recipient and each recipient group. Data expressed as Mean ± SEM.

6.3.4 CX3CR1 deficiency in recipient tissue does not affect leukocyte recruitment to the eye throughout disease

CX3CR1 deficiency on recipient tissue does not affect disease induction and by OCT imaging does not appear to affect the disease course within the two groups.

To further analyse the differences in disease course across the two groups of recipients that received Ly5 uveitogenic cells (CX3CR1 heterozygous and CX3CR1 knockout) flow cytometric analysis was performed at several time points throughout clinical disease course to support the OCT imaging collected.

At day 2, endogenous recruitment of CD4+ T cells to the eye is similar between the two groups this is also seen within the transferred population at this time point (figure 6.6a and 6.6d). Within the CD8 T cell compartment endogenous recruitment and transferred recruitment is comparable across the two recipient groups (figure 6.8b and 6.8e), this is also seen within the CD11b+ cell compartment (figure 6.8c and 6.8f).

As observed within the OCT imaging in figure 6.6 and 6.7 clinical disease has developed in the recipients of both groups illustrated by severe retinal infiltrate, made up of several different leukocyte populations including CD4+ T cells, CD8+ T cells and CD11b+ cells. CD4+ T cell recruitment has increased in both groups to mediate disease. Transferred CD4 T cell number has increased and the ratio of endogenous to transferred cells is ~1:1 illustrating recruitment of both uveitogenic transferred CD4+ T cells and endogenous CD4+ T cells (figure 6.8a and 6.8d). At peak disease, endogenous CD8+ T cells are found in increased numbers in the retinal infiltrate (figure 6.8a), but in contrast transferred CD8+ T cells have a small increase in number at peak disease which has also been observed in previous chapters (*chapter 4)* (figure 6.8b). The same pattern is observed in the CD11b+ compartment, many endogenous cells within the retinal infiltrate but minimal transferred cells (figure 6.8c and 6.8f).

At day 14 total CD4+ retinal infiltrate in the endogenous compartment has remained from day 7 (figure 6.8a) but within the transferred compartment there is now a statistically significant difference between the transferred CD4+ T cell population within the eyes of the CX3CR1 heterozygous recipients and the CX3CR1 knockout recipients. This is due to a decrease in transferred cells in the CX3CR1 knockout recipients in comparison to the CX3CR1 heterozygous recipients (figure 6.8d). Endogenous CD8+ T cells have persisted through to day 14 in the CX3CR1 heterozygous group (figure 6.8b), whereas in the CX3CR1 knockout group a

drop in endogenous CD8+ numbers is observed (figure 6.6b). In the transferred CD8+ population a minimal population is still observed in both groups of recipients (figure 6.8e). CD11b+ cell number is reduced in both groups in the endogenous compartment, but no statistical difference is observed between the two groups (figure 6.6c). As seen at day 7, the transferred CD11b+ cell number continues to be minimal through peak disease with very little recruitment of transferred cells (figure 6.8f).

Finally, at day 21 when active disease has begun to resolve based on OCT clinical imaging (figure 6.6). Endogenous CD4+ T cell numbers have dropped in both groups in comparison to day 14 but no statistically significant difference between the two groups is observed (figure 6.6a). Whereas in the transferred CD4+ T cell population a reduction in cell number in both groups of recipients is observed but a statistically significant difference between the two groups based on cell number is present. Similarly, to day 14 a statistically significant difference between the two recipient groups based on transferred CD4+ T cell number due to a larger decrease of transferred CD4+ cells in the CX3CR1 knockout group when compared to the CX3CR1 heterozygous group (figure 6.8d).

CD8+ T cell number at the day 21 time point appears to be similar in total endogenous cell number across the two recipient groups (figure 6.8b). As seen throughout clinical disease, very little recruitment of the transferred CD8+ population is seen. This pattern continues through to day 21 (figure 6.8e).

Endogenous CD11b+ cell number decreases at day 21 back to a similar number that is seen at day 2 (figure 6.c8). Transferred CD11b+ cells were recruited in small numbers throughout the disease and this persists through to day 21 (figure 6.8f).

Overall, the only difference between disease in the two recipient groups is observed in the transferred CD4+ T cell number at day 14 and day 21.

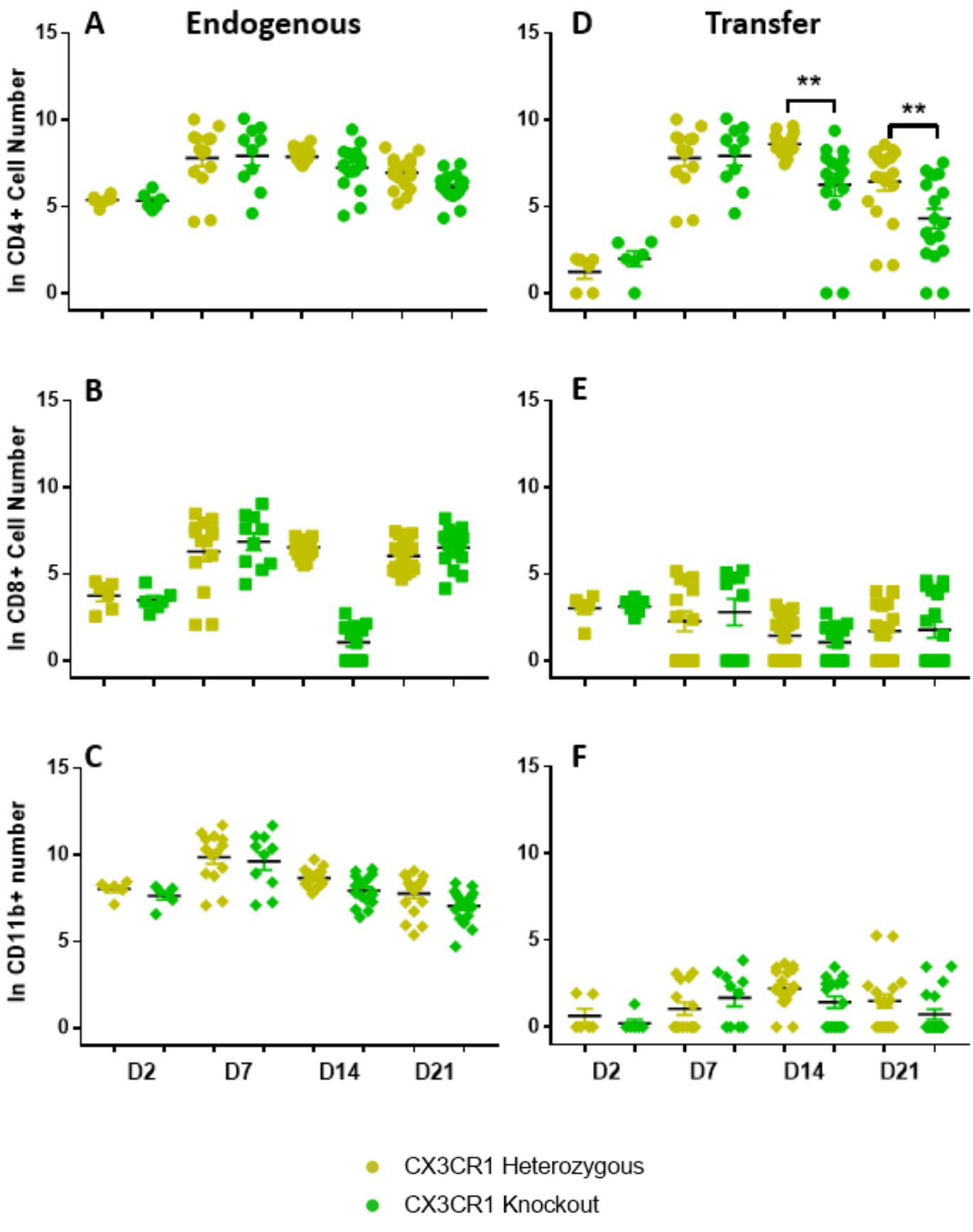
A
Endogenous
D
Transfer
ln CD4+ Cell Number
B
E
ln CD8+ Cell Number
C
F
ln CD11b+ number
15
10
5
0
**
**
D2
D7
D14
D21
CX3CR1 Heterozygous
CX3CR1 Knockout

CD4 ENDOGENOUS

	CX3CR1 Heterozygous	CX3CR1 Homozygous
D2	225	231
D7	6004	5997
D14	2802	2721
D21	1496	588

CD8 ENDOGENOUS		
	CX3CR1 Heterozygous	CX3CR1 Homozygous
D2	53	38
D7	1538	1931
D14	801	1846
D21	686	1016

CD11B ENDOGENOUS		
	CX3CR1 Heterozygous	CX3CR1 Homozygous
D2	3296	2330
D7	38502	29860
D14	6344	3796
D21	3645	1579

CD4 TRANSFER

	CX3CR1 Heterozygous	CX3CR1 Homozygous
D2	4	9
D7	1929	2709
D14	6483	2233
D21	1950	401
CD8 TRANSFER		
	CX3CR1 Heterozygous	CX3CR1 Homozygous
D2	24	24
D7	51	59
D14	2	4
D21	14	26
CD11B TRANSFER		
	CX3CR1 Heterozygous	CX3CR1 Homozygous
D2	2	0
D7	7	9
D14	13	7
D21	19	4

Figure 6.8: Flow cytometric analysis of retinal infiltrate throughout clinical disease in CX3CR1 heterozygous or CX3CR1 knockout recipients that received a Ly5 uveitogenic cell transfer. Retinas from CX3CR1 heterozygous recipients or CX3CR1 knockout recipients were taken and processed at each clinical imaging time point to analyse leukocytes present within the retinal infiltrate. Time course of endogenous CD4+ retinal infiltrate through clinical disease (A). Time course of transferred CD4+ retinal infiltrate through clinical disease (D). Time course of endogenous and transferred CD8+ T cell number through clinical disease (B+E). Time course of endogenous and transferred CD11b+ cell number through clinical disease (C+F). Data expressed as Mean $\pm$SEM. Statistical analysis performed: One-Way ANOVA multiple comparisons (A-F). **p<0.01.

6.3.5 CX3CR1 upregulation on CD4+ T cells in the eye during EAU

In a model studied by Mionnet et al, expression of CX3CR1 on CD4+ T cells is required for the development of clinical asthma, suggesting that expression by Th2 cells is required for airway disease (151). Further to this, expression of CX3CR1 denoted by GFP is highly increased on T cells in the inflamed lung (20-30%) in comparison to T cells in naïve CX3CR1 heterozygous mice (0.5%) (151). The studies further highlighted that CX3CR1 gives a selective advantage to Th2 cells, inflammation was not enough to induce infiltrating Th2 cells to express CX3CR1 but also required TCR engagement (151). And finally, CX3CR1 provided a survival signal to lung Th2 cells (151).

To analyse the role of expression of CX3CR1 on CD4+ T cells in EAU, uveitogenic CX3CR1 heterozygous cells were adoptively transferred into Ly5 recipients. Disease course was monitored using OCT imaging (figure 6.9) and CX3CR1 expression quantified by flow cytometric analysis at each time point by GFP expression on CD4+ T cells. Leukocyte infiltrate data and OCT imaging and scoring was previously presented in *chapter 4*.

Figure 6.10a illustrates the frequency of transferred CD4+ cells expressing CX3CR1 from pre-clinical disease at day 2 through peak disease to day 21. At day 2 GFP therefore CX3CR1 expression was at 10% on the small number of recruited transfer cells at this time point. By day 7, CX3CR1 expression on CD4 T cells has increased slightly to ~20%. Peak frequency of transferred CD4+ T cells expressing CX3CR1 occurs at day 14 where 40% of the transferred population is GFP+ which then plateaus off at day 21.

To support the large CX3CR1 CD4+ T cell population present within the eye during clinical disease figure 6.10b illustrates an increased population of CX3CR1 CD4+ T cells present within the eye in comparison to the other organs analysed including blood and liver.

Throughout clinical disease, CX3CR1 expression on CD4+ T cells present within the liver and blood is reduced in comparison to the eye.

D0

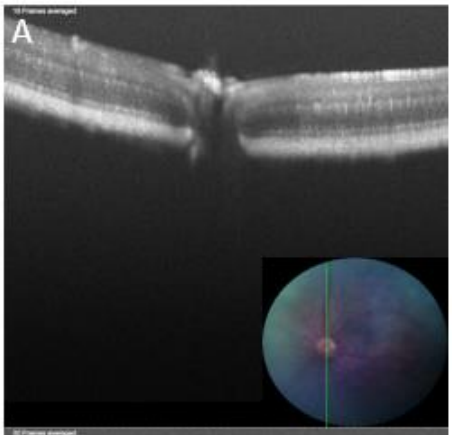

D9

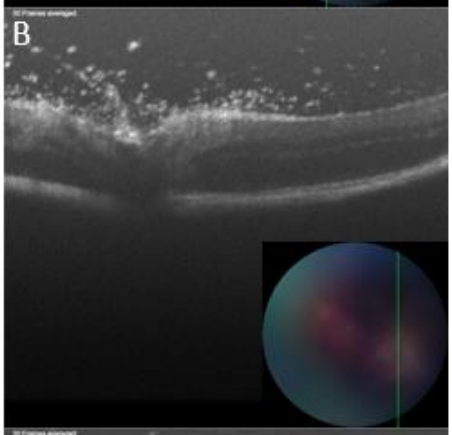

D15

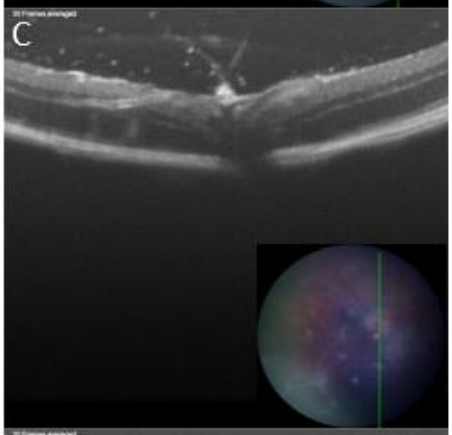

D21

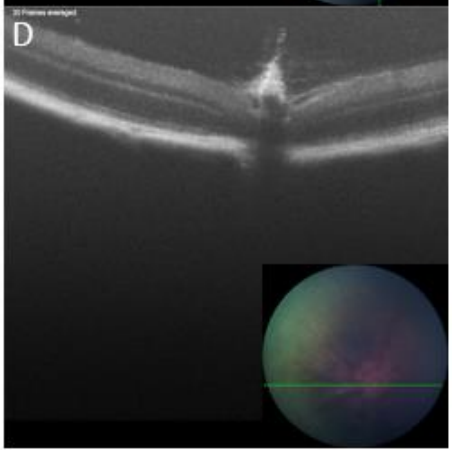

Figure 6.9: Clinical imaging of disease course after CX3CR1 heterozygous transfer of uveitogenic cells into Ly5 mice. As previously described in figure 4.5, clinical disease course after uveitogenic cell transfer. Peak disease is present at day 7-10, but by day 14 infiltrate has reduced and is not visible by OCT at day 21.

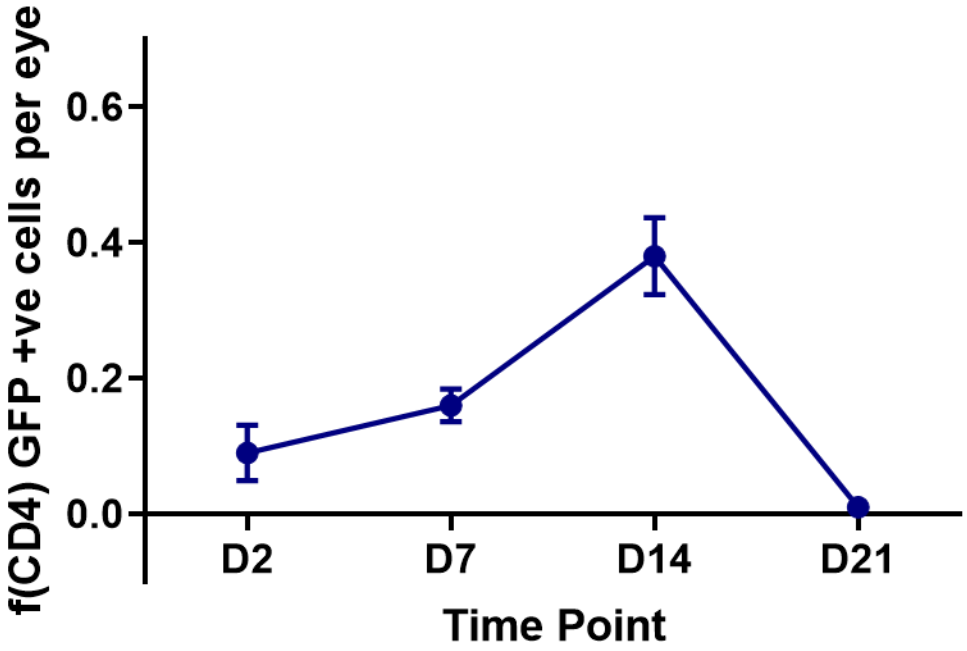
f(CD4) GFP +ve cells per eye
0.6
0.4
0.2
0.0
D2
D7
D14
D21
Time Point

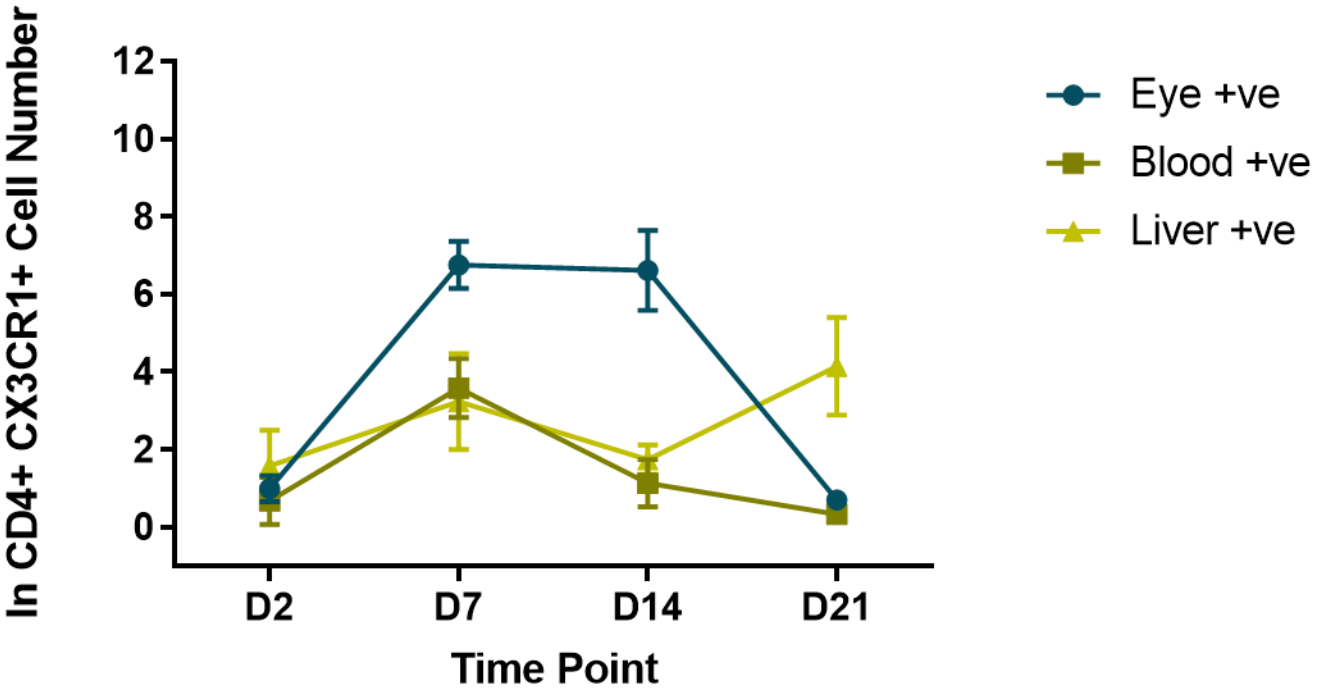
ln CD4+ CX3CR1+ Cell Number
12
10
8
6
4
2
0
D2
D7
D14
D21
Time Point
Eye +ve
Blood +ve
Liver +ve

Figure 6.10: Frequency of CX3CR1+ CD4+ T cells in the eye throughout disease, and total number of CX3CR1+ CD4+ T cells in the eye in comparison to blood and liver. (A) CD4+ CX3CR1+ transferred cells as a fraction of the total CD4+ transferred population recruited to the eye at each time point through EAU. (B) Comparison of CD4+ CX3CR1+ cells present within the eye, blood, and liver throughout EAU. (A) frequency calculated by dividing total CD4+ CX3CR1+ cell number by total transferred CD4+ T cell number at each time point. (B) Total CX3CR1+ CD4+ cell number (log transformed). Data expressed as Mean ± SEM.

6.3.6 Pathogenic cells express CX3CR1 during EAU but when transferred together non-pathogenic cells do not express CX3CR1 during EAU

As illustrated in figure 6.10, CX3CR1 is expressed on transferred uveitogenic CD4+ T cells during EAU. As peak disease progresses, the frequency of CX3CR1 expression on CD4+ T cells increases to ~40% (figure 6.10a).

To further investigate if the upregulation of CX3CR1 on CD4+ T cells is observed solely on pathogenic transferred CD4+ T cells, CX3CR1 expression was quantified from the double cell transfer (described in figure 5.13). Pathogenic CX3CR1 heterozygous leukocytes and OTII activated non-pathogenic leukocytes were transferred in a 1:1 mixture into Ly5 recipients. Leukocyte infiltrate data and OCT imaging was previously presented in *chapter 5.*

OCT imaging (figure 6.11) shows a similar clinical disease course as the CX3CR1 heterozygous transfer alone into Ly5 recipients (figure 6.9). From data presented in *chapter 5,* CD4+ infiltrate during peak disease was quantified and 3 populations were observed: endogenous, antigen-specific (pathogenic) and non-antigen specific OTII (TCR transgenic activated with OVA peptide). In both the transferred antigen-specific and the activated non-antigen specific OTII populations there is a heterozygous CX3CR1 GFP tag present. Using GFP expression as a measure of CX3CR1 expression on both these populations total CD4+ CX3CR1+ retinal infiltrate is quantifiable in each recipient.

At day 5-7, peak disease is observed by OCT clinical imaging (figure 6.11b), retinas were then isolated from recipients and CX3CR1 expression on CD4+ T cells quantified in the antigen-specific and non-antigen specific OTII transferred populations. Figure 6.12 shows a difference in the frequency of CX3CR1 expression on CD4+ T cells on the transferred antigen-specific pathogenic cells in comparison to the activated non-antigen specific OTII transferred cell population.

At day 14, active disease appears to have begun to resolve by OCT imaging (figure 6.11c). But a statistically significant difference between CX3CR1 expression on CD4+ T cells is observed between the transferred antigen-specific and the transferred non-antigen specific OTII cells (figure 6.12).

D0

D5

D14

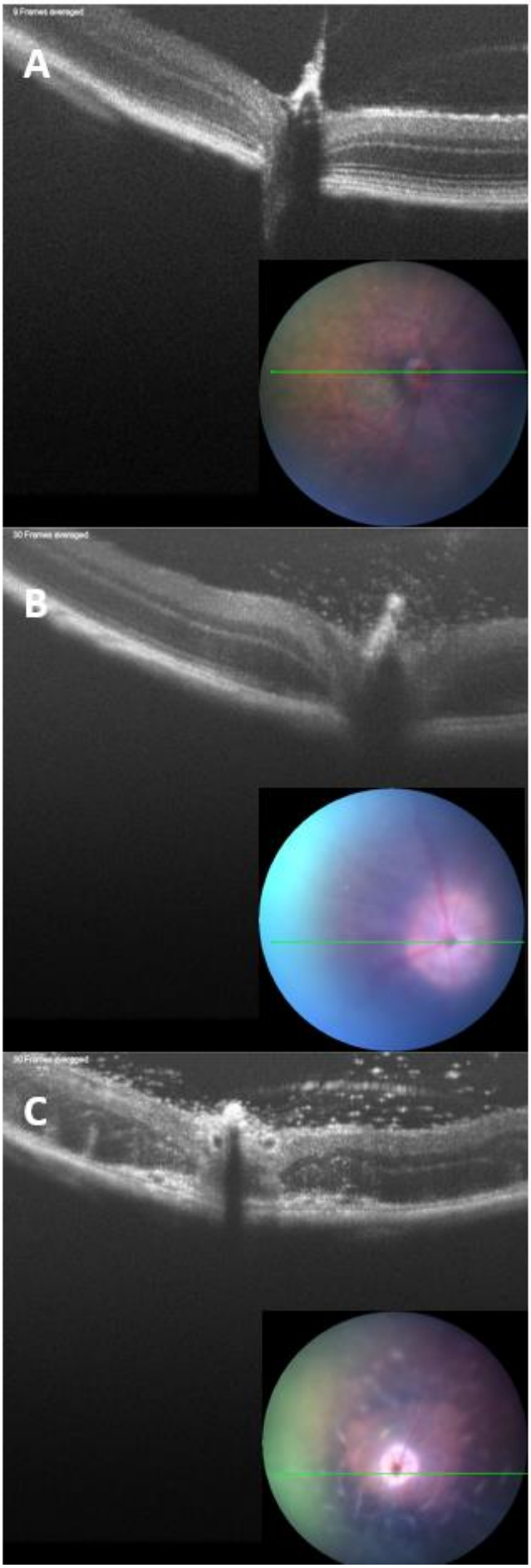

Figure 6.11: OCT Clinical imaging of EAU disease course after double transfer of antigen - specific and non-antigen specific leukocytes. Recipients were imaged from day 0 to day 14 to monitor clinical disease course. Peak clinical disease was observed by day 5, denoted by swelling of the retina and optic disc combined with high levels of retinal infiltrate (B). At day 14, active disease is still present within the eyes of recipients, but disease is post-peak so retinal infiltrate is mildly reduced and retinal layers are again visible by OCT (C).

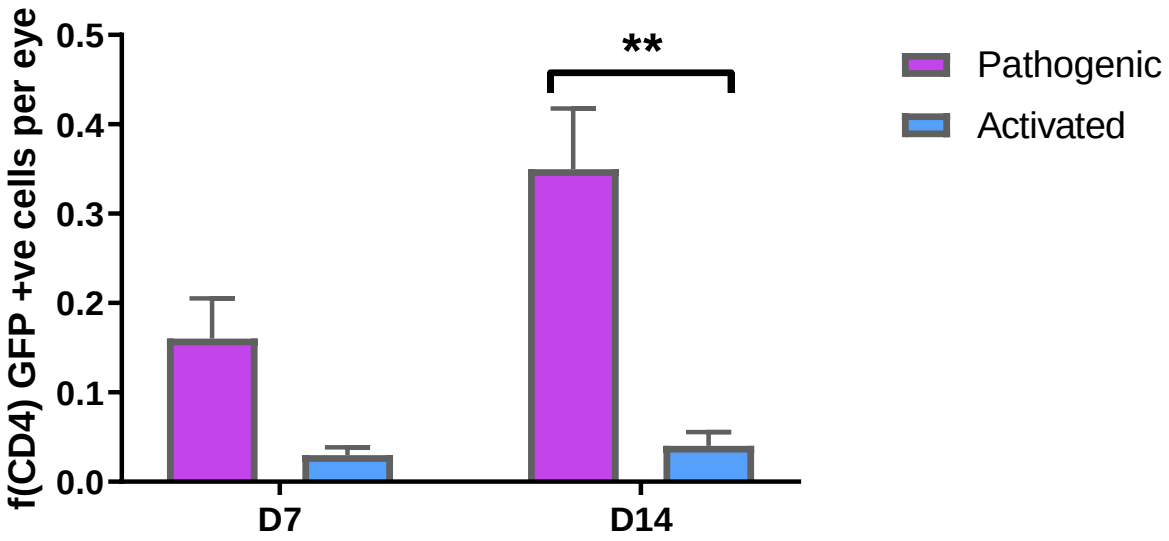

Figure 6.12: Flow cytometric analysis of retinal infiltrate at day 7 and day 14 quantifying CX3CR1+ CD4+ cells as a frequency of total transferred RBP3 antigen specific or RBP3 non-specific (OVA specific) populations. CX3CR1 expression was measured using the GFP tag on the CX3CR1 heterozygous antigen-specific (pathogenic cells) and the CX3CR1 knockout cross onto OTII TCR transgenic mouse OVA specific (Non-pathogenic cells). The frequency of CD4+ CX3CR1+ was calculated for both the RBP3 specific (pathogenic) cell population and the OVA specific (activated) cell population. Data expressed as Mean $\pm$ SEM. Statistical analysis performed unpaired non-parametric Mann-Whitney Test **$p < 0.01$

6.3.7 CX3CR1 upregulation on CD4+ T cells is due to an antigen-specific signal to the cells in vivo

As seen in figure 6.12, more than 35% of antigen specific, pathogenic transferred CD4+ T cells express CX3CR1 during clinical disease, in comparison ~4% of the transferred non-pathogenic, OVA specific CD4+ T cells expressed CX3CR1 during clinical disease.

To further investigate this observation that an antigen specific component is involved in CX3CR1 expression on CD4+ T cells. CX3CR1 expression was measured using the OVA intravitreal transfers described previously into C57BL/6 CX3CR1 heterozygous knockout mice. Leukocyte infiltrate data and OCT imaging was previously presented in *chapter 5.*

Recipients firstly received an intravitreal injection of ovalbumin into the left eye and a PBS or L144 intravitreal control injection into the right eye. OTII TCR transgenic leukocytes were then transferred by intraperitoneal injection after activation by ovalbumin. Recruitment of leukocytes to both eyes were then monitored by OCT and endogenous and transferred leukocytes quantified by flow cytometry.

At day 2, by clinical imaging no infiltrate is observed by OCT and overall, the fundus and OCT images look normal (figure 6.13a and 6.13b). By flow cytometry, endogenous recruitment to both eyes are comparable with low numbers of CX3CR1 expression, minimal transferred cell recruitment is observed at this time point.

At day 4, some retinal infiltrate is observed by OCT in the left eye but not within the right (figure 6.13c and 6.13d), when CX3CR1 expression is analysed in the infiltrate from both eyes, no difference is observed in the total number of CX3CR1 CD4+ T cells expressing in both eyes at this time point (figure 6.14a and 6.14b).

By day 8 after intravitreal injection of ovalbumin peptide and cell transfer, peak disease is present within the left eye (that received the OVA peptide) of the recipients, whereas in the right eye minimal infiltrate is observed (figure 6.11e and 6.11f). This continues to day 15 where obvious infiltrate and retinal swelling is present within the left eye but not within the right eye (figure 6.13g and 6.13h). Total CD4+ CX3CR1+ T cells were increased in the endogenous and transferred compartment of the left eye, but in the right eye remained at similar reduced numbers as at day 4 (figure 6.14a and 6.14b).

At day 25, retinal infiltrate is still observed within the left eye, but disease is past peak at this time point (figure 6.13i). The right eye of each recipient has not changed throughout the

disease course of the left eye by clinical imaging (6.13j). CX3CR1 is also still increased in the left eye over the right eye, although total CX3CR1+ CD4+ T cells does decrease after peak disease (figure 6.14a and 6.14b). CX3CR1 expression on CD4+ T cells is increased in the left eye in comparison to the right eye throughout the whole disease course.

CX3CR1 expression on CD4+ T cells during EAU is observed when an antigen-specific interaction in vivo has taken place and therefore activation alone with a non-specific antigen is not sufficient to induce expression, the data presented in this chapter supports this hypothesis.

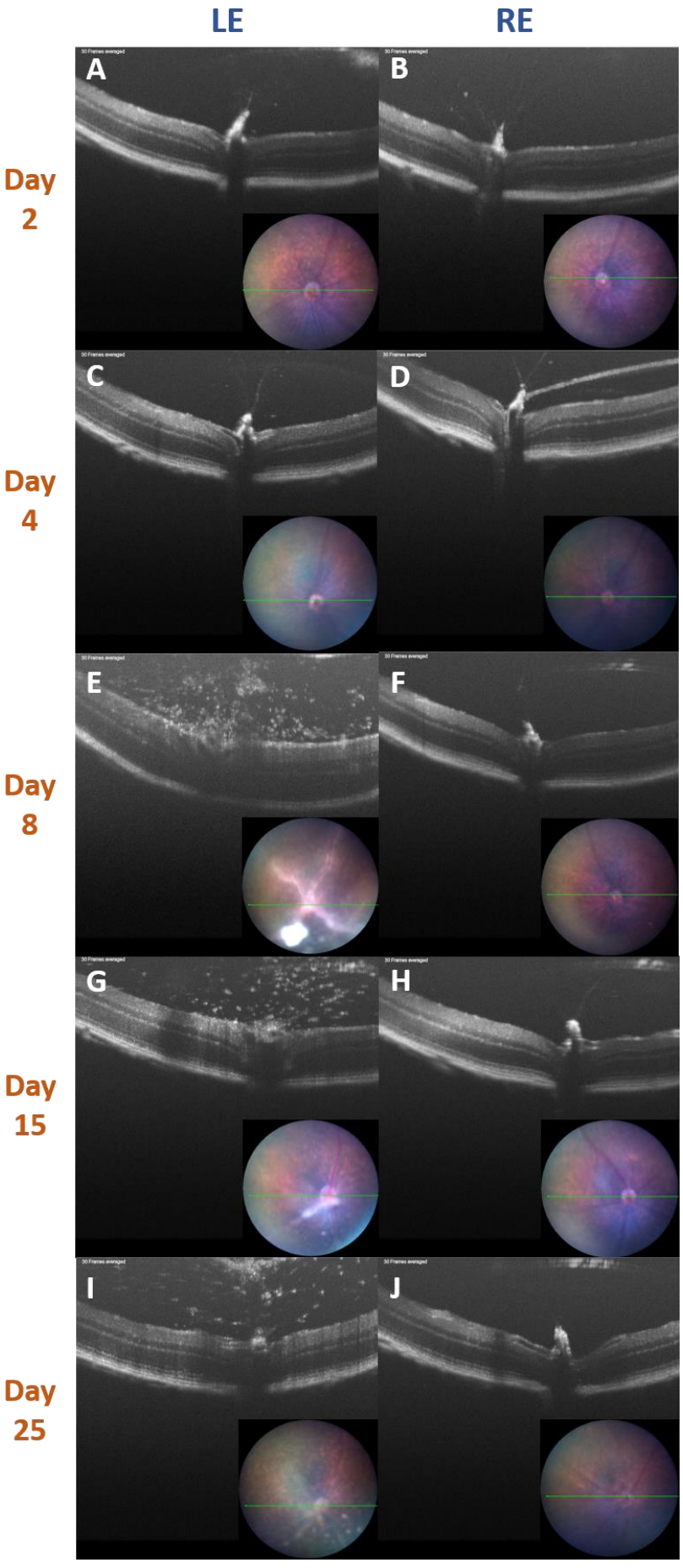
LE
RE
Day 2
Day 4
Day 8
Day 15
Day 25
A
B
C
D
E
F
G
H
I
J

Figure 6.13: OCT clinical imaging of disease course after cell transfer and intravitreal injection of OVA or L144 control peptide Disease was monitored in both eyes from day 2-day 25. Disease was observed in the left eye (A,C.E,G,I). But no clinical disease was seen in the right eye (B, D, F, H, J) (Data presented with average disease scores in *Chapter 5*)

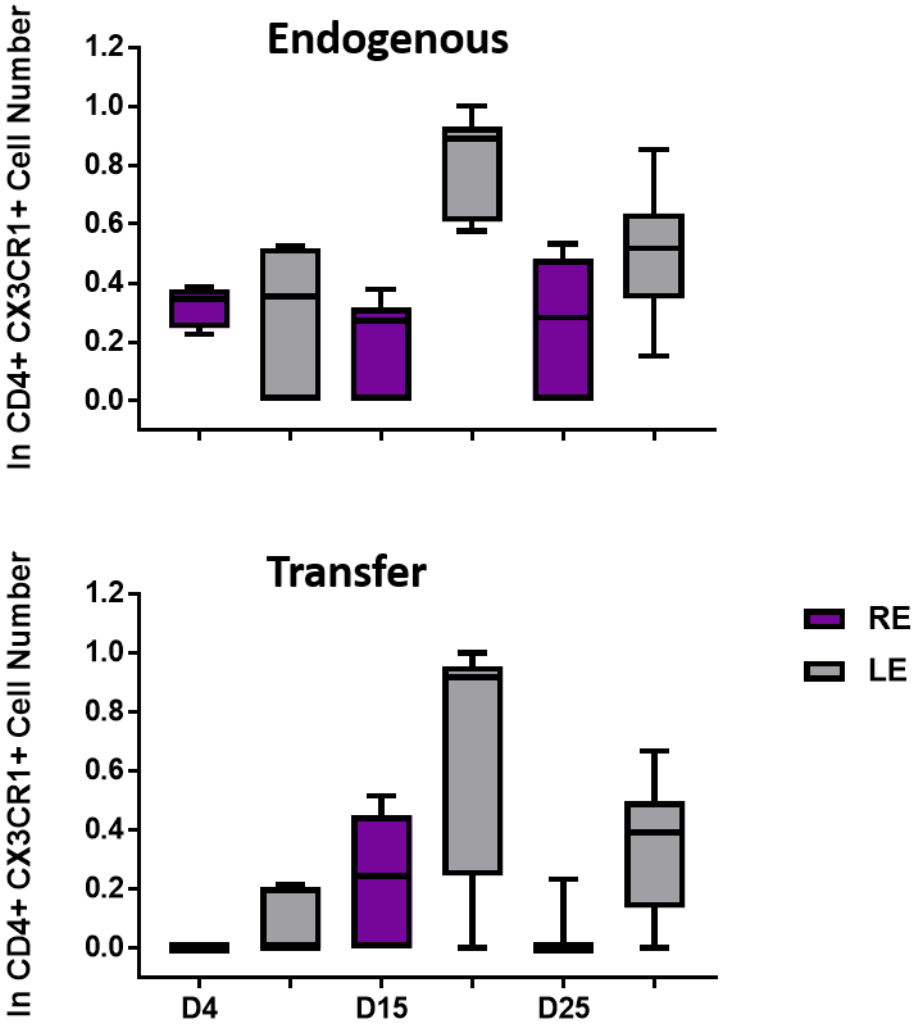

LE				RE			
ENDOGENOUS				**ENDOGENOUS**			
	Lowest Value	Highest Value	Mean		Lowest Value	Highest Value	Mean
D4	0	27	12	D4	0	10	7
D15	0	556	250	D15	0	10	4
D25	0	216	49	D25	0	28	9
TRANSFER				**TRANSFER**			
	Lowest Value	Highest Value	Mean		Lowest Value	Highest Value	Mean
D4	0	4	1	D4	0	0	0
D15	0	1243	570	D15	0	38	11
D25	0	116	23	D25	0	4	0

Figure 6.14: Total CX3CR1+ CD4+ T cells within the retinal infiltrate at each time point. Flow cytometric analysis at each time point during clinical disease of total CD4+ CX3CR1+ T cells present within the endogenous compartment of each eye (A) and transferred CX3CR1+ CD4+ T cells (B). (Left eye received OVA intravitreal injection, Right eye received control peptide L144 or PBS) Data Expressed as Mean ± SEM. Data obtained from 3 experiments and 8-17 eyes per time point

6.4 Discussion

The role of CX3CR1 in EAU is controversial. A study by Kezic et al (248) suggests that the CX3CR1 receptor does not play a significant role in the pathogenesis of EAU (248), this was based on disease scores following active induction of disease between wildtype, CX3CR1 heterozygous and CX3CR1 knockout mice not being significantly different at disease onset (248). Conversely, a study by Dagkalis et al (47) defined an association between CX3CR1-deficiency and increased severity of disease in EAU in the active immunisation model. CX3CR1 knockout mice had increased disease severity at day 23 post-immunisation in comparison to CX3CR1 heterozygous mice, with increased recruitment of monocytes to the retina in response to EAU induction (47).

The studies presented in this chapter extend these findings by illustrating a role for CX3CR1 expression on CD4+ T cells during EAU using the adoptive transfer technique of disease induction, showing that there is a selective retention or recruitment of CX3CR1+ CD4+ T cells during active clinical disease.

To investigate the role of CX3CR1 expression has on disease initiation and progress in the adoptive transfer model of EAU, cells of different CX3CR1 expression (wildtype, CX3CR1 heterozygous and CX3CR1 knockout) were transferred into $RAG2^{-/-}$ mice. These experiments allow the analysis of the effect of CX3CR1 deficiency on donor cells with CX3CR1 intact in the recipient tissue.

Wildtype cells initiate disease within the $RAG2^{-/-}$ recipients by day 7, whereas disease initiation within the CX3CR1 heterozygous and CX3CR1 knockout transfer recipients occurred at the later time point of day 14. The delay in disease induction in the CX3CR1 deficient transfers (figure 6.1 and 6.2) is consistent with a role for CX3CR1 on the transferred population that even in the heterozygote animals influences efficacy of recruitment during disease initiation but does not limit maximum severity of the disease. Because normal Treg function is deficient, it is not possible to interpret disease duration.

To complement this set of experiments, CX3CR1 deficiency in recipient tissue was investigated. Wildtype cells were transferred into CX3CR1 heterozygous and CX3CR1 knockout mice. No difference was observed in disease initiation or course by OCT imaging (figure 6.5) but there was a statistically significant difference in the transferred WT CD4+ T cell number within the retinal infiltrate at day 14 and day 21 (figure 6.6). Which indicates that

CX3CR1 expression within the tissue can have an effect on CD4+ T cell recruitment throughout active clinical disease.

These data sets illustrate a role for CX3CR1 in disease initiation in donor uveitogenic cells, but not disease severity. Further to this the wildtype transferred cells preferentially survived during clinical disease in CX3CR1 heterozygous mice over the CX3CR1 knockout mice.

As demonstrated in *chapter 4*, within the leukocyte population that is transferred into naïve recipients the surviving population is CD4+ T cells. This suggests that the effect on disease within donor CX3CR1 deficient cells is based on CX3CR1 being expressed on CD4+ T cells during EAU.

Mionnet et al (151), suggested a role for CX3CR1 expression on CD4+ T cells in survival and maintenance during airway inflammation (151). Further to this, a study conducted by Staumont-Sallé et al concluded that CX3CR1 deficiency does not affect antigen presentation or T cell proliferation upon skin sensitisation in experimental models of atopic dermatitis and that expression of CX3CR1 by both Th1 and Th2 cells was required for induction of disease (247). The study also used adoptive transfer experiments to establish CX3CR1 as a key regulator of CD4+ T cell retention in inflamed skin (247). However, the role of CX3CR1 on CD4+ T cells in EAU has not yet been published.

Adoptive transfer of CX3CR1 heterozygous cells into Ly5 (wildtype) C57BL/6 recipients investigated expression of CX3CR1 using the GFP on CD4+ T cells. At day 7 which is considered to be peak disease, CX3CR1 expression is observed on transferred CD4+ T cells recovered from the eye at a frequency of ~0.2 on total transferred CD4+ T cells, when followed to day 14 the frequency increases to ~0.4 showing an increase in the relative frequency of transferred CD4+ T cell expressing CX3CR1 within the ocular tissue. The increase in CX3CR1 expression could be due to a selective recruitment of transferred CX3CR1 expressing cells, specific retention, and survival of CX3CR1 expressing CD4+ T cells or stimuli within the eye causing local CX3CR1 upregulation.

To investigate if the local environment was sufficient to drive CX3CR1 expression by recruited CD4+ T cells, experiments were performed using pathogenic antigen specific cell transfers mixed with an activated non-antigen specific OTII transfer (non-pathogenic cells that do not cause uveitis alone as described in *chapter 5)*. Both transferred cell populations were CX3CR1 heterozygous, so CX3CR1 expression was monitored on both antigen specific and non-antigen specific CD4+ T cells recruited to the ocular tissue during active disease using GFP expression.

CX3CR1 expression on the antigen-specific population is at a frequency of ~0.2 of the pathogenic transfer population at day 7 but increases to >0.4 by day 14. Confirming as previously observed that there is a local enrichment of CX3CR1 CD4+ transferred T cells. In contrast, the non-antigen specific transferred cell population had minimal CX3CR1 expression on CD4+ T cells at both time points. These findings demonstrate that the local environment alone is not sufficient to stimulate CX3CR1 on CD4+ T cells during the disease course.

To determine if expression of CX3CR1 on CD4+ T cells is due to antigen-specific stimulus within the tissue, ovalbumin peptide was injected intravitreally into the eye (described in *chapter 5*) TCR transgenic ovalbumin specific leukocytes (OTII) were then transferred intraperitoneally. As shown in *chapter 5* figure 5.2 activated OTII cells do not localise to the retina following transfer in the absence of uveitis, however, when the antigen is present within ocular tissue, recruitment of the ovalbumin-specific T cells is observed to the eye that received the ovalbumin peptide compared with the eye that received PBS or L144 (data presented in *chapter 5*, figures 5.6-5.10). CX3CR1 expression was then quantified on the endogenous and transferred recruited CD4+ T cells using GFP expression. There is a significant difference between the two eyes both in terms of recruitment of endogenous and transferred cells and also in CX3CR1 expression on CD4+ T cells between the endogenous and transferred population. A significant increase in CD4+ T cell recruitment is observed in the eye that received the OVA intravitreal injection throughout disease course and an increase in CX3CR1 expression is also observed, whereas in the contralateral eye where no disease progression is observed and no OVA antigen is present CX3CR1 expression is minimal within the CD4+ T cells that are present. The data produced further supported the hypothesis that an antigen-specific stimulus is involved in the expression of CX3CR1 on CD4+ T cells.

In conclusion, as expected from previous studies, CX3CR1 expression is not necessary either for CD4+ uveitogenic cells to cause uveitis or to provide an ocular environment in which it can develop. Partial or complete CX3CR1 deficiency in donor T cells delays disease initiation in comparison to WT cells but does not then affect disease course. While deficiency of CX3CR1 in the recipient animals supports greater persistence of the WT cell population in the heterozygous background (figure 6.8). This is consistent with the findings Dagkalis et al (47) that the knockout background had more severe disease. However, before cells are transferred the culture supernatant of the CX3CR1 heterozygous and CX3CR1 deficient mice show similar levels of IFN-γ production whereas the wildtype supernatant shows an increase in IFN-γ

production and therefore a more Th1 phenotype is present within the cell culture (figure 3.7). Due to the transferred CD4+ population being the sole surviving population this data suggested a role for CX3CR1 on CD4+ T cells.

To investigate the mechanism of CX3CR1 expression within the uveitogenic antigen specific transferred population. The double transfer of antigen specific and non-antigen specific cells suggested an antigen specific mechanism and TCR engagement is involved in CX3CR1 expression on CD4+ T cells. This was further confirmed by the transfer of non RBP specific TCR transgenic OTII leukocytes concurrently with an intravitreal injection of ovalbumin peptide illustrating CX3CR1 expression on transferred CD4+ T cells recruited to the ovalbumin injected eye. This data demonstrates that bystander activation in the target tissue is not sufficient to induce CX3CR1 expression on CD4+ T cells, but instead it requires an antigen specific signal. However, before transfer antigen specific in vitro activation leads to only very limited CX3CR1 expression (less than 5%), it is only when the cells come back into contact with the same antigen during active clinical disease that CX3CR1 expression is seen at higher frequencies on CD4+ T cells. Together this data illustrates the maintenance of CX3CR1 expressing CD4+ T cells in the eye throughout active EAU when they are in the presence of their cognate antigen.

Chapter 7. The effect of IL-27Rα on clinical disease course of EAU

7.1 Introduction

Cytokines are involved in most biological processes including disease pathogenesis, non-specific response to infection, specific responses to antigen, embryonic development, changes in cognitive function and the degenerative process of ageing (249). Cytokines can be divided into functional classes such as lymphocyte growth factors, pro-inflammatory cytokines, anti-inflammatory cytokines or cytokines involved in polarising the response to a specific antigen (249).

Polymorphisms in cytokines and cytokine receptors are associated with susceptibility to disease in many autoimmune conditions (249). After autoimmunity is initiated, it results in a persistent inflammatory response against self-tissue with the release of inflammatory mediators such as cytokines, the production of autoantibodies, the formation of immune complexes and the extravasation and activation of cytotoxic T cells, natural killer cells, macrophages and polymorphonuclear leukocytes (250).

7.1.1 Cytokines in Experimental Autoimmune Uveitis

T cell cytokines in uveitis

Th1 cells can be defined by their expression of the transcription factor T-bet and secretion of IFN-γ (251). IL-12 produced by dendritic cells and macrophages, plays a key role in inducing Th1 cells, the roles of IL-12 and IFN-γ (the main signature cytokine of the Th1 lineage) have been intensively studied in models of EAU (252).

Th2 cells are defined by the transcription factor GATA binding protein 3 and secretion of IL-4, IL-13 and IL-5 and are responsible for developing the humoral response, the timing and cellular source of Th2 cytokines can determine whether Th2 cells play a pathogenic or protective role in the progression of uveitis (251, 252).

Tregs are important for peripheral tolerance and the control of autoimmune disease and are identifiable by forkhead box P3 (FoxP3) transcription factor expression and production of transforming growth factor beta (TGFβ), IL-10 and IL-35 (251).

Th17 cells and IL-17 in uveitis

IL-17 is part of the IL-17 family of cytokines, including IL-17 (IL17A), IL-17B, IL-17C, IL-17D, IL-25 and IL-17F. In uveitis Th17 cells produce IL-17A and IL-17F and have an important role for driving inflammation. Pathogenic Th17 cells are capable of inducing uveitis alone and treatment with anti-IL-17 antibody can block development of EAU (251, 253).

IL-23 and its roles in uveitis

The IL-12 superfamily of cytokines consists of ; IL-12, IL-23, IL-27 and IL-35 (251). IL-23 is made up of the unique subunit p19 (only found in IL-23) and the shared subunit p40 (also comprising IL-12). Due to IL-23 comprising of two subunits it is known as a heterodimeric protein (251, 254). In the maturation and development of a population of pathogenic Th17 cells IL-23 is a very important checkpoint, if IL-23 is not present the population will not be pathogenic when developed (251, 254). Lack of the IL-12p40 or IL-23p19 subunits in mice has shown protection against the development of EAU (255). Increased serum levels of IL-23 in humans has been linked to increased risk of uveitic disease (251).

IL-6 and its roles in uveitis

IL-6 is an established innate cytokine and a principal mediator of autoinflammatory disease which includes uveitis. IL-6 family cytokines include cardiotrophin-1 (CT-1), ciliary neurotrophic factor (CNTF), leukaemia inhibitory factor (LIF), oncostatin M (OSM), osteopontin (OPN), IL-11 and IL-31 (251, 256).

In EAU, IL-6 deficient animals have a significantly attenuated disease phenotype and treatment with intravitreal anti- IL-6 reduces inflammation (251, 256). Elevated IL-6 levels in humans have been detected in the aqueous humor, similarly to the mouse model intravitreal anti-IL-6 is capable of reducing inflammation (251).

7.1.2 Interleukin 6 and Interleukin 12 family of cytokines

Interleukin 6 (IL-6)

Type-I cytokines include IL-6 and IL-12 families that are both made up of proteins related structurally due to the presence of four-helix proteins. Members of the IL-6 family of cytokines are secreted in the form of single-subunit monomers (257). The dimeric IL-12 family α subunits, including p19, p28 and p35 pair with potential β subunits for example p40 and

EBI3. The α subunits are structurally homologous to IL-6 cytokines while the β subunits can be compared structurally to membrane-bound receptors of IL-6 cytokines (257).

The IL-6 cytokine family comprises of a number of cytokines including IL-6 and IL-11, these cytokines have been implicated to play important roles in autoimmunity, cancer, chronic inflammation and infectious diseases (258). The defining characteristic of this family of cytokines is many of the cytokines share the common cytokine receptor subunits. Further to this, phylogenetic analysis suggests a close relationship between the IL-6 and IL-12 cytokine families (257, 258).

Interleukin 12 (IL-12)

IL-12 was first purified in 1989, it was discovered to have the unique molecular structure of a covalently linked heterodimer composed of p40 and p35 (259, 260). The sequence of p35 is homologous to that of IL-6 and G-CSF comprised of a four-α- helix structure that is typically seen in cytokines (260). The sequence of the p40 chain is structurally similar to the IL-6 receptor-α chain and ciliary neurotrophic factor receptor which are both members of the hemopoietin family. The similarities found in these chains are present in the extracellular portion of specific members of the hemopoietin family (260). The extracellular portion of the receptor α chain of the IL-6 family is capable of being secreted as a soluble molecule to form complexes with cytokines, these complexes can bind to transmembrane chains of the receptor complex to induce signal transduction. The membrane receptor complex of IL-12 is composed of two chains IL-12Rβ1 and Il-12Rβ2 that are both homologous to gp130, IL12Rβ1 binds to IL-12p40 and is associated with Tyk2, whereas IL-12Rβ2 recognises the heterodimer or the p35 chain and is associated with Jak2 (260). The production of IL-12 is mostly found by activated innate cells such as neutrophils and dendritic cells and adaptive immune cells including macrophages and monocytes. The production of IL-12 by these activated cell types is capable of inducing IFN- γ production in populations of T cells including Th1 cells and NK cells (260). Most biological responses to IL-12 are mediated by STAT4 but signalling through the IL-12 receptor complex also includes a number of STAT transcription factors such as: STAT1, STAT3 and STAT5 inducing nuclear translocation, phosphorylation and dimerisation in these transcription factors (260).

IL-12 was originally thought to be the only heterodimeric cytokine, however IL-23, IL-27 and IL-35 have been determined to have a similar structure to form part of the family of

heterodimeric cytokines (260). IL-23 and IL-27 affect the production of IFN-γ by T and NK cells, and in the case of IL-23 share part of the IL-12 receptor complex (figure 7.1)

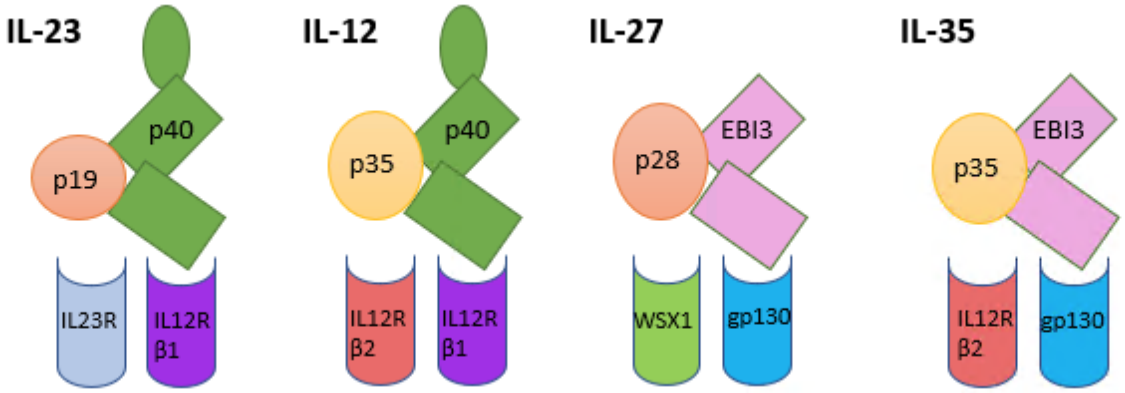

Figure 7.1: IL-12 family of cytokines and their receptors. Architecture of the IL-12 family of cytokines and their receptors. Figure adapted from Vignali et al (2012) (261).

7.1.4 Role of interleukin 27 (IL-27) and Interleukin 27 Receptor (IL-27R) in vivo

IL-27 is a heterodimeric cytokine made up of EBI3 and IL-27p28. Receptors of class I cytokines are made up of α and β heterodimers. The α subunit being a primary cytokine in the case of IL-27 receptor (IL-27R) this is the IL-27Rα (also known as WSX-1 or TCCR) and a β subunit that is used for high affinity binding and signal transduction which in the case of IL27R is gp130 (39).

WSX-1 consists of 2 tyrosine residues that can be phosphorylated in humans whereas in mice there are 3 tyrosine residues including one residue that is conserved (39). WSX-1 contains a Trp-Gly-Glu-Trp-Ser (WGEWS) fitting with other proteins from the same family (WSXWS motif) (262). IL-27Rα is expressed highly in spleen, thymus, and lymph nodes, specifically in the CD4+ T cell compartment.

The IL-6 receptor family of cytokines shares the gp130 subunit with several other receptor partners (39), IL-27Rα is capable of forming homodimers that are capable of activating the JAK-STAT pathway that is associated with myeloid cell transformation but gp130 is considered to be the main partner of the IL-27Rα (40, 263). In memory B cells IL-27 mainly signals through STAT1 in humans whereas activated T cells signal mainly through STAT3 (39, 264).

Upon activation of CD4+ T cells increased surface expression of Il-27Rα has been observed this is significantly different to naïve T cells where minimal expression is present (40).

Studies have illustrated both naïve and activated CD8+ T cells are responsive to IL-27, however downregulation of gp130 expression render memory CD8+ T cells non-responsive to IL-27 and therefore do not produce an IL-10 response(265). A study by Perona-Wright et al (265), showed mice lacking in IL-10 down regulated the cytokine receptor gp130 due to the persistent loss of IL-27 responsiveness in memory CD8+ T cells. Impaired IL-27 responsiveness on human memory CD8+ T cells has shown the same effects as the mouse models (265).

In order to study the effect of IL-27Rα in vivo, IL-27Rα knockout mice were generated.

A study by Wang et al (266) have shown when administered in recombinant heterodimer form to mice with EAU it was able to inhibit cellular infiltrate including Th1 and Th17 responses and stimulated an expansion in the Treg population to decrease disease (40, 266). Dominant cellular sources of IL-27 include myeloid cell populations such as; macrophages, inflammatory monocytes, microglia and dendritic cells but it has also been observed to be expressed by plasma cells, endothelial cells and epithelial cells (40). Specifically, within the eye, IL-27 is produced by the microglia, retinal ganglion cells and throughout the neuroretina especially during peak EAU (267).

In a study by Chihara et al (268), the co-inhibitory receptor protein C receptor and podoplanin were functionally validated and are co-expressed in both CD4+ and CD8+ T cells, that forms part of a larger programme that is driven by IL-27 of a co-inhibitory nature shared by non-responsive T cells in many physiological contexts(268), illustrating the role of IL-27 as an immunoregulatory cytokine.

The immunoregulatory properties of IL-27 centre around the idea of its ability to induce T cells to perform functions necessary for suppressing ongoing inflammation (40). Il-27 promotes Th1-type immune responses while inhibiting Th17 responses, inducing Il-10 expression and the promotion of a Treg specific population specialised to limit the Th1 response. Further to this IL-27 is also capable of limiting IL-2 production while increasing IFN-γ production during an immune response (40).

7.1.5 IL-27Rα$^{-/-}$/ WSX-1$^{-/-}$ mice

IL27Rα$^{-/-}$ mice were generated in 2001 by Yoshida et al. (262). The mice were produced by homologous recombination and have been used in studies to define the role of IL-27Rα$^{-/-}$ in vivo (262).

Development of hematopoietic and lymphoid systems in the mice appeared normal but isolated T cells from the knockout animals produced reduced levels of IFN-γ when treated in vitro with IL-12 and concanavalin A (ConA) or anti-CD3 antibody (262). When fully differentiated, if cells from IL-27Rα$^{-/-}$ are subjected to a secondary stimulation they produce similar levels of IFN-γ to wild type mice (262).

Studies in arthritis using this mouse model in the experimental model adjuvant induced arthritis (AIA) have illustrated that IL-27Rα$^{-/-}$ mice displayed a more severe inflammatory arthritis indicated by increased leukocyte infiltration, synovial exudate, hypertrophy and hallmarks of cartilage and bone erosion (269).

Along with a more severe inflammatory arthritis, IL27Rα$^{-/-}$ mice with AIA showed heightened synovial T cell infiltration and the presence of discrete CD3+ aggregates (ectopic lymphoid structures (ELS)) within the synovium (269). In this study by Jones et al (269), at day 3 after AIA induction a small portion of the IL-27Rα$^{-/-}$ mice presented with small CD3+ aggregates but by day 10 all IL-27Rα$^{-/-}$ mice had developed multiple CD3+ aggregates throughout the synovium, in contrast wildtype mice developed fewer lymphoid aggregates and a less severe infiltrate in the synovium (269).

These studies have suggested a role for IL-27 in regulating autoimmune disease, further studies in the EAE model using the IL-27Rα$^{-/-}$ mouse gave severe neuroinflammation and a more severe Th17 response (270). Further studies support this hypothesis when autoimmune disease is treated with IL-27, limited immunopathology associated with a Th17 response is present. This occurs in models of uveitis including EAU, collagen induced arthritis (CIA),EAE and colitis (270).

IL-27Rα$^{-/-}$ mice are a useful tool to study interactions and properties of IL-27 receptor in vivo, and the role of IL-27 in disease processes in autoimmune models such as models of arthritis (AIA) and uveitis (EAU).

7.1.6 Anti-inflammatory properties of IL-27

A role for IL-27 in the promotion of Th1-type immunity has been suggested in early studies of the cytokine but further studies have instead highlighted a function for IL-27 in limiting immune hyperactivity (40). One report that illustrated this was using IL27Rα$^{-/-}$ mice that were infected by *Toxoplasma gondii.* Parasite replication was efficiently controlled but was not

capable of downregulating the response of CD8+ and CD4+ T cells induced by infection and instead the mice developed increased levels of IFN-γ and a lethal CD4+ T cell mediated immune pathology (40, 271). Similarly, in a model of Trypanosoma *cruzi* infection IL27Rα$^{-/-}$ mice had exacerbated IFN-γ production and lethal inflammatory disease (40, 272).

7.1.7 Pro-inflammatory properties of IL-27

IL-27 is considered a growth and survival factor for T cells that has a positive affect on many aspects of T cell function (40, 273). Upregulation of expression of lymphocyte function-associate antigen-1, ICAM-1 and sphingosine-1-phosphate has been linked to IL-27 but inhibition of CCR5 expression has also been observed, this illustrates a need for further study of IL-27 on trafficking and behaviour of lymphocyte populations (40).

Using IL-27Rα$^{-/-}$ mice this chapter aims to compare disease course assessed using OCT and total retinal infiltrate in groups of animals that have received either wildtype pathogenic cell transfer or IL-27Rα$^{-/-}$ pathogenic cell transfer. The fate of transferred IL27Rα$^{-/-}$ and wildtype cells will be analysed using allelic markers. The adoptive transfer model was used as a way of specifically studying the effect of the knockout phenotype on T cells in an environment where there is normal IL27Rα regulation in the tissue.

7.2 Materials and Methods

7.2.1 Adoptive transfer technique

EAU was induced in C57BL/6 or IL-27Rα$^{-/-}$ CD45.2 donors using RBP3 peptide, donor cells were then transferred using i.p injection into C57BL/6 CD45.1 recipients at variable cell concentrations to determine the optimum number of cells needed to induce a disease.

7.2.2 Flow cytometry analysis

Flow cytometry was used to identify subsets of cells within the endogenous and transferred cell population present in the retinal infiltrate using extracellular and intracellular staining. Within transferred recipients, allelic markers CD45.1 and CD45.2 were used to identify endogenous and transferred populations of cells within the retina.

7.2.3 Clinical imaging

OCT scans and fundus images standardised across recipients during transfer optimisation were taken weekly for both groups to study disease course.

7.2.4 Immunohistochemistry

Eyes were frozen in OCT and kept at -80°C before being sectioned at ~20 microns. Sections were then stained for CD3, CD4 and CD8 or CD3, CD4 and CD19 to identify leukocyte infiltrate.

7.2.5 Fluorescence Microscopy

Whole retina mounts were isolated and fixed for analysis by light sheet fluorescence microscopy or confocal microscopy. Retinas were stained using CD3, CD4 and CD8 antibodies.

7.3 Results

7.3.1 Flow cytometric analysis of naïve mice

As previously discussed in *chapter 4* naïve baseline quantification of leukocytes in unmanipulated mice is a useful tool in understanding leukocyte presence in the eye before induction of EAU.

IL27Rα$^{-/-}$ mice do not display major defects in mounting a Th1 response, but in a limited number of scenarios the Th1 response is delayed in these animals (274). These mice have exacerbated inflammation in response to a wide variety of immune challenges, including pathogens that cause a Th1 and Th2 response in models of inflammation that rely on Th2 and Th17 activity (274). Several mechanisms have been suggested to be linked to the role of IL-27 in immunomodulatory activities including; IL-27 is known to antagonise Th17 development (275), induce IL-10 production (276) and suppress IL-6-induced T cell proliferation under inflammatory conditions (275).

To determine at baseline if there are any changes within leukocyte recruitment to the eyes of IL27Rα$^{-/-}$ mice, leukocyte infiltration was quantified in naïve IL27Rα$^{-/-}$ mice. This data was then compared to the C57BL/6 naïve leukocyte data previously presented in *chapter 4* figure 4.1.

The CD4+ T cells present within the naïve eyes of both the C57BL/6 and Il27Rα$^{-/-}$ mice are similar in number (figure 7.2a). However, there is a statistically significant increase in CD8+ T cell number and CD11b+ cell number present within the eye in the Il27Rα$^{-/-}$ mice in a naïve state in comparison to the naïve C57BL/6 group (figure 7.2b and 7.2c). No effect is seen between the two groups when looking at Ly6G+ cell number and Ly6C+ cell number (figure 7.2d and 7.2e).

C57BL/6

IL27RKO

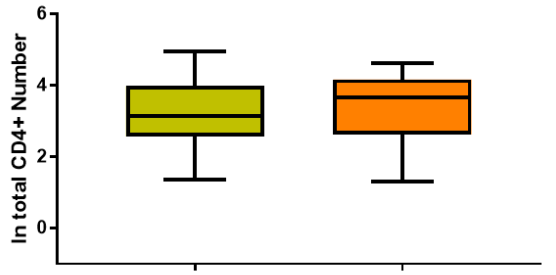

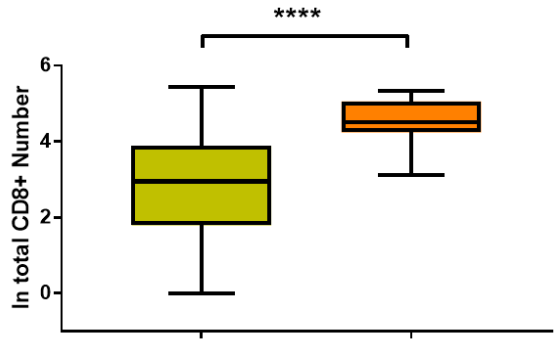

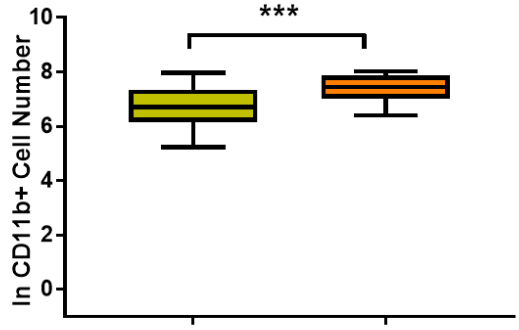

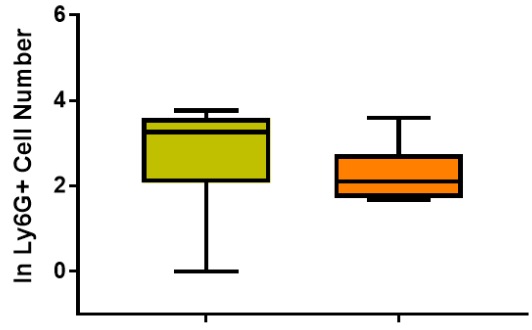

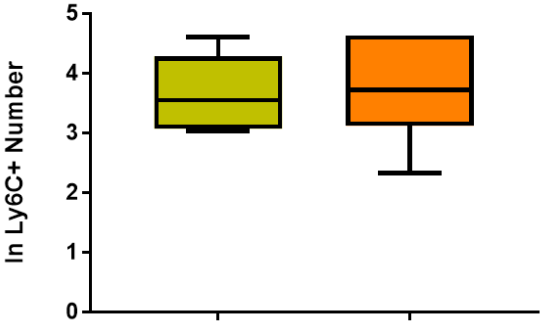

IL-27RA$^{-/-}$	LOWER LIMIT	UPPER LIMIT	MEAN
CD4	3	102	41
CD8	22	204	106
CD11B	598	3028	1786
LY6G	4	35	12
LY6C	9	103	55

Figure 7.2: Quantified leukocyte cell number in naïve eyes of unmanipulated C57BL/6 or C57BL/6 IL-27Rα$^{-/-}$ mice. Using a standard curve acquired by flow cytometry leukocytes present within the eyes of naïve mice were quantified. CD4+ T cell number within the two groups is comparable (A). A statistically significant difference is observed between the two groups in the CD8+ and CD11b+ cell compartment (B+C). The final leukocyte populations quantified, Ly6C+ and Ly6G+ cell number in the two groups are also similar (D+E). Numbers expressed as Mean ±SEM. Unpaired non-parametric Mann-Whitney Test ***p<0.001, ****p<0.0001.

7.3.2 Analysis of adoptive transfer donor C57BL/6 eyes vs C57BL/6 IL-27Rα$^{-/-}$ eyes at day 11 after active immunisation.

In order to perform the adoptive transfer of uveitogenic leukocytes into naïve recipients, donors are immunised using RBP3 peptide emulsified in CFA administered subcutaneously with a concurrent intraperitoneal injection of pertussis toxin. After 11 days, spleen and lymph nodes were isolated for cell culture to produce leukocytes for adoptive transfer.

To quantify disease severity of the donors at cell harvest, donor eyes were analysed across a number of experiments to quantify total leukocyte populations present within the eye at day 11 after immunisation and intracellular cytokine staining in the two groups immunised (C57BL/6 mice and the C57BL/6 IL-27Rα$^{-/-}$ mice).

Eyes from donor mice 11 days after immunisation were analysed by extracellular staining to isolate the CD4+ T cell population then further analysed based on cytokine secretion within the isolated CD4+ T cell population (figure 7.3). Overall in the Il-27Rα$^{-/-}$ immunised donors have an increase in cytokine production in comparison to the C57BL/6 immunised donors and a statistically significant increase in IFN-γ secretion within the Il-27Rα$^{-/-}$ is also observed (figure 7.3). The increase in IFN-γ production is accompanied by an increased percentage of IFN-γ in the eyes of the donors (presented underneath) an increased overall percentage of IL-17 production is also observed in the IL-27Rα$^{-/-}$ donor mice.

CD4+, CD8+ and CD11b+ cells were quantified to determine disease stage in both groups of immunised animals (figure 7.4). Overall, there is a statistically significant increase in the number of leukocytes present within the eyes of the IL-27Rα$^{-/-}$ in comparison to the C57BL/6 control group. Specifically, a statistically significant increase in CD4+, CD8+ and CD11b+ cell number is observed in the IL-27Rα$^{-/-}$ mice in comparison to wildtype, suggesting a more severe clinical disease is present within the eyes of the IL-27Rα$^{-/-}$ mice.

C57BL/6

IL27RKO

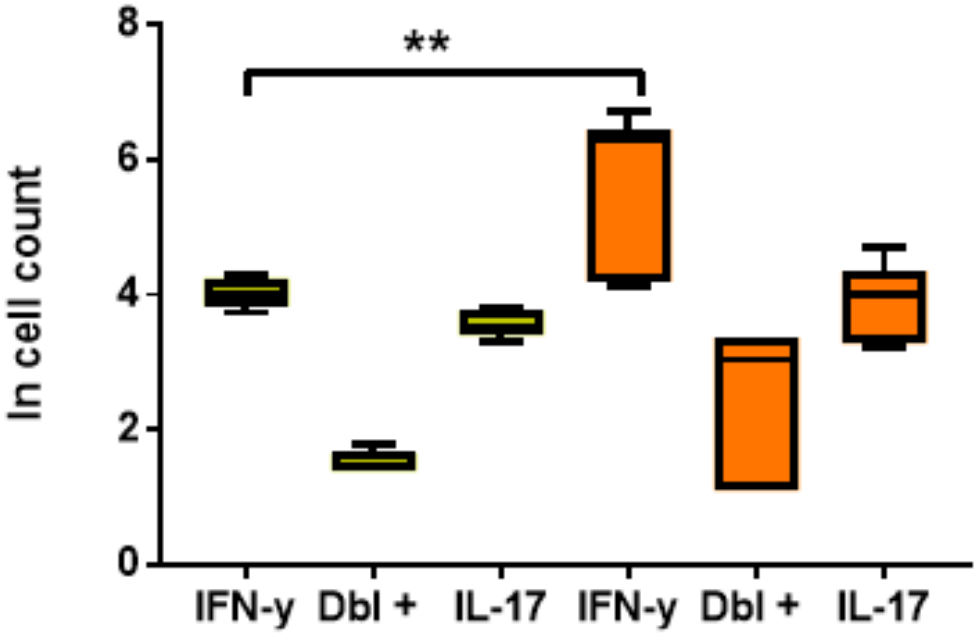

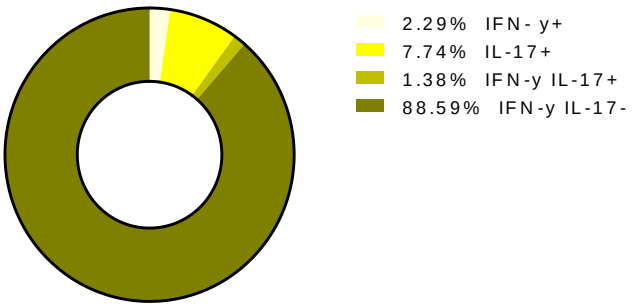

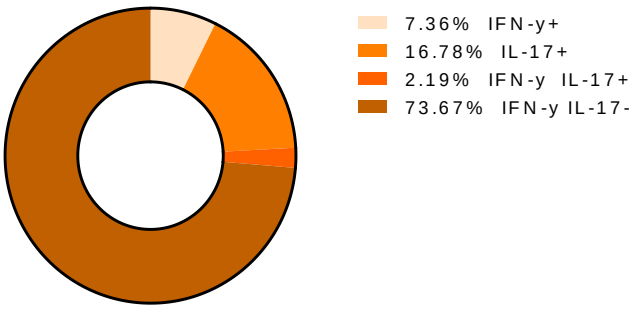

Figure 7.3: Intracellular staining of CD4+ T cells to detect cytokines expressed at day 11 after immunisation. Extracellular staining was performed on retinal and vitreous infiltrate, gating through CD4+ cells to analyse cytokine production in this compartment. IFN-γ, IL-17 and double positive expression was analysed in both sets of eyes from the donor groups. Numbers expressed as Mean ±SEM. One-Way ANOVA multiple comparisons **p<0.01.

C57BL/6

IL27RKO

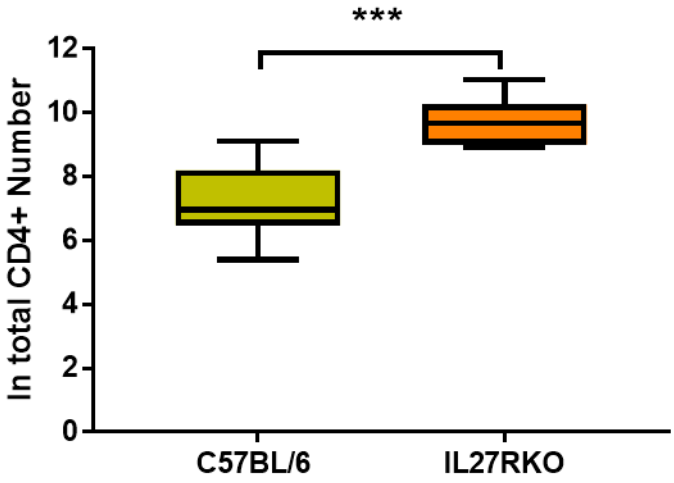

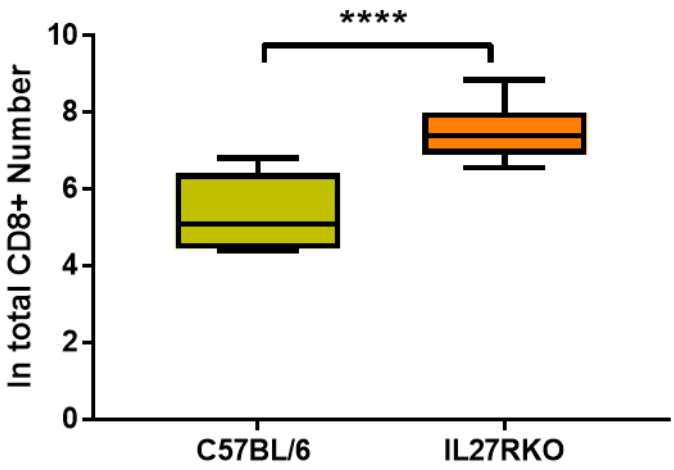

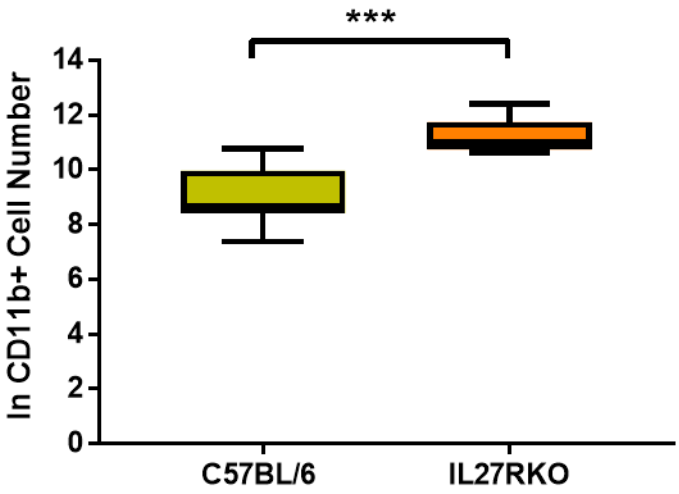

C57BL/6	LOWER LIMIT	UPPER LIMIT	MEAN
CD4	219	9096	2542
CD8	79	910	327
CD11B	1586	47396	13821

IL-27RA$^{-/-}$	LOWER LIMIT	UPPER LIMIT	MEAN
CD4	7434	62711	21655
CD8	703	6955	2321
CD11B	41414	242324	91789

Figure 7.4: Quantified leukocyte numbers present within the eyes of the donor mice at day 11. At day 11, 8-10 eyes were analysed from both donor groups and leukocytes quantified. CD4+ T cell number was quantified and compared across the two donor groups (A). CD8+ T cell number was quantified and compared across the two donor groups (B). CD11b+ cell number quantified and compared across the two donor groups (C). Numbers expressed as Mean $\pm$SEM. Unpaired non-parametric Mann-Whitney Test ***p<0.001, ****p<0.0001.

7.3.3 Clinical disease onset in IL-27Rα$^{-/-}$ mice

Because the clinical disease within the immunised IL-27Rα$^{-/-}$ adoptive transfer donors was more severe when analysed by leukocyte quantification in comparison to the control C57BL/6 donor this suggested that disease induction in the IL-27Rα$^{-/-}$ mice has an earlier onset when compared to other C57BL/6 mice. This contrasts with EAE studies which reported that the induction of disease in IL-27Rα$^{-/-}$ mice is not accelerated.

To characterise the initiation of clinical disease in IL-27Rα$^{-/-}$ mice, IL-27Rα$^{-/-}$ were immunised and analysed by clinical imaging and flow cytometry at day 7 after immunisation.

A statistically significant increase in leukocyte number is observed by day 7 in the eyes of the IL-27Rα$^{-/-}$ mice. When quantified, CD4+ T cell number is significantly increased in the IL-27Rα$^{-/-}$ mice after immunisation in comparison to the baseline obtained from mice of the same phenotype (figure 7.5a).

The same affect is observed within the CD8+ compartment, where a significant increase is observed in comparison to a naïve baseline (figure 7.5b), similarly in CD11b+, Ly6G+ and Ly6C+ cell number is also increased (figure 7.5c, 7.5d and 7.5e).

The statistically significant increase shows that initiation of clinical disease occurs earlier within the IL-27Rα$^{-/-}$ animals and early clinical disease is seen by day 7 after active immunisation.

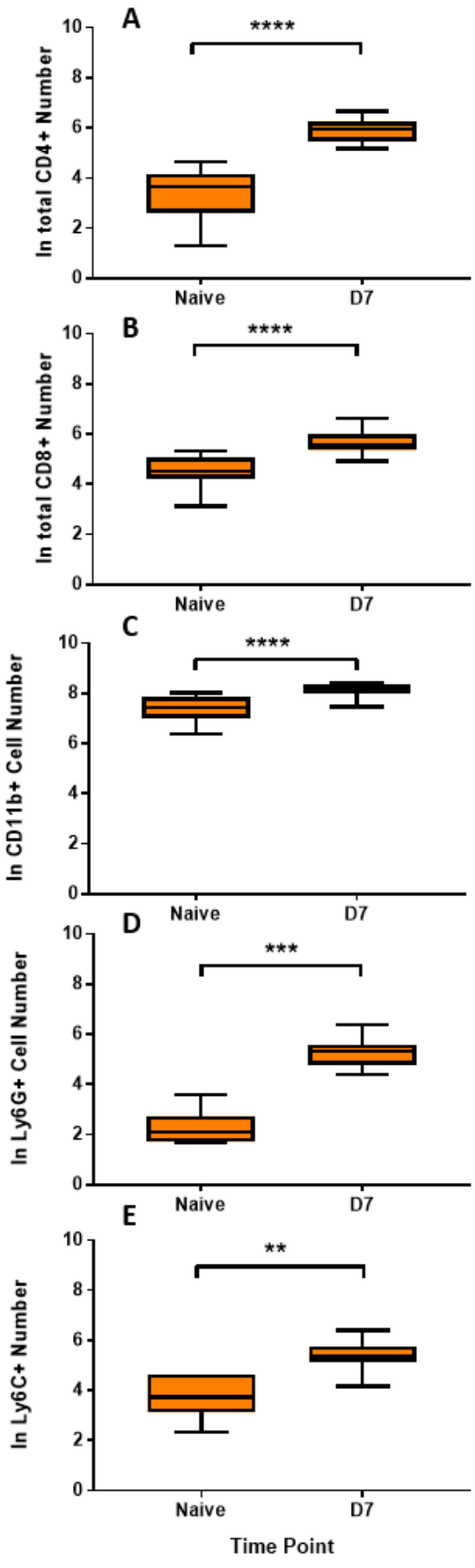
A
****
ln total CD4+ Number
10
8
6
4
2
0
Naive
D7
B
****
ln total CD8+ Number
10
8
6
4
2
0
Naive
D7
C
****
ln CD11b+ Cell Number
10
8
6
4
2
0
Naive
D7
D
***
ln Ly6G+ Cell Number
10
8
6
4
2
0
Naive
D7
E
**
ln Ly6C+ Number
10
8
6
4
2
0
Naive
D7
Time Point

IL-27RA$^{-/-}$	LOWER LIMIT	UPPER LIMIT	MEAN
CD4	176	534	400
CD8	135	745	320
CD11B	1725	4574	3445
LY6G	78	581	226
LY6C	64	611	256

Figure 7.5: Early onset of EAU in actively immunised IL-27Rα$^{-/-}$ mice. To further analyse onset of clinical disease in IL-27Rα$^{-/-}$ mice, active immunisation was performed. 8 eyes were analysed by flow cytometry at day 7. Overall leukocyte recruitment appeared to be increased in comparison to baseline (day 0). (A-E) Quantified leukocyte cell number at day 0 and at day 7 after active immunisation. Numbers expressed as Mean ±SEM. Unpaired non-parametric Mann-Whitney Test **p<0.01, ***p<0.001, ****p<0.0001.

7.3.4 Analysis of donor supernatant and donor cells before adoptive transfer

Due to the early onset of clinical disease in IL-27Rα$^{-/-}$ and statistically significant differences between leukocyte recruitment in the donor IL-27Rα$^{-/-}$ mice in comparison to the C57BL/6 control group, analysis of the leukocyte population used for adoptive transfer was carried out using a Legendplex assay.

At day 11 after active immunisation, spleen and lymph nodes were processed for cell culture to prepare for adoptive transfer into naïve recipients. At this time point, eyes were also obtained from the donors and analysed by flow cytometry (figure 7.3 and figure 7.4). The differences in leukocyte infiltration suggested differences in clinical disease course.

To determine the cytokine secretion of the whole culture supernatants, supernatant was taken at the end of the 72-hour cell culture before transfer. Cytokine secretion was then measured using a LegendPlex assay to determine differences between the two cultures. Overall, the IL-27Rα$^{-/-}$ culture was determined to be secreting increased levels of cytokines. Specifically, a statistically significant increase in IL-1α, IFN-γ, TNF-α, MCP-1, IL-10, IL-6, IL-17A and GM-CSF (figure 7.6b, 7,6c, 7.6d, 7.6e, 7.6h, 7.6i, 7.6k, 7.6m) is observed in the IL-27Rα$^{-/-}$ cultures suggesting a more potent cell phenotype present within the cell cultures denoted by increased cytokine expression per cells and in the fraction of cells present within the culture expressing cytokine. Although a statistically significant increase in specific cytokines quantified within the IL-27Rα$^{-/-}$ cultures in comparison to the control C57BL/6 cultures, other cytokines analysed including: IL-23, IL-12p70, IL-1β, IL-27 and IFN-β (figure 7.6a, 7.6f, 7.6g, 7.6j and 7.6l) although not statistically significant has a general effect of increased cytokine secretion within the IL-27Rα$^{-/-}$ cultures raising the possibility that a more pathogenic type of cell is present within the culture.

Another observation made about the difference in the IL-27Rα$^{-/-}$ cultures in comparison to the C57BL/6 culture is the difference in total cell number yield from the cultures. Comparable numbers of mice were originally immunised to create the same number of flasks at the same cell density at 0 hours of cell culture. After leukocytes were isolated using Ficoll density centrifugation at 72 hours of cell culture a large difference in leukocyte number obtained from the two cell cultures is observed. The IL-27Rα$^{-/-}$ cultures yield more than double the cell number of the C57BL/6 cultures.

For cell transfer we used equivalent numbers of CD4+ T cells , so it was important when analysing the transferred leukocyte population to determine the percentage of a number of leukocyte populations present within the transferred populations including; CD4+ T cells, CD8+ T cells, CD11b+ cells and other leukocytes (figure 7.7). Despite the overall increase in cell numbers, the transferred CD4+ T cell population isolated from each cell culture is comparable in percentage in both C57BL/6 and IL-27Rα$^{-/-}$ leukocyte populations (figure 7.7). The same is also seen within the CD8+ and CD11b+ cell compartment (figure 7.7). Thus suggesting that although the leukocytes present within the IL-27Rα$^{-/-}$ cultures expand more than the C57BL/6 control, the total percentage of CD4+ T cells present within each culture is comparable so there is no difference at disease induction in CD4+ T cell number transferred.

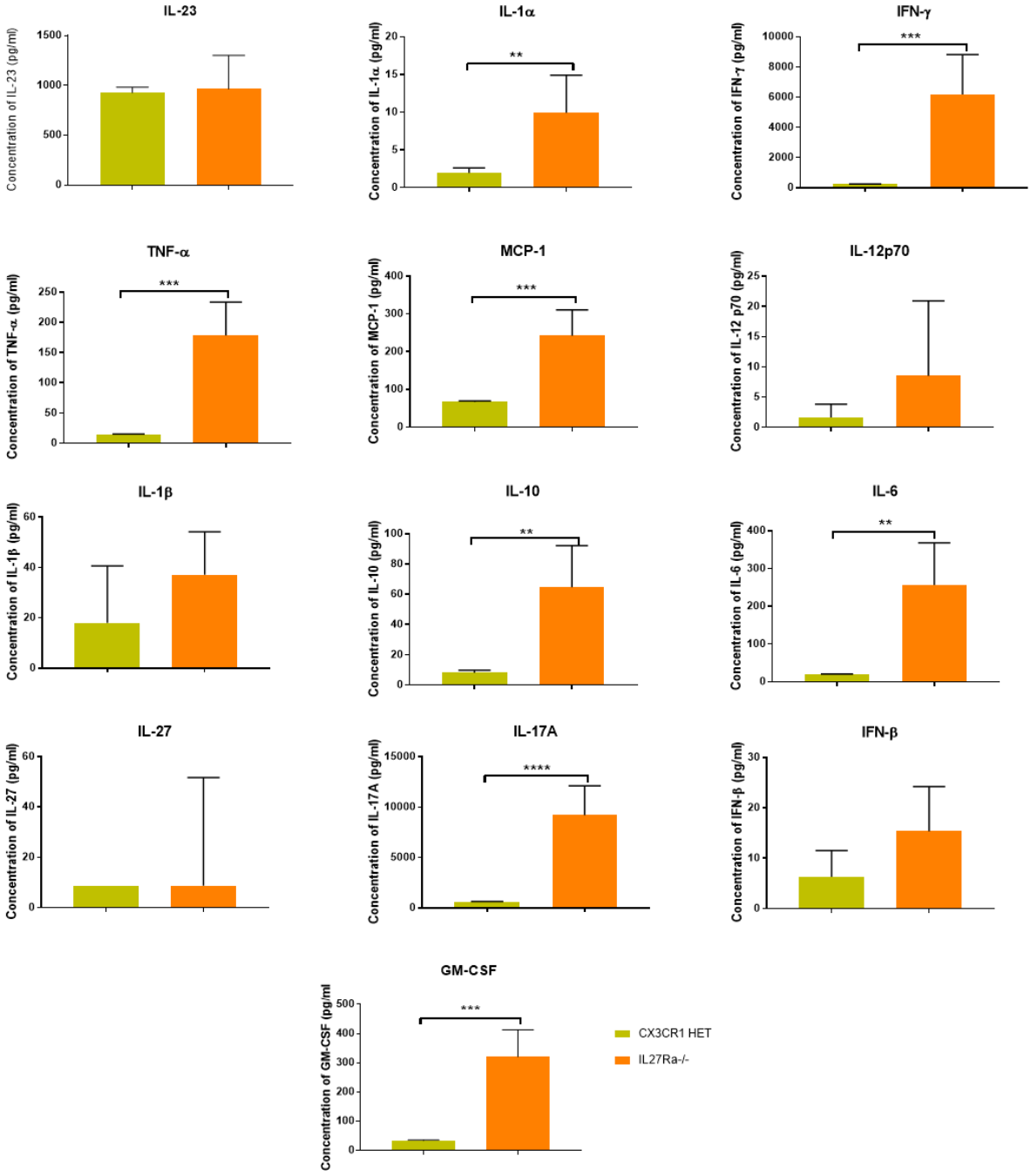
IL-23
Concentration of IL-23 (pg/ml)
1500
1000
500
0
IL-1α
Concentration of IL-1α (pg/ml)
20
15
10
5
0
**
IFN-γ
Concentration of IFN-γ (pg/ml)
10000
8000
6000
4000
2000
0
***
TNF-α
Concentration of TNF-α (pg/ml)
250
200
150
100
50
0
***
MCP-1
Concentration of MCP-1 (pg/ml)
400
300
200
100
0
***
IL-12p70
Concentration of IL-12 p70 (pg/ml)
25
20
15
10
5
0
IL-1β
Concentration of IL-1β (pg/ml)
60
40
20
0
IL-10
Concentration of IL-10 (pg/ml)
100
80
60
40
20
0
**
IL-6
Concentration of IL-6 (pg/ml)
400
300
200
100
0
**
IL-27
Concentration of IL-27 (pg/ml)
60
40
20
0
IL-17A
Concentration of IL-17A (pg/ml)
15000
10000
5000
0
****
IFN-β
Concentration of IFN-β (pg/ml)
30
20
10
0
GM-CSF
Concentration of GM-CSF (pg/ml
500
400
300
200
100
0
***
CX3CR1 HET
IL27Ra-/-

Figure 7.6: Analysis of supernatant obtained from cultures of C57BL/6 leukocytes or IL-27Rα$^{-/-}$ leukocytes. To analyse cytokine secretion within both cultures a sample of supernatant was obtained from each culture and analysed using LegendPlex analysis. Overall, increased levels of cytokines are observed with the analysed IL-27Rα$^{-/-}$ culture in comparison to the C57BL/6 cultures. (A-L) Cytokine expression within the supernatant of the C57BL/6 culture in comparison to the IL-27Rα$^{-/-}$. Numbers expressed as Mean ±SEM. One-Way ANOVA multiple comparisons **p<0.01, ***p<0.001, ****p<0.0001.

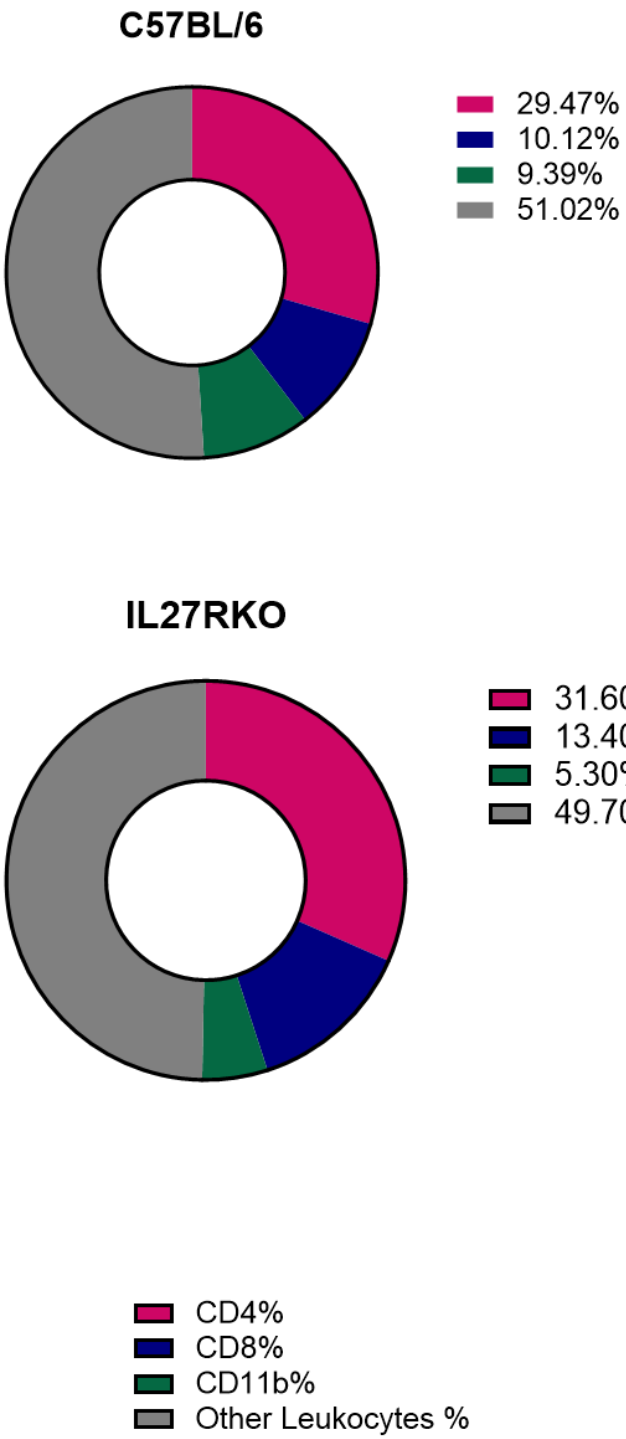
C57BL/6
29.47%
10.12%
9.39%
51.02%
IL27RKO
31.60%
13.40%
5.30%
49.70%
CD4%
CD8%
CD11b%
Other Leukocytes %

Figure 7.7: Flow cytometric analysis of transferred leukocyte populations from C57BL/6 cultures and IL-27Rα$^{-/-}$ cultures. After leukocytes were isolated for adoptive transfer a sample was analysed by flow cytometry to determine the percentage of CD4+ T cells, CD8+ T cells and CD11b+ cells transferred into the naïve recipients by extracellular staining. Data expressed as Mean percentage. 3-10 samples per donor group.

7.3.5 OCT imaging throughout clinical disease in the C57BL/6 and IL-27Rα$^{-/-}$ adoptive transfer recipients

At day 7 both groups of recipients have peak disease, but differences are observed in the severity of the peak disease in each group of recipients that received either the C57BL/6 leukocyte transfer or the IL-27Rα$^{-/-}$ leukocyte transfer. The disease within the recipients that received C57BL/6 cells (figure 7.8c) is severe with obvious retinal and optic disc swelling within the OCT image coinciding with the large cell numbers present in the vitreous stopping a clear signal within the OCT image. Within the fundal image cellular infiltrate causes a reflection of light also causing the image to be blurry.

However, in the IL-27Rα$^{-/-}$ recipients the disease is so severe that an OCT image cannot be obtained due to the severity of the disease present (figure 7.8d). Due to the severity of the cellular infiltrate the OCT cannot give a clean image of the optic disc, retina or vitreous including the infiltrate. This is supported by the fundus image which due to the severity of the cellular infiltrate the image is unclear, and the optic disc or blood vessels are no longer obviously present (as seen in figure 7.8a and 7.8b).

By day 13, disease is resolving and is less severe in comparison to the disease present at day 7 but is still active and of a severe phenotype. At this time point the OCT images are comparable between the two recipient groups (figure 7.8e and 7.8f), although the thickness of the retina has reduced in both groups, the optic disc is still swollen and severe vitreal infiltrate is present. When looking at the fundus image there is obvious differences between the two groups. In the C57BL/6 recipients the vitreal haze is not obscuring the optic disc and blood vessels, whereas, within the IL-27Rα$^{-/-}$ transfer recipients the fundus remains full of leukocyte infiltrate and the vessels and optic disc are not clear due to the presence of this infiltrate within the vitreous.

At day 28, active disease has mostly resolved within the C57BL/6 recipients (figure 7.8g) with minimal cellular infiltrate present within the vitreous in the OCT image, the retina and optic disc has thinned and is now thinner than the OCT images taken at baseline day 0 (figure 7.8a). The fundus image is much clearer due to reduced infiltrate present within the vitreous. In the IL-27Rα$^{-/-}$ transfer recipients the OCT image shows continued active disease including severe infiltrate present within the vitreous. However, the retina appears to have thinned and swelling of the optic disc has resolved (figure 7.8h).

Based on the resolution of active clinical disease in the C57BL/6 recipients the OCT disease course has been split into two stages the early disease highlighted in figure 7.8 and the later stages of disease observed in figure 7.9.

At day 40, the disease remains inactive in the C57BL/6 recipients (figure 7.9a). In the OCT image, there is a lack of infiltrate present within the vitreous, the retina remains thin but the optic disc has returned to its original thickness observed at baseline. In the fundus image the vitreal haze has completely resolved and the retina, blood vessels and optic disc are now seen clearly within the image. In the IL-27Rα$^{-/-}$ recipients, the OCT image shows that active disease has persisted to this time point, vitreal infiltrate remains present within the eyes of the recipients. Although the retina remains thinned, the optic disc appears slightly swollen (figure 7.9b). The fundus image is still blurry due to the vitreal infiltrate, the retina and vessels are visible but not defined and the optic disc remains swollen with infiltrate.

By day 51, the disease continues to be quiescent and not active within the C57BL/6 recipients, a small amount of infiltrate is observed within the OCT image but not enough to suggest any active disease (figure 7.9c). The retina remains thinned due to scarring from disease severity and has not returned to a baseline state and the optic disc has remained similar to baseline state that was observed at previous time points. In the IL-27Rα$^{-/-}$ recipients active disease persists to this time point (figure 7.9d). The infiltrate present within the vitreous has further persisted to this stage in disease, the retina remains thinned, but the optic disc is swollen due to the infiltrate.

At day 67, eyes were analysed by flow cytometry to quantify leukocyte infiltrate present within the eyes of both groups of recipients. Before the eyes were analysed, they were imaged using OCT at this time point to deduce disease severity in the two groups before flow cytometric analysis.

The C57BL/6 group continues to be quiescent in the recipients by studying the OCT image (figure 7.9e). The number of leukocytes present within the vitreous is minimal, the retina remained thinned and the optic disc consistent with the baseline OCT image. The fundus image shows some retinal scarring, but the image is clear, and the optic disc and blood vessels are clearly present within the image. The IL-27Rα$^{-/-}$ recipients as seen in previous time points still has persistent active disease that has shown no signs of resolution throughout the entire disease course. There is obvious swelling of the optic disc and infiltrate present within the

vitreous (figure 7.9f). In the fundus image, the fundus remains blurry due to the cells present within the vitreous, because of this the blood vessels and the optic disc remain out of focus.

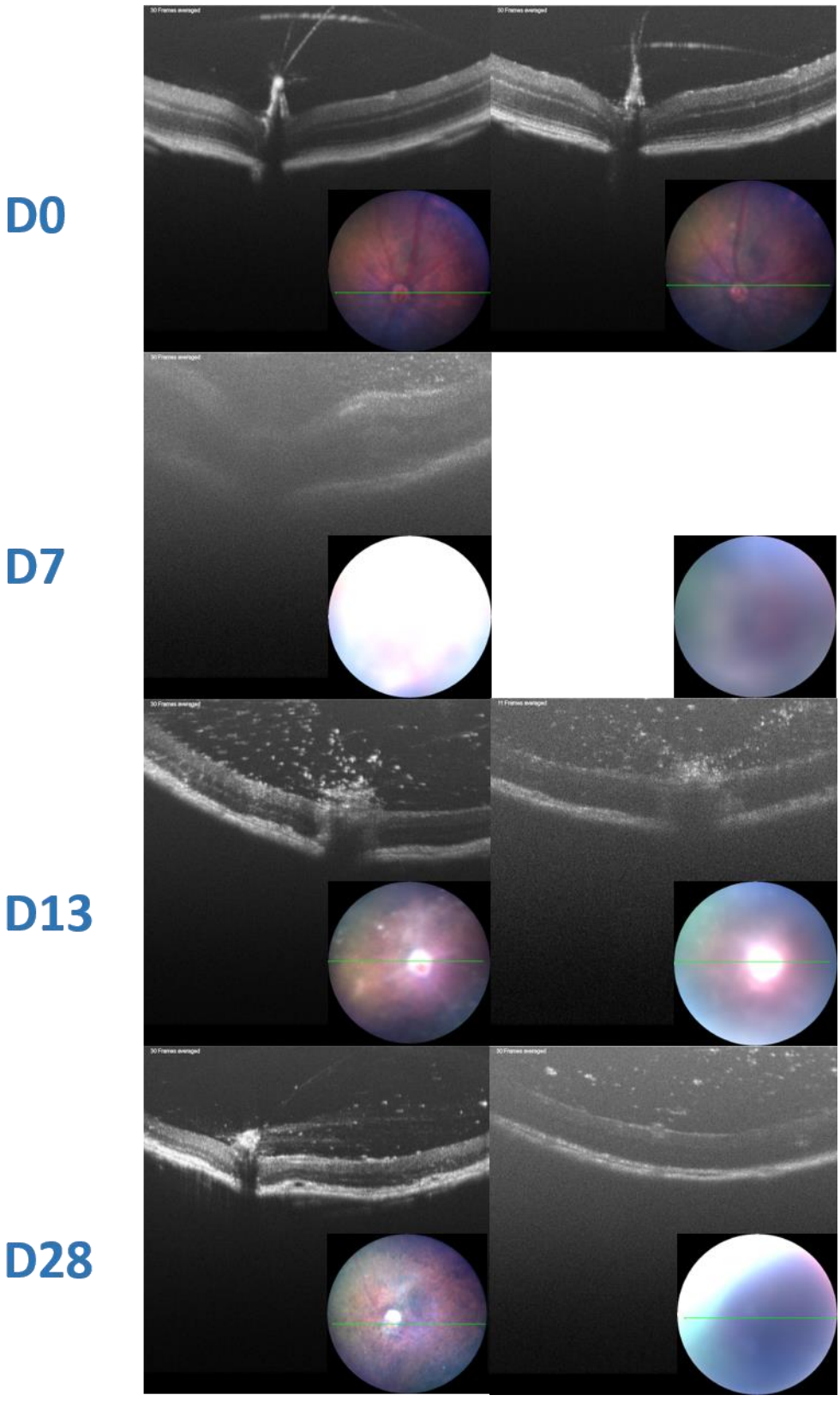
C57BL/6
IL27RKO
D0
D7
D13
D28

Figure 7.8: OCT time course of early clinical disease in C57BL/6 transfer recipients and IL-27Rα$^{-/-}$ transfer recipients. OCT and fundus imaging from baseline through to day 28 to monitor early clinical disease in both recipient groups. (A+B) Baseline day 0 imaging illustrates the naïve eyes showing no signs of clinical disease in both groups before disease induction by leukocyte transfer. (C+D) Day 7 imaging illustrating peak disease in both groups with severe vitreal infiltrate and swelling of the retina and optic disc visible in the OCT. (E+F) Day 14 imaging illustrating early disease resolution in both groups but still with severe clinical disease present within both groups. (G+H) Day 28 imaging of the recipient groups illustrating further resolving in the C57BL/6 transfer group but active disease persisting in the IL-27Rα$^{-/-}$ group.

(A+C+E+G) C57BL/6 transfer recipients

(B+D+F+H) IL-27Rα$^{-/-}$ transfer recipients

D40

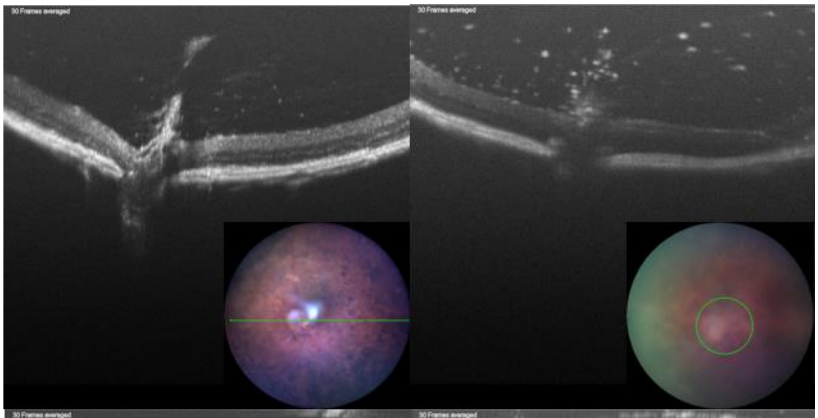

D51

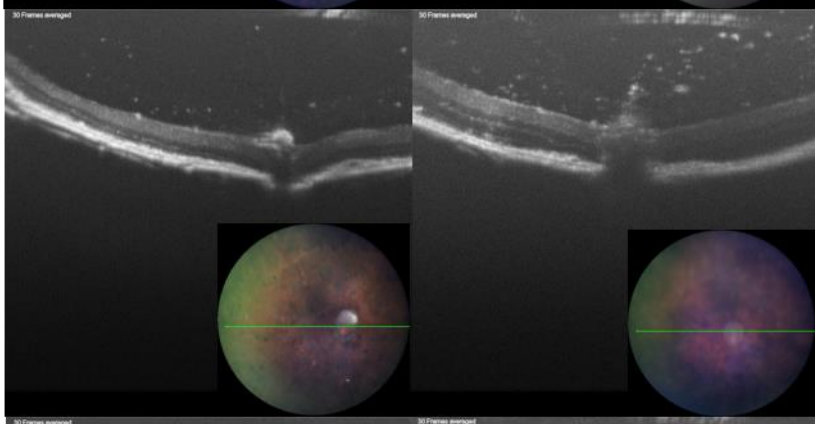

D67

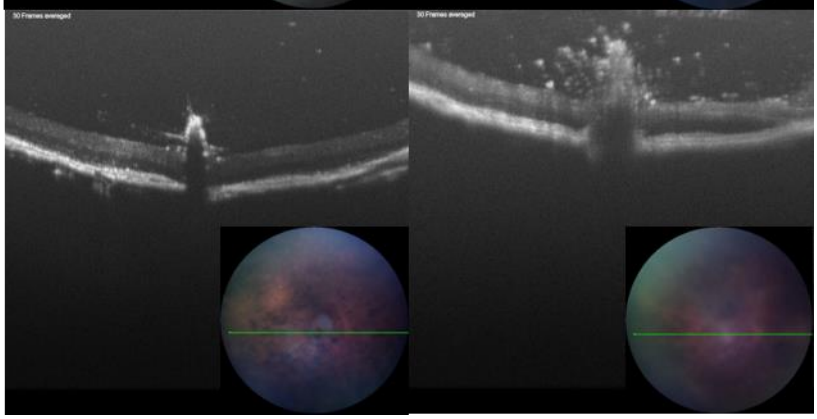

Figure 7.9: OCT time course of late clinical disease in C57BL/6 transfer recipients and IL-27Rα$^{-/-}$ transfer recipients. OCT and fundus imaging from day 40 through to day 67 to monitor late clinical disease in both recipient groups. (A+B) Day 40 imaging of both groups to illustrate disease severity and persistence in each group at this time point. (C+D) Day 51 imaging of both groups of recipients to compare disease severity and persistence within the two groups of recipients. (E+F) Day 67 imaging was obtained before eyes were analysed by flow cytometry to quantify leukocytes present within the eye. The imaging allows a final comparison of disease severity to correlate with leukocyte numbers obtained by flow cytometry.

(A+C+E) C57BL/6 transfer recipients

(B+D+F) IL-27Rα$^{-/-}$ transfer recipients

7.3.6 Flow cytometric analysis of leukocyte infiltrate at day 67 after adoptive transfer of uveitogenic leukocytes into C57BL/6 or IL-27Rα$^{-/-}$ recipients

Disease course was monitored in the two recipient groups using OCT imaging from baseline through to day 67 (figure 7.8 and 7.9). At day 67, disease within the IL-27Rα$^{-/-}$ recipients remains active in the OCT image with large levels of vitreal infiltrate (figure 7.9f), whereas in the C57BL/6 recipients active disease resolved by day 28 (figure 7.8g) and remained in a quiescent state through to day 67 (figure 7.9e). Data from the C57BL/6 recipients previously presented in *chapter 4*.

One eye from each recipient was isolated and prepared for analysis by flow cytometry and the corresponding eye was used for light sheet analysis, flat mount analysis by confocal microscope or sectioned for staining by immunofluorescence.

Retinas and vitreous were isolated from one eye from each recipient in both groups. CD4+, CD8+, CD11b+, Ly6G+ and Ly6C+ cells were quantified in the endogenous and transferred compartment of each eye using allelic markers.

Figure 7.10a illustrates endogenous and transferred CD4+ T cells present within recipients' eyes at day 67. In recipients that received the C57BL/6 transfer, a small population of transferred CD4+ T cells persists within the eye to day 67 which corresponds with a small increase in the endogenous population. In the IL-27Rα$^{-/-}$ recipient group a large group of transferred CD4+ T cells have persisted through to day 67 driving disease to continue; this is accompanied by a large endogenous CD4+ T cell population within the ocular tissue at day 67. The large CD4+ T cell number present within the IL-27Rα$^{-/-}$ recipients supports the observation made by the OCT images taken at day 67.

There is a statistically significant difference between the endogenous populations of CD4+ T cells within the recipients of each group which coincides with a statistically significant difference between the transferred populations present within the eyes of recipients at day 67 due to differences in disease state.

Figure 7.10b shows the endogenous and transferred CD8+ T cell number at day 67 in both groups of recipients. Transferred CD8+ T cells in both groups do not survive within the eye, this was previously observed in *chapter 4* from day 14. Due to the transferred cells not persisting within the eye there is a statistically significant difference between the endogenous and transferred populations. But no statistically significant difference is observed between

the endogenous populations of the two groups. This observation suggests that differences in disease are driven by the CD4+ compartment by both the endogenous and transferred population and other endogenous leukocyte compartments such as macrophages and neutrophils.

Figure 7.10c shows the endogenous and transfer CD11b+ populations present within the eye of the two groups of recipients at day 67. Similarly, to the transferred CD8+ T cell population the CD11b+ does not persist within the eye in both groups of recipients so there is a large statistically significant difference between the endogenous and transferred populations in both groups. There is also a small statistically significant increase in the CD11b+ cell number present within the eyes of the IL-27Rα$^{-/-}$ recipients in comparison to the C57BL/6 recipients.

Figure 7.11a represents the Ly6G+ cell number present within the eyes of the recipients in both groups at day 67. In both groups the transferred leukocyte population is not present within the ocular tissue at day 67, this causes a large statistically significant difference between the endogenous and transferred populations in each group of recipients. In the C57BL/6 recipients a small population of Ly6G+ cells are observed within the eye, whereas within the IL-27Rα$^{-/-}$ a statistically significant increase in the Ly6G+ population is present within the eyes of recipients at day 67.

Ly6C+ and Ly6C- numbers are expressed in figure 7.11b and 7.11c. As observed previously the transferred population does not survive within the eye, therefore a statistically significant difference between the endogenous and transferred populations is present in both recipient groups. There is also a statistically significant increase in the Ly6C+ cell number between the two groups, specifically an increase is present within the IL-27Rα$^{-/-}$ recipients in comparison to the C57BL/6 recipients. The same effect is also seen within the Ly6C- population present within the eyes of the recipients. The IL-27Rα$^{-/-}$ recipients have an increased Ly6C- population present within the eye in comparison to the C57BL/6 recipients.

Overall the IL-27Rα$^{-/-}$ recipients have increased endogenous leukocyte recruitment in comparison to the C57BL/6 control group. Transferred CD4+ T cells persist in high numbers to drive active disease in the IL-27Rα$^{-/-}$ recipients due to the transferred population not being shut down, whereas the transferred CD4+ T cells in the C57BL/6 recipients persist in low numbers that do not drive an active disease phenotype which suggests the cells are more readily shut down to limit active disease.

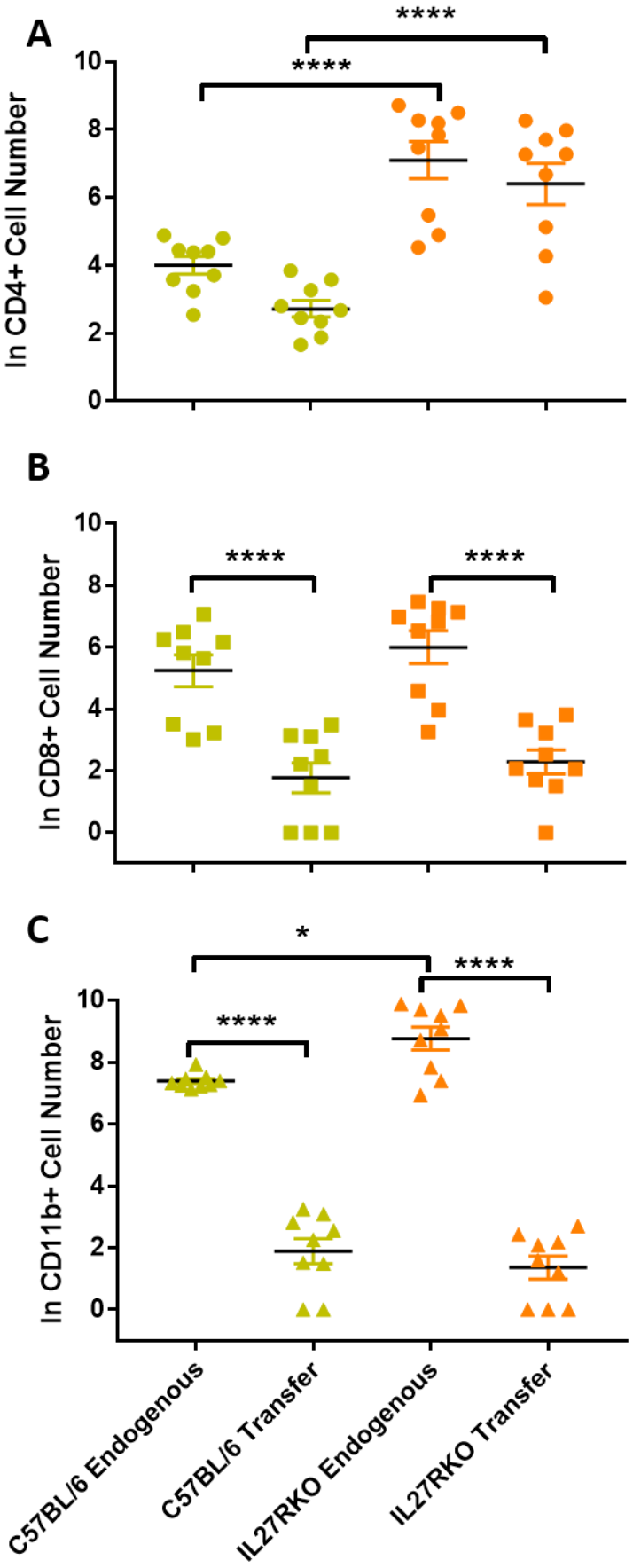
A
****
****
ln CD4+ Cell Number
10
8
6
4
2
0
B
****
****
ln CD8+ Cell Number
10
8
6
4
2
0
C
*
****
****
ln CD11b+ Cell Number
10
8
6
4
2
0
C57BL/6 Endogenous
C57BL/6 Transfer
IL27RKO Endogenous
IL27RKO Transfer

ENDOGENOUS				TRANSFER			
IL-27RA$^{-/-}$	**Lower Limit**	**Upper Limit**	**Mean**	**IL-27Rα$^{-/-}$**	**Lower Limit**	**Upper Limit**	**Mean**
CD4	92	6148	2602	**CD4**	71	3900	1441
CD8	25	1748	808	**CD8**	0	45	16
CD11B	1021	19482	9730	**CD11b**	0	14	5
LY6G	147	3101	1884	**LY6G**	0	0	0
LY6C	311	5673	1989	**LY6C**	0	0	0
C57BL/6	**Lower Limit**	**Upper Limit**	**Mean**	**C57BL/6**	**Lower Limit**	**Upper Limit**	**Mean**
CD4	12	132	68	**CD4**	4	46	18
CD8	20	1175	390	**CD8**	0	32	11
CD11B	1242	2756	1660	**CD11b**	0	25	10
LY6G	7	108	40	**LY6G**	0	0	0
LY6C	21	149	73	**LY6C**	0	0	0

Figure 7.10: **Leukocytes present within eyes of recipients processed at day 67 after adoptive transfer of C57BL/6 cells or IL-27Rα$^{-/-}$ cells.** Leukocytes were quantified from retinas and vitreous in one eye of each recipient at day 67 after adoptive transfer of C57BL/6 or IL-27Rα$^{-/-}$leukocytes into naïve C57BL/6 recipients. (A) Quantification of CD4+ T cell infiltrate present in eyes of recipients at day 67, using allelic markers endogenous and transferred population can be deduced. (B) Quantification of CD8+ T cell infiltrate present in eyes of recipients at day 67. Endogenous and transferred populations are quantified in each recipient within each group. (C) CD11b+ cell quantification at day 67 after adoptive transfer. Endogenous and transferred populations are quantified in each recipient within each group. Numbers expressed as Mean ±SEM. One-Way ANOVA multiple comparisons **p<0.1 and ****p<0.0001.

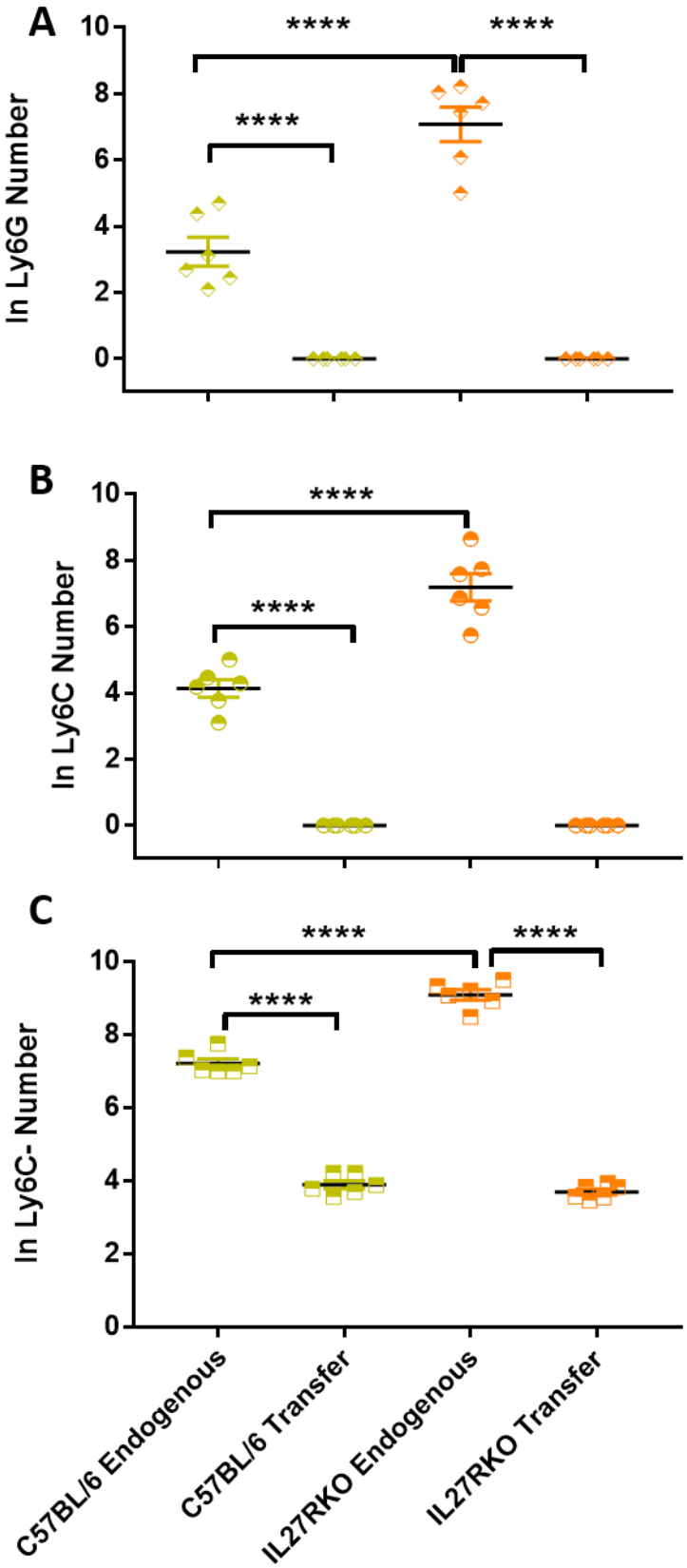
A
B
C
****
****
****
****
****
****
ln Ly6G Number
ln Ly6C Number
ln Ly6C- Number
0
2
4
6
8
10
C57BL/6 Endogenous
C57BL/6 Transfer
IL27RKO Endogenous
IL27RKO Transfer

ENDOGENOUS				TRANSFER			
IL-27RA$^{-/-}$	**Lower Limit**	**Upper Limit**	**Mean**	**IL-27Rα$^{-/-}$**	**Lower Limit**	**Upper Limit**	**Mean**
CD4	92	6148	2602	**CD4**	71	3900	1441
CD8	25	1748	808	**CD8**	0	45	16
CD11B	1021	19482	9730	**CD11b**	0	14	5
LY6G	147	3101	1884	**LY6G**	0	0	0
LY6C	311	5673	1989	**LY6C**	0	0	0
C57BL/6	**Lower Limit**	**Upper Limit**	**Mean**	**C57BL/6**	**Lower Limit**	**Upper Limit**	**Mean**
CD4	12	132	68	**CD4**	4	46	18
CD8	20	1175	390	**CD8**	0	32	11
CD11B	1242	2756	1660	**CD11b**	0	25	10
LY6G	7	108	40	**LY6G**	0	0	0
LY6C	21	149	73	**LY6C**	0	0	0

Figure 7.11: Leukocytes present within eyes of recipients processed at day 67 after adoptive transfer of C57BL/6 cells or IL-27Rα$^{-/-}$ cells. Leukocytes were quantified from retinas and vitreous from one eye from each recipient at day 67 after adoptive transfer of C57BL/6 or IL-27Rα$^{-/-}$leukocytes into naïve C57BL/6 recipients. (A) Quantification of Ly6G+ cell number present within the eyes of recipients at day 67 after disease induction by adoptive transfer. Endogenous and transferred populations were quantified individually in each eye. (B) Quantification of Ly6C+ cell number present within the eyes of recipients at day 67 after disease induction by adoptive transfer. Endogenous and transferred populations were quantified individually in each eye. (C) Quantification of Ly6C- cell number present within the eyes of recipients ta day 67 after disease induction by adoptive transfer. Endogenous and transferred populations were quantified individually in each eye. Numbers expressed as Mean ±SEM. One-Way ANOVA multiple comparisons ****p<0.0001.

7.3.7 Lightsheet, Confocal and EVOS imaging of immunofluorescence staining of whole eyes or retinas from C57BL/6 or IL-27Rα$^{-/-}$ recipients

At day 67, recipient's eyes were analysed by OCT to determine disease severity. One eye from each recipient was then analysed by flow cytometry to quantify differences in cellular infiltrate between the two groups.

Imaging techniques were used to analyse the differences between groups using the remaining eye from each recipient. Firstly, one eye from each recipient group was used for analysis by Lightsheet fluorescence microscopy (Zeiss Z.1 Lightsheet microscope).

Lightsheet fluorescence microscopy (LSFM) uses a thin plane of light to optically section transparent tissue of whole organisms that have been labelled by a fluorophore (277). An IL-27Rα$^{-/-}$ recipient was imaged using lightsheet microscopy, as seen in figure 7.12 the retina holds its shape whilst being imaged using the lightsheet and the leukocytes present within the retina are visible due to the fluorophore staining. CD4+ T cells (figure 7.12a) are present throughout the retinal tissue indicating active clinical disease as previously described in OCT and flow cytometry data presented in figures 7.8, 7.9, 7.10 and 7.11. CD8+ T cells are dispersed throughout the retina in high numbers (figure 7.12b) as previously highlighted by the flow cytometry analysis presented in figure 7.10. The CD3e stain indicates high levels of T cell infiltrate present in the retina (figure 7.12c). Figure 7.14d merges the stains together to create a complete image of the retina, unfortunately due to the active state of disease the vessel stain was not possible to image due to leaking.

2 eyes from each recipient group were also prepared for flat mount imaging by confocal microscopy. Confocal microscopy is capable of providing high-resolution microscopic images of cells within tissues under inspection especially using z-axis scans (278). The eyes were punctured and placed into fixative for two hours before the anterior was removed and the eye placed into fixative overnight. The retina is then removed carefully to keep fully intact. The retina was stained with antibodies conjugated to fluorophores to stain for leukocytes present within the retina such as CD3e, CD4 and CD8 and a DAPI cellular stain was also used to orientate the eye when imaging. The retina is the petallated and mounted onto a slide for imaging.

Figure 7.13 are images taken using a confocal microscope of a retina taken from a C57BL/6 leukocyte transfer recipient. CD4+ T cells are detected in low numbers within the retina of

the C57BL/6 recipient (figure 7.13), this supports the OCT imaging data and the flow cytometry data previously presented in figure 7.8, 7.10 and 7.11 that no active disease was present in the eyes of the C57BL/6 recipients. Increased CD8+ infiltrate in comparison to the CD4+ infiltrate is detected within the flat mounted retina by confocal microscopy (figure 7.13) which supports the flow cytometry data obtained and presented in figure 7.10. Figure 7.13 illustrates the CD3e stain to detect all T cells present within the retina. As the greatest number of T cells present within the retina are CD8+ T cells this stain is predominantly staining the CD8+ T cells.

Figure 7.14 contains images taken using a confocal microscope of a retina taken from an IL-27Rα$^{-/-}$ leukocyte transfer recipient. As previously discussed, the stains for the flat mount are also present in figure 7.13. CD4+ T cells (figure 7.14) are present in high numbers in the retina of the IL-27Rα$^{-/-}$ recipients, further indicating active disease that was previously suggested in previous figures. CD8+ T cell number is detected in figure 7.14, supporting the flow cytometry data previously presented in figure 7.10. The CD8+ T cell number present in the retinas of both groups are comparable, this is detected by flow cytometry and confocal microscopy. Figure 7.14 also illustrates CD3e staining within the retina to detect all T cells present within the retina.

The final imaging technique used for analysis of eyes at day 67 after adoptive transfer with C57BL/6 leukocytes or IL-27Rα$^{-/-}$ leukocytes is by cryostat slicing of the eyes to image using the EVOS fluorescence microscope. Firstly, eyes are frozen in OCT medium using liquid nitrogen and then stored at -80°C until sectioned. Sections were then obtained from the eyes using a cryostat to obtain 20micron sections through the eye. The sections were then stained using fluorescently conjugated antibodies specific for CD3e and CD4 along with a DAPI stain for orientation of the eye when imaging. Sections were then mounted onto slides for imaging. Fluorescence microscopy requires that the objects of interest fluoresce (279). The sections were then imaged using a fluorescence microscope.

Representative images are observed in figure 7.15, figure 7.15a is a section from a C57BL/6 transfer recipient stained with a CD3e stain to detect all T cells present within the section. The CD3e+ cells within the section are low in number which was also illustrated in previous figures regarding disease severity and leukocyte infiltrate.

Figure 7.15b is a section from an IL-27Rα$^{-/-}$ leukocyte transfer recipient stained with a CD3e stain to detect all T cells within the section. The large levels of CD3+ T cells present within the section support the active disease present in the eye described in previous figures.

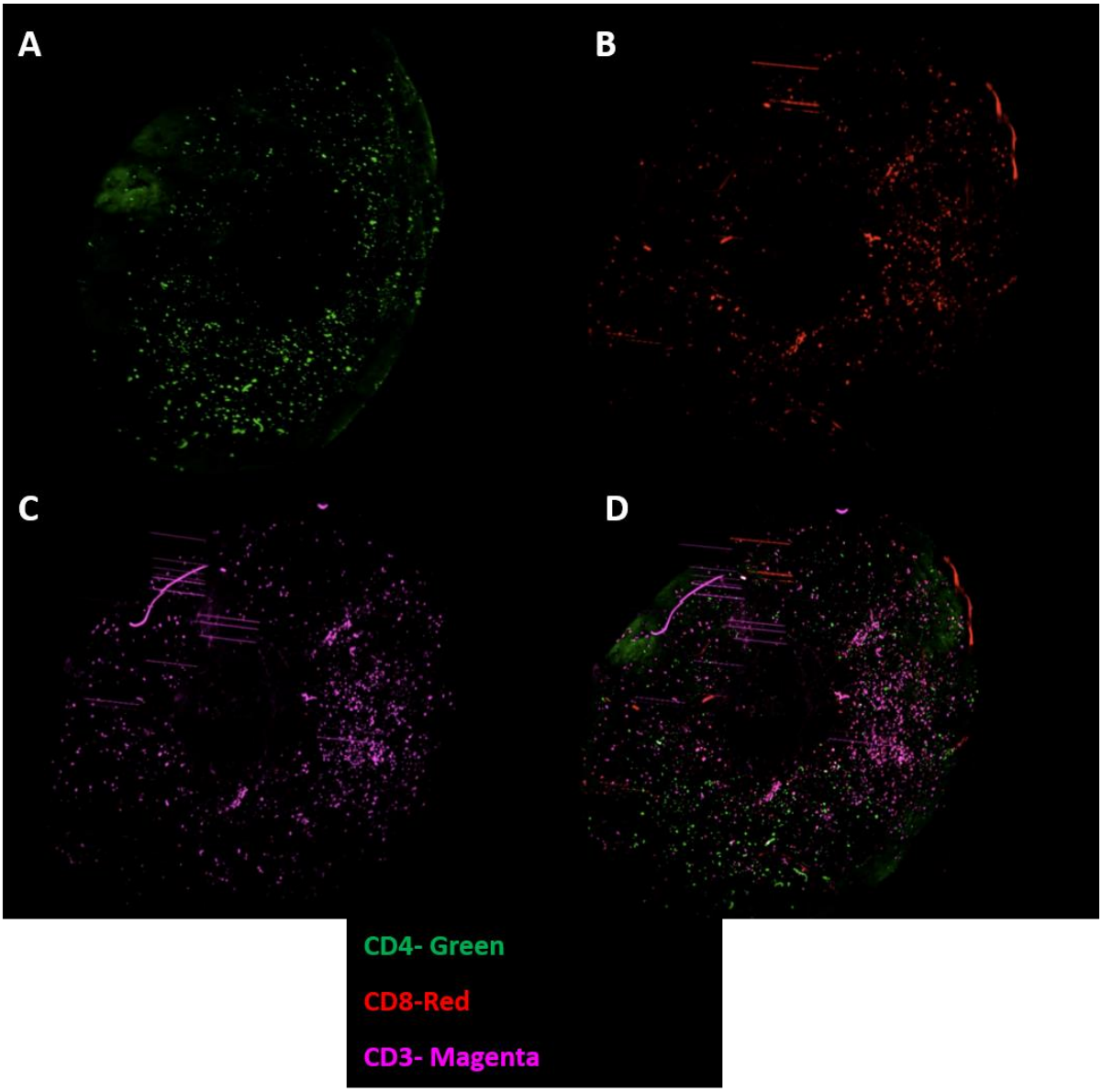

Figure 7.12: Images taken using lightsheet fluorescence microscopy to image a whole retina of an IL-27Rα$^{-/-}$ leukocyte transfer recipient. Whole retina imaging using lightsheet fluorescence microscopy was used to detect leukocytes throughout the retina. (A) CD4+ AF488 stain to indicate disease severity based on CD4+ T cell infiltrate. (Green) (B) CD8+ AF594 stain to determine infiltrate within the whole retina (Red) (C) CD3e AF647 stain to illustrate all T cell infiltrate within the retina at day 67 (Magenta) (D) Merged image to analyse all T cell infiltrate within the retina. 20x Magnification.

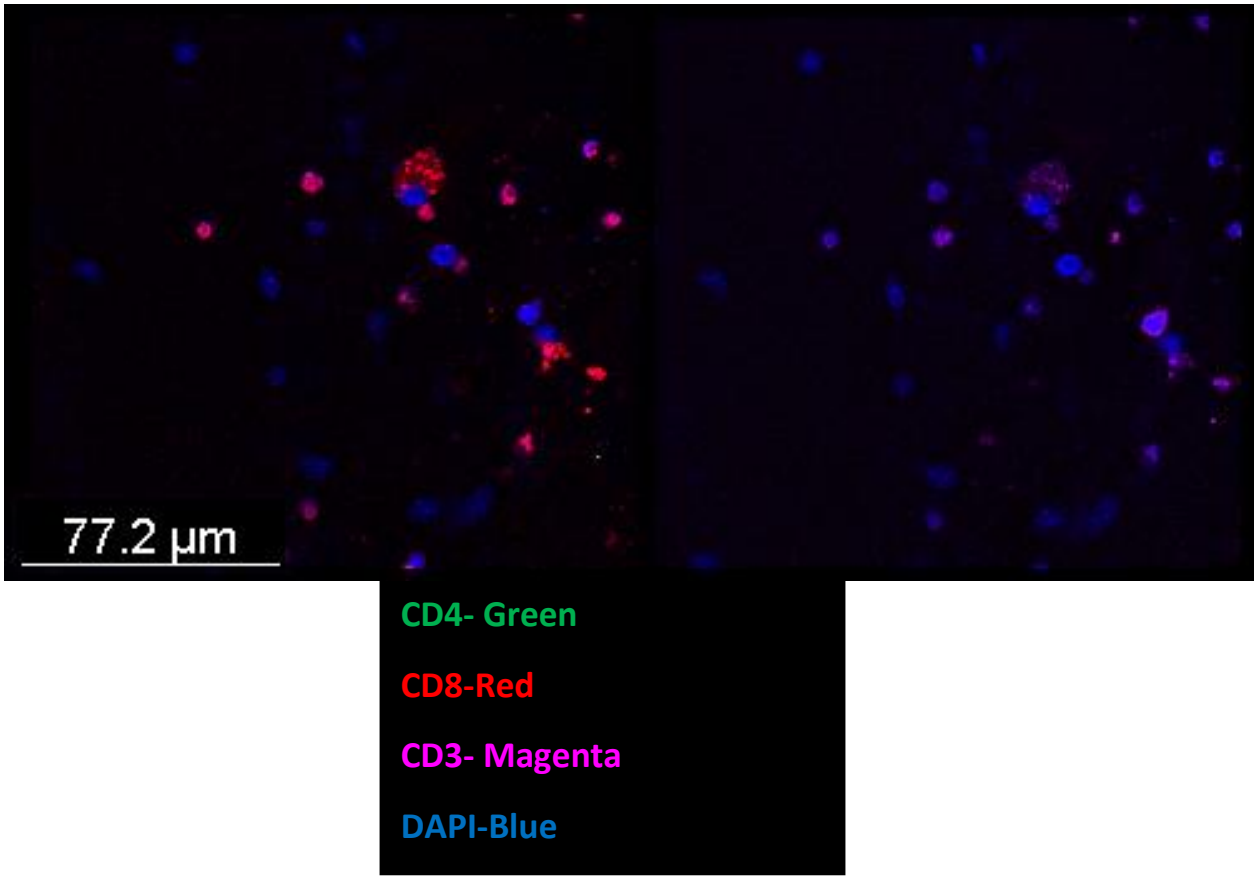

Figure 7.13: Images taken by confocal microscopy of a flat mount of a retina obtained from a C57BL/6 transfer recipient at day 67. Images obtained using confocal microscopy of a whole flat mounted retina. DAPI cellular stain used to orientate the retina to image specific sections of the retina. The CD3+, CD4+ and CD8+ stain illustrates total T cell infiltrate within the sections observed to compare across the two recipient groups. 40x Magnification.

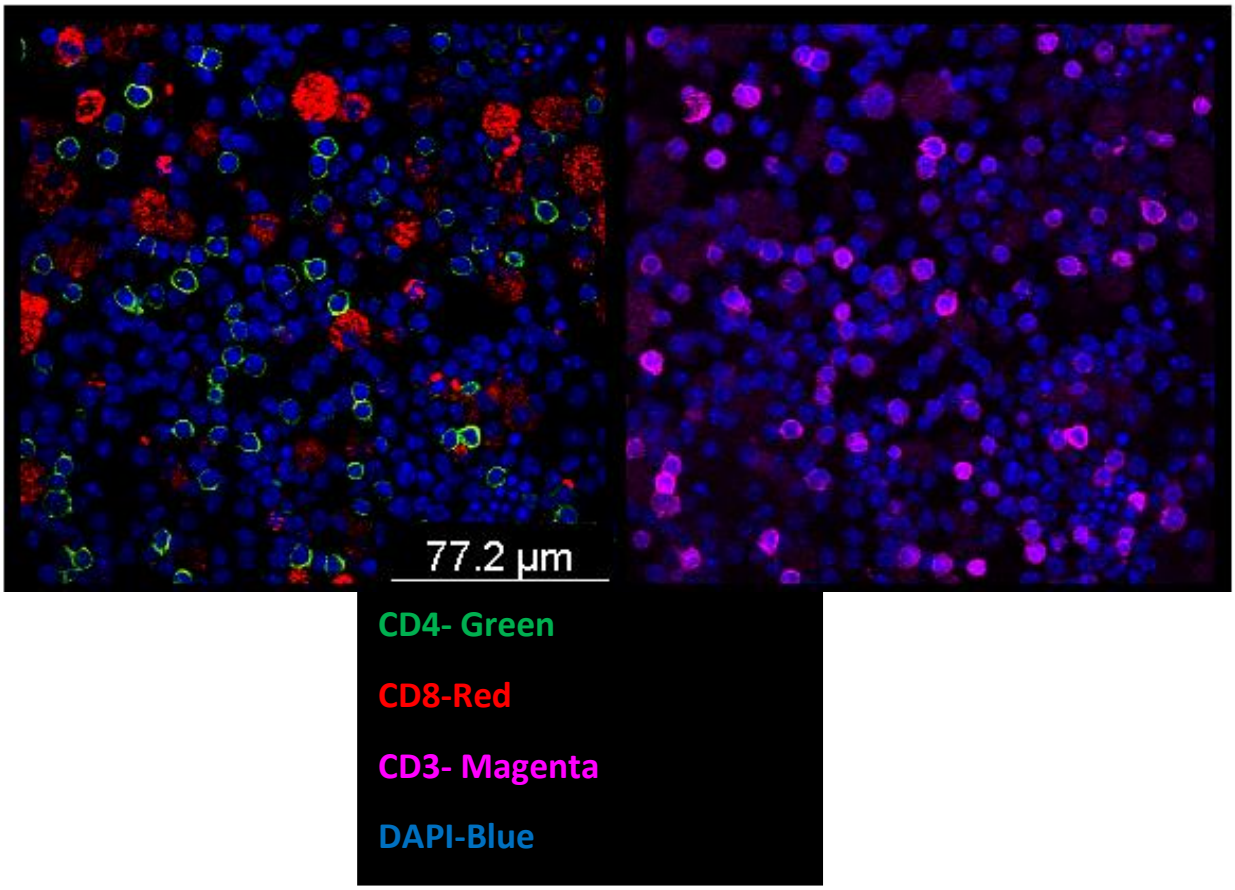

Figure 7.14: Images taken by confocal microscopy of a flat mount of a retina obtained from an IL-27Rα$^{-/-}$ transfer recipient at day 67. Images obtained using confocal microscopy of a whole flat mounted retina. DAPI cellular stain used to orientate the retina to image specific sections of the retina. The CD3+, CD4+ and CD8+ stain illustrates total T cell infiltrate within the sections observed to compare across the two recipient groups.40x Magnification.

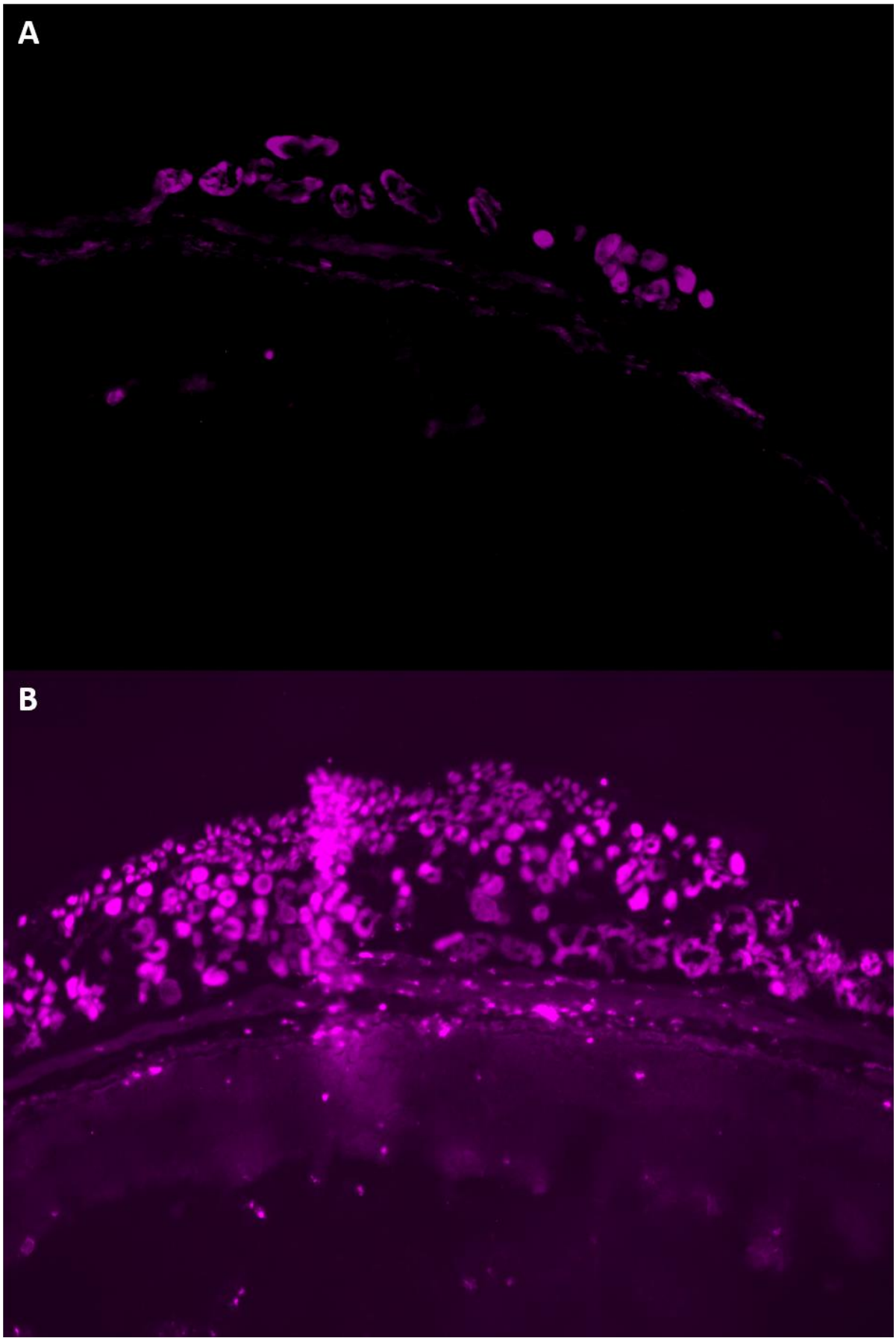
A
B

Figure 7.15: Images taken from 40micron sections obtained from frozen whole eyes of C57BL/6 or IL-27Rα$^{-/-}$ transfer recipients. Sections from whole eyes frozen in OCT medium were obtained from eyes of both groups of recipients. (A) CD3e AF647 stain on sections obtained from C57BL/6 transfer recipients. Reduced infiltrate is present in comparison to the IL-27Rα$^{-/-}$ recipients due to resolution of active disease within the recipient at day 67. (B) CD3e AF647 stain on sections obtained from IL-27Rα$^{-/-}$ transfer recipients. Increased infiltrate is present within the eyes due to persistent active disease. Images show retinal infiltrate from both eyes.10x Magnification.

7.3.8 Analysis of leukocyte transfer recipients by OCT and flow cytometry through to day 144 after adoptive transfer.

After analysis of transfer recipients at day 67 and differences in disease activity observed, further recipients were then taken through to day 144 to determine differences in disease activity by disease monitoring using OCT imaging and final time point analysis by flow cytometry leukocyte quantification.

C57BL/6 and IL-27Rα$^{-/-}$ recipients were monitored to assess clinical disease across the two groups using OCT from day 76 to day 143. Figure 7.16a demonstrates that the active clinical disease within the C57BL/6 recipients remains resolved at day 76 as described previously in figure 7.9 where active disease resolution occurred within this recipient group at day 28 and continued to be in a quiescent state through the time course to day 67. Whereas at day 76 in the IL-27Rα$^{-/-}$ recipients (figure 7.16b) some signs of active disease are still present, obvious vitreal infiltrate and cells are present around the optic disc. At day 84, disease continues to be in a quiescent state in the C57BL/6 recipients (figure 7.16c) that is previously seen in figure 7.16a. No vitreal infiltrate is observed and no swelling of the retina or optic disc. At day 84 in the IL-27Rα$^{-/-}$ recipients (figure 7.16d) obvious vitreal infiltrate is present suggesting active disease is persisting. There are obvious cells around the optic disc and retinal folds present within the OCT. The fundus image is slightly hazy due to cellular infiltrate.

At day 123, the disease continues to be in a quiescent state in the C57BL/6 transfer recipients (figure 7.16e), in the OCT image no cellular infiltrate is present and there is no obvious swelling of the retina or infiltrate present around the optic disc. The fundus image is clear due to lack of infiltrate. In comparison, the IL-27Rα$^{-/-}$ recipient mice still show some signs of clinical disease in the OCT image such as swelling or fluid accumulation within the retina and vitreal infiltrate present. The fundus image remains slightly hazy due to vitreal infiltrate.

Day 143 is the final OCT time point for both groups of recipients, the C57BL/6 recipients remains in a quiescent state (figure 7.16g). The fundus image remains clear due to the lack of active disease present in the recipients. As seen throughout the time course, active disease persists within the IL-27Rα$^{-/-}$ transfer recipients (figure 7.18h), in the OCT image cellular infiltrate remains present within the vitreous and cells are surrounding the optic disc. The corresponding fundus image remains hazy due to persistent active disease.

At day 144, eyes were dissected to isolate the retina and vitreous to quantify specific leukocyte infiltrate within the recipient's eyes. Total CD4+ T cells were quantified from each of the recipient's eyes (figure 7.19a) and compared to naïve baseline CD4+ T cell number. The total number of CD4+ T cells recovered from eyes of C57BL/6 animals at D144 was within the normal range established in naïve eyes (3->68) of which transferred cells comprised 25-30% in the C57BL/6 recipient transfer suggesting the CD4+ T cell number had returned to naïve baseline limits. The transferred population persisted within the C57BL/6 recipients in small numbers, a mean of 10 transferred cells per eye (data shown as total CD4+ T cell population). In contrast, the IL-27Rα$^{-/-}$ transfer recipients (figure 7.18a) have an increase in total CD4+ T cells present within the eyes of the recipients at day 144 in comparison to naïve baseline. Active disease was clear in 2/5 animals and CD4+ cells were above normal levels in a further 2/5 of the recipients with one animal appearing as if infiltrative disease had resolved. Transferred cells were present in the majority of eyes.

The same pattern is also seen in the CD8+ T cell compartment, no significant change is seen within the C57BL/6 recipients in comparison to the naïve baseline number (figure 7.19b). But as seen in the CD4+ compartment, an increase is observed between the naïve baseline and the total CD8+ T cell population present within the IL-27Rα$^{-/-}$ recipients. As previously discussed, transferred CD8+ T cells do not persist in either transfer model.

In the CD11b+ cell compartment, total cell numbers are comparable between the two recipient groups. Transferred CD11b+ cells do not survive throughout disease course as mentioned in previous figures.

Overall, transferred IL-27Rα$^{-/-}$ CD4+ T cells cause a more severe clinical disease phenotype and drive a more persistent active disease in comparison to the C57BL/6 transfer. Increased endogenous leukocyte recruitment is also seen in the IL-27Rα$^{-/-}$ recipients including neutrophils and macrophages.

C57BL/6 IL27RKO

D76

D84

D123

D143

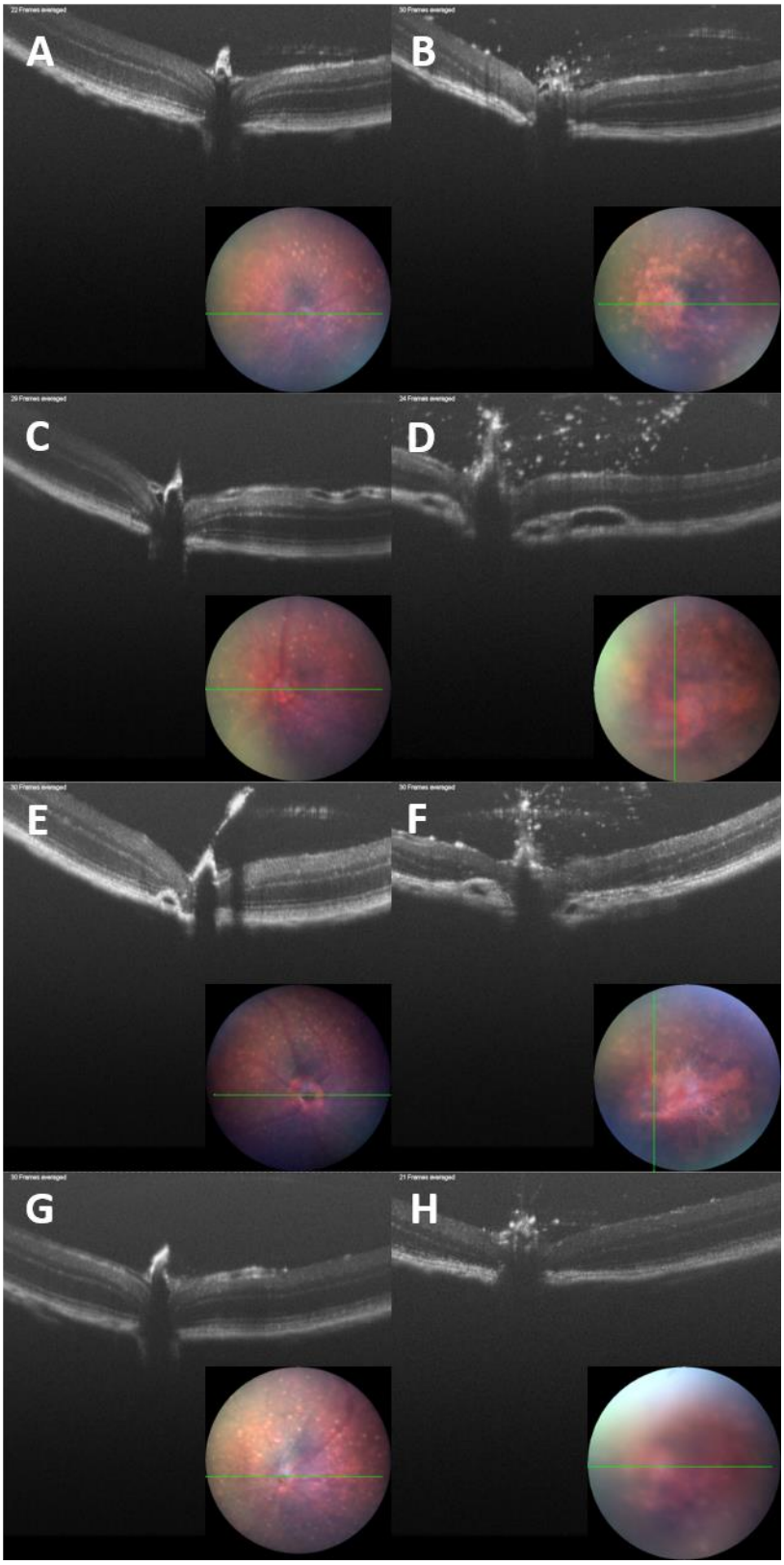

Figure 7.16: OCT imaging between day 76 to day 143 to monitor disease course between the two recipient groups. Disease course was monitored using OCT imaging across the two recipient groups that received a C57BL/6 leukocyte transfer or IL-27Rα$^{-/-}$ leukocyte transfer. (A-H) OCT and fundal imaging obtained from day 76 after transfer from C57BL/6 or IL-27Rα$^{-/-}$ donors into wildtype recipients.

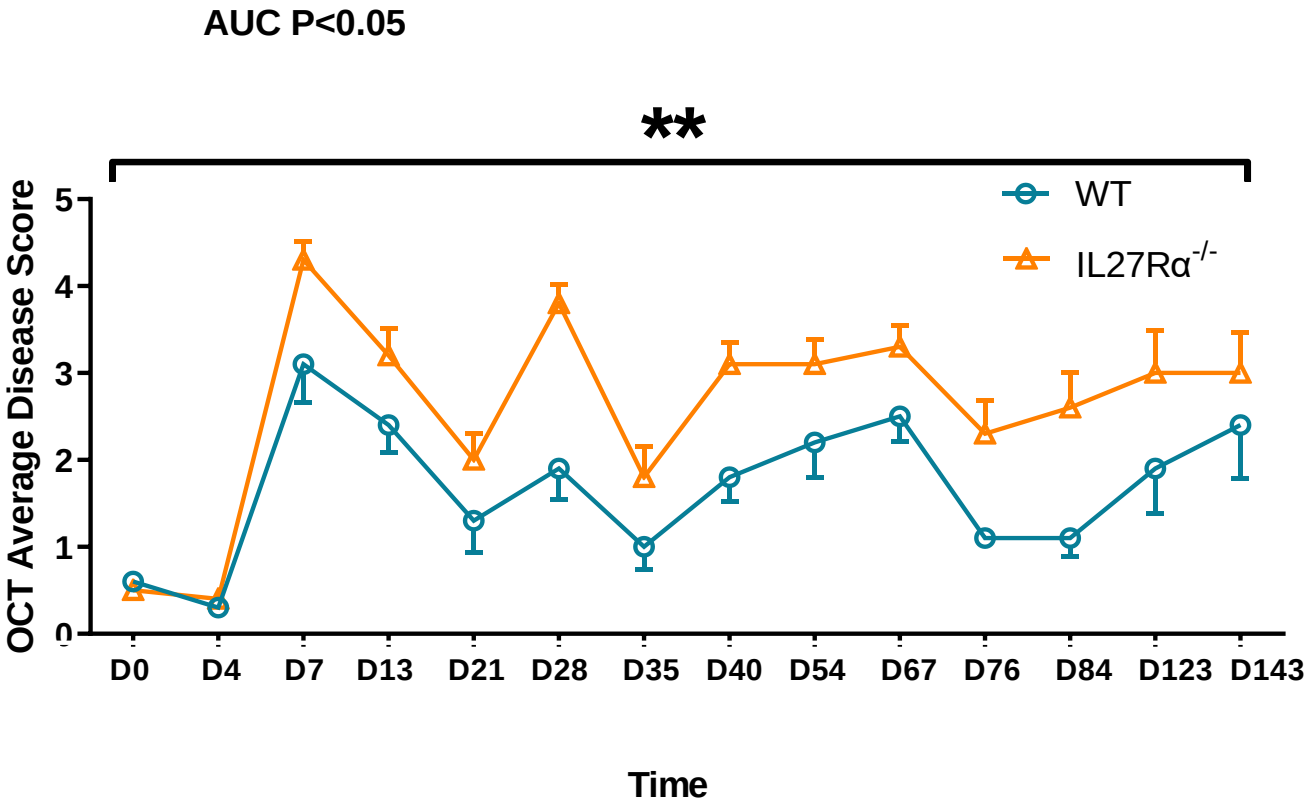

Figure 7.17: Average clinical scores of recipients over full disease course. OCT imaging was used to acquire fundal images of wildtype and IL-27Rα$^{-/-}$ recipients throughout disease course. The images were then scored blind using the criteria described in *chapter 2* and the average score taken from each eye at each time point. Data expressed as Mean ±SEM. Area under the curve calculated and statistical significance determined by an unpaired T test **p<0.05

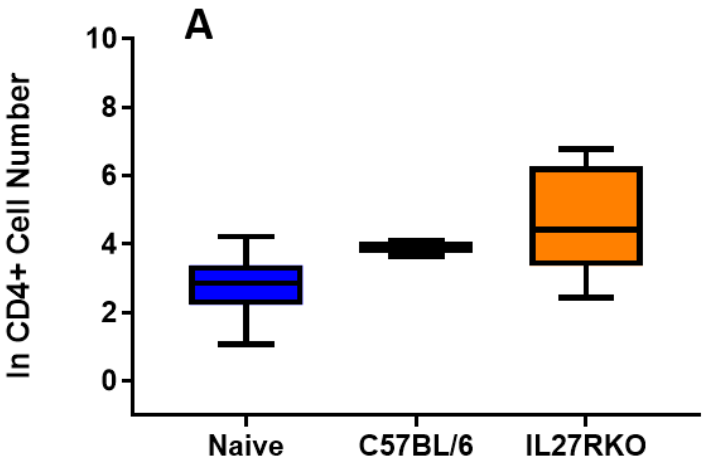
A
ln CD4+ Cell Number
10
8
6
4
2
0
Naive
C57BL/6
IL27RKO

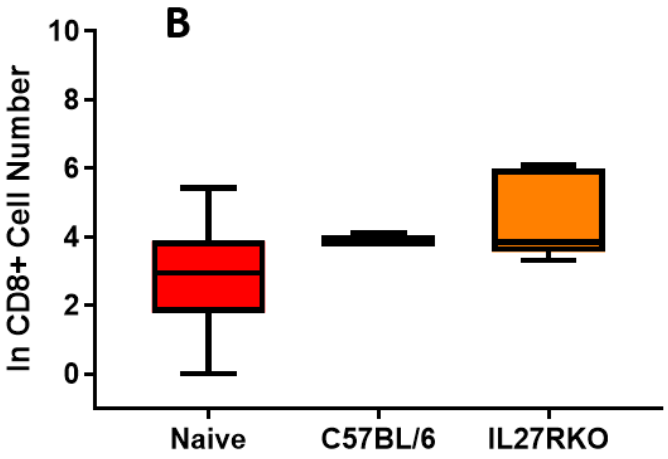
B
ln CD8+ Cell Number
10
8
6
4
2
0
Naive
C57BL/6
IL27RKO

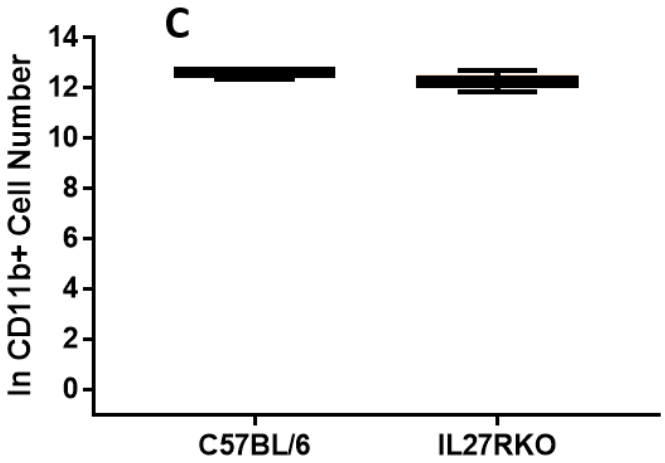
C
ln CD11b+ Cell Number
14
12
10
8
6
4
2
0
C57BL/6
IL27RKO

C57BL/6	LOWER LIMIT	UPPER LIMIT	MEAN
CD4	37	59	48
CD8	43	60	50
CD11B	2227	3381	2852
IL-27RA$^{-/-}$	**LOWER LIMIT**	**UPPER LIMIT**	**MEAN**
CD4	10	872	270
CD8	26	437	182
CD11B	1761	6068	3607

Figure 7.18: Quantification of leukocytes present within the vitreous and retina in transfer recipients at day 143 after adoptive transfer of C57BL/6 leukocytes or IL-27Rα$^{-/-}$ leukocytes. Quantification of leukocytes present in the eyes of recipients at day 143 after adoptive transfer. (A) Total CD4+ T cells present in the eyes of C57BL/6 and IL-27Rα$^{-/-}$ recipients in comparison the naïve baseline (B) Total CD8+ T cells present in the eyes of C57BL/6 recipients and IL-27Rα$^{-/-}$ recipients in comparison to the naïve baseline (C) Total CD11b+ cells present in the eyes of C57BL/6 recipients and IL-27Rα$^{-/-}$ recipients. Total eyes analysed at D143 3 per recipient group. Stats was not performed due to low numbers of eyes at D143.

7.4 Discussion

Studies have shown that IL-27 plays an important role in a variety of autoimmune diseases (156). IL-27Rα is quite widely expressed, therefore, to investigate the effect of IL-27Rα specifically on T cell pathogenicity and disease the adoptive transfer model was used.

In mouse models of autoimmune diseases IL-27Rα deficiency has been implicated in a more severe disease phenotype. In the murine model of rheumatoid arthritis, formation of ectopic lymphoid tissues has been reported (269) and in the experimental model of multiple sclerosis, using a Treg conditional knockout of IL-27Rα$^{-/-}$, a more severe disease phenotype due to dysregulated Tregs was seen (280).

This chapter presents work showing the effect of the IL-27Rα knockout in EAU, on disease induction analysed in the actively immunised model and in disease progression and severity analysed in the previously optimised adoptive transfer model.

In the eyes of unmanipulated IL-27Rα$^{-/-}$ mice total CD8+ T cells recovered (day 0 baseline) are significantly increased when compared to naïve C57BL/6 mice. The same effect was observed within the kidney of the IL-27Rα$^{-/-}$ mice (appendix 3) but not the liver. This could be caused by slower leukocyte trafficking throughout the periphery in comparison to the wildtype group, perhaps associated with tight endothelial barriers or potential differences in MHC expression within the tissue of the IL-27Rα$^{-/-}$ mice but more study is needed to determine the exact cause.

It has been previously published that in the IL-27Rα$^{-/-}$ mouse a more severe and persistent disease is present in comparison to a control C57BL/6 group in models such as AIA and EAE (269, 275). Following from this observation, donor eyes from both immunised recipient groups at day 11 were analysed by extracellular staining of cell markers and intracellular staining of cytokines. In the mouse model of arthritis using the IL-27Rα$^{-/-}$ mice robust Th1 responses are characterised by IFN-γ and IL-2 production (281). In EAU there is an increase in leukocyte number and disease severity in the IL-27Rα$^{-/-}$ mice (figure 7.4) and a statistically significant increase in overall IFN-γ production in the IL-27Rα$^{-/-}$ donors is observed. A further observation at day 11, is accelerated disease onset in the IL-27Rα$^{-/-}$ donors particularly within the CD4+ T cell compartment. This statistically significant increase in CD4+ T cells in the IL-27Rα$^{-/-}$ immunised donors in comparison to the C57BL/6 immunised donors demonstrates an earlier onset of clinical disease in the IL-27Rα$^{-/-}$ mice in comparison to the C57BL/6 control

group. This is further supported by data acquired at day 7 (figure 7.5) showing a more fast-moving clinical disease.

Considering the differences observed within the eyes of the donor mice, cytokine secretion and leukocyte cell number was analysed within the cell cultures before the adoptive transfer of leukocytes into recipients. Overall, the IL-27Rα$^{-/-}$ cultures expressed increased levels of numerous cytokines including IFN-γ and IL-17 reflecting the larger number of CD4+ T cells are present within the cultures. To understand further if the increase in cytokine secretion is purely per culture or if there are more cytokines produced by individual cells intra-cytoplasmic staining of cell cultures could be obtained. The increase in overall cytokine secretion in the IL-27Rα$^{-/-}$ culture suggests a more pathogenic or potent phenotype present. The total cell number in the IL-27Rα$^{-/-}$ cultures is nearly doubled in comparison to the C57BL/6, but the percentage of CD4+ T cells is comparable in both, equal cell numbers were then transferred into recipients, therefore any difference in disease is due to the difference in the pathogenicity of the leukocytes transferred not any difference in cell number. Further analysis of growth factors present within the cultures would explain the increase in total leukocytes present in the IL-27Rα$^{-/-}$ cultures.

Whereas early onset of clinical disease was observed in immunised IL-27Rα$^{-/-}$ mice in comparison to the C57BL/6 immunised group, in the adoptive transfer model of IL-27Rα$^{-/-}$ or C57BL/6 T cells into C57BL/6 Ly5 recipients, no difference is observed in the two groups. This could be due to the cells being transferred already having an activated, antigen-specific phenotype whereas the immunisation of mice in both groups has had no pre-priming of CD4+ T cells and therefore when the two groups were immunised the more rapid expansion of the IL-27Rα$^{-/-}$ causes an earlier onset and more severe disease phenotype.

OCT of early disease shows no differences between clinical disease onset and a similar disease severity at peak disease in both groups. Resolution of active clinical disease in the C57BL/6 group occurs by day 28, whereas in the IL-27Rα$^{-/-}$ recipient group clinical disease remains active. When studying late disease by OCT, clinical disease in the C57BL/6 recipient group remains generally inactive throughout the time course. In the IL-27Rα$^{-/-}$ recipient group disease is generally more severe and clinical infiltration remains through to day 67. This observation further confirms that T cells isolated from an IL-27Rα$^{-/-}$ mouse are more potent and drive a more severe persistent disease phenotype consistent with active immunisation models of AIA and EAE (269, 275).

At day 67 the recipient's eyes from both groups were isolated and analysed by flow cytometry or fluorescence microscopy.

The data obtained from quantification of leukocytes by flow cytometry supports the observations made by OCT in relation to disease severity across the two groups. Firstly, total number of leukocytes within the eyes of the IL-27Rα$^{-/-}$ recipients is increased in comparison to the C57BL/6 recipient group.

When studying the ratio of endogenous and transferred leukocytes present within the eyes of both groups of recipients in these long-term experiments most transferred leukocyte populations, except CD4+ cells, did not survive from the donor groups. In the CD4+ T cell compartment, transferred C57BL/6 CD4+ T cells are found in low numbers in the eyes of recipients at all time points studied. The decrease in transfer cell number is consistent with the resolution of active clinical disease in these recipients. In the eyes of the IL-27Rα$^{-/-}$ recipients a large transferred CD4+ T cell population persists within the eyes of recipients through to day 67. This is the only transferred leukocyte population to persist long-term within the eyes of recipients suggesting that it is the absence of IL-27Rα specifically on CD4+ T cells that is required to drive a more severe persistent disease. Even with intact Treg function within recipients, the transferred cells are still highly pathogenic, driving active clinical disease and causing recruitment of endogenous CD4+ T cells.

To study if during clinical disease any ectopic lymphoid tissue aggregates form, fluorescence microscopy was performed on whole retinas by flat mount or lightsheet microscopy. Both forms of analysis showed no signs of ectopic lymphoid structures being present using a CD3 stain to mark formation. Further analysis was performed using whole eye sections stained with fluorescence, but this further analysis also showed no ectopic lymphoid structure formations. However, the differences in CD4+ T cell number between the two groups is further supportive of the OCT and flow cytometry analysis at the same time point, illustrating more active disease in the IL-27Rα$^{-/-}$ recipient mice. The CD8+ population present within the retinas are larger and therefore suggests an active environment, specifically in the IL-27Rα$^{-/-}$ recipients where an increased number of larger more activated CD8+ T cells are present in comparison to the C57BL/6 transfer.

To extend the analysis of the effect of IL-27Rα$^{-/-}$ on transferred CD4+ T cells, in a small number of animals, disease was monitored through to day 144. As previously observed in earlier OCT images the recipients of the C57BL/6 transfer show no signs of active clinical disease from day

28 and disease appears to be quiescent through to day143 (figure 7.17) when eyes are analysed by flow cytometry to quantify total CD4+ T cell number (figure 7.18) the total number is not increased when compared to a naïve control, although damage to the retina is present in the OCT the disease does not remain active. In contrast in the OCT images of the IL-27Rα$^{-/-}$ recipients active disease is present but has reduced in severity when compared to previous OCT acquired at day 67. However, the disease, remains active in some animals through to day 144. Flow cytometric quantification shows an increase in the total CD4+ T cell number present within the eyes at day 144 and persistence of transferred IL-27Rα$^{-/-}$ CD4+ T cells. Overall, using the adoptive transfer technique has highlighted the IL-27Rα knockout CD4+ T cells persist throughout clinical disease and continue to recruit endogenous cells including CD4+ T cells and neutrophils specifically to drive active disease to persist. Suggesting that in the active immunisation model the effect observed is based on the presence of a more pathogenic and potent CD4+ T cell.

In conclusion, IL-27Rα knockout on leukocytes causes a more potent pathogenic phenotype that induces a more severe and persistent autoimmune disease in models of active immunisation. Using the adoptive transfer technique highlights that IL-27Rα$^{-/-}$ specifically within the CD4+ T cell population is sufficient to induce a more severe and persistent disease phenotype even in the presence of functional Tregs. This data also supports IL-27 as an immunoregulatory cytokine as active clinical disease persists within the IL-27Rα$^{-/-}$ recipients but within the C57BL/6 recipients with functional IL-27 present active clinical disease has resolved by day 28. The IL-27Rα$^{-/-}$ CD4+ T cells are also more long lived and continue to drive clinical disease in comparison to the small numbers found in the C57BL/6 transfer group suggesting a more pathogenic and potent phenotype of CD4+ T cell.

Chapter 8. Discussion

8. Discussion

8.1 General Discussion

CD4+ T cells are important mediators and drivers of autoimmune disease. To induce EAU it is well established that immunisation of susceptible animals with a uveitogenic peptide triggers an immune response within the periphery of the animal, characterised by the activation and clonal expansion of pathogenic autoreactive T cells. T cells then cross the blood-retinal barrier this induces leukocyte recruitment and retinal disruption (1).

Research presented in this thesis investigated the role of antigen-specific pathogenic T cells in the EAU model of uveitis. The effects of upregulation of specific chemokines and knock-out of cytokine receptors on transferred antigen-specific T cells was also investigated using the model. In coordination with these studies non-antigen specific recruitment to the ocular tissue was analysed with or without an antigen-specific stimulus and the work demonstrated the effects of antigen-specific T cell recruitment on the endothelium of the ocular tissue. Key findings were:

- Transfer of pathogenic leukocytes causes increased retention of endogenous CD4+ cells to the eye in addition to sticking of transferred CD4+ T cells. (*chapter 5*)
- Active uveitis enhances the recruitment of non-antigen specific activated T cells. (*chapter 5*)
- CX3CR1 is upregulated on CD4+ T cells in the eye during EAU. The upregulation of CX3CR1 is due to antigen-specific response by CD4+ T cells. (*chapter 6*)
- IL-27R$\alpha^{-/-}$ CD4+ T cells cause a more severe persistent clinical disease when adoptively transferred into wildtype C57BL/6 recipients. CD4+ T cells that are IL-27R$\alpha^{-/-}$ are more pathogenic and persist long term within the eye driving clinical disease. (*chapter 7*)

Thus, this work provides new insights into the role of antigen-specific uveitogenic CD4+ T cells, disease-associated non-antigen-specific CD4+ T cells and the important role of IL-27 in the regulation of disease.

8.2 Induction of EAU by adoptive transfer

The work presented in this thesis uses the adoptive transfer of antigen-specific or non-antigen-specific leukocytes. The adoptive transfer of antigen-specific uveitogenic leukocytes efficiently induces EAU in naive C57BL/6 recipients. As demonstrated in RAG2$^{-/-}$ mice in *Chapter 3*, disease induction and progression are CD4+ T cell mediated. Using the adoptive transfer of whole leukocyte populations allows the transferred and endogenous T cell populations to be distinguished and therefore gives us the ability to determine the long-term fate of the initial transferred cells, including the CD4+ transferred population.

8.2.1 The fate of transferred antigen specific CD4+ T cells throughout clinical disease

Transferred pathogenic antigen-specific cells are capable of inducing clinical disease in wildtype C57BL/6 (Ly5) recipients. The transferred CD4+ T cells give rise to a population that persists within the eye throughout clinical disease course this is highlighted in *Chapter 4*. This leads to a recruitment of endogenous CD4+ T cells that is observed from day 2 and increases as peak disease is reached at day 7-10 thus suggesting the host's own immune response responds to the pathogenic stimulus of the transferred antigen-specific T cells.

At day 2, the number of endogenous CD4+ T cells present within the eyes of recipient mice increases concurrently with the presence of transferred CD4+ T cells at this time point, suggesting an activation of the endothelium has occurred due to the transfer of antigen specific activated CD4+ T cells. We hypothesised that activation of the endothelium could be due to an antigen-specific stimulus due to the pathogenic nature of the transferred CD4+ T cells or alternatively due to the activation status of the transferred CD4+ T cells. This question will be discussed later on in this section.

Analysis of clinical disease course after adoptive transfer was achieved by OCT imaging and by quantification of leukocyte number by flow cytometry. These methods of analysis allowed active clinical disease to be monitored and the proportion of endogenous and transferred cells. It has previously been reported that initial disease causing CD4+ T cells or the progeny of these cells do not persist within the inflamed tissue throughout active disease and go through apoptosis as active clinical disease is resolving (282), however the data presented in *chapter 4*, suggests that in EAU the original antigen specific transferred

CD4+ T cells or their progeny have persisted within the eyes of the recipient mice and have driven the disease process or have been recruited to the eye during the disease process and have persisted within the tissue past active clinical disease. This finding is in contrast to a study by Oh et al where they describe the fate of autoreactive T cells that mediate uveitis to reside in the bone marrow after acute uveitic disease and not the ocular tissue (283). However, fate mapping would be required to understand the population of transferred cells that have survived within the tissue.

8.2.2 Transferred cells activate the endothelium after adoptive transfer causing a recruitment of both endogenous and transferred CD4+ T cells

After adoptive transfer of leukocytes, recipients were monitored using OCT imaging to assess early signs of clinical disease. Active disease was not detected on OCT before day 5, at this point swelling of the optic disc was a sign of early active clinical disease.

Although changes are not detectable by OCT at day 2 in many recipients, quantification of leukocytes at day 2 after adoptive transfer is a more sensitive measure of active clinical disease. As highlighted in *Chapter 4* at day 2 after adoptive transfer an increase in endogenous CD4+ T cell number is observed. Concurrently with this observation a population of transferred CD4+ T cells is detected within the ocular tissue which is not seen after transfer of non-antigen specific cells.

The presence of transferred CD4+ T cells and the increased number of endogenous CD4+ T cells suggests a mechanism involved in disease induction has already begun to impact the ocular tissue. We hypothesised that the recruitment of transferred CD4 cells to the ocular tissue by day 2 after adoptive transfer is due to an activation of the endothelium due to the activation status or antigen-specific nature of the transferred cells.

The role of endothelial cells in the recruitment of lymphocytes, monocytes, neutrophils and dendritic cells into lymph nodes and tissues depends on an intimate relationship between endothelial cells and immune cells (284). The recruitment of immune cells is selective and can be influenced by an immune stimulus to trigger the trafficking process along with mediators produced by endothelial cells (284). Therefore, the endothelium can play a vital role in the immune response and in the adoptive transfer model of EAU a role in disease initiation.

Further investigation into the immune stimulus linked to the recruitment of transferred CD4+ T cells that induces the increased recruitment and sticking of endogenous CD4+ T cells will be discussed with the relevant data presented from *chapter 5.*

8.3 Antigen specific and non-antigen specific CD4+ T cell recruitment in EAU

8.3.1 Increased recruitment and retention of endogenous CD4+ T cells at day 2 after adoptive transfer of CD4+ T cells is due to an antigen-specific stimulus

At day 2 after adoptive transfer of uveitogenic, antigen specific CD4+ T cells there is an increase in recruitment and retention of endogenous CD4+ T cells.

Further experimentation investigated whether the endothelium becomes activated in response to the transferred CD4+ T cells being in an activated state or due to their antigen specificity. Therefore, using OVA TCR transgenic leukocytes allowed us to address the question of activation versus antigen-specificity facilitating increased endogenous CD4+ T cell recruitment and transferred cells sticking within the ocular tissue to cause clinical disease.

Adoptive transfer of activated non retinal antigen specific leukocytes from an OVA TCR transgenic mouse does not initiate activation of the endothelium to the level seen with an antigen specific response, this is suggested by no increase in endogenous CD4+ T cell recruitment and almost no retention of the transferred OVA- specific activated. However, previous studies have highlighted the ability of activated T cells to migrate across normal, non-inflamed endothelium at day 1 ~44 cells had infiltrated the eyes of recipient mice when $10x10^6$ activated T cells are transferred (285).

An i.p injection of PBS, without activated or unactivated cells will still initiate a measurable and statistically significant increase in recruitment and retention of endogenous CD4+ T cells at day 2 after injection, this effect could be caused by endotoxin release at the site of injection that stimulates the endothelium to upregulate molecules that retain CD4+ T cells at this early time point. Increased trafficking does not lead to initiation of uveitic disease and by day 7 has resolved, thus suggesting that without a pathogenic stimulus the endothelium does not become activated to recruit and retain endogenous and transferred cells that cause disease.

Therefore, this data suggests a local antigen-specific response is required to induce disease progression through endothelial activation that leads to endogenous and transferred CD4+ T cell recruitment. This conclusion was further confirmed using the OVA TCR specific cell transfer of activated OVA antigen-specific OTII cells with a concurrent intravitreal injection of OVA given just prior to cell transfer presented in *chapter 5*. This data confirmed that the recruitment of transferred and endogenous cells observed at day 2 after adoptive transfer is not retinal antigen specific but an antigen-specific response to any antigen in the local environment and has the ability to induce recruitment of endogenous and transferred CD4+ T cells.

8.3.2 Antigen-specific transferred CD4+ T cells initiate recruitment of antigen and non-antigen specific CD4+ T cells throughout ocular inflammation

As previously discussed, activated non-antigen specific CD4+ T cells are not capable of inducing endothelial activation defined by significant endogenous cell recruitment and do not remain within the ocular tissue past day 2 after adoptive transfer. Although the endogenous CD4+ T cell number does increase due to the release of endotoxin at the site of injection.

Data has demonstrated an antigen-specific stimulus induces the activation of the endothelium. However, further experiments including the co-transfer of retinal antigen specific activated CD4+ T cells with OVA specific activated CD4+ T cells at a 1:1 ratio. These experiments allowed for tracking of transferred 'pathogenic' retinal antigen specific CD4+ T cells, 'activated' OVA specific CD4+ T cells and endogenous CD4+ T cells.

The concurrent transfer of 'pathogenic' and 'activated' CD4+ T cells illustrated a recruitment and retention of 'activated' OVA specific CD4+ T cells that are not specific for retinal antigen, which is compatible with a non-antigen specific CD4+ T cell role in active clinical disease. However, what this data also suggests is that activation alone on T cells is not sufficient enough to induce clinical disease.

However, an antigen specific stimulus is capable of inducing disease and when the stimulus is present in the form of 'pathogenic' cells to facilitate, recruitment of the OVA specific 'activated' CD4+ T cells occurs. Therefore, suggesting a non-specific recruitment of CD4+ T cells throughout clinical disease that is contributing to clinical disease course. Looking at the total cell number of the endogenous, 'pathogenic' and 'activated'

populations, it illustrates that the number of activated cells is proportionate to the other CD4+ T cell population present within the eye during active clinical disease.

Further to this the endogenous cells accumulating within the eye at this time point may also be of an activated phenotype. Due to the size of this 'activated' non-retinal specific CD4+ T cell population it suggests these cells play a role in clinical disease progression and that the recruitment of these cells suggest a non-retinal antigen specific drive takes place during disease course, the minimal CX3CR1 expression present on this population supports the hypothesis that these cells are recruited non-specifically. This data also suggests that without the pathogenic stimulus activated non-retinal specific CD4+ T cells don't remain within the ocular tissue, whereas with a pathogenic retinal antigen specific stimulus present activated non-retinal antigen specific cells are recruited to the eye and they or their progeny remain within the eye throughout clinical disease and contribute to active disease progression.

8.4 CX3CR1 in EAU

8.4.1 CX3CR1 deficiency does not affect disease severity in donor cells or recipient tissue

After determining disease course using the adoptive transfer technique in *chapter 3*, experiments investigated how knocking out both or one of the alleles of the CX3CR1 receptor effected disease course. The literature surrounding the effect of CX3CR1 on disease course in EAU is conflicted.

Firstly, comparing CX3CR1 heterozygous or total CX3CR1 allelic knockout transferred cells in RAG2$^{-/-}$ recipient mice. In comparison to the wildtype transferred cell control group, the data presented in *chapter 6* suggests no effect on severity of disease caused in recipients between the three groups, although differences in timing of disease induction is observed within the three groups. Active clinical disease is observed in the wildtype group at day 7 whereas in both the CX3CR1 heterozygous and knockout groups, active disease was not observed until day 14 after adoptive transfer. The delay in disease onset suggests that CX3CR1 heterozygous or knockout cells have reduced or slower trafficking in comparison to the wildtype control group.

On the other hand, when wildtype cells were transferred into CX3CR1 heterozygous knockout or CX3CR1 knockout recipient mice no difference in disease induction, severity

or incidence was observed. Therefore, suggesting CX3CR1 has a modest effect on disease when one or both alleles are knocked out on the transferred population in contrast to being knocked out on the endogenous population. CX3CR1 is known to be involved in leukocyte trafficking and therefore by knocking out the chemokine trafficking is slowed to the ocular tissue in the transferred population, whereas due to CX3CR1 receptor being intact on the transferred wild type cells trafficking of the cells to the ocular tissue is not effected and the host responds to the trafficking of the transferred population. However more experimentation is needed to further investigate this effect.

8.4.2 CX3CR1 is upregulated on CD4+ T cells throughout active EAU

CX3CR1 is known to be expressed on cells of myeloid lineage, but recent studies have started to investigate a role for CX3CR1 expression on CD4+ and CD8+ T cells in models of inflammation.

CX3CR1 heterozygous knockout leukocytes were transferred into wildtype Ly5 recipients to assess using the GFP present in place of one CX3CR1 allele to track CX3CR1 expression. Data presented in *chapter 6* suggests that in EAU disease progression CX3CR1 is expressed on CD4+ T cells present within the eye during disease. The proportion of transferred cells expressing CX3CR1 increases as disease progresses and reaches its peak in the eye at day 14 after adoptive transfer of leukocytes in comparison to non-lymphoid tissue. Thus, suggesting that these cells have switched on CX3CR1 expression when recruited to the eye and then have been retained throughout disease making up by day 14 a larger population of the transferred CD4+ T cells.

Previous studies have suggested that CX3CR1 upregulation on CD4+ T cells has led to increased survival and retention in the inflamed tissue. The data presented in this thesis suggests a similar potentially selective retention in the diseased tissue during active EAU of the CX3CR1 expressing CD4+ T cells. However, the mechanism for the switching on of expression of CX3CR1 requires further investigation.

8.4.3 CX3CR1 is not expressed on CD4+ T cells unless the cognate antigen is present within the tissue

The previous observation that CX3CR1 is expressed on CD4+ T cells during active clinical disease specifically in the ocular tissue in contrast to non-lymphoid tissues suggested the involvement of TCR activation directly or indirectly in CX3CR1 expression.

In *chapter 5* a double transfer technique was described utilising pathogenic retinal antigen specific CD4+ T cells transferred concurrently with a population of CD4+ T cells that are activated, OVA antigen specific. Both cell populations had one allele of the CX3CR1 locus replaced by a green fluorescent protein so in both populations CX3CR1 expression on CD4+ T cells can be monitored throughout disease course.

Data presented in *chapter 6* using this method of disease induction illustrates a specific expression of CX3CR1 on CD4+ T cells that are retinal antigen specific within the eyes in comparison to minimal CX3CR1 expression on activated OVA specific CD4+ T cells that remain in the eye sticking non-specifically during active disease. This observation suggests that activation alone is not sufficient to induce CX3CR1 expression on CD4+ T cells. Further to this, activation using an antigen in vitro (RBP or OVA) does not induce CX3CR1 expression on CD4+ T cells in both populations. However in vivo CX3CR1 expression is upregulated on retinal antigen specific CD4+ T cells that have been re-exposed to retinal antigen present in the eye, in contrast the OVA specific activated CD4+ T cell population present within the eye express minimal levels of CX3CR1. This data supports a model that when antigen specific cells are re-exposed to the antigen in vivo the response engages the TCR and therefore induces CX3CR1 on CD4+ retinal antigen specific cells that enter the eye. At time of transfer CX3CR1 expression on CD4+ T cells is <2% of the population. Whereas in the OVA specific activated CD4+ T cells, the OVA antigen is not present within the recipient mice so therefore the cells do not come into contact with the antigen in vivo. Minimal CX3CR1 expression is observed on these cells suggesting that because the cells are not re-exposed to the antigen CX3CR1 expression is not induced in these cells.

This data suggests that activation alone with the antigen is not sufficient to induce CX3CR1 expression, however when re-exposed to the antigen in vivo, CX3CR1 expression on CD4+ T cells is present.

8.4.4 CX3CR1 expression on CD4+ T cells is due to re-exposure to antigen in vivo

To determine if the expression of CX3CR1 on CD4+ T cells is retinal antigen specific in vivo, the experimental design described in *chapter 5* was used, OVA specific CD4+ CX3CR1 heterozygous cells were activated in culture similarly to the uveitogenic cell transfer technique but are stimulated using OVA peptide instead of the RBP3. After the cell culture stage recipient CX3CR1 heterozygous mice receive an intravitreal injection of OVA peptide when cells are transferred. Data presented in *chapter 5* illustrates a peak in disease at day 7/8 using clinical imaging and flow cytometry and the presence of both endogenous and transferred CD4+ T cells within the eye.

Analysis of CX3CR1 expression on CD4+ T cells using the OVA intravitreal transfer is presented in *chapter 6*. The eye injected with OVA peptide gets clinical disease that recruits both endogenous and transferred CD4+ T cells whereas the eye that receives PBS or control peptide has elevated endogenous CD4+ T cell numbers in comparison to naïve eyes but minimal transferred CD4+ are detected throughout active disease in the ocular tissue.

CX3CR1 expression is observed on both the transferred and endogenous CD4+ T cell population especially within the eye that received the intravitreal OVA. The expression of CX3CR1 on transferred CD4+ OVA specific cells support the hypothesis that CX3CR1 is expressed on CD4+ T cells in the presence of the antigen the cells are familiar with and therefore the TCR is involved in the expression of CX3CR1. However, upregulation of CX3CR1 on the endogenous CD4+ T cell population suggests expression of CX3CR1 on the endogenous CD4+ population indicates at least some of this population are interacting in the eye with cognate antigen. Therefore, suggesting CX3CR1 expression on endogenous CD4+ T cells is switched on when cells are recruited to the eye during active disease where they encounter the ocular antigen and are activated which switches CX3CR1 expression on in CD4+ T cells. In the transferred compartment it can be concluded that CX3CR1 expression is not just retinal antigen specific but specific to any antigen the CD4+ T cells are able to recognise within the tissue when activated.

8.5 The role of IL-27 in EAU

8.5.1 Disease onset is earlier in the IL-27Rα$^{-/-}$ after active immunisation

Using the adoptive transfer technique described in *chapter 3* combined with the data presented in *chapter 4* that describes a conventional disease course gives a robust technique and comparable data set to manipulate donor or recipient leukocytes (as previously demonstrated using the CX3CR1 heterozygous or CX3CR1 knockout). Due to recent studies in models of arthritis and multiple sclerosis illustrating an effect on clinical disease when inducing disease in the IL-27Rα$^{-/-}$ mouse, experiments were designed to utilise these mice as donors for adoptive transfer.

Firstly, eyes and organs from naïve IL-27Rα$^{-/-}$ mice were analysed to give a baseline for the study to detect changes in leukocyte number within the eyes of immunised mice. At day 7 after immunisation, increased leukocyte recruitment is observed in immunised mice in comparison to the naïve baseline obtained from naïve IL-27Rα$^{-/-}$ mice. Further to this, eyes from donor mice immunised for adoptive transfer from IL-27Rα$^{-/-}$ and C57BL/6 mice were analysed, and leukocytes quantified using flow cytometry. By day 11 after immunisation the IL-27Rα$^{-/-}$ mice have leukocyte numbers similar to that of peak disease in a C57BL/6 whereas in the eyes of C57BL/6 mice at day 11 after immunisation elevated leukocyte numbers are present within the eye but not comparable to peak clinical disease. In contrast to studies of EAE this data demonstrates that uveitis onset is accelerated in IL-27Rα$^{-/-}$ animals when using the active immunisation method. This could be down to the pathogenicity of the CD4+ T cells that lack the IL-27Rα$^{-/-}$ initiating a more severe response when immunised with the RBP3 antigen. Studies (280) have also suggested dysfunction of the Treg population due to the lack of the IL-27Rα could contribute to disease induction and severity due to lack of regulation.

8.5.2 IL-27Rα$^{-/-}$ leukocytes are more pathogenic and cause a more severe and persistent disease phenotype when disease is induced using the adoptive transfer technique

The evidence presented in this thesis leads to the conclusion that CD4+ T cells are more pathogenic from an IL-27Rα$^{-/-}$ mouse in comparison to CD4+ T cells from a wildtype C57BL/6. Firstly, after immunisation leukocytes were isolated and stimulated in cell culture, after this step supernatant from the cell cultures was obtained and analysed using

the LegendPLex platform. Concentration of cytokines within the supernatant of both the IL-27Rα$^{-/-}$ and wildtype C57BL/6 cell cultures were calculated. There is a significant increase in the concentration of cytokines present within the IL-27Rα$^{-/-}$ leukocyte cultures in comparison to the wildtype C57BL/6 cultures. The increase in cytokine production in the IL-27Rα$^{-/-}$ culture supernatant suggests a more pathogenic phenotype is present.

This is further supported by observations made about disease phenotype after the adoptive transfer of IL-27Rα$^{-/-}$ leukocytes into wildtype C57BL/6 recipients. At early time points a more severe disease is present within the eyes of recipients in comparison to the wildtype transfer with the same number of CD4+ T cells. The differences in disease severity between the two groups cannot be attributed to Tregs as the recipient wildtype mice have intact Treg populations. But no difference was observed in disease initiation between the two groups which was observed within the active immunisation group of IL-27Rα$^{-/-}$ mice, which further supports the hypothesis that dysfunctional Tregs due to IL-27Rα$^{-/-}$ initiates early onset disease.

Using OCT imaging to follow clinical disease course allows analysis of disease throughout active disease and during disease resolution. The imaging data illustrates a persistent and more severe disease phenotype in the IL-27Rα$^{-/-}$ transfer recipients in comparison to the C57BL/6 transfer. IL-27Rα$^{-/-}$ has been implicated in causing a more severe and persistent disease phenotype in other models of autoimmune disease including adjuvant induced arthritis and experimental autoimmune encephalitis. AIA was induced in IL-27Rα$^{-/-}$mice and disease monitored in comparison to a wildtype group, exacerbated joint pathology denoted by increased leukocyte infiltration, synovial exudate, hypertrophy and hallmarks of cartilage and bone erosion (269). This data suggests IL-27 is a key mediator of immune response homeostasis in autoimmune conditions such as arthritis. The same pattern of more severe disease pathology is observed within the adoptive transfer model of EAU. Further to this using the clinical imaging to monitor clinical disease, the IL-27Rα$^{-/-}$ recipients illustrate no disease resolution and persistence of active clinical disease through to day 67. Analysis of clinical disease from day 67 to day 144 using clinical imaging illustrates active disease resolution in some recipients however in others active disease persisted to day 144 after adoptive transfer when samples were taken for flow cytometric analysis.

8.5.3 IL-27Rα$^{-/-}$ CD4+ T cells persist within the eyes of recipients through to day 144 after adoptive transfer

Clinical imaging allows disease monitoring throughout active disease and to compare disease phenotype across recipient groups. Combined with quantification of leukocytes present within the eyes of recipient's differences in leukocyte infiltration can be attributed to differences in disease severity or phenotype.

At day 67 after adoptive transfer the only population to persist within the eyes of the IL-27Rα$^{-/-}$ recipients are transferred CD4+ T cells, and in large enough numbers to drive clinical disease whereas in the wildtype transfer group minimal numbers of transferred and endogenous leukocytes are present within the recipient tissue. This data suggests that the persistence of the IL-27Rα$^{-/-}$ CD4+ T cells is driving active disease and initiating recruitment of endogenous CD4+ T cells along with other endogenous leukocytes such as neutrophils and myeloid cells.

Continuing disease course through to day 144 illustrates a further persistence of the IL-27Rα$^{-/-}$ CD4+ T cells. With many recipients still with active clinical disease at this time point due to the persistence of this CD4+ T cell population driving disease.

This collated data suggests a more potent and persistent phenotype of CD4+ T cell that can survive within the tissue and drive disease through to day 144 after adoptive transfer.

8.6 Final Discussion

This study investigates the basic mechanisms underlying the induction and progression of EAU. The basic mechanism underpinning clinical symptoms is poorly understood within human uveitis, in order to develop new treatments for the disease it is important to understand how and why disease develops. The work in this thesis can help with further understanding on the disease process.

The work in this thesis illustrates manipulation of disease using IL-27Rα$^{-/-}$ and CX3CR1$^{+/GFP}$ and CX3CR1$^{GFP/GFP}$ knockout mice, therefore using the adoptive transfer model optimised in previous chapters more detailed investigation of how these targets affect disease course and determine further targets for treatment of uveitis can be determined. Further studies of the effects of different cytokines and chemokines on disease course could be

achieved by combining different knockout mouse strains or by CRISPR/Cas9 knockout of genes of interest.

Overall, the data in this thesis gives an optimised method of tracking antigen specific cells that drive disease and non-retinal antigen specific cells which are non-specifically recruited throughout disease course. The adoptive transfer technique further allows expression of chemokines to be monitored throughout disease and how receptor knockouts influence disease course.

Further to this from the original hypothesis set out for this thesis we have developed and optimised sensitive method of analysis of naïve and diseased ocular tissue and used this method to track allelically marked CD4+ T cells that drive disease and persist within the tissue after active clinical disease has resolved along with the recruitment of endogenous CD4+ T cells and studied their role in disease. The mechanism of recruitment of endogenous and transferred cells to the ocular tissue has been observed to be of antigen-specific nature but recruitment of transferred non-antigen specific cells is observed when a pathogenic cell stimulus is present. Upregulation of CX3CR1 in increased frequencies was observed during active clinical disease due to an antigen-specific response and finally IL-27R$\alpha^{-/-}$ T cells cause a more long-lived and severe disease phenotype and persist within the ocular tissue in increased numbers for longer to drive active clinical disease.

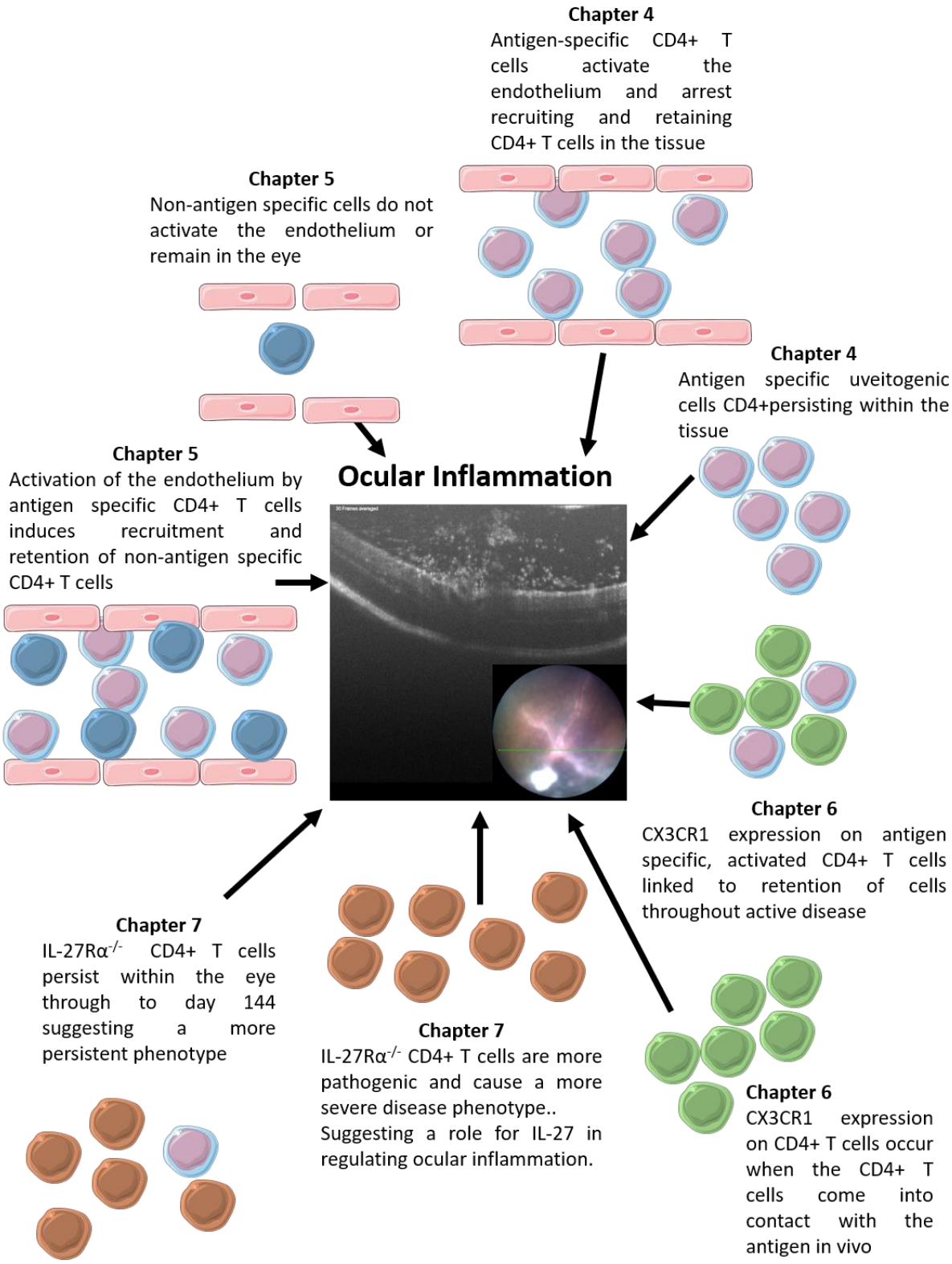

Figure 8.1: Overview of thesis findings

Chapter 9. Future Directions

9. Future Directions

9.1 Nonspecific recruitment of CD4+ T cells throughout clinical disease

As illustrated in *chapter 5* recruitment of non-antigen specific CD4+ T cells when a uveitogenic stimulus is present was observed throughout active clinical disease. Further experimentation into what is causing the retention of non-specific CD4+ T cells within the eye could be achieved by the use of endothelial cell markers that are upregulated during active disease course that would influence retention of non-antigen specific CD4+ T cells. Distribution within the tissue of the antigen-specific and non-specific cells are retained specifically if they are resting on the endothelium or dispersed throughout the retina and vitreous.

Further to this, the CRISPR/Cas9 system of gene editing could be utilised to knock out genes that effect disease progression and could be involved in the non-specific retention of CD4+ T cells. Firstly, to test if virally transduced cells survive in vivo and are capable of causing disease. Using a retroviral construct of F-tractin tagged GFP. CRISPR/Cas9 can then be utilised to knockout genes that can be assumed to cause a more severe disease phenotype including CTLA-4 or from the work presented in this thesis IL-27Rα or knockout genes that can be assumed to cause a less severe disease phenotype including CD28. After optimisation of this platform specific genes can be selected to target on OVA antigen specific CD4+ T cells before concurrent adoptive transfer with retinal antigen specific CD4+ T cells to monitor if the OVA specific cells are retained throughout active disease after specific genes are knocked out to manipulate disease course and reduce disease severity.

9.2 The role of initial disease-causing antigen specific cells in EAU disease course

The persistence of the disease initiating antigen specific CD4+ T cells throughout clinical disease is highlighted within this thesis (*chapter 4*). Using RNA sequencing at a number of late disease time points could identify genes present in the total CD4+ and CD8+ T cell population to identify differences in gene expression in cells retained in the eye past active clinical disease. This technique allows comparisons between clinical disease points past active disease but also could be used to analyse differential gene expression in endogenous and transferred CD4+ T cell populations during active disease.

The role of the transferred antigen specific cells in disease initiation by activation of the endothelium was highlighted in (*chapter 4*) but further analysis into how transferred cells are involved in the initiation and progression of clinical disease can be investigated using antibody depletion of the transferred population before active peak disease occurs. This experiment will determine the role of transferred antigen specific cells in continuing active disease course and whether the endogenous compartment of CD4+ T cells is capable of continuing disease course without the presence of the antigen specific pathogenic transferred CD4+ T cells.

Further to this the proliferation status of the transferred CD4+ population during active disease. Using a Ki67 antibody stain we can determine if the cells are in the active phase of the cell cycle and are therefore proliferating or the increase in transferred number present in the eye during active clinical disease is due purely to recruitment of transferred cells from the blood, spleen and lymph nodes.

9.3 CX3CR1 expression on CD4+ T cells throughout clinical disease

The expression of CX3CR1 on CD4+ T cells due to an antigen specific response is presented in *chapter 6*. To investigate if CX3CR1 is also expressed on CD4+ T cells in vitro cultures, OVA specific CD4+ T cells cocultured with antigen and CD3 CD28 stimulation to quantify CX3CR1 expression on CD4+ T cells.

Further experiments include utilising the $RAG2^{-/-}$ mice to transfer cells from transfer recipients at peak disease in Ly5 recipients. CD4+ transferred T cells from recipient eyes at peak disease can be sorted into CX3CR1+ CD4+ T cells and transferred into one group of recipients and sort CX3CR1- CD4+ T cells to transfer into another group of recipients. This experiment will allow differences in disease course based on CX3CR1 expression of CD4+ T cells with the hypothesis that CX3CR1+ CD4+ T cells are more capable of causing disease and persisting during active disease in comparison to the CX3CR1- CD4+ T cell population.

Analysis of differential gene expression in these recipients could be investigated by focussed analysis of the expression of functional gene sets that are associated with changes in T cell effector potential specifically analysing intracellular cytokine expression including IFN-γ, IL-17 and TNF. Regulatory and activation threshold markers including; FoxP3, CD5, CD39 and CD73, coinhibitory markers BTLA, TIM3, CTLA4, LAG3, PD1 and TIGIT and costimulatory markers (41BB, CD25, CD28, GITR, ICOS and OX40 using flow cytometry antibody panels.

Further to this RNA seq analysis of levels of mRNA followed by unsupervised analysis of differential gene expression will complement the previous study. Using total cell count of CD4+ T cells at different time points throughout disease course and with differing CX3CR1 expression levels to compare cross different disease-causing cells.

Due to the antigen specific nature of CX3CR1 expression on CD4+ T cells analysis of the TCR of CX3CR1+ CD4+ T cells using single cell sequencing. This platform allows single cell analysis at the transcript level with concurrent analysis of the TCR repertoire of each individual cell. Firstly, using the OTII transfer model with intravitreal OVA followed by analysis of the uveitogenic transfer model.

9.4 IL-27Rα$^{-/-}$ causes a more potent CD4+ T cell phenotype

As described in *chapter 7* knocking out the IL-27Rα in transferred CD4+ T cells causes a more severe cell phenotype that persists throughout active disease and continues to drive disease to cause a longer more severe disease within the recipients. Further experimentation could include phenotyping the CD4+ T cell populations within both groups of recipients to identify the role of CD4+ T cell phenotype in disease progression including early disease time points and late disease time points such as staining for IFN-γ, IL-17 and FoxP3 using flow cytometry antibodies before including analysis of differential gene expression in recipients by quantifying expression of functional gene sets that are associated with changes in T cell effector potential specifically analysing intracellular cytokine expression including IFN-γ, IL-17 and TNF. Regulatory and activation threshold markers including FoxP3, CD5, CD39 and CD73, coinhibitory markers BTLA, TIM3, CTLA4, LAG3, PD1 and TGIT and costimulatory markers (41BB, CD25, CD28, GITR, ICOS and OX40.

The effect of IL-27Rα knockout on CD4+ T cells has contributed to differences in disease phenotype but how this difference in clinical disease affects the structure and function of the tissue. Using histological sections to analyse the structures present within the eye to determine any abnormalities across disease groups, alternatively further analysis using whole retina flat mounts allows study of dispersion within the retina of immune infiltrate.

- T cells to the eye in addition to sticking of transferred CD4+ T cells. (*chapter 5*)
- Active uveitis enhances the recruitment of non-antigen specific activated T cells. (*chapter 5*)

- CX3CR1 is upregulated on CD4+ T cells in the eye during EAU. The upregulation of CX3CR1 is due to antigen-specific response by CD4+ T cells. (*chapter 6*)
- IL-27Rα$^{-/-}$ CD4+ T cells cause a more severe persistent clinical disease when adoptively transferred into wildtype C57BL/6 recipients. CD4+ T cells that are IL-27Rα$^{-/-}$ are more pathogenic and persist long term within the eye driving clinical disease. (*chapter 7*)

Thus, this work provides new insights into the role of antigen-specific uveitogenic CD4+ T cells, disease-associated non-antigen-specific CD4+ T cells and the important role of IL-27 in the regulation of disease.

8.2 Induction of EAU by adoptive transfer

The work presented in this thesis uses the adoptive transfer of antigen-specific or non-antigen-specific leukocytes. The adoptive transfer of antigen-specific uveitogenic leukocytes efficiently induces EAU in naive C57BL/6 recipients. As demonstrated in RAG2$^{-/-}$ mice in *Chapter 3*, disease induction and progression are CD4+ T cell mediated. Using the adoptive transfer of whole leukocyte populations allows the transferred and endogenous T cell populations to be distinguished and therefore gives us the ability to determine the long-term fate of the initial transferred cells, including the CD4+ transferred population.

8.2.1 The fate of transferred antigen specific CD4+ T cells throughout clinical disease

Transferred pathogenic antigen-specific cells are capable of inducing clinical disease in wildtype C57BL/6 (Ly5) recipients. The transferred CD4+ T cells give rise to a population that persists within the eye throughout clinical disease course this is highlighted in *Chapter 4*. This leads to a recruitment of endogenous CD4+ T cells that is observed from day 2 and increases as peak disease is reached at day 7-10 thus suggesting the host's own immune response responds to the pathogenic stimulus of the transferred antigen-specific T cells.

At day 2, the number of endogenous CD4+ T cells present within the eyes of recipient mice increases concurrently with the presence of transferred CD4+ T cells at this time point, suggesting an activation of the endothelium has occurred due to the transfer of antigen specific activated CD4+ T cells. We hypothesised that activation of the endothelium could be due to an antigen-specific stimulus due to the pathogenic nature of the transferred CD4+ T cells or alternatively due to the activation status of the transferred CD4+ T cells. This question will be discussed later on in this section.

Analysis of clinical disease course after adoptive transfer was achieved by OCT imaging and by quantification of leukocyte number by flow cytometry. These methods of analysis allowed active clinical disease to be monitored and the proportion of endogenous and transferred cells. It has previously been reported that initial disease causing CD4+ T cells or the progeny of these cells do not persist within the inflamed tissue throughout active disease and go through apoptosis as active clinical disease is resolving (282), however the data presented in *chapter 4*, suggests that in EAU the original antigen specific transferred CD4+ T cells or their progeny have persisted within the eyes of the recipient mice and have driven the disease process or have been recruited to the eye during the disease process and have persisted within the tissue past active clinical disease. This finding is in contrast to a study by Oh et al where they describe the fate of autoreactive T cells that mediate uveitis to reside in the bone marrow after acute uveitic disease and not the ocular tissue (283). However, fate mapping would be required to understand the population of transferred cells that have survived within the tissue.

8.2.2 Transferred cells activate the endothelium after adoptive transfer causing a recruitment of both endogenous and transferred CD4+ T cells

After adoptive transfer of leukocytes, recipients were monitored using OCT imaging to assess early signs of clinical disease. Active disease was not detected on OCT before day 5, at this point swelling of the optic disc was a sign of early active clinical disease.

Although changes are not detectable by OCT at day 2 in many recipients, quantification of leukocytes at day 2 after adoptive transfer is a more sensitive measure of active clinical disease. As highlighted in *Chapter 4* at day 2 after adoptive transfer an increase in endogenous CD4+ T cell number is observed. Concurrently with this observation a

population of transferred CD4+ T cells is detected within the ocular tissue which is not seen after transfer of non-antigen specific cells.

The presence of transferred CD4+ T cells and the increased number of endogenous CD4+ T cells suggests a mechanism involved in disease induction has already begun to impact the ocular tissue. We hypothesised that the recruitment of transferred CD4 cells to the ocular tissue by day 2 after adoptive transfer is due to an activation of the endothelium due to the activation status or antigen-specific nature of the transferred cells.

The role of endothelial cells in the recruitment of lymphocytes, monocytes, neutrophils and dendritic cells into lymph nodes and tissues depends on an intimate relationship between endothelial cells and immune cells (284). The recruitment of immune cells is selective and can be influenced by an immune stimulus to trigger the trafficking process along with mediators produced by endothelial cells (284). Therefore, the endothelium can play a vital role in the immune response and in the adoptive transfer model of EAU a role in disease initiation.

Further investigation into the immune stimulus linked to the recruitment of transferred CD4+ T cells that induces the increased recruitment and sticking of endogenous CD4+ T cells will be discussed with the relevant data presented from *chapter 5.*

8.3 Antigen specific and non-antigen specific CD4+ T cell recruitment in EAU

8.3.1 Increased recruitment and retention of endogenous CD4+ T cells at day 2 after adoptive transfer of CD4+ T cells is due to an antigen-specific stimulus

At day 2 after adoptive transfer of uveitogenic, antigen specific CD4+ T cells there is an increase in recruitment and retention of endogenous CD4+ T cells.

Further experimentation investigated whether the endothelium becomes activated in response to the transferred CD4+ T cells being in an activated state or due to their antigen specificity. Therefore, using OVA TCR transgenic leukocytes allowed us to address the question of activation versus antigen-specificity facilitating increased endogenous CD4+ T cell recruitment and transferred cells sticking within the ocular tissue to cause clinical disease.

Adoptive transfer of activated non retinal antigen specific leukocytes from an OVA TCR transgenic mouse does not initiate activation of the endothelium to the level seen with

an antigen specific response, this is suggested by no increase in endogenous CD4+ T cell recruitment and almost no retention of the transferred OVA- specific activated. However, previous studies have highlighted the ability of activated T cells to migrate across normal, non-inflamed endothelium at day 1 ~44 cells had infiltrated the eyes of recipient mice when $10x10^6$ activated T cells are transferred (285).

An i.p injection of PBS, without activated or unactivated cells will still initiate a measurable and statistically significant increase in recruitment and retention of endogenous CD4+ T cells at day 2 after injection, this effect could be caused by endotoxin release at the site of injection that stimulates the endothelium to upregulate molecules that retain CD4+ T cells at this early time point. Increased trafficking does not lead to initiation of uveitic disease and by day 7 has resolved, thus suggesting that without a pathogenic stimulus the endothelium does not become activated to recruit and retain endogenous and transferred cells that cause disease.

Therefore, this data suggests a local antigen-specific response is required to induce disease progression through endothelial activation that leads to endogenous and transferred CD4+ T cell recruitment. This conclusion was further confirmed using the OVA TCR specific cell transfer of activated OVA antigen-specific OTII cells with a concurrent intravitreal injection of OVA given just prior to cell transfer presented in *chapter 5*. This data confirmed that the recruitment of transferred and endogenous cells observed at day 2 after adoptive transfer is not retinal antigen specific but an antigen-specific response to any antigen in the local environment and has the ability to induce recruitment of endogenous and transferred CD4+ T cells.

8.3.2 Antigen-specific transferred CD4+ T cells initiate recruitment of antigen and non-antigen specific CD4+ T cells throughout ocular inflammation

As previously discussed, activated non-antigen specific CD4+ T cells are not capable of inducing endothelial activation defined by significant endogenous cell recruitment and do not remain within the ocular tissue past day 2 after adoptive transfer. Although the endogenous CD4+ T cell number does increase due to the release of endotoxin at the site of injection.

Data has demonstrated an antigen-specific stimulus induces the activation of the endothelium. However, further experiments including the co-transfer of retinal antigen

specific activated CD4+ T cells with OVA specific activated CD4+ T cells at a 1:1 ratio. These experiments allowed for tracking of transferred 'pathogenic' retinal antigen specific CD4+ T cells, 'activated' OVA specific CD4+ T cells and endogenous CD4+ T cells.

The concurrent transfer of 'pathogenic' and 'activated' CD4+ T cells illustrated a recruitment and retention of 'activated' OVA specific CD4+ T cells that are not specific for retinal antigen, which is compatible with a non-antigen specific CD4+ T cell role in active clinical disease. However, what this data also suggests is that activation alone on T cells is not sufficient enough to induce clinical disease.

However, an antigen specific stimulus is capable of inducing disease and when the stimulus is present in the form of 'pathogenic' cells to facilitate, recruitment of the OVA specific 'activated' CD4+ T cells occurs. Therefore, suggesting a non-specific recruitment of CD4+ T cells throughout clinical disease that is contributing to clinical disease course. Looking at the total cell number of the endogenous, 'pathogenic' and 'activated' populations, it illustrates that the number of activated cells is proportionate to the other CD4+ T cell population present within the eye during active clinical disease.

Further to this the endogenous cells accumulating within the eye at this time point may also be of an activated phenotype. Due to the size of this 'activated' non-retinal specific CD4+ T cell population it suggests these cells play a role in clinical disease progression and that the recruitment of these cells suggest a non-retinal antigen specific drive takes place during disease course, the minimal CX3CR1 expression present on this population supports the hypothesis that these cells are recruited non-specifically. This data also suggests that without the pathogenic stimulus activated non-retinal specific CD4+ T cells don't remain within the ocular tissue, whereas with a pathogenic retinal antigen specific stimulus present activated non-retinal antigen specific cells are recruited to the eye and they or their progeny remain within the eye throughout clinical disease and contribute to active disease progression.

8.4 CX3CR1 in EAU

8.4.1 CX3CR1 deficiency does not affect disease severity in donor cells or recipient tissue

After determining disease course using the adoptive transfer technique in *chapter 3*, experiments investigated how knocking out both or one of the alleles of the CX3CR1

receptor effected disease course. The literature surrounding the effect of CX3CR1 on disease course in EAU is conflicted.

Firstly, comparing CX3CR1 heterozygous or total CX3CR1 allelic knockout transferred cells in RAG2$^{-/-}$ recipient mice. In comparison to the wildtype transferred cell control group, the data presented in *chapter 6* suggests no effect on severity of disease caused in recipients between the three groups, although differences in timing of disease induction is observed within the three groups. Active clinical disease is observed in the wildtype group at day 7 whereas in both the CX3CR1 heterozygous and knockout groups, active disease was not observed until day 14 after adoptive transfer. The delay in disease onset suggests that CX3CR1 heterozygous or knockout cells have reduced or slower trafficking in comparison to the wildtype control group.

On the other hand, when wildtype cells were transferred into CX3CR1 heterozygous knockout or CX3CR1 knockout recipient mice no difference in disease induction, severity or incidence was observed. Therefore, suggesting CX3CR1 has a modest effect on disease when one or both alleles are knocked out on the transferred population in contrast to being knocked out on the endogenous population. CX3CR1 is known to be involved in leukocyte trafficking and therefore by knocking out the chemokine trafficking is slowed to the ocular tissue in the transferred population, whereas due to CX3CR1 receptor being intact on the transferred wild type cells trafficking of the cells to the ocular tissue is not effected and the host responds to the trafficking of the transferred population. However more experimentation is needed to further investigate this effect.

8.4.2 CX3CR1 is upregulated on CD4+ T cells throughout active EAU

CX3CR1 is known to be expressed on cells of myeloid lineage, but recent studies have started to investigate a role for CX3CR1 expression on CD4+ and CD8+ T cells in models of inflammation.

CX3CR1 heterozygous knockout leukocytes were transferred into wildtype Ly5 recipients to assess using the GFP present in place of one CX3CR1 allele to track CX3CR1 expression. Data presented in *chapter 6* suggests that in EAU disease progression CX3CR1 is expressed on CD4+ T cells present within the eye during disease. The proportion of transferred cells expressing CX3CR1 increases as disease progresses and reaches its peak in the eye at day 14 after adoptive transfer of leukocytes in comparison to non-lymphoid tissue. Thus,

suggesting that these cells have switched on CX3CR1 expression when recruited to the eye and then have been retained throughout disease making up by day 14 a larger population of the transferred CD4+ T cells.

Previous studies have suggested that CX3CR1 upregulation on CD4+ T cells has led to increased survival and retention in the inflamed tissue. The data presented in this thesis suggests a similar potentially selective retention in the diseased tissue during active EAU of the CX3CR1 expressing CD4+ T cells. However, the mechanism for the switching on of expression of CX3CR1 requires further investigation.

8.4.3 CX3CR1 is not expressed on CD4+ T cells unless the cognate antigen is present within the tissue

The previous observation that CX3CR1 is expressed on CD4+ T cells during active clinical disease specifically in the ocular tissue in contrast to non-lymphoid tissues suggested the involvement of TCR activation directly or indirectly in CX3CR1 expression.

In *chapter 5* a double transfer technique was described utilising pathogenic retinal antigen specific CD4+ T cells transferred concurrently with a population of CD4+ T cells that are activated, OVA antigen specific. Both cell populations had one allele of the CX3CR1 locus replaced by a green fluorescent protein so in both populations CX3CR1 expression on CD4+ T cells can be monitored throughout disease course.

Data presented in *chapter 6* using this method of disease induction illustrates a specific expression of CX3CR1 on CD4+ T cells that are retinal antigen specific within the eyes in comparison to minimal CX3CR1 expression on activated OVA specific CD4+ T cells that remain in the eye sticking non-specifically during active disease. This observation suggests that activation alone is not sufficient to induce CX3CR1 expression on CD4+ T cells. Further to this, activation using an antigen in vitro (RBP or OVA) does not induce CX3CR1 expression on CD4+ T cells in both populations. However in vivo CX3CR1 expression is upregulated on retinal antigen specific CD4+ T cells that have been re-exposed to retinal antigen present in the eye, in contrast the OVA specific activated CD4+ T cell population present within the eye express minimal levels of CX3CR1. This data supports a model that

when antigen specific cells are re-exposed to the antigen in vivo the response engages the TCR and therefore induces CX3CR1 on CD4+ retinal antigen specific cells that enter the eye. At time of transfer CX3CR1 expression on CD4+ T cells is <2% of the population. Whereas in the OVA specific activated CD4+ T cells, the OVA antigen is not present within the recipient mice so therefore the cells do not come into contact with the antigen in vivo. Minimal CX3CR1 expression is observed on these cells suggesting that because the cells are not re-exposed to the antigen CX3CR1 expression is not induced in these cells.

This data suggests that activation alone with the antigen is not sufficient to induce CX3CR1 expression, however when re-exposed to the antigen in vivo, CX3CR1 expression on CD4+ T cells is present.

8.4.4 CX3CR1 expression on CD4+ T cells is due to re-exposure to antigen in vivo

To determine if the expression of CX3CR1 on CD4+ T cells is retinal antigen specific in vivo, the experimental design described in *chapter 5* was used, OVA specific CD4+ CX3CR1 heterozygous cells were activated in culture similarly to the uveitogenic cell transfer technique but are stimulated using OVA peptide instead of the RBP3. After the cell culture stage recipient CX3CR1 heterozygous mice receive an intravitreal injection of OVA peptide when cells are transferred. Data presented in *chapter 5* illustrates a peak in disease at day 7/8 using clinical imaging and flow cytometry and the presence of both endogenous and transferred CD4+ T cells within the eye.

Analysis of CX3CR1 expression on CD4+ T cells using the OVA intravitreal transfer is presented in *chapter 6*. The eye injected with OVA peptide gets clinical disease that recruits both endogenous and transferred CD4+ T cells whereas the eye that receives PBS or control peptide has elevated endogenous CD4+ T cell numbers in comparison to naïve eyes but minimal transferred CD4+ are detected throughout active disease in the ocular tissue.

CX3CR1 expression is observed on both the transferred and endogenous CD4+ T cell population especially within the eye that received the intravitreal OVA. The expression of CX3CR1 on transferred CD4+ OVA specific cells support the hypothesis that CX3CR1 is expressed on CD4+ T cells in the presence of the antigen the cells are familiar with and therefore the TCR is involved in the expression of CX3CR1. However, upregulation of

CX3CR1 on the endogenous CD4+ T cell population suggests expression of CX3CR1 on the endogenous CD4+ population indicates at least some of this population are interacting in the eye with cognate antigen. Therefore, suggesting CX3CR1 expression on endogenous CD4+ T cells is switched on when cells are recruited to the eye during active disease where they encounter the ocular antigen and are activated which switches CX3CR1 expression on in CD4+ T cells. In the transferred compartment it can be concluded that CX3CR1 expression is not just retinal antigen specific but specific to any antigen the CD4+ T cells are able to recognise within the tissue when activated.

8.5 The role of IL-27 in EAU

8.5.1 Disease onset is earlier in the IL-27Rα$^{-/-}$ after active immunisation

Using the adoptive transfer technique described in *chapter 3* combined with the data presented in *chapter 4* that describes a conventional disease course gives a robust technique and comparable data set to manipulate donor or recipient leukocytes (as previously demonstrated using the CX3CR1 heterozygous or CX3CR1 knockout). Due to recent studies in models of arthritis and multiple sclerosis illustrating an effect on clinical disease when inducing disease in the IL-27Rα$^{-/-}$ mouse, experiments were designed to utilise these mice as donors for adoptive transfer.

Firstly, eyes and organs from naïve IL-27Rα$^{-/-}$ mice were analysed to give a baseline for the study to detect changes in leukocyte number within the eyes of immunised mice. At day 7 after immunisation, increased leukocyte recruitment is observed in immunised mice in comparison to the naïve baseline obtained from naïve IL-27Rα$^{-/-}$ mice. Further to this, eyes from donor mice immunised for adoptive transfer from IL-27Rα$^{-/-}$ and C57BL/6 mice were analysed, and leukocytes quantified using flow cytometry. By day 11 after immunisation the IL-27Rα$^{-/-}$ mice have leukocyte numbers similar to that of peak disease in a C57BL/6 whereas in the eyes of C57BL/6 mice at day 11 after immunisation elevated leukocyte numbers are present within the eye but not comparable to peak clinical disease. In contrast to studies of EAE this data demonstrates that uveitis onset is accelerated in IL-27Rα$^{-/-}$ animals when using the active immunisation method. This could be down to the

pathogenicity of the CD4+ T cells that lack the IL-27Rα$^{-/-}$ initiating a more severe response when immunised with the RBP3 antigen. Studies (280) have also suggested dysfunction of the Treg population due to the lack of the IL-27Rα could contribute to disease induction and severity due to lack of regulation.

8.5.2 IL-27Rα$^{-/-}$ leukocytes are more pathogenic and cause a more severe and persistent disease phenotype when disease is induced using the adoptive transfer technique

The evidence presented in this thesis leads to the conclusion that CD4+ T cells are more pathogenic from an IL-27Rα$^{-/-}$ mouse in comparison to CD4+ T cells from a wildtype C57BL/6. Firstly, after immunisation leukocytes were isolated and stimulated in cell culture, after this step supernatant from the cell cultures was obtained and analysed using the LegendPLex platform. Concentration of cytokines within the supernatant of both the IL-27Rα$^{-/-}$ and wildtype C57BL/6 cell cultures were calculated. There is a significant increase in the concentration of cytokines present within the IL-27Rα$^{-/-}$ leukocyte cultures in comparison to the wildtype C57BL/6 cultures. The increase in cytokine production in the IL-27Rα$^{-/-}$ culture supernatant suggests a more pathogenic phenotype is present.

This is further supported by observations made about disease phenotype after the adoptive transfer of IL-27Rα$^{-/-}$ leukocytes into wildtype C57BL/6 recipients. At early time points a more severe disease is present within the eyes of recipients in comparison to the wildtype transfer with the same number of CD4+ T cells. The differences in disease severity between the two groups cannot be attributed to Tregs as the recipient wildtype mice have intact Treg populations. But no difference was observed in disease initiation between the two groups which was observed within the active immunisation group of IL-27Rα$^{-/-}$ mice, which further supports the hypothesis that dysfunctional Tregs due to IL-27Rα$^{-/-}$ initiates early onset disease.

Using OCT imaging to follow clinical disease course allows analysis of disease throughout active disease and during disease resolution. The imaging data illustrates a persistent and more severe disease phenotype in the IL-27Rα$^{-/-}$ transfer recipients in comparison to the C57BL/6 transfer. IL-27Rα$^{-/-}$ has been implicated in causing a more severe and persistent disease phenotype in other models of autoimmune disease including adjuvant induced arthritis and experimental autoimmune encephalitis. AIA was induced in IL-27Rα$^{-/-}$mice and disease monitored in comparison to a wildtype group, exacerbated joint pathology

denoted by increased leukocyte infiltration, synovial exudate, hypertrophy and hallmarks of cartilage and bone erosion (269). This data suggests IL-27 is a key mediator of immune response homeostasis in autoimmune conditions such as arthritis. The same pattern of more severe disease pathology is observed within the adoptive transfer model of EAU. Further to this using the clinical imaging to monitor clinical disease, the IL-27Rα$^{-/-}$ recipients illustrate no disease resolution and persistence of active clinical disease through to day 67. Analysis of clinical disease from day 67 to day 144 using clinical imaging illustrates active disease resolution in some recipients however in others active disease persisted to day 144 after adoptive transfer when samples were taken for flow cytometric analysis.

8.5.3 IL-27Rα$^{-/-}$ CD4+ T cells persist within the eyes of recipients through to day 144 after adoptive transfer

Clinical imaging allows disease monitoring throughout active disease and to compare disease phenotype across recipient groups. Combined with quantification of leukocytes present within the eyes of recipient's differences in leukocyte infiltration can be attributed to differences in disease severity or phenotype.

At day 67 after adoptive transfer the only population to persist within the eyes of the IL-27Rα$^{-/-}$ recipients are transferred CD4+ T cells, and in large enough numbers to drive clinical disease whereas in the wildtype transfer group minimal numbers of transferred and endogenous leukocytes are present within the recipient tissue. This data suggests that the persistence of the IL-27Rα$^{-/-}$ CD4+ T cells is driving active disease and initiating recruitment of endogenous CD4+ T cells along with other endogenous leukocytes such as neutrophils and myeloid cells.

Continuing disease course through to day 144 illustrates a further persistence of the IL-27Rα$^{-/-}$ CD4+ T cells. With many recipients still with active clinical disease at this time point due to the persistence of this CD4+ T cell population driving disease.

This collated data suggests a more potent and persistent phenotype of CD4+ T cell that can survive within the tissue and drive disease through to day 144 after adoptive transfer.

8.6 Final Discussion

This study investigates the basic mechanisms underlying the induction and progression of EAU. The basic mechanism underpinning clinical symptoms is poorly understood within human uveitis, in order to develop new treatments for the disease it is important to understand how and why disease develops. The work in this thesis can help with further understanding on the disease process.

The work in this thesis illustrates manipulation of disease using IL-27Rα$^{-/-}$ and CX3CR1$^{+/GFP}$ and CX3CR1$^{GFP/GFP}$ knockout mice, therefore using the adoptive transfer model optimised in previous chapters more detailed investigation of how these targets affect disease course and determine further targets for treatment of uveitis can be determined. Further studies of the effects of different cytokines and chemokines on disease course could be achieved by combining different knockout mouse strains or by CRISPR/Cas9 knockout of genes of interest.

Overall, the data in this thesis gives an optimised method of tracking antigen specific cells that drive disease and non-retinal antigen specific cells which are non-specifically recruited throughout disease course. The adoptive transfer technique further allows expression of chemokines to be monitored throughout disease and how receptor knockouts influence disease course.

Further to this from the original hypothesis set out for this thesis we have developed and optimised sensitive method of analysis of naïve and diseased ocular tissue and used this method to track allelically marked CD4+ T cells that drive disease and persist within the tissue after active clinical disease has resolved along with the recruitment of endogenous CD4+ T cells and studied their role in disease. The mechanism of recruitment of endogenous and transferred cells to the ocular tissue has been observed to be of antigen-specific nature but recruitment of transferred non-antigen specific cells is observed when a pathogenic cell stimulus is present. Upregulation of CX3CR1 in increased frequencies was observed during active clinical disease due to an antigen-specific response and finally IL-27Rα$^{-/-}$ T cells cause a more long-lived and severe disease phenotype and persist within the ocular tissue in increased numbers for longer to drive active clinical disease.

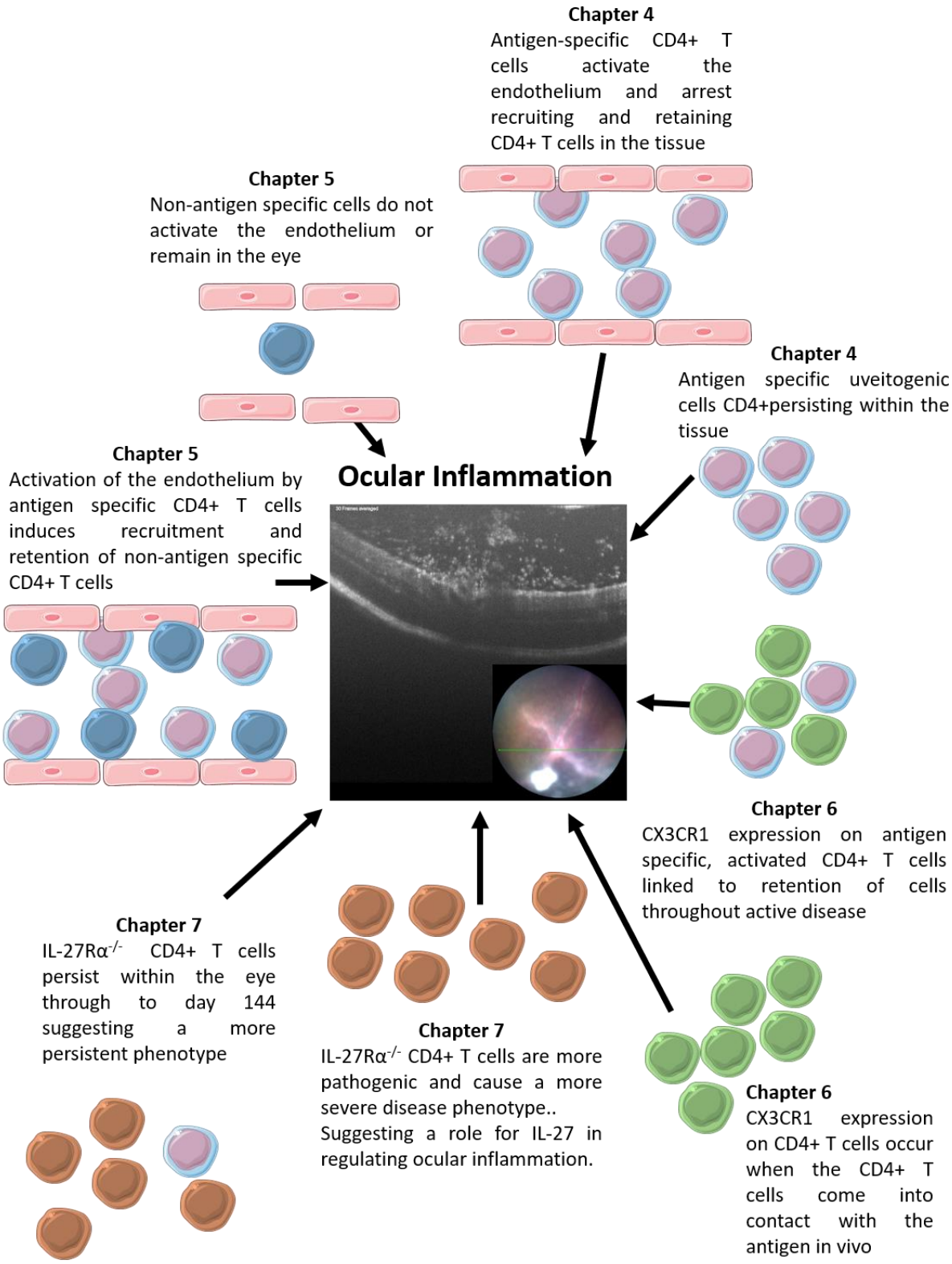

Figure 8.1: Overview of thesis findings

Chapter 9. Future Directions

9. Future Directions

9.1 Nonspecific recruitment of CD4+ T cells throughout clinical disease

As illustrated in *chapter 5* recruitment of non-antigen specific CD4+ T cells when a uveitogenic stimulus is present was observed throughout active clinical disease. Further experimentation into what is causing the retention of non-specific CD4+ T cells within the eye could be achieved by the use of endothelial cell markers that are upregulated during active disease course that would influence retention of non-antigen specific CD4+ T cells. Distribution within the tissue of the antigen-specific and non-specific cells are retained specifically if they are resting on the endothelium or dispersed throughout the retina and vitreous.

Further to this, the CRISPR/Cas9 system of gene editing could be utilised to knock out genes that effect disease progression and could be involved in the non-specific retention of CD4+ T cells. Firstly, to test if virally transduced cells survive in vivo and are capable of causing disease. Using a retroviral construct of F-tractin tagged GFP. CRISPR/Cas9 can then be utilised to knockout genes that can be assumed to cause a more severe disease phenotype including CTLA-4 or from the work presented in this thesis IL-27Rα or knockout genes that can be assumed to cause a less severe disease phenotype including CD28. After optimisation of this platform specific genes can be selected to target on OVA antigen specific CD4+ T cells before concurrent adoptive transfer with retinal antigen specific CD4+ T cells to monitor if the OVA specific cells are retained throughout active disease after specific genes are knocked out to manipulate disease course and reduce disease severity.

9.2 The role of initial disease-causing antigen specific cells in EAU disease course

The persistence of the disease initiating antigen specific CD4+ T cells throughout clinical disease is highlighted within this thesis (*chapter 4*). Using RNA sequencing at a number of late disease time points could identify genes present in the total CD4+ and CD8+ T cell population to identify differences in gene expression in cells retained in the eye past active clinical disease. This technique allows comparisons between clinical disease points past active disease but also could be used to analyse differential gene expression in endogenous and transferred CD4+ T cell populations during active disease.

The role of the transferred antigen specific cells in disease initiation by activation of the endothelium was highlighted in (*chapter 4*) but further analysis into how transferred cells are involved in the initiation and progression of clinical disease can be investigated using antibody depletion of the transferred population before active peak disease occurs. This experiment will determine the role of transferred antigen specific cells in continuing active disease course and whether the endogenous compartment of CD4+ T cells is capable of continuing disease course without the presence of the antigen specific pathogenic transferred CD4+ T cells.

Further to this the proliferation status of the transferred CD4+ population during active disease. Using a Ki67 antibody stain we can determine if the cells are in the active phase of the cell cycle and are therefore proliferating or the increase in transferred number present in the eye during active clinical disease is due purely to recruitment of transferred cells from the blood, spleen and lymph nodes.

9.3 CX3CR1 expression on CD4+ T cells throughout clinical disease

The expression of CX3CR1 on CD4+ T cells due to an antigen specific response is presented in *chapter 6*. To investigate if CX3CR1 is also expressed on CD4+ T cells in vitro cultures, OVA specific CD4+ T cells cocultured with antigen and CD3 CD28 stimulation to quantify CX3CR1 expression on CD4+ T cells.

Further experiments include utilising the $RAG2^{-/-}$ mice to transfer cells from transfer recipients at peak disease in Ly5 recipients. CD4+ transferred T cells from recipient eyes at peak disease can be sorted into CX3CR1+ CD4+ T cells and transferred into one group of recipients and sort CX3CR1- CD4+ T cells to transfer into another group of recipients. This experiment will allow differences in disease course based on CX3CR1 expression of CD4+ T cells with the hypothesis that CX3CR1+ CD4+ T cells are more capable of causing disease and persisting during active disease in comparison to the CX3CR1- CD4+ T cell population.

Analysis of differential gene expression in these recipients could be investigated by focussed analysis of the expression of functional gene sets that are associated with changes in T cell effector potential specifically analysing intracellular cytokine expression including IFN-γ, IL-17 and TNF. Regulatory and activation threshold markers including; FoxP3, CD5, CD39 and CD73, coinhibitory markers BTLA, TIM3, CTLA4, LAG3, PD1 and TIGIT and costimulatory markers (41BB, CD25, CD28, GITR, ICOS and OX40 using flow cytometry antibody panels.

Further to this RNA seq analysis of levels of mRNA followed by unsupervised analysis of differential gene expression will complement the previous study. Using total cell count of CD4+ T cells at different time points throughout disease course and with differing CX3CR1 expression levels to compare cross different disease-causing cells.

Due to the antigen specific nature of CX3CR1 expression on CD4+ T cells analysis of the TCR of CX3CR1+ CD4+ T cells using single cell sequencing. This platform allows single cell analysis at the transcript level with concurrent analysis of the TCR repertoire of each individual cell. Firstly, using the OTII transfer model with intravitreal OVA followed by analysis of the uveitogenic transfer model.

9.4 IL-27Rα$^{-/-}$ causes a more potent CD4+ T cell phenotype

As described in *chapter 7* knocking out the IL-27Rα in transferred CD4+ T cells causes a more severe cell phenotype that persists throughout active disease and continues to drive disease to cause a longer more severe disease within the recipients. Further experimentation could include phenotyping the CD4+ T cell populations within both groups of recipients to identify the role of CD4+ T cell phenotype in disease progression including early disease time points and late disease time points such as staining for IFN-γ, IL-17 and FoxP3 using flow cytometry antibodies before including analysis of differential gene expression in recipients by quantifying expression of functional gene sets that are associated with changes in T cell effector potential specifically analysing intracellular cytokine expression including IFN-γ, IL-17 and TNF. Regulatory and activation threshold markers including FoxP3, CD5, CD39 and CD73, coinhibitory markers BTLA, TIM3, CTLA4, LAG3, PD1 and TGIT and costimulatory markers (41BB, CD25, CD28, GITR, ICOS and OX40.

The effect of IL-27Rα knockout on CD4+ T cells has contributed to differences in disease phenotype but how this difference in clinical disease affects the structure and function of the tissue. Using histological sections to analyse the structures present within the eye to determine any abnormalities across disease groups, alternatively further analysis using whole retina flat mounts allows study of dispersion within the retina of immune infiltrate.

Chapter 10. Appendix

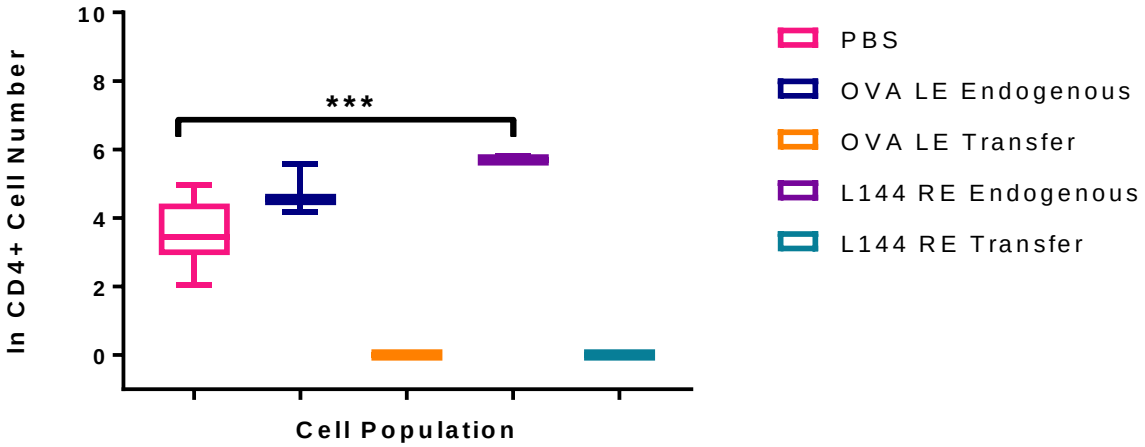

Appendix 1: Control experiment OVA and L144 control invit with no cell transfer performed to monitor changes in endogenous cell number

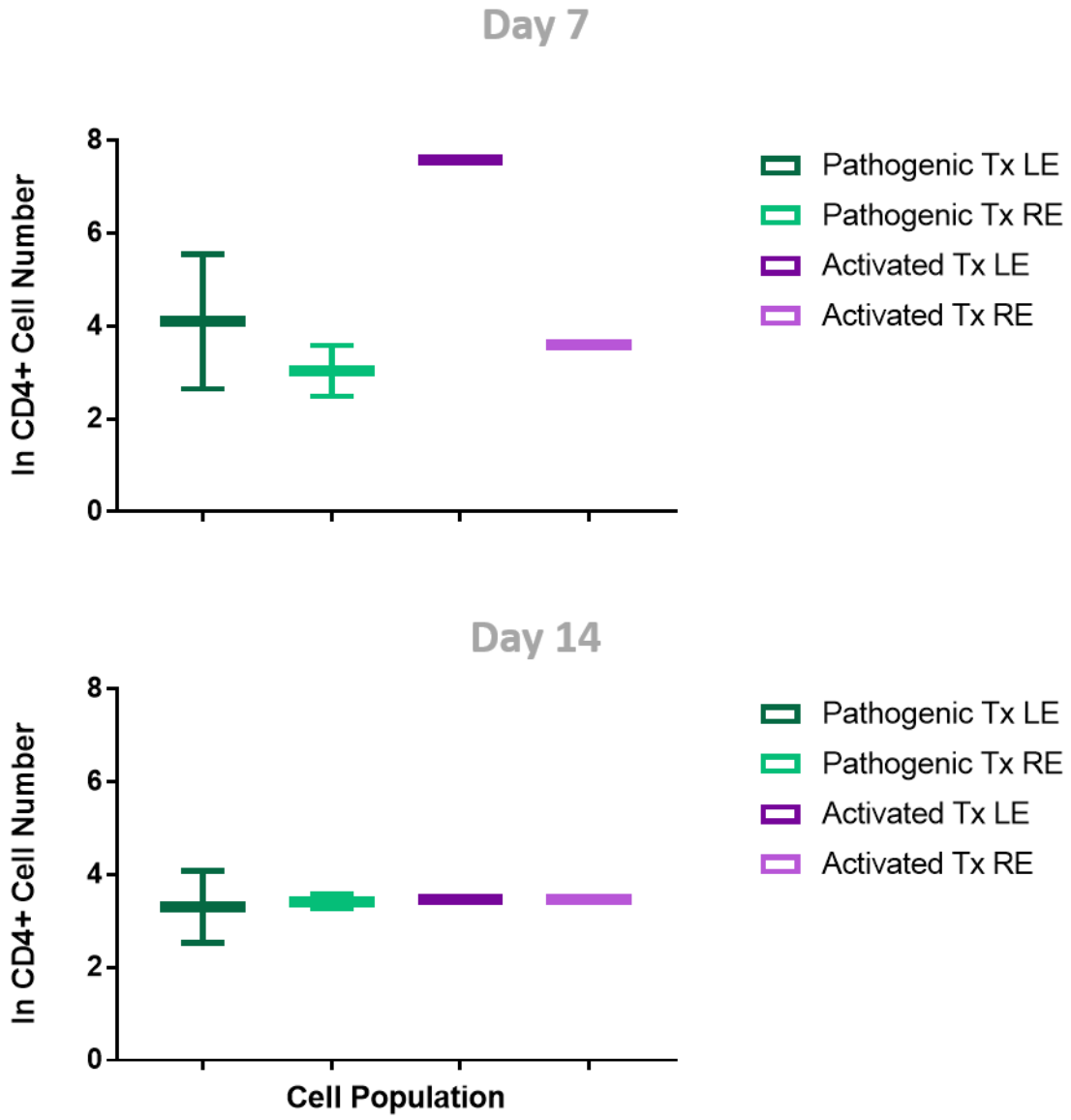
Day 7
ln CD4+ Cell Number
8
6
4
2
0
Pathogenic Tx LE
Pathogenic Tx RE
Activated Tx LE
Activated Tx RE
Day 14
ln CD4+ Cell Number
8
6
4
2
0
Cell Population
Pathogenic Tx LE
Pathogenic Tx RE
Activated Tx LE
Activated Tx RE

Appendix 2: Pathogenic or OTII activated intravitreal injection of cells into the left eye of RAG2$^{-/-}$ mice. Eyes were then analysed by flow cytometry at day 7 and 14 to quantify presence of transferred cells in each eye.

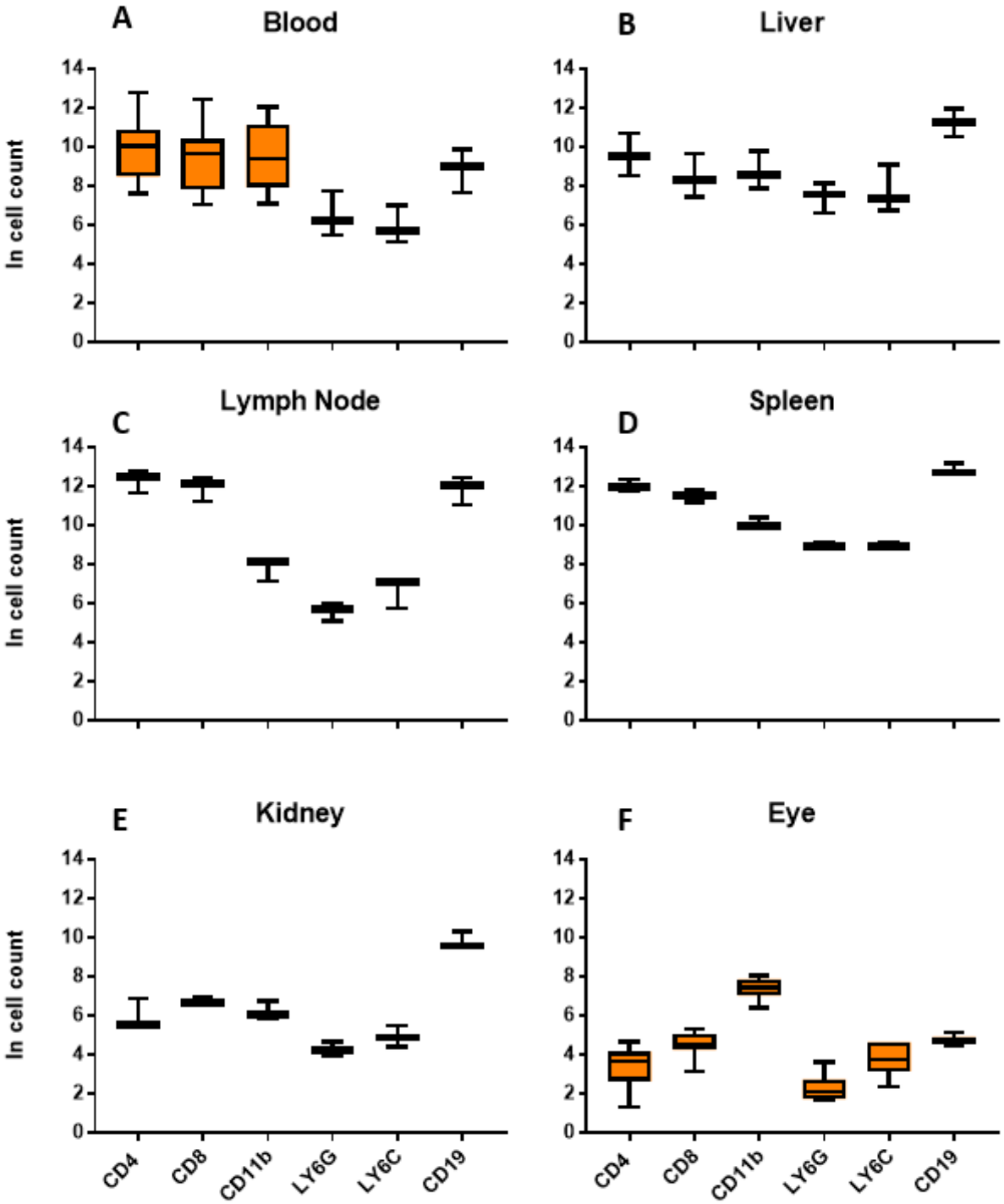
A
Blood
B
Liver
C
Lymph Node
D
Spleen
E
Kidney
F
Eye
ln cell count
0
2
4
6
8
10
12
14
CD4
CD8
CD11b
LY6G
LY6C
CD19

Appendix 3: Leukocytes quantified in organs from IL-27Rα$^{-/-}$ mice to compare to leukocyte numbers present within the eye.

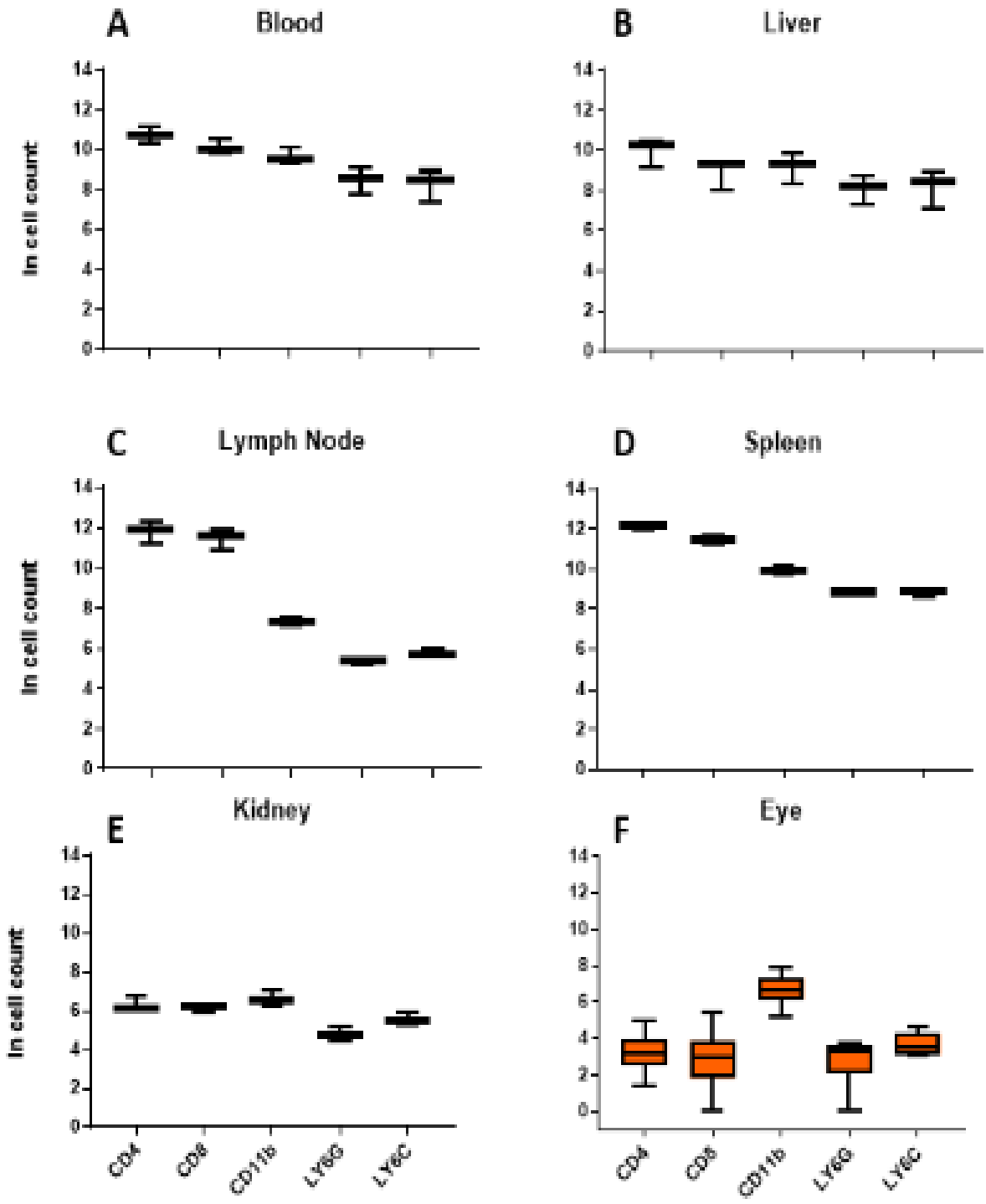
A
Blood
B
Liver
C
Lymph Node
D
Spleen
E
Kidney
F
Eye
ln cell count
0
2
4
6
8
10
12
14
CD4
CD8
CD11b
LY6G
LY6C

Appendix 4: Leukocytes quantified in organs from C57BL/6 mice to compare to leukocyte numbers present within the eye.

Chapter 11. References

References

1. Kerr EC, Copland DA, Dick AD, Nicholson LB. The dynamics of leukocyte infiltration in experimental autoimmune uveoretinitis. Progress in Retinal and Eye Research. 2008;27(5):527-35.
2. Chaplin DD. Overview of the immune response. The Journal of allergy and clinical immunology. 2010;125(2 Suppl 2):S3-S23.
3. Howell M, Shepherd M. The immune system. Anaesthesia & Intensive Care Medicine. 2018;19(10):575-8.
4. Porcelli SA, Firestein GS, Budd RC, Gabriel SE, McInnes IB, O'Dell JR. Chapter 17 - Innate Immunity. Kelley and Firestein's Textbook of Rheumatology (Tenth Edition): Elsevier; 2017. p. 274-87.
5. Italiani P, Boraschi D. From Monocytes to M1/M2 Macrophages: Phenotypical vs. Functional Differentiation. Frontiers in immunology. 2014;5:514-.
6. Iwasaki A, Medzhitov R. Control of adaptive immunity by the innate immune system. Nature immunology. 2015;16(4):343-53.
7. Vijay K. Toll-like receptors in immunity and inflammatory diseases: Past, present, and future. International Immunopharmacology. 2018;59:391-412.
8. Kolaczkowska E, Kubes P. Neutrophil recruitment and function in health and inflammation. Nature Reviews Immunology. 2013;13(3):159-75.
9. Kierdorf K, Prinz M, Geissmann F, Gomez Perdiguero E. Development and function of tissue resident macrophages in mice. Seminars in immunology. 2015;27(6):369-78.
10. Varol C, Mildner A, Jung S. Macrophages: Development and Tissue Specialization. Annual Review of Immunology. 2015;33(1):643-75.
11. Mosser DM, Edwards JP. Exploring the full spectrum of macrophage activation. Nature reviews Immunology. 2008;8(12):958-69.
12. Wculek SK, Cueto FJ, Mujal AM, Melero I, Krummel MF, Sancho D. Dendritic cells in cancer immunology and immunotherapy. Nature Reviews Immunology. 2019.
13. Banchereau J, Briere F, Caux C, Davoust J, Lebecque S, Liu YJ, et al. Immunobiology of dendritic cells. Annu Rev Immunol. 2000;18:767-811.
14. Wen T, Rothenberg ME. The Regulatory Function of Eosinophils. Microbiology spectrum. 2016;4(5):10.1128/microbiolspec.MCHD-0020-2015.
15. Siracusa MC, Kim BS, Spergel JM, Artis D. Basophils and allergic inflammation. The Journal of allergy and clinical immunology. 2013;132(4):789-8.
16. Ebbo M, Crinier A, Vély F, Vivier E. Innate lymphoid cells: major players in inflammatory diseases. Nature Reviews Immunology. 2017;17(11):665-78.
17. Vivier E, Tomasello E, Baratin M, Walzer T, Ugolini S. Functions of natural killer cells. Nature Immunology. 2008;9(5):503-10.
18. Bonilla FA, Oettgen HC. Adaptive immunity. Journal of Allergy and Clinical Immunology. 2010;125(2, Supplement 2):S33-S40.
19. Pennock ND, White JT, Cross EW, Cheney EE, Tamburini BA, Kedl RM. T cell responses: naive to memory and everything in between. Advances in physiology education. 2013;37(4):273-83.
20. Cooper MD, Alder MN. The Evolution of Adaptive Immune Systems. Cell. 2006;124(4):815-22.
21. Cota AM, Midwinter MJ. The immune system. Anaesthesia & Intensive Care Medicine. 2015;16(7):353-5.
22. Tomayko MM, Allman D. What B cell memories are made of. Current Opinion in Immunology. 2019;57:58-64.
23. Hoffman W, Lakkis FG, Chalasani G. B Cells, Antibodies, and More. Clinical journal of the American Society of Nephrology : CJASN. 2016;11(1):137-54.
24. Hombach J, Tsubata T, Leclercq L, Stappert H, Reth M. Molecular components of the B-cell antigen receptor complex of the IgM class. Nature. 1990;343(6260):760-2.

25. Sant'Angelo DB, Lucas B, Waterbury PG, Cohen B, Brabb T, Goverman J, et al. A Molecular Map of T Cell Development. Immunity. 1998;9(2):179-86.
26. Schmitt TM, Zúñiga-Pflücker JC. Induction of T Cell Development from Hematopoietic Progenitor Cells by Delta-like-1 In Vitro. Immunity. 2002;17(6):749-56.
27. Angus KL, Griffiths GM. Cell polarisation and the immunological synapse. Curr Opin Cell Biol. 2013;25(1):85-91.
28. Romagnani S. Regulation of the T cell response. Clinical and experimental allergy : journal of the British Society for Allergy and Clinical Immunology. 2006;36(11):1357-66.
29. Romagnani S. Th1/Th2 cells. Inflamm Bowel Dis. 1999;5(4):285-94.
30. Romagnani S. Regulation of the T cell response. Clinical & Experimental Allergy. 2006;36(11):1357-66.
31. Romano M, Fanelli G, Albany CJ, Giganti G, Lombardi G. Past, Present, and Future of Regulatory T Cell Therapy in Transplantation and Autoimmunity. Frontiers in immunology. 2019;10:43-.
32. Groux H, O'Garra A, Bigler M, Rouleau M, Antonenko S, de Vries JE, et al. A CD4+T-cell subset inhibits antigen-specific T-cell responses and prevents colitis. Nature. 1997;389(6652):737-42.
33. Zeng H, Zhang R, Jin B, Chen L. Type 1 regulatory T cells: a new mechanism of peripheral immune tolerance. Cellular & Molecular Immunology. 2015;12(5):566-71.
34. Varricchi G, Harker J, Borriello F, Marone G, Durham SR, Shamji MH. T follicular helper (Tfh) cells in normal immune responses and in allergic disorders. Allergy. 2016;71(8):1086-94.
35. Clark GJ, Angel N, Kato M, López JA, MacDonald K, Vuckovic S, et al. The role of dendritic cells in the innate immune system. Microbes and Infection. 2000;2(3):257-72.
36. Sprent J. Antigen-Presenting Cells: Professionals and amateurs. Current Biology. 1995;5(10):1095-7.
37. Zhang J-M, An J. Cytokines, inflammation, and pain. International anesthesiology clinics. 2007;45(2):27-37.
38. Kastelein RA, Hunter CA, Cua DJ. Discovery and biology of IL-23 and IL-27: related but functionally distinct regulators of inflammation. Annu Rev Immunol. 2007;25:221-42.
39. Carl JW, Bai X-F. IL27: its roles in the induction and inhibition of inflammation. International journal of clinical and experimental pathology. 2008;1(2):117-23.
40. Yoshida H, Hunter CA. The immunobiology of interleukin-27. Annu Rev Immunol. 2015;33:417-43.
41. Owaki T, Asakawa M, Morishima N, Hata K, Fukai F, Matsui M, et al. A role for IL-27 in early regulation of Th1 differentiation. J Immunol. 2005;175(4):2191-200.
42. Jones GW, Hill DG, Cardus A, Jones SA. IL-27: a double agent in the IL-6 family. Clinical & Experimental Immunology. 2018;193(1):37-46.
43. Le Texier L, Thebault P, Carvalho-Gaspar M, Vignard V, Merieau E, Usal C, et al. Immunoregulatory function of IL-27 and TGF-β1 in cardiac allograft transplantation. Transplantation. 2012;94(3):226-33.
44. Zlotnik A, Yoshie O. Chemokines: A New Classification System and Their Role in Immunity. Immunity. 2000;12(2):121-7.
45. Fallahi P, Ferrari SM, Ragusa F, Ruffilli I, Elia G, Paparo SR, et al. Th1 Chemokines in Autoimmune Endocrine Disorders. The Journal of Clinical Endocrinology & Metabolism. 2019;105(4):1046-60.
46. Pucci S, Mazzarelli P, Zonetti MJ, Fisco T, Bonanno E, Spagnoli LG, et al. CX3CR1 receptor polymorphisms, Th1 cell recruitment, and acute myocardial infarction outcome: looking for a link. BioMed research international. 2013;2013:451349.
47. Dagkalis A, Wallace C, Hing B, Liversidge J, Crane IJ. CX3CR1-deficiency is associated with increased severity of disease in experimental autoimmune uveitis. Immunology. 2009;128(1):25-33.
48. Ansel KM, Ngo VN, Hyman PL, Luther SA, Förster R, Sedgwick JD, et al. A chemokine-driven positive feedback loop organizes lymphoid follicles. Nature. 2000;406(6793):309-14.

49. Stein JV, Nombela-Arrieta C. Chemokine control of lymphocyte trafficking: a general overview. Immunology. 2005;116(1):1-12.
50. Waldmann H. Immunological Tolerance. Reference Module in Biomedical Sciences: Elsevier; 2014.
51. Mackay IR. Tolerance and autoimmunity. Western Journal of Medicine. 2001;174(2):118-23.
52. Mathis D, Benoist C. Back to Central Tolerance. Immunity. 2004;20(5):509-16.
53. Anderson MS, Venanzi ES, Klein L, Chen Z, Berzins SP, Turley SJ, et al. Projection of an immunological self shadow within the thymus by the aire protein. Science. 2002;298(5597):1395-401.
54. Klein L, Kyewski B, Allen PM, Hogquist KA. Positive and negative selection of the T cell repertoire: what thymocytes see (and don't see). Nature Reviews Immunology. 2014;14(6):377-91.
55. Mueller DL. Mechanisms maintaining peripheral tolerance. Nature Immunology. 2010;11(1):21-7.
56. ElTanbouly MA, Noelle RJ. Rethinking peripheral T cell tolerance: checkpoints across a T cell's journey. Nat Rev Immunol. 2021;21(4):257-67.
57. Schwartz RH. Historical overview of immunological tolerance. Cold Spring Harbor perspectives in biology. 2012;4(4):a006908-a.
58. Rosenblum MD, Remedios KA, Abbas AK. Mechanisms of human autoimmunity. The Journal of Clinical Investigation. 2015;125(6):2228-33.
59. Smith DA, Germolec DR. Introduction to immunology and autoimmunity. Environ Health Perspect. 1999;107 Suppl 5(Suppl 5):661-5.
60. Farh KK-H, Marson A, Zhu J, Kleinewietfeld M, Housley WJ, Beik S, et al. Genetic and epigenetic fine mapping of causal autoimmune disease variants. Nature. 2015;518(7539):337-43.
61. Palmer MT, Weaver CT. Autoimmunity: increasing suspects in the CD4+ T cell lineup. Nature Immunology. 2009;11:36.
62. Dardalhon V, Korn T, Kuchroo VK, Anderson AC. Role of Th1 and Th17 cells in organ-specific autoimmunity. Journal of autoimmunity. 2008;31(3):252-6.
63. Zambrano-Zaragoza JF, Romo-Martínez EJ, Durán-Avelar MdJ, García-Magallanes N, Vibanco-Pérez N. Th17 cells in autoimmune and infectious diseases. International journal of inflammation. 2014;2014:651503-.
64. McCaa CS. The eye and visual nervous system: anatomy, physiology and toxicology. Environmental health perspectives. 1982;44:1-8.
65. Masland RH. The fundamental plan of the retina. Nature Neuroscience. 2001;4(9):877-86.
66. McMenamin PG, Saban DR, Dando SJ. Immune cells in the retina and choroid: Two different tissue environments that require different defenses and surveillance. Progress in Retinal and Eye Research. 2019;70:85-98.
67. Simó R, Villarroel M, Corraliza L, Hernández C, Garcia-Ramírez M. The retinal pigment epithelium: something more than a constituent of the blood-retinal barrier--implications for the pathogenesis of diabetic retinopathy. Journal of biomedicine & biotechnology. 2010;2010:190724-.
68. Masland Richard H. The Neuronal Organization of the Retina. Neuron. 2012;76(2):266-80.
69. Zhou R, Caspi RR. Ocular immune privilege. F1000 Biology Reports. 2010;2:3.
70. Medawar PB. Immunity to homologous grafted skin; the fate of skin homografts transplanted to the brain, to subcutaneous tissue, and to the anterior chamber of the eye. British journal of experimental pathology. 1948;29(1):58-69.
71. Niederkorn JY. Ocular immune privilege and ocular melanoma: parallel universes or immunological plagiarism? Frontiers in immunology. 2012;3:148-.
72. Griffith TS, Brunner T, Fletcher SM, Green DR, Ferguson TA. Fas ligand-induced apoptosis as a mechanism of immune privilege. Science. 1995;270(5239):1189-92.
73. Kaplan HJ, Streilein JW, Stevens TR. Transplantation Immunology of the Anterior Chamber of the Eye. II Immune Response to Allogeneic Cells. 1975;115(3):805-10.

74. Kaplan HJ, Streilein JW. Immune Response to Immunization Via the Anterior Chamber of the Eye. I F₁ Lymphocyte-Induced Immune Deviation. 1977;118(3):809-14.
75. Niederkorn JY. Mechanisms of Immune Privilege in the Eye and Hair Follicle. Journal of Investigative Dermatology Symposium Proceedings. 2003;8(2):168-72.
76. Ohta K, Wiggert B, Taylor AW, Streilein JW. Effects of Experimental Ocular Inflammation on Ocular Immune Privilege. Invest Ophthalmol Vis Sci. 1999;40(9):2010-8.
77. Epps SJ, Boldison J, Stimpson ML, Khera TK, Lait PJP, Copland DA, et al. Re-programming immunosurveillance in persistent non-infectious ocular inflammation. Progress in retinal and eye research. 2018;65:93-106.
78. Ransohoff RM, Engelhardt B. The anatomical and cellular basis of immune surveillance in the central nervous system. Nature Reviews Immunology. 2012;12(9):623-35.
79. Engelhardt B, Ransohoff RM. The ins and outs of T-lymphocyte trafficking to the CNS: anatomical sites and molecular mechanisms. Trends Immunol. 2005;26(9):485-95.
80. Stein-Streilein J. Immune regulation and the eye. Trends in Immunology. 2008;29(11):548-54.
81. Bharadwaj AS, Appukuttan B, Wilmarth PA, Pan Y, Stempel AJ, Chipps TJ, et al. Role of the retinal vascular endothelial cell in ocular disease. Progress in Retinal and Eye Research. 2013;32:102-80.
82. Michiels C. Endothelial cell functions. Journal of Cellular Physiology. 2003;196(3):430-43.
83. Hunt BJ, Jurd KM. Endothelial cell activation. A central pathophysiological process. BMJ (Clinical research ed). 1998;316(7141):1328-9.
84. Adams DH, Shaw S. Leucocyte-endothelial interactions and regulation of leucocyte migration. The Lancet. 1994;343(8901):831-6.
85. Muller WA. Leukocyte-endothelial cell interactions in the inflammatory response. Laboratory Investigation. 2002;82(5):521-33.
86. McEver RP, Zhu C. Rolling cell adhesion. Annual review of cell and developmental biology. 2010;26:363-96.
87. Sugita S, Shimizu J, Makabe K, Keino H, Watanabe T, Takahashi M. Inhibition of T cell-mediated inflammation in uveitis by a novel anti-CD3 antibody. Arthritis Research & Therapy. 2017;19(1):176.
88. Bi H-S, Liu Z-F, Cui Y. Pathogenesis of innate immunity and adaptive immunity in the mouse model of experimental autoimmune uveitis. Journal of the Chinese Medical Association. 2015;78(5):276-82.
89. de Smet MD, Taylor SRJ, Bodaghi B, Miserocchi E, Murray PI, Pleyer U, et al. Understanding uveitis: The impact of research on visual outcomes. Progress in Retinal and Eye Research. 2011;30(6):452-70.
90. Pan J, Kapur M, McCallum R. Noninfectious Immune-Mediated Uveitis and Ocular Inflammation. Current Allergy and Asthma Reports. 2013;14(1):409.
91. Voigt V, Wikstrom ME, Kezic JM, Schuster IS, Fleming P, Makinen K, et al. Ocular antigen does not cause disease unless presented in the context of inflammation. Scientific reports. 2017;7(1):14226-.
92. BODAGHI B, CASSOUX N, WECHSLER B, HANNOUCHE D, FARDEAU C, PAPO T, et al. Chronic Severe Uveitis: Etiology and Visual Outcome in 927 Patients from a Single Center. Medicine. 2001;80(4):263-70.
93. Lee JH, Agarwal A, Mahendradas P, Lee CS, Gupta V, Pavesio CE, et al. Viral posterior uveitis. Survey of ophthalmology. 2017;62(4):404-45.
94. Liberman P, Gauro F, Berger O, Urzua CA. Causes of Uveitis in a Tertiary Center in Chile: A Cross-sectional Retrospective Review. Ocular immunology and inflammation. 2015;23(4):339-45.
95. Llorenc V, Mesquida M, Sainz de la Maza M, Keller J, Molins B, Espinosa G, et al. Epidemiology of uveitis in a Western urban multiethnic population. The challenge of globalization. Acta Ophthalmol. 2015;93(6):561-7.

96. Venkatesh P, Gogia V, Shah B, Gupta S, Sagar P, Garg S. Patterns of uveitis at the Apex Institute for Eye Care in India: Results from a prospectively enrolled patient data base (2011-2013). Int Ophthalmol. 2016;36(3):365-72.
97. Guly CM, Forrester JV. Investigation and management of uveitis. BMJ. 2010;341:c4976.
98. Mitchel Opremcak E. Symptoms and Signs of Uveitis. Uveitis: A Clinical Manual for Ocular Inflammation. New York, NY: Springer New York; 1995. p. 14-30.
99. de Smet MD, Nussenblatt RB. Clinical Use of Cyclosporine in Ocular Disease. International Ophthalmology Clinics. 1993;33(4):31-45.
100. Sudharshan S, Ganesh SK, Biswas J. Current approach in the diagnosis and management of posterior uveitis. Indian journal of ophthalmology. 2010;58(1):29-43.
101. Birnbaum AD, Oh F, Sahin O, Little DM, Tessler HH, Goldstein DA. Chlorambucil and Malignancy. Ophthalmology. 2010;117(7):1466-.e1.
102. Pujari SS, Kempen JH, Newcomb CW, Gangaputra S, Daniel E, Suhler EB, et al. Cyclophosphamide for Ocular Inflammatory Diseases. Ophthalmology. 2010;117(2):356-65.
103. Imrie FR, Dick AD. Biologics in the treatment of uveitis. Current Opinion in Ophthalmology. 2007;18(6):481-6.
104. Nussenblatt RB, Fortin E, Schiffman R, Rizzo L, Smith J, Van Veldhuisen P, et al. Treatment of noninfectious intermediate and posterior uveitis with the humanized anti-Tac mAb: a phase I/II clinical trial. Proc Natl Acad Sci U S A. 1999;96(13):7462-6.
105. Occhiutto ML, Freitas FR, Maranhao RC, Costa VP. Breakdown of the blood-ocular barrier as a strategy for the systemic use of nanosystems. Pharmaceutics. 2012;4(2):252-75.
106. Cunha-Vaz JG. The blood-retinal barriers. Doc Ophthalmol. 1976;41(2):287-327.
107. Worakul N, Robinson JR. Ocular pharmacokinetics/pharmacodynamics. European Journal of Pharmaceutics and Biopharmaceutics. 1997;44(1):71-83.
108. Crane IJ, Liversidge J. Mechanisms of leukocyte migration across the blood–retina barrier. Seminars in immunopathology. 2008;30(2):165-77.
109. Lin P, Suhler EB, Rosenbaum JT. The Future of Uveitis Treatment. Ophthalmology.121(1):365-76.
110. Caspi RR, Chan C-C, Fujino Y, Najafian F, Grover S, Hansen CT, et al. Recruitment of antigen-nonspecific cells plays a pivotal role in the pathogenesis of a T cell-mediated organ-specific autoimmune uveoretinitis. Journal of Neuroimmunology. 1993;47(2):177-88.
111. Pennesi G, Mattapallil MJ, Sun S-H, Avichezer D, Silver PB, Karabekian Z, et al. A humanized model of experimental autoimmune uveitis in HLA class II transgenic mice. The Journal of Clinical Investigation.111(8):1171-80.
112. Xu H, Rizzo LV, Silver PB, Caspi RR. Uveitogenicity Is Associated with a Th1-like Lymphokine Profile: Cytokine-Dependent Modulation of Early and Committed Effector T Cells in Experimental Autoimmune Uveitis. Cellular Immunology. 1997;178(1):69-78.
113. Commodaro AG, Peron JPS, Lopes CT, Arslanian C, Belfort JR, Rizzo LV, et al. Evaluation of Experimental Autoimmune Uveitis in Mice Treated with FTY720. Invest Ophthalmol Vis Sci. 2010;51(5):2568-74.
114. Kerr EC, Raveney BJE, Copland DA, Dick AD, Nicholson LB. Analysis of retinal cellular infiltrate in experimental autoimmune uveoretinitis reveals multiple regulatory cell populations. Journal of Autoimmunity. 2008;31(4):354-61.
115. Fang S, Meng X, Zhang Z, Wang Y, Liu Y, You C, et al. Vorinostat Modulates the Imbalance of T Cell Subsets, Suppresses Macrophage Activity, and Ameliorates Experimental Autoimmune Uveoretinitis. NeuroMolecular Medicine. 2016;18(1):134-45.
116. Dick AD, Cheng YF, Liversidge J, Forrester JV. Immunomodulation of experimental autoimmune uveoretinitis: A model of tolerance induction with retinal antigens. Eye. 1994;8(1):52-9.
117. Agarwal RK, Silver PB, Caspi RR. Rodent Models of Experimental Autoimmune Uveitis. Methods in molecular biology (Clifton, NJ). 2012;900:10.1007/978-1-60761-720-4_22.

118. Caspi RR, Roberge FG, McAllister CG, el-Saied M, Kuwabara T, Gery I, et al. T cell lines mediating experimental autoimmune uveoretinitis (EAU) in the rat. The Journal of Immunology. 1986;136(3):928-33.
119. Sanui H, Redmond TM, Kotake S, Wiggert B, Hu LH, Margalit H, et al. Identification of an immunodominant and highly immunopathogenic determinant in the retinal interphotoreceptor retinoid-binding protein (IRBP). The Journal of experimental medicine. 1989;169(6):1947-60.
120. Pfister C, Chabre M, Plouet J, Tuyen VV, De Kozak Y, Faure JP, et al. Retinal S antigen identified as the 48K protein regulating light-dependent phosphodiesterase in rods. Science. 1985;228(4701):891-3.
121. Bansal S, Barathi VA, Iwata D, Agrawal R. Experimental autoimmune uveitis and other animal models of uveitis: An update. Indian Journal of Ophthalmology. 2015;63(3):211-8.
122. Adler AJ, Martin KJ. Retinol-binding proteins in bovine interphotoreceptor matrix. Biochemical and Biophysical Research Communications. 1982;108(4):1601-8.
123. Chader GJ, Wiggert B. Interphotoreceptor retinoid-binding protein: Characteristics in bovine and monkey retina. Vision Research. 1984;24(11):1605-14.
124. Borst DE, Redmond TM, Elser JE, Gonda MA, Wiggert B, Chader GJ, et al. Interphotoreceptor retinoid-binding protein. Gene characterization, protein repeat structure, and its evolution. J Biol Chem. 1989;264(2):1115-23.
125. Chan CC, Caspi RR, Ni M, Leake WC, Wiggert B, Chader GJ, et al. Pathology of experimental autoimmune uveoretinitis in mice. J Autoimmun. 1990;3(3):247-55.
126. Gery I, Chanaud NP, 3rd, Anglade E. Recoverin is highly uveitogenic in Lewis rats. Invest Ophthalmol Vis Sci. 1994;35(8):3342-5.
127. Danner S, Lohse MJ. Phosducin is a ubiquitous G-protein regulator. Proc Natl Acad Sci U S A. 1996;93(19):10145-50.
128. Caspi RR, Grubbs BG, Chan CC, Chader GJ, Wiggert B. Genetic control of susceptibility to experimental autoimmune uveoretinitis in the mouse model. Concomitant regulation by MHC and non-MHC genes. The Journal of Immunology. 1992;148(8):2384-9.
129. Silver PB, Chan C-C, Wiggert B, Caspi RR. The Requirement for Pertussis to Induce EAU Is Strain-Dependent: B10.RIII, but Not B10.A Mice, Develop EAU and Th1 Responses to IRBP without Pertussis Treatment. Invest Ophthalmol Vis Sci. 1999;40(12):2898-905.
130. Su SB, Silver PB, Zhang M, Chan C-C, Caspi RR. Pertussis Toxin Inhibits Induction of Tissue-Specific Autoimmune Disease by Disrupting G Protein-Coupled Signals. The Journal of Immunology. 2001;167(1):250-6.
131. Caspi RR, Silver PB, Chan CC, Sun B, Agarwal RK, Wells J, et al. Genetic susceptibility to experimental autoimmune uveoretinitis in the rat is associated with an elevated Th1 response. The Journal of Immunology. 1996;157(6):2668-75.
132. Mochizuki M, Kuwabara T, McAllister C, Nussenblatt RB, Gery I. Adoptive transfer of experimental autoimmune uveoretinitis in rats. Immunopathogenic mechanisms and histologic features. Invest Ophthalmol Vis Sci. 1985;26(1):1-9.
133. Pennesi G, Mattapallil MJ, Sun SH, Avichezer D, Silver PB, Karabekian Z, et al. A humanized model of experimental autoimmune uveitis in HLA class II transgenic mice. J Clin Invest. 2003;111(8):1171-80.
134. Broekhuyse RM, Kuhlmann ED, Winkens HJ. Experimental melanin-protein induced uveitis (EMIU) is the sole type of uveitis evoked by a diversity of ocular melanin preparations and melanin-derived soluble polypeptides. Jpn J Ophthalmol. 1996;40(4):459-68.
135. Broekhuyse RM, Kuhlmann ED, Winkens HJ. Experimental autoimmune anterior uveitis (EAAU). II. Dose-dependent induction and adoptive transfer using a melanin-bound antigen of the retinal pigment epithelium. Exp Eye Res. 1992;55(3):401-11.
136. Smith JR, Hart PH, Williams KA. Basic pathogenic mechanisms operating in experimental models of acute anterior uveitis. Immunol Cell Biol. 1998;76(6):497-512.

137. Okumura A, Mochizuki M. Endotoxin-induced uveitis in rats: morphological and biochemical study. Jpn J Ophthalmol. 1988;32(4):457-65.
138. Szpak Y, Vieville JC, Tabary T, Naud MC, Chopin M, Edelson C, et al. Spontaneous retinopathy in HLA-A29 transgenic mice. Proc Natl Acad Sci U S A. 2001;98(5):2572-6.
139. Horai R, Silver PB, Chen J, Agarwal RK, Chong WP, Jittayasothorn Y, et al. Breakdown of immune privilege and spontaneous autoimmunity in mice expressing a transgenic T cell receptor specific for a retinal autoantigen. Journal of Autoimmunity. 2013;44:21-33.
140. DeVoss J, Hou Y, Johannes K, Lu W, Liou GI, Rinn J, et al. Spontaneous autoimmunity prevented by thymic expression of a single self-antigen. The Journal of experimental medicine. 2006;203(12):2727-35.
141. Gadjanski I, Williams SK, Hein K, Sättler MB, Bähr M, Diem R. Correlation of optical coherence tomography with clinical and histopathological findings in experimental autoimmune uveoretinitis. Experimental Eye Research. 2011;93(1):82-90.
142. de Kozak Y, Thillaye B, Renard G, Faure JP. Hyperacute form of experimental autoimmune uveo-retinitis in lewis rats; electron microscopic study. Albrecht von Graefes Archiv für klinische und experimentelle Ophthalmologie. 1978;208(1):135-42.
143. McMenamin PG, Broekhuyse RM, Forrester JV. Ultrastructural pathology of experimental autoimmune uveitis: A review. Micron. 1993;24(5):521-46.
144. Damsker JM, Hansen AM, Caspi RR. Th1 and Th17 cells: Adversaries and collaborators. Annals of the New York Academy of Sciences. 2010;1183:211-21.
145. Wekerle H, Kojima K, Lannes-Vieira J, Lassmann H, Linington C. Animal models. Annals of neurology. 1994;36 Suppl:S47-53.
146. Dornmair K, Goebels N, Weltzien H-U, Wekerle H, Hohlfeld R. T-cell-mediated autoimmunity: novel techniques to characterize autoreactive T-cell receptors. The American journal of pathology. 2003;163(4):1215-26.
147. Jiang G, Ke Y, Sun D, Han G, Kaplan HJ, Shao H. Reactivation of uveitogenic T cells by retinal astrocytes derived from experimental autoimmune uveitis-prone B10RIII mice. Invest Ophthalmol Vis Sci. 2008;49(1):282-9.
148. Papotto PH, Marengo EB, Sardinha LR, Goldberg AC, Rizzo LV. Immunotherapeutic strategies in autoimmune uveitis. Autoimmunity Reviews. 2014;13(9):909-16.
149. Chen X, Kezic JM, Forrester JV, Goldberg GL, Wicks IP, Bernard CC, et al. In vivo multi-modal imaging of experimental autoimmune uveoretinitis in transgenic reporter mice reveals the dynamic nature of inflammatory changes during disease progression. Journal of Neuroinflammation. 2015;12:17.
150. Jones BA, Beamer M, Ahmed S. Fractalkine/CX3CL1: A Potential New Target for Inflammatory Diseases. Molecular Interventions. 2010;10(5):263-70.
151. Mionnet C, Buatois V, Kanda A, Milcent V, Fleury S, Lair D, et al. CX3CR1 is required for airway inflammation by promoting T helper cell survival and maintenance in inflamed lung. Nat Med. 2010;16(11):1305-12.
152. Jung S, Aliberti J, Graemmel P, Sunshine MJ, Kreutzberg GW, Sher A, et al. Analysis of Fractalkine Receptor CX(3)CR1 Function by Targeted Deletion and Green Fluorescent Protein Reporter Gene Insertion. Molecular and Cellular Biology. 2000;20(11):4106-14.
153. Fong AM, Robinson LA, Steeber DA, Tedder TF, Yoshie O, Imai T, et al. Fractalkine and CX(3)CR1 Mediate a Novel Mechanism of Leukocyte Capture, Firm Adhesion, and Activation under Physiologic Flow. The Journal of Experimental Medicine. 1998;188(8):1413-9.
154. Shinkai Y, Rathbun G, Lam K-P, Oltz EM, Stewart V, Mendelsohn M, et al. RAG-2-deficient mice lack mature lymphocytes owing to inability to initiate V(D)J rearrangement. Cell. 1992;68(5):855-67.
155. Leung S, Smith D, Myc A, Morry J, Baker Jr JR. OT-II TCR transgenic mice fail to produce anti-ovalbumin antibodies upon vaccination. Cellular Immunology. 2013;282(2):79-84.
156. Meka RR, Venkatesha SH, Dudics S, Acharya B, Moudgil KD. IL-27-induced modulation of autoimmunity and its therapeutic potential. Autoimmunity Reviews. 2015;14(12):1131-41.

157. Hunter Christopher A, Kastelein R. Interleukin-27: Balancing Protective and Pathological Immunity. Immunity. 2012;37(6):960-9.
158. Villarino AV, Huang E, Hunter CA. Understanding the Pro- and Anti-Inflammatory Properties of IL-27. 2004;173(2):715-20.
159. Boldison J, Khera TK, Copland DA, Stimpson ML, Crawford GL, Dick AD, et al. A novel pathogenic RBP-3 peptide reveals epitope spreading in persistent experimental autoimmune uveoretinitis. Immunology. 2015;146(2):301-11.
160. Nicholson LB, Murtaza A, Hafler BP, Sette A, Kuchroo VK. A T cell receptor antagonist peptide induces T cells that mediate bystander suppression and prevent autoimmune encephalomyelitis induced with multiple myelin antigens. Proceedings of the National Academy of Sciences. 1997;94(17):9279-84.
161. Chisolm DA, Cheng W, Colburn SA, Silva-Sanchez A, Meza-Perez S, Randall TD, et al. Defining Genetic Variation in Widely Used Congenic and Backcrossed Mouse Models Reveals Varied Regulation of Genes Important for Immune Responses. Immunity. 2019;51(1):155-68.e5.
162. Copland DA, Wertheim MS, Armitage WJ, Nicholson LB, Raveney BJ, Dick AD. The clinical time-course of experimental autoimmune uveoretinitis using topical endoscopic fundal imaging with histologic and cellular infiltrate correlation. Invest Ophthalmol Vis Sci. 2008;49(12):5458-65.
163. Paques M, Guyomard JL, Simonutti M, Roux MJ, Picaud S, Legargasson JF, et al. Panretinal, high-resolution color photography of the mouse fundus. Invest Ophthalmol Vis Sci. 2007;48(6):2769-74.
164. Copland DA, Liu J, Schewitz-Bowers LP, Brinkmann V, Anderson K, Nicholson LB, et al. Therapeutic Dosing of Fingolimod (FTY720) Prevents Cell Infiltration, Rapidly Suppresses Ocular Inflammation, and Maintains the Blood-Ocular Barrier. The American journal of pathology. 2012;180(2):672-81.
165. Li W, Germain RN, Gerner MY. High-dimensional cell-level analysis of tissues with Ce3D multiplex volume imaging. Nature Protocols. 2019;14(6):1708-33.
166. Avichezer D, Grajewski RS, Chan C-C, Mattapallil MJ, Silver PB, Raber JA, et al. An immunologically privileged retinal antigen elicits tolerance: major role for central selection mechanisms. The Journal of experimental medicine. 2003;198(11):1665-76.
167. Egwuagu CE, Charukamnoetkanok P, Gery I. Thymic expression of autoantigens correlates with resistance to autoimmune disease. The Journal of Immunology. 1997;159(7):3109-12.
168. Caspi RR. A look at autoimmunity and inflammation in the eye. J Clin Invest. 2010;120(9):3073-83.
169. Dittel BN. CD4 T cells: Balancing the coming and going of autoimmune-mediated inflammation in the CNS. Brain, behavior, and immunity. 2008;22(4):421-30.
170. Miyagawa F, Gutermuth J, Zhang H, Katz SI. The use of mouse models to better understand mechanisms of autoimmunity and tolerance. Journal of autoimmunity. 2010;35(3):192-8.
171. Aronson SB, McMaster PRB. Passive Transfer of Experimental Allergic Uveitis. JAMA Ophthalmology. 1971;86(5):557-63.
172. Oh HM, Yu CR, Lee Y, Chan CC, Maminishkis A, Egwuagu CE. Autoreactive memory CD4+ T lymphocytes that mediate chronic uveitis reside in the bone marrow through STAT3-dependent mechanisms. J Immunol. 2011;187(6):3338-46.
173. Gery I, Mochizuki M, Nussenblatt RB. Chapter 3 Retinal specific antigens and immunopathogenic processes they provoke. Progress in Retinal Research. 1986;5:75-109.
174. Kotake S, Wiggert B, Zhang XY, Redmond TM, Chader GJ, Gery I. Stimulation in vitro of lymphocytes for induction of uveoretinitis without any significant proliferation. The Journal of Immunology. 1990;145(2):534-9.
175. Langrish CL, Chen Y, Blumenschein WM, Mattson J, Basham B, Sedgwick JD, et al. IL-23 drives a pathogenic T cell population that induces autoimmune inflammation. The Journal of experimental medicine. 2005;201(2):233-40.

176. Zhang L, Bell BA, Yu M, Chan CC, Peachey NS, Fung J, et al. Complement anaphylatoxin receptors C3aR and C5aR are required in the pathogenesis of experimental autoimmune uveitis. Journal of leukocyte biology. 2016;99(3):447-54.
177. Moon JJ, Chu HH, Hataye J, Pagán AJ, Pepper M, McLachlan JB, et al. Tracking epitope-specific T cells. Nature protocols. 2009;4(4):565-81.
178. van Os R, Sheridan TM, Robinson S, Drukteinis D, Ferrara JLM, Mauch PM. Immunogenicity of Ly5 (CD45)-Antigens Hampers Long-Term Engraftment Following Minimal Conditioning in a Murine Bone Marrow Transplantation Model. STEM CELLS. 2001;19(1):80-7.
179. Lefrançois L, Parker CM, Olson S, Muller W, Wagner N, Schön MP, et al. The role of beta7 integrins in CD8 T cell trafficking during an antiviral immune response. The Journal of experimental medicine. 1999;189(10):1631-8.
180. Dysli C, Enzmann V, Sznitman R, Zinkernagel MS. Quantitative Analysis of Mouse Retinal Layers Using Automated Segmentation of Spectral Domain Optical Coherence Tomography Images. Transl Vis Sci Technol. 2015;4(4):9.
181. Chu CJ, Herrmann P, Carvalho LS, Liyanage SE, Bainbridge JWB, Ali RR, et al. Assessment and In Vivo Scoring of Murine Experimental Autoimmune Uveoretinitis Using Optical Coherence Tomography. PloS one. 2013;8(5):e63002.
182. Meyers RL, Pettit TH. Pathogenesis of experimental allergic uveitis induced by retinal rod outer segments and pigment epithelium. J Immunol. 1975;114(4):1269-74.
183. Caspi RR. Animal models of autoimmune and immune-mediated uveitis. Drug Discovery Today: Disease Models. 2006;3(1):3-9.
184. Thurau SR, Mempel TR, Flügel A, Diedrichs-Möhring M, Krombach F, Kawakami N, et al. The fate of autoreactive, GFP+ T cells in rat models of uveitis analyzed by intravital fluorescence microscopy and FACS. International Immunology. 2004;16(11):1573-82.
185. Venkatesha SH, Durai M, Moudgil KD, Shoenfeld Y, Agmon-Levin N, Rose NR. Chapter 4 - Epitope Spreading in Autoimmune Diseases. Infection and Autoimmunity (Second Edition). Amsterdam: Academic Press; 2015. p. 45-68.
186. Vanderlugt CJ, Miller SD. Epitope spreading. Current Opinion in Immunology. 1996;8(6):831-6.
187. Vanderlugt CL, Miller SD. Epitope spreading in immune-mediated diseases: implications for immunotherapy. Nature Reviews Immunology. 2002;2(2):85-95.
188. Boldison J, Khera TK, Kerr EC, Copland DA, Dick AD, Nicholson LB. rRBP-3 Subunit 3 can Induce Severe Experimental Autoimmune Uveitis. Invest Ophthalmol Vis Sci. 2011;52(14):2954-.
189. Van den Elsen JHM, Van den Broek MF, Klasen IS, Van den Berg WB. Stimulation of antigen-specific murine T cell clones in vitro with antigen-pulsed adherent cells fixed to a carrier. Journal of Immunological Methods. 1988;112(1):15-22.
190. Basu S, Ray A, Dittel BN. Differential representation of B cell subsets in mixed bone marrow chimera mice due to expression of allelic variants of CD45 (CD45.1/CD45.2). Journal of immunological methods. 2013;396(1-2):163-7.
191. Pacheco Y, Acosta-Ampudia Y, Monsalve DM, Chang C, Gershwin ME, Anaya J-M. Bystander activation and autoimmunity. Journal of Autoimmunity. 2019;103:102301.
192. Bluestone JA, Bour-Jordan H, Cheng M, Anderson M. T cells in the control of organ-specific autoimmunity. J Clin Invest. 2015;125(6):2250-60.
193. Slavin AJ, Tarner IH, Nakajima A, Urbanek-Ruiz I, McBride J, Contag CH, et al. Adoptive cellular gene therapy of autoimmune disease. Autoimmunity Reviews. 2002;1(4):213-9.
194. Caspi R. Autoimmunity in the immune privileged eye: pathogenic and regulatory T cells. Immunologic research. 2008;42(1-3):41-50.
195. Thorlacius-Ussing G, Sørensen JF, Wandall HH, Pedersen AE. Auto-reactive T cells revised. Overestimation based on methodology? Journal of Immunological Methods. 2015;420:56-9.
196. Kronenberg M, Rudensky A. Regulation of immunity by self-reactive T cells. Nature. 2005;435(7042):598-604.

197. Huber SA-O, Gagliani N, O'Connor WJA-O, Geginat J, Caprioli F. CD4(+) T Helper Cell Plasticity in Infection, Inflammation, and Autoimmunity. (1466-1861 (Electronic)).
198. Yamamoto K. T cells and autoimmune diseases. Allergology International. 2001;50(1):1-4.
199. Pullen AM, Wade T, Marrack P, Kappler JW. Identification of the region of T cell receptor β chain that interacts with the self-superantigen MIs-1a. Cell. 1990;61(7):1365-74.
200. Wucherpfennig KW. Mechanisms for the induction of autoimmunity by infectious agents. The Journal of Clinical Investigation. 2001;108(8):1097-104.
201. Benoist C, Mathis D. The pathogen connection. Nature. 1998;394(6690):227-8.
202. Arata N, Ando T, Unger P, Davies TF. By-stander activation in autoimmune thyroiditis: Studies on experimental autoimmune thyroiditis in the GFP+ fluorescent mouse. Clinical Immunology. 2006;121(1):108-17.
203. McCully ML, Kouzeli A, Moser B. Peripheral Tissue Chemokines: Homeostatic Control of Immune Surveillance T Cells. Trends in Immunology. 2018;39(9):734-47.
204. Streilein JW, Ksander BR, Taylor AW. Immune deviation in relation to ocular immune privilege. The Journal of Immunology. 1997;158(8):3557-60.
205. Lechner O, Lauber J, Franzke A, Sarukhan A, von Boehmer H, Buer J. Fingerprints of anergic T cells. Current Biology. 2001;11(8):587-95.
206. Mai J, Virtue A, Shen J, Wang H, Yang X-F. An evolving new paradigm: endothelial cells--conditional innate immune cells. Journal of hematology & oncology. 2013;6:61-.
207. Rajendran P, Rengarajan T, Thangavel J, Nishigaki Y, Sakthisekaran D, Sethi G, et al. The vascular endothelium and human diseases. International journal of biological sciences. 2013;9(10):1057-69.
208. Pober JS, Sessa WC. Evolving functions of endothelial cells in inflammation. Nature Reviews Immunology. 2007;7(10):803-15.
209. Ley K, Reutershan J. Leucocyte-Endothelial Interactions in Health and Disease. In: Moncada S, Higgs A, editors. The Vascular Endothelium II. Berlin, Heidelberg: Springer Berlin Heidelberg; 2006. p. 97-133.
210. Bonfanti R, Furie B, Furie B, Wagner D. PADGEM (GMP140) is a component of Weibel-Palade bodies of human endothelial cells. Blood. 1989;73(5):1109-12.
211. Middleton J, Neil S, Wintle J, Clark-Lewis I, Moore H, Lam C, et al. Transcytosis and Surface Presentation of IL-8 by Venular Endothelial Cells. Cell. 1997;91(3):385-95.
212. Lipski DA, Foucart V, Dewispelaere R, Caspers LE, Defrance M, Bruyns C, et al. Retinal endothelial cell phenotypic modifications during experimental autoimmune uveitis: a transcriptomic approach. BMC Ophthalmology. 2020;20(1):106.
213. Xu H, From the Department of Ophthalmology AUMS, Scotland, United Kingdom., Forrester JV, From the Department of Ophthalmology AUMS, Scotland, United Kingdom., Liversidge J, From the Department of Ophthalmology AUMS, Scotland, United Kingdom., et al. Leukocyte Trafficking in Experimental Autoimmune Uveitis: Breakdown of Blood–Retinal Barrier and Upregulation of Cellular Adhesion Molecules. Invest Ophthalmol Vis Sci. 2016;44(1):226-34.
214. Razakandrainibe R, Pelleau S, Grau GE, Jambou R. Antigen presentation by endothelial cells: what role in the pathophysiology of malaria? Trends in Parasitology. 2012;28(4):151-60.
215. Wagner CR, Vetto RM, Burger DR. The mechanism of antigen presentation by endothelial cells. Immunobiology. 1984;168(3-5):453-69.
216. Fujikawa LS, Chan CC, McAllister C, Gery I, Hooks JJ, Detrick B, et al. Retinal vascular endothelium expresses fibronectin and class II histocompatibility complex antigens in experimental autoimmune uveitis. Cell Immunol. 1987;106(1):139-50.
217. Fujikawa LS, Reay C, Morin ME. Class II antigens on retinal vascular endothelium, pericytes, macrophages, and lymphocytes of the rat. Invest Ophthalmol Vis Sci. 1989;30(1):66-73.
218. Marelli-Berg FM, Jarmin SJ. Antigen presentation by the endothelium: a green light for antigen-specific T cell trafficking? Immunology Letters. 2004;93(2):109-13.

219. Ghani S, Feuerer M, Doebis C, Lauer U, Loddenkemper C, Huehn J, et al. T cells as pioneers: antigen-specific T cells condition inflamed sites for high-rate antigen-non-specific effector cell recruitment. Immunology. 2009;128(1pt2):e870-e80.
220. Yadav UCS, Subramanyam S, Ramana KV. Prevention of endotoxin-induced uveitis in rats by benfotiamine, a lipophilic analogue of vitamin B1. Invest Ophthalmol Vis Sci. 2009;50(5):2276-82.
221. Salvador B, Arranz A, Francisco S, Córdoba L, Punzón C, Llamas MÁ, et al. Modulation of endothelial function by Toll like receptors. Pharmacological Research. 2016;108:46-56.
222. Reynolds JM, Martinez GJ, Chung Y, Dong C. Toll-like receptor 4 signaling in T cells promotes autoimmune inflammation. Proceedings of the National Academy of Sciences of the United States of America. 2012;109(32):13064-9.
223. Ager A, Drayson M. Migration and homing of lymphoid cells. 1988.
224. Reinhardt RL, Khoruts A, Merica R, Zell T, Jenkins MK. Visualizing the generation of memory CD4 T cells in the whole body. Nature. 2001;410(6824):101-5.
225. Reinhardt RL, Bullard DC, Weaver CT, Jenkins MK. Preferential accumulation of antigen-specific effector CD4 T cells at an antigen injection site involves CD62E-dependent migration but not local proliferation. J Exp Med. 2003;197(6):751-62.
226. Doebis C, Menning A, Neumann K, Ghani S, Schlawe K, Lauer U, et al. Accumulation and local proliferation of antigen-specific CD4+ T cells in antigen-bearing tissue. Immunology & Cell Biology. 2011;89(4):566-72.
227. Hwang JM, Yamanouchi J, Santamaria P, Kubes P. A critical temporal window for selectin-dependent CD4+ lymphocyte homing and initiation of late-phase inflammation in contact sensitivity. The Journal of experimental medicine. 2004;199(9):1223-34.
228. Moser B, Wolf M, Walz A, Loetscher P. Chemokines: multiple levels of leukocyte migration control☆. Trends in Immunology. 2004;25(2):75-84.
229. Kufareva I, Gustavsson M, Zheng Y, Stephens BS, Handel TM. What Do Structures Tell Us About Chemokine Receptor Function and Antagonism? Annu Rev Biophys. 2017;46:175-98.
230. Baggiolini M. Chemokines and leukocyte traffic. (0028-0836 (Print)).
231. Mackay CR. Chemokines: immunology's high impact factors. (1529-2908 (Print)).
232. Youn BS, Mantel C Fau - Broxmeyer HE, Broxmeyer HE. Chemokines, chemokine receptors and hematopoiesis. (0105-2896 (Print)).
233. Koch AE, Polverini Pj Fau - Kunkel SL, Kunkel Sl Fau - Harlow LA, Harlow La Fau - DiPietro LA, DiPietro La Fau - Elner VM, Elner Vm Fau - Elner SG, et al. Interleukin-8 as a macrophage-derived mediator of angiogenesis. (0036-8075 (Print)).
234. Belperio JA, Keane Mp Fau - Arenberg DA, Arenberg Da Fau - Addison CL, Addison Cl Fau - Ehlert JE, Ehlert Je Fau - Burdick MD, Burdick Md Fau - Strieter RM, et al. CXC chemokines in angiogenesis. (0741-5400 (Print)).
235. Miller MC, Mayo KH. Chemokines from a Structural Perspective. International journal of molecular sciences. 2017;18(10):2088.
236. Borish LC, Steinke JW. 2. Cytokines and chemokines. Journal of Allergy and Clinical Immunology. 2003;111(2, Supplement 2):S460-S75.
237. Fernandez EJ, Lolis E. Structure, function, and inhibition of chemokines. (0362-1642 (Print)).
238. Roy I, Evans DB, Dwinell MB. Chemokines and chemokine receptors: update on utility and challenges for the clinician. Surgery. 2014;155(6):961-73.
239. Szczuciński A, Losy J. Chemokines and chemokine receptors in multiple sclerosis. Potential targets for new therapies. Acta Neurologica Scandinavica. 2007;115(3):137-46.
240. Fernandez EJ, Lolis E. Structure, Function, and Inhibition of Chemokines. Annual Review of Pharmacology and Toxicology. 2002;42(1):469-99.
241. Kufareva I, Salanga CL, Handel TM. Chemokine and chemokine receptor structure and interactions: implications for therapeutic strategies. Immunology and cell biology. 2015;93(4):372-83.
242. Bennett LD, Fox JM, Signoret N. Mechanisms regulating chemokine receptor activity. Immunology. 2011;134(3):246-56.

243. Bazan JF, Bacon KB, Hardiman G, Wang W, Soo K, Rossi D, et al. A new class of membrane-bound chemokine with a CX3C motif. Nature. 1997;385(6617):640-4.
244. Schulz O, Hammerschmidt SI, Moschovakis GL, Förster R. Chemokines and Chemokine Receptors in Lymphoid Tissue Dynamics. Annual Review of Immunology. 2016;34(1):203-42.
245. Ruth JH, Volin MV, Haines GK, 3rd, Woodruff DC, Katschke KJ, Jr., Woods JM, et al. Fractalkine, a novel chemokine in rheumatoid arthritis and in rat adjuvant-induced arthritis. Arthritis Rheum. 2001;44(7):1568-81.
246. Liu H, Jiang D. Fractalkine/CX3CR1 and atherosclerosis. Clinica Chimica Acta. 2011;412(13):1180-6.
247. Staumont-Sallé D, Fleury S, Lazzari A, Molendi-Coste O, Hornez N, Lavogiez C, et al. CX_3CL1 (fractalkine) and its receptor CX_3CR1 regulate atopic dermatitis by controlling effector T cell retention in inflamed skin. The Journal of experimental medicine. 2014;211(6):1185-96.
248. Kezic J, McMenamin PG. The Monocyte Chemokine Receptor CX3CR1 Does Not Play a Significant Role in the Pathogenesis of Experimental Autoimmune Uveoretinitis. Invest Ophthalmol Vis Sci. 2010;51(10):5121-7.
249. Dinarello CA. Historical insights into cytokines. European journal of immunology. 2007;37 Suppl 1(Suppl 1):S34-S45.
250. Andreakos ET, Foxwell BM, Brennan FM, Maini RN, Feldmann M. Cytokines and anti-cytokine biologicals in autoimmunity: present and future. Cytokine & Growth Factor Reviews. 2002;13(4):299-313.
251. Weinstein JE, Pepple KL. Cytokines in uveitis. Current Opinion in Ophthalmology. 2018;29(3):267-74.
252. Horai R, Caspi RR. Cytokines in autoimmune uveitis. J Interferon Cytokine Res. 2011;31(10):733-44.
253. Zhang R, Qian J, Guo J, Yuan YF, Xue K. Suppression of experimental autoimmune uveoretinitis by Anti-IL-17 antibody. Curr Eye Res. 2009;34(4):297-303.
254. Sun L, He C, Nair L, Yeung J, Egwuagu CE. Interleukin 12 (IL-12) family cytokines: Role in immune pathogenesis and treatment of CNS autoimmune disease. Cytokine. 2015;75(2):249-55.
255. Luger D, Silver PB, Tang J, Cua D, Chen Z, Iwakura Y, et al. Either a Th17 or a Th1 effector response can drive autoimmunity: conditions of disease induction affect dominant effector category. J Exp Med. 2008;205(4):799-810.
256. Lin P. Targeting interleukin-6 for noninfectious uveitis. Clin Ophthalmol. 2015;9:1697-702.
257. Jones LL, Vignali DAA. Molecular interactions within the IL-6/IL-12 cytokine/receptor superfamily. Immunologic research. 2011;51(1):5-14.
258. Jones SA, Jenkins BJ. Recent insights into targeting the IL-6 cytokine family in inflammatory diseases and cancer. Nature Reviews Immunology. 2018;18(12):773-89.
259. Trinchieri G. Interleukin-12 and the regulation of innate resistance and adaptive immunity. Nat Rev Immunol. 2003;3(2):133-46.
260. Trinchieri G, Pflanz S, Kastelein RA. The IL-12 Family of Heterodimeric Cytokines: New Players in the Regulation of T Cell Responses. Immunity. 2003;19(5):641-4.
261. Vignali DAA, Kuchroo VK. IL-12 family cytokines: immunological playmakers. Nature immunology. 2012;13(8):722-8.
262. Yoshida H, Hamano S, Senaldi G, Covey T, Faggioni R, Mu S, et al. WSX-1 Is Required for the Initiation of Th1 Responses and Resistance to L. major Infection. Immunity. 2001;15(4):569-78.
263. Pradhan A, Lambert QT, Reuther GW. Transformation of hematopoietic cells and activation of JAK2-V617F by IL-27R, a component of a heterodimeric type I cytokine receptor. Proceedings of the National Academy of Sciences of the United States of America. 2007;104(47):18502-7.
264. Larousserie F, Charlot P, Bardel E, Froger J, Kastelein RA, Devergne O. Differential effects of IL-27 on human B cell subsets. J Immunol. 2006;176(10):5890-7.
265. Perona-Wright G, Kohlmeier JE, Bassity E, Freitas TC, Mohrs K, Cookenham T, et al. Persistent loss of IL-27 responsiveness in CD8+memory T cells abrogates IL-10 expression in a recall response.

Proceedings of the National Academy of Sciences of the United States of America. 2012;109(45):18535-40.
266. Wang R-X, Yu C-R, Mahdi RM, Egwuagu CE. Novel IL27p28/IL12p40 Cytokine Suppressed Experimental Autoimmune Uveitis by Inhibiting Autoreactive Th1/Th17 Cells and Promoting Expansion of Regulatory T Cells. The Journal of Biological Chemistry. 2012;287(43):36012-21.
267. Amadi-Obi A, Yu CR, Liu X, Mahdi RM, Clarke GL, Nussenblatt RB, et al. TH17 cells contribute to uveitis and scleritis and are expanded by IL-2 and inhibited by IL-27/STAT1. Nat Med. 2007;13(6):711-8.
268. Chihara N, Madi A, Kondo T, Zhang H, Acharya N, Singer M, et al. Induction and transcriptional regulation of the co-inhibitory gene module in T cells. Nature. 2018;558(7710):454-9.
269. Jones GW, Bombardieri M, Greenhill CJ, McLeod L, Nerviani A, Rocher-Ros V, et al. Interleukin-27 inhibits ectopic lymphoid-like structure development in early inflammatory arthritis. The Journal of experimental medicine. 2015;212(11):1793-802.
270. Tait Wojno ED, Hunter CA, Stumhofer JS. The Immunobiology of the Interleukin-12 Family: Room for Discovery. Immunity. 2019;50(4):851-70.
271. Villarino A, Hibbert L, Lieberman L, Wilson E, Mak T, Yoshida H, et al. The IL-27R (WSX-1) is required to suppress T cell hyperactivity during infection. Immunity. 2003;19(5):645-55.
272. Hamano S, Himeno K, Miyazaki Y, Ishii K, Yamanaka A, Takeda A, et al. WSX-1 is required for resistance to Trypanosoma cruzi infection by regulation of proinflammatory cytokine production. Immunity. 2003;19(5):657-67.
273. Pflanz S, Timans JC, Cheung J, Rosales R, Kanzler H, Gilbert J, et al. IL-27, a heterodimeric cytokine composed of EB13 and p28 protein, induces proliferation of naive CD4(+) T cells. Immunity. 2002;16(6):779-90.
274. Cox JH, Kljavin NM, Ramamoorthi N, Diehl L, Batten M, Ghilardi N. IL-27 promotes T cell-dependent colitis through multiple mechanisms. The Journal of experimental medicine. 2011;208(1):115-23.
275. Batten M, Li J, Yi S, Kljavin NM, Danilenko DM, Lucas S, et al. Interleukin 27 limits autoimmune encephalomyelitis by suppressing the development of interleukin 17-producing T cells. Nat Immunol. 2006;7(9):929-36.
276. Awasthi A, Carrier Y, Peron JP, Bettelli E, Kamanaka M, Flavell RA, et al. A dominant function for interleukin 27 in generating interleukin 10-producing anti-inflammatory T cells. Nat Immunol. 2007;8(12):1380-9.
277. Santi PA. Light sheet fluorescence microscopy: a review. The journal of histochemistry and cytochemistry : official journal of the Histochemistry Society. 2011;59(2):129-38.
278. Kaufman SC, Musch DC, Belin MW, Cohen EJ, Meisler DM, Reinhart WJ, et al. Confocal microscopy: A report by the American Academy of Ophthalmology. Ophthalmology. 2004;111(2):396-406.
279. Lichtman JW, Conchello JA. Fluorescence microscopy. Nat Methods. 2005;2(12):910-9.
280. Do J, Kim D, Kim S, Valentin-Torres A, Dvorina N, Jang E, et al. Treg-specific IL-27Rα deletion uncovers a key role for IL-27 in Treg function to control autoimmunity. Proceedings of the National Academy of Sciences of the United States of America. 2017;114(38):10190-5.
281. Cao Y, Doodes PD, Glant TT, Finnegan A. IL-27 Induces a Th1 Immune Response and Susceptibility to Experimental Arthritis. The Journal of Immunology. 2008;180(2):922-30.
282. Schmied M, Breitschopf H, Gold R, Zischler H, Rothe G, Wekerle H, et al. Apoptosis of T lymphocytes in experimental autoimmune encephalomyelitis. Evidence for programmed cell death as a mechanism to control inflammation in the brain. The American journal of pathology. 1993;143(2):446-52.
283. Oh H-M, Yu C-R, Lee Y, Chan C-C, Maminishkis A, Egwuagu CE. Autoreactive Memory CD4(+) T Lymphocytes that mediate Chronic Uveitis Reside in the Bone Marrow through STAT3-dependent Mechanisms. Journal of Immunology (Baltimore, Md : 1950). 2011;187(6):3338-46.

284. Young MR. Endothelial cells in the eyes of an immunologist. Cancer immunology, immunotherapy : CII. 2012;61(10):1609-16.
285. Xu H, Manivannan A, Liversidge J, Sharp PF, Forrester JV, Crane IJ. Requirements for passage of T lymphocytes across non-inflamed retinal microvessels. Journal of Neuroimmunology. 2003;142(1):47-57.